Journal of Double Star Observations

VOLUME 15 NUMBER 3 July 1, 2019

Inside this issue:

Inside this issue:

Study and Description of a New Wide Binary in Dissolution Process

Antonio Agudo Azcona and Francisco Rica Romero

Astronomical forum of Extremadura (Spain)
agudo.fyq@gmail.com

Abstract: In this paper we report the study of a new wide binary according the common parallax and proper motion located at 37 pc and separated by 183 arcsec (data from Gaia-DR2). The system is composed of two stars of 11.5 and 15.9 V-band magnitudes with K8V and M4V spectral types. Despite the wide separation, this system has non-negligible probability of being a comoving binary system. Our dynamical study showed that is a stellar system in process of dissolution. We suggest that this pair be included in the WDS catalog with the name AZC189.

1. Introduction

Wide binaries are important tracers of many processes of star formation, early dynamical evolution (Allen and Monroy-Rodríguez 2014) and galactic shaping (Oh et al. 2017). It may be assumed that wide fragile binaries (by definition with semi-major axis > 100 AU) have evolved independently and therefore they are unaffected by some processes such as mass exchange or tidal coupling that complicate the evolution of close pairs. It may also be considered that members of such binaries are coeval (Zhao et al. 2012).

Coeval stars are born together and have the same metallicity and kinematics. Even if these systems don't orbit around a common center of mass, they should be consider as 'co-moving' binaries because they really form an independent entity by themselves (Benavides et al. 2010). Co-moving pairs with separations smaller than 1 pc are wide binaries (or multiples) that are either weakly gravitationally bound or slowly separating, but at separations larger than 1 pc, they are likely members of (potentially dissolving) moving groups, associations, and star clusters or disrupted wide binaries (Oh et al. 2017).

The orbital properties of the wide binaries are unaltered after their formation, unless perturbed by the galactic tidal field or the interaction with masses encountered during their lifetimes, as they travel in the galactic environment. The widest binaries are quite fragile and easily disrupted by encounters with various influences, be they passing stars, molecular clouds, spiral arms, MACHOs (massive compact halo objects) or the galactic tidal field (Allen & Monroy-Rodríguez 2014). The study of wide binaries can be used as probes to establish the nature of the astronomical objects they interact with as well as their own formation and evolution.

In this work is presented a new wide binary candidate, so far not listed in the Washington Double Star Catalog (WDS), because of its common parallax and kinematic and its large projected separation about 6800 AU. We also report the estimation of the spectral type and masses of the components, other astrophysical properties and the study of the nature of the system.

2. Discovery

The pair discussed in this paper was discovered by filtering a high parallax catalogue obtained from Gaia DR2. Its existence was confirmed visually using Aladin Sky Atlas (Bonnarel et al. 2000) as it is shown in Figure 1. The designations and J2000 precise coordinates for both components are:

- Gaia DR2 47322641158530560 (AR = 04 18 47.54 DEC = +17 32 17.1)
- Gaia DR2 47322297561027712 (AR = 04 18 35.99 DEC = +17 30 58.1)

Parallax and proper motions from Gaia DR2 are shown in Table 1. The common parallax in addition to the high common proper motions and the relative astrometry (rho = 183.14" and theta = 244.4 deg) suggest

Study and Description of a New Wide Binary in Dissolution Process

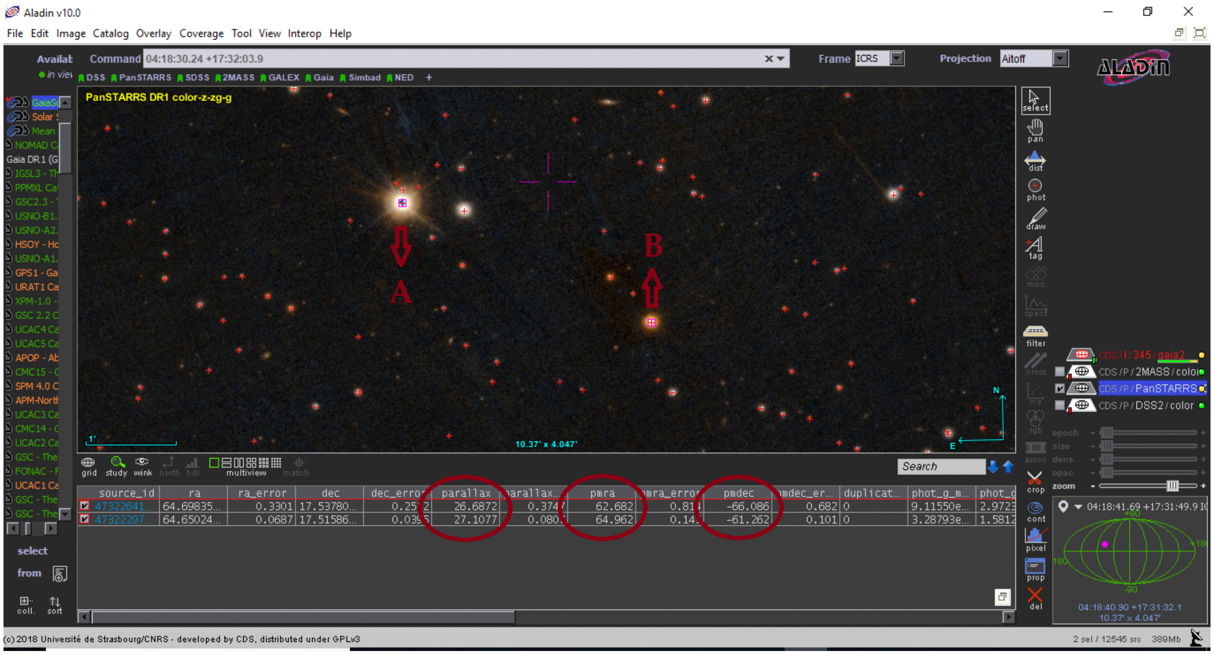

Figure 1. The pair was identified visually using Aladin Sky Atlas.

a wide common proper motion pair. A common value of radial velocity would support even more this assessment, but unfortunately radial velocity from Gaia DR2 is only available for A component (28.80 ± 0.55 km/s)

3. Methodology

The procedure used to study this pair was as follows:

- Astrophysical data collection from diverse sources
- Estimation of spectral type and confirmation of dwarf nature of both components
- Estimation of masses and other astrophysical parameters
- Determination of relative astrometry and calculation of the relative proper motion
- Estimation of the projected separation and the expected semimajor axis
- Estimation of metallicity

4. Results

4.1. Collecting data from astronomical literature

Aladin Sky Atlas and Vizier, the astronomical catalogue service of the Centre de Données Astronomiques de Strasbourg (Ochsenbein et al, 2000), were consulted in order to obtain photometric and other astrophysical data. Table 2 lists the photometric and astrophysical data obtained from the literature. To summarize, Table 2 also include all the astrophysical parameters computed or estimated in this work.

V mag and B-V index were collected from AAVSO Photometric All Sky Survey (APASS) DR9 (Henden et al. 2016). For the A component, the standard deviation is included, but for the B component the value is only from one measure. Therefore, in order to confirm these measures, we collected ugriz photometry from 'The SDSS Photometric Catalog, Release 9' (Adelman-McCarthy+, 2012) and we computed for the secondary the V and B magnitude using Jordi et al. (2006) trans-

Table 1

Component	Parallax (mas)	pmRA (mas/yr)	pmDE (mas/yr)
A	26.6872 ± 0.3747	62.682 ± 0.814	-66.086 ± 0.682
B	27.1077 ± 0.0807	64.962 ± 0.145	-61.262 ± 0.101

formations. Only g and r filter were used for the computation. The results, V = 15.84 and B = 17.39, are quite in agreement with APASS values, therefore we decided to use those ones. We didn't use the SDSS photometric data for the primary because it is likely to be saturated.

J, H and Ks photometry were collected from Two Micron All Sky Survey (2MASS). In addition, other astrophysical parameters like effective temperature, luminosity (only for A component) and radius (only for A component) were collected from Gaia DR2.

4.2. Determination of the Spectral Type

Firstly, we made a J-H vs H-Ks color-color diagram in order to confirm the dwarf nature of both components. As shown in Figure 2, the diagram agrees with this assessment.

Before doing the determination of the spectral type, we estimated the reddening and extinction for the system using the "Galactic Dust Reddening and Extinction" web site (http://irsa.ipac.caltech.edu/applications/DUST/). This web site computes the reddening in the line of sight by Schlafly & Finkbeiner (2011). We scaled down this value to obtain the reddening at distance of the system using the exponential law of Anthony-Twarog & Twarog (1994):

Where $E(B\text{-}V)_d$ is the reddening at distance,

$$E\left(B-V\right)_d = E\left(B-V\right)_\infty \cdot \left(1-e^{-\left(0.008d\sin|b|\right)}\right)$$

$E(B\text{-}V)_\infty$ is the reddening in the line of sight, d is the distance in parsec and b the galactic latitude. We estimated a reddening $E(B\text{-}V)_d$ = 0.045 and an extinction $Av = 0.140$.

Reddening was used to calculate the intrinsic index $B\text{-}V$, called $(B\text{-}V)_o$, and the extinction to compute the absolute visual magnitude using the well-known expression:

$$V - Mv - Mv = 5\log d - 5$$

We obtained the values shown in Table 3.

Table 2

	A component	B component	Source
V	11.528 ± 0.017	15.934	APASS
B-V	1.405 ± 0.029	1.592	APASS
u	16.409 ± 0.011	19.346 ± 0.011	SDSS9
g	12.507 ± 0.001	16.701 ± 0.001	SDSS9
r	10.940 ± 0.001	15.196 ± 0.001	SDSS9
i	10.202 ± 0.001	13.637 ± 0.001	SDSS9
z	10.664 ± 0.004	12.817 ± 0.004	SDSS9
J	8.627 ± 0.020	11.352 ± 0.021	2MASS
H	7.966 ± 0.023	10.769 ± 0.022	2MASS
Ks	7.759 ± 0.021	10.504 ± 0.019	2MASS
Distance (pc)	37.47 ± 0.53	36.89 ± 0.11	This work
Mv	8.52 ± 0.04	12.96 ± 0.02	This work
Teff‡ (K)	4047 (3974...4100)	3335 (3117...4020)	Gaia DR2
Spectral type	K8V	M4V	This work
Luminosity (solL)	0.082	0.006‡‡	Gaia DR2
Radius (solRad)	0.58	0.26‡‡	Gaia DR2
Mass (solMass)	0.62	0.22	This work

‡ It's included the lower and upper uncertainty at 16th and 84th percentile

‡‡ estimated Luminosity and radius for B component from http://www.pas.rochester.edu/~emamajek/EEM_dwarf_UBVIJHK_colors_Teff.txt

Study and Description of a New Wide Binary in Dissolution Process

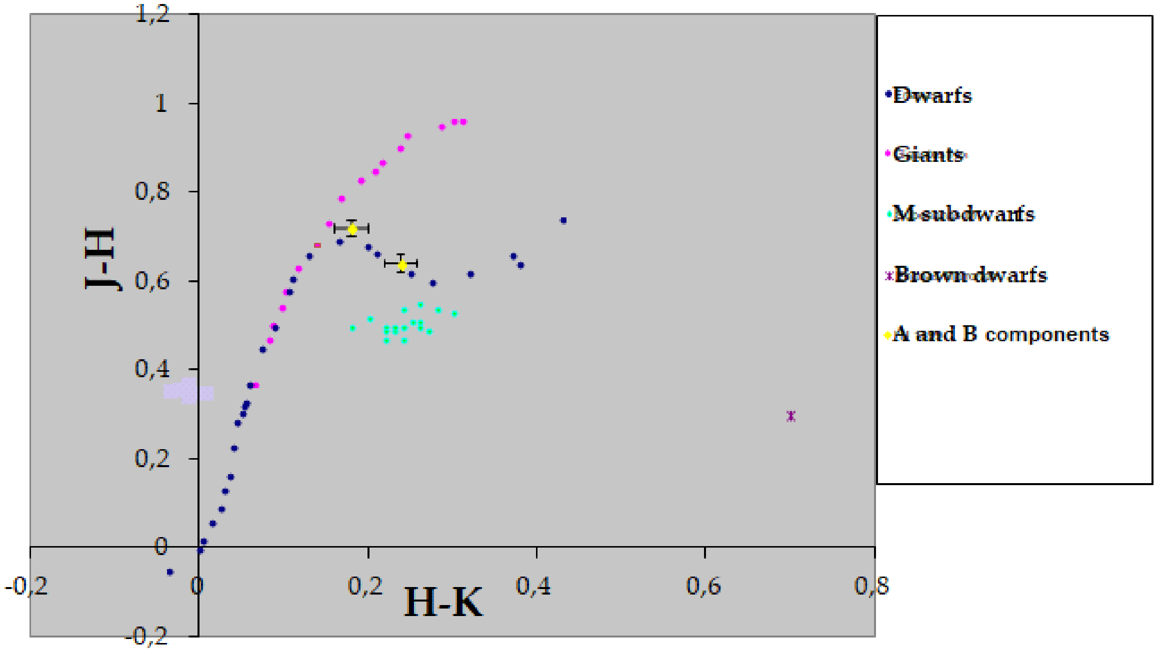

Figure 2: JHK color-color diagram by Francisco Rica's spreadsheets

To determine the spectral type we used as input parameters Teff, Mv, (B-V)o, J-H and H-Ks in the Mamajek tables‡ (Version 2018.08.02) and we selected those spectral types that produced a better fit between the input parameters. The estimated spectral types were K8V for the A component and M4V for the B component.

4.3. Estimation of masses and other astrophysical parameters

The luminosity and the radius of the A component were obtained from Gaia DR2. Nevertheless, these parameters were not available for the B component, but we could get them immediately from the Mamajek tables‡ as it is shown in Table 2.

The masses of both components were computed in terms of solar masses using the next equation in K absolute magnitude by Delfosse et al. (2000):

$$\log\left(\frac{M}{M_{\odot}}\right) = 10^{-3} \cdot \left(1.8 + 6.2M_k + 13.205{M_k}^2 - 6.2315{M_k}^3 + 0.37529{M_k}^4\right)$$

This equation is valid for stars with K absolute magnitude from 4.5 to 9.5. Previously we compute the K absolute magnitude using the relation between Mv and V-K colour. The Mk magnitudes were 4.9 and 7.7, respectively, and the masses obtained 0.68 M¤ and 0.21 M¤.

‡ *"A Modern Mean Dwarf Stellar Color and Effective Temperature Sequence" by Eric Mamajek.* http://www.pas.rochester.edu/~emamajek/EEM_dwarf_UBVIJHK_colors_Teff.txt

Table 3

	A component	B component
$(B-V)_o$	1.36 ± 0.05	1.55 ± 0.05
Mv	8.51 ± 0.05	12.96 ± 0.05

Table 4 compares the masses just like are obtained from Mamajek tables with the values obtained previously.

4.4. Relative Astrometry and relative proper motion

Fourteen astrometric positions (RA and DE J2000) for each component were obtained from different catalogs or surveys by querying Aladin Sky Atlas and Vizier. These equatorial coordinates were transformed into polar coordinates in order to get the relative astrometry, rho and theta. The results are shown in Table 5.

Using the relative astrometry which covers a 65-year period, the relative proper motion of the secondary with respect to the primary was obtained. This parameter gives us an estimate of the relative orbital velocity of the system assuming both stellar components be bound. The relative astrometry X (= ρ*sinθ) and Y (= ρ*cosθ) was plotted *vs* Epoch in two separated diagrams (Figures 3 and 4). Data of these diagrams are

Study and Description of a New Wide Binary in Dissolution Process

Table 4.

	Mass (solMass)	
	Delfosse et al. (2000)	Mamajek tables
A component	0.68	0.59
B component	0.21	0.22

shown in Table 6.

The slopes of each regression line fit are the relative proper motion in RA and DE expressed in mas/year. The vectorial sum produces the total relative proper motion. The results are reported in Table 7.

The total relative proper motion also can be obtained as the difference between the individual proper motions of each component, listed in GAIA DR2, and subsequent vectoral sum. Using this procedure with data of Table 1:

$$\Delta\mu_{total} = \sqrt{\left(pmRA(B) = pmRA(A)\right)^2 + \left(pmDE(B) - pmDE(A)\right)^2}$$

We obtained the total relative proper motion $\Delta\mu_{total}$= (5.34 ± 0.71) mas·yr^{-1}. As can be seen there is a good agreement between the two methods. The small value of the relative proper motion supports the idea of a co-moving pair.

4.5. Projected separation

For these wide binaries, the separation between components usually can't be computed because the Z component of the secondary respect to the primary is unknown. Instead, the projected separation along the celestial plane is computed by the next equation:

$$s = \rho \cdot d \text{ (AU)}$$

where ρ is the angular separation in arc seconds and d is

Table 5

Source	Epoch	Theta	Rho
USNO-A2.0	1950.936	244.42	183.41
POSS-I	1950.937	244.34	182.93
GSC 2.2	1982.959	244.51	182.64
POSS-II Red	1989.845	244.37	183.11
POSS-II Red	1989.973	244.35	183.42
POSS-II Blue	1990.063	244.42	183.49
POSS-II Blue	1991.792	244.51	183.09
POSS-II N	1995.718	244.40	182.88
POSS-II N	1995.726	244.36	183.02
2MASS	1997.763	244.45	182.94
CMC15	2001.120	244.46	183.03
WISE	2010.559	244.47	183.05
URAT1	2013.736	244.44	183.08
GAIA-DR2	2015.5	244.46	183.02

Table 6

Epoch	X	Y
1950.936	-165.43	-79.19
1950.937	-164.89	-79.21
1982.959	-164.86	-78.60
1989.845	-165.09	-79.21
1989.973	-165.34	-79.40
1990.063	-165.50	-79.23
1991.792	-165.27	-78.79
1995.718	-164.93	-79.01
1995.726	-164.99	-79.21
1997.763	-165.05	-78.90
2001.120	-165.15	-78.91
2010.559	-165.18	-78.89
2013.736	-165.16	-78.99
2015.5	-165.14	-78.91

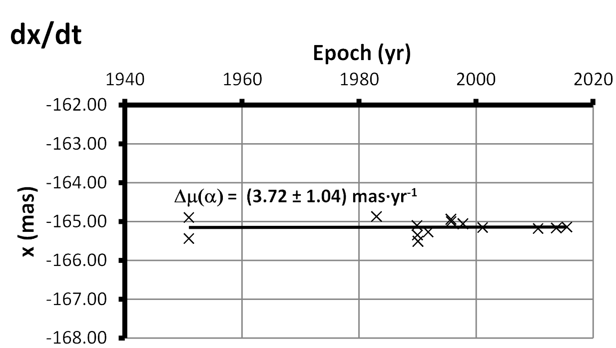

Figure 3. Relative proper motion in RA from the X versus epoch diagram

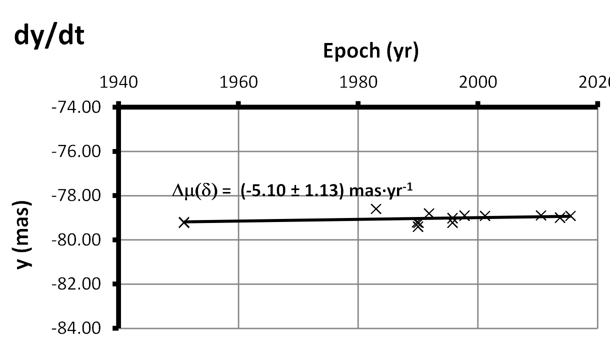

Figure 4. Relative proper motion in DE from the Y versus epoch diagram

Table 7

Δm(α) (mas·yr^{-1})	Δm(δ) (mas·yr^{-1})	Δm$_{total}$ (mas·yr^{-1})
3.72 ± 1.04	-5.10 ± 1.13	6.31 ± 1.54

the distance in parsecs. The value obtained for this system was (6790 ± 102) AU.

4.6. Metallicity

We use two polynomial relations described by Bonfils et al (2005) for low mass stars in order to estimate the metallicities of both components. The first associates the K absolute magnitude, the V-Ks color and the metallicity:

$$[\mathrm{Fe/H}] = 0.196 - 1.527M_K + 0.091{M_K}^2 + 1.886(V-K) - 0.142(V-K)^2$$
$$\text{valid for } M_K \in [4,7.5],\ (V-K) \in [2.5,6], \text{ and } [\mathrm{Fe/H}] \in [-1.5,+0.2]$$

The second relates the absolute visual magnitude, the mass of the star in solar mass units and the metallicity:

$$M_V = 15.884 - 16.534M_\odot + 0.091M_\odot^2 - 7.411M_\odot^2 + 1.153[\mathrm{Fe/H}]$$
$$\text{valid for } M_\odot \in [0.2,0.8] \text{ and } [\mathrm{Fe/H}] \in [-1.5,+0.2]$$

The results obtained are shown in Table 8

The metallicities agree for both components using the first polynomial relation, but don´t agree using the second.

5. Study of the Nature of the System

In order to evaluate the optical or physical nature of the system, we first evaluated the Halbwachs' criterion (Halbwachs 1986) and then the criterion that compares the relative velocity with the escape velocity as was proposed by Rica (2011).

The Halbwachs' criterion studies the kinematics of the components of a double star. Halbwachs set as necessary, but not absolute conditions for a physical binary that the stars have common proper motion (CPM). The critical condition for a common proper motion system (95 % similarity level) is:

$$(\mu_1 - \mu_2)^2 < -2\left({\sigma_1}^2 + {\sigma_2}^2\right)\ln 0.05$$

where μ_1 and μ_2 are the proper motions of each component and σ_1 and σ_2 their standard deviations. The system studied in this work fits the Halbwachs' criterion, therefore is a CPM pair.

For the common proper motion systems we can define the T parameter as the ρ/μ ratio, which is the time used by the system to travel with its motion μ its angular separation ρ. Rica (2004) used this parameter to do an assessment of the probability that a system is a physical binary. Our system has T = 2050, so using this criterion we estimate a 60 % of probability that it is a physical binary.

Table 8

	[Fe/H]	
	A component	B component
1st polynomial relation	-0.2	-0.2
2nd polynomial relation	-0.2	0.0

The relative velocity of the secondary with respect to the primary (or tangential velocity in km·s^{-1}) can be computed from the relative proper motion. The escape velocity is the velocity of the secondary needed to escape from the gravity of the companion star and can be computed by the equation

$$v_{esc} = \sqrt{\frac{2G(M_A + M_B)}{s}}$$

obtained from the conservation of energy equation (Rica 2011).

In a physical binary the relative velocity must be lower than the escape velocity. For this system the relative velocity is (1.11 ± 0.19) km·s^{-1} and the escape velocity (0.48 ± 0.02) km·s^{-1}. We designed a Monte Carlo simulation using the dynamical parameters and their errors to determine the probability of $v_{tan} < v_{esc}$. The result was 0%. Even if the primary star has a twin companion (increasing v_{esc}) this probability will be still 0%. Therefore, this system can't be considered a bound physical binary, but the small difference between both values doesn't reject a possible co-moving system. In Table 9 we list the dynamical parameters for this system.

We calculated a galactocentric velocity (U, V, W) of (-28, -15, -11) km·s^{-1}. According to the plot of Eggen (1969), we conclude that the stars belong to the young disk, as shown in Figure 5. The Grenon parameter (Grenon 1987), fG = 0.15, corresponds to a thin disk of young-medium age (3-4 Gyr).

The star components are in the same region of the sky as the Hyades open cluster. To determine if they belong to this open cluster we used the web site **BANYAN Σ: Bayesian Analysis for Nearby Young AssociatioN**:(http://www.exoplanetes.umontreal.ca/banyan/banyansigma.php). The result was that the star components are field stars with no possibility of be-

Table 9

Mean Epoch	1983.218
θ (deg)	244.47 ± 0.01
ρ (arcsec)	182.908 ± 0.033
x (AU). [E-W]	-6107 ± 61
y (AU). [N-S]	-2917 ± 29
dρ/dt (mas·yr^{-1})	5.65 ± 1.09
dθ/dt (deg·yr^{-1})	-0.0009 ± 0.0003
dx/dt (mas·yr^{-1}) [E-W]	-3.72 ± 1.04
dy/dt (deg·yr^{-1}) [N-S]	-5.10 ± 1.13
Vx (km·s^{-1}) [E-W]	-0.65 ± 0.18
Vy (km·s^{-1}) [N-S]	-0.90 ± 0.20
Vz (km·s^{-1})	---
Vtot (km·s^{-1})	1.11 ± 0.19
Vesc max (km·s^{-1})	0.48 ± 0.02
Mass A (solMass)	0.68 ± 0.07
Mass B (solMass)	0.21 ± 0.02
Distance (pc)	37.0 ± 0.4
Expected max Vz (km·s^{-1})	0.5

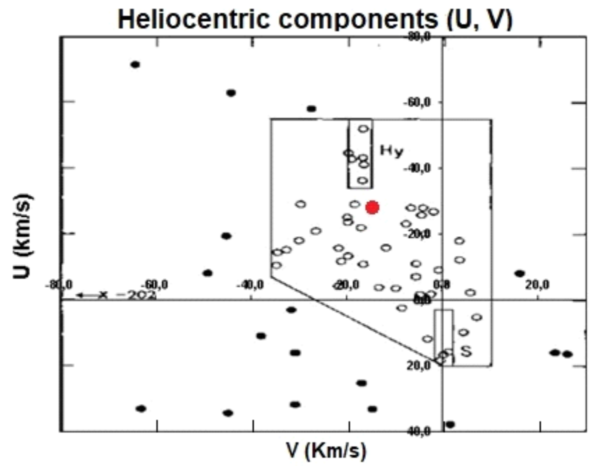

Figure 5. Eggen diagram with galactocentric velocities. The Red circle is the position for this pair.

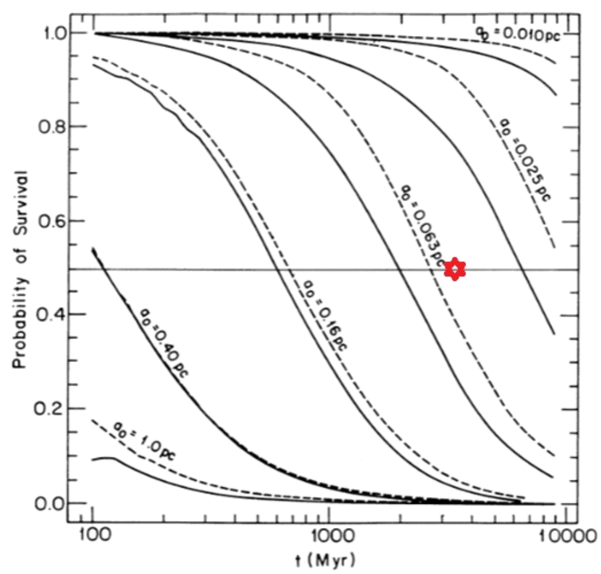

Figure 6. Survival plots of Weinberg et al. (1987).

longing to young stellar associations.

Weinberg et al. (1987) studied the probability of survival for very wide systems (see Figure 6). In this plot the author assumes, for the binaries, a total mass of 1 solar mass. The system we are studying has a gravitationally energy of -2.93·10^{41} ergs, very similar to that of binaries plotted as the curve a_o = 0.065 pc. Binaries similar to the one studied in this work have a survival probability of about 50% at 3-4 Gyr of age.

Our dynamical study allow us conclude that this system is not gravitationally bound but they are probably in the process of dissolution.

6. Conclusions

We have presented the discovery of a new wide binary of common proper motion with both components at the same distance and a projected separation about 6700 UA (~0.033 pc). According to our dynamical study this system can't be considered as a physically bound binary, but the T parameter of the Halbwachs' criterion indicate that the system has a high probability of being a co-moving pair. In our opinion, this pair may be in the initial status of slow disconnection, according to the findings of some researches (Oh et al. 2017). Unfortunately, the estimated values of metallicity are not conclusive and we can't affirm that the components of the system are coeval.

Both components are dwarf stars of the main sequence with K8V and M4V spectral types, respectively. We have estimated the masses and other physical parameters. The kinematic obtained from Gaia DR2 and by an historical review of 65-years period are in a good agreement.

Study and Description of a New Wide Binary in Dissolution Process

This pair is proposed for its inclusion in the Washington Double Star Catalog as a new double star named AZC189.

7. Acknowledgements

This research has made use of the Washington Double Star, USNOA.2 and URAT1 Catalogs maintained at the U.S. Naval Observatory.

This work has made use of data from the European Space Agency (ESA) mission Gaia (https://www.cosmos.esa.int/gaia), processed by the Gaia Data Processing and Analysis Consortium (DPAC, https://www.cosmos.esa.int/web/gaia/dpac/consortium). Funding for the DPAC has been provided by national institutions, in particular the institutions participating in the Gaia Multilateral Agreement.

This work has made use of The Guide Star Catalogue-II, a joint project of the Space Telescope Science Institute and the Osservatorio Astronomico di Torino. Space Telescope Science Institute is operated by the Association of Universities for Research in Astronomy, for the National Aeronautics and Space Administration under contract NAS5-26555. The participation of the Osservatorio Astronomico di Torino is supported by the Italian Council for Research in Astronomy. Additional support is provided by European Southern Observatory, Space Telescope European Coordinating Facility, the International GEMINI project and the European Space Agency Astrophysics Division.

This research has made use of data from the Two Micron All Sky Survey (2MASS), which is a joint project of the University of Massachusetts and the Infrared Processing and Analysis Center/California Institute of Technology, funded by the National Aeronautics and Space Administration and the National Science Foundation.

This publication has made use of data products from the Wide-field Infrared Survey Explorer, which is a joint project of the University of California, Los Angeles, and the Jet Propulsion Laboratory/California Institute of Technology, funded by the National Aeronautics and Space Administration.

This publication has made use of DSS2 surveys produced at the Space Telescope Science Institute through its Guide Star Survey group. The images of these surveys are based on photographic data obtained using the Oschin Schmidt Telescope on Palomar Mountain and the UK Schmidt Telescope. The plates were processed into the present compressed digital form with the permission of these institutions

This publication has made use of the Pan-STARRS1 Surveys (PS1) and the PS1 public science archive that have been made possible through contributions by the Institute for Astronomy, the University of Hawaii, the Pan-STARRS Project Office, the Max-Planck Society and its participating institutes, the Max Planck Institute for Astronomy, Heidelberg and the Max Planck Institute for Extraterrestrial Physics, Garching, The Johns Hopkins University, Durham University, the University of Edinburgh, the Queen's University Belfast, the Harvard-Smithsonian Center for Astrophysics, the Las Cumbres Observatory Global Telescope Network Incorporated, the National Central University of Taiwan, the Space Telescope Science Institute, the National Aeronautics and Space Administration under Grant No. NNX08AR22G issued through the Planetary Science Division of the NASA Science Mission Directorate, the National Science Foundation Grant No. AST-1238877, the University of Maryland, Eotvos Lorand University (ELTE), the Los Alamos National Laboratory, and the Gordon and Betty Moore Foundation.

The study here presented also has made use of the SIMBAD astronomical database and VizieR astronomical catalogs service, both maintained and operated by the Center de Données Astronomiques de Strasbourg (http://cdsweb.u-strasbg.fr/). This research has made use of "Aladin sky atlas" also developed at CDS, Strasbourg Observatory, France.

8. References

Adelman-McCarthy, J., 2012, *ApJS*, **203**, 21A.

Allen, C. & Monroy-Rodríguez, M.A., 2014, *ApJ*, **790**, 158.

Anthony-Twarog B. J., Twarog B. A., 1994, *AJ*, **107**, 1577.

Benavides, R., Rica, F., Reina, E., Castellano, J, Naves, R., Lahuerta, L., Lahuerta, S., 2010, *JDSO*, *6*, 30.

Bonfils, X., Delfosse, X., Udry, S., Santos, N. C., Forveille, T., Ségransan, D., 2005, *A&A*, **442**, 635.

Bonnarel, F., Fernique, P., Bienaymé, O., Egret, D., Genova, F., Louys, M., Ochsenbein, F., Wenger, M., Bartlett, J. G. 2000, *A&AS*, **143**, 33.

Delfosse, X.; Forveille, T.; Ségransan, D.; Beuzit, J.-L.; Udry, S.; Perrier, C.; Mayor, M., 2000, *A&A*, **364**, 217.

Eggen, O. J. 1969, *PASP*, 81, 741E

Fischer, D. A. & Marcy, G. W., 1992, *ApJ*, **396**, 178.

Grenon, M. 1987, JA&A, 8, 123.

Halbwachs, J. L., 1986, *Bull. Inf. Centre Donnees Stellaires*, **30**, 129.

Henden, A.A., Templeton, M., Terrell, D., Smith, T. C., Levine S., Welch, D., 2016, AAS Meeting #225, id.336.16.

Jordi, K., Grebel, E. K., Ammon, K., 2006, *A&A*, **460**, 339.

Ochsenbein, F., Bauer, P., Marcout, J., 2000, *A&AS*, **143**, 23.

Oh, S., Price-Whelan, A. M., Hogg, D. W., Morton, T. D., Spergel, D. N., 2017, *AJ*, **153**, 257.

Rica, F. 2004, Circular Nº 6 Sección Estrellas Dobles LIADA, 33.

Rica, F. 2011, *JDSO*, **7**, 254.

Schlafly, E. F., and Finkbeiner, D.P., 2011, *ApJ*, **737**, 103.

Weinberg, M.D., Shapiro, S.L., and Wasserman, I., 1987, *ApJ*, **312**, 367.

Zhao J. K., Oswalt T. D. & Zhao G., 2012, *AJ*, **143**, 31.

Antonio Agudo-Azcona has a PhD in Chemistry at the University of Extremadura and works as a Physics and Chemistry High School teacher in Olivenza (Badajoz-Spain). He is an amateur astronomer and holds the 'Observatorio Las Vaguadas' MPC I54.

Measurements of Visual Binary Stars: 2018 Report

J. Sérot

jocelyn.serot@free.fr

Abstract: This paper presents the measurements of 113 visual binary stars obtained between January and December 2018 with an 11" reflector telescope and an ASI 290MM CMOS-based camera. Observations focused on close binaries (71 of them having a separation smaller 1 arcsec) and not observed for decades (82 of them were last observed before 2008 and 45 before 1998). In the continuation of some of our previously published papers [1,2], a significant part of these stars are binaries discovered by R.G. Aitken. All measurements were obtained using the bispectrum-based reduction technique described in our previous paper. The observed set also includes 13 binaries having an orbit in the Sixth Catalog of Orbits, for which O-C values are reported. For one of these binaries (A 2157), our observation, along with the previously recorded ones, seems to indicate that an orbit recalculation is required. Finally, for each observed pair, we give, when available, an indication of the probability of being physical, as derived from a score computed from Gaia DR2 data, as described by Harshaw in [9].

1. Instrumental Setup

The instrumental setup is the same as that described in [1,2]. The telescope is a 280 mm Schmidt-Cassegrain reflector (Celestron C11) and the camera an ASI 290MM camera, A 2x Barlow focal length amplificator gives a plate scale of 0.095 arcsec/pixel. Observations are performed with a broad L-band filter (λ_c = 530 nm, $\Delta\lambda$ = 300 nm) and an Atmospheric Dispersion Corrector providing a full correction down to $\delta = 0°$ for our latitude (45° N).

2. Image acquisition and analysis

Acquisition is carried out with the Genika Astro software [3] controlling the ASI 290MM camera. Compared to our previous work the camera gain has been set to a lower value (400 instead of 550). This setting significantly reduces the amount of noise in the raw images. Comparison to our previous results shows that this does not impact the maximum magnitude of the pairs which can be successfully reduced – at least when using bispectrum-based techniques. Exposure time for individual images range from 10 to 80 ms typically.

For each target, N+1 distinct sequences of 1000 images are typically acquired: N of the target itself and one of a nearby reference single star – with similar magnitude and spectral type – to be used for deconvolution later. For most of observations, N=4.

Calibration is carried out using the sideral drift method using the dedicated module of the SpeckleToolBox software [4], again as described in [1,2].

3. Data reduction

All acquired sequences are pre-processed using Reduc [5] and reduced using the bispectrum reconstruction technique described in [1,2] and supported by the latest version of the SpeckleToobox software. The global processing pipeline is sketched in Figure 1.

For each pair, each of the N acquired cube is first dark-subtracted and cropped to 128x128 dimension to speedup subsequent processing and limit the amount of storage needed for archiving. All the resulting cubes are then processed separately (using the reference star cube for deconvolution) and the final results (PA, SEP and Δm) are obtained by computing the statistical mean of the corresponding values. The associated standard error is computed as

$$e = f\sqrt{\frac{\sum_{i=1}^{N}(x_i-\mu)^2}{N-1}}$$

where the x_i are the individual measurements, μ the statistical mean, N the total number of measurements and f a correction factor introduced here to compensate the

Measurements of Visual Binary Stars: 2018 Report

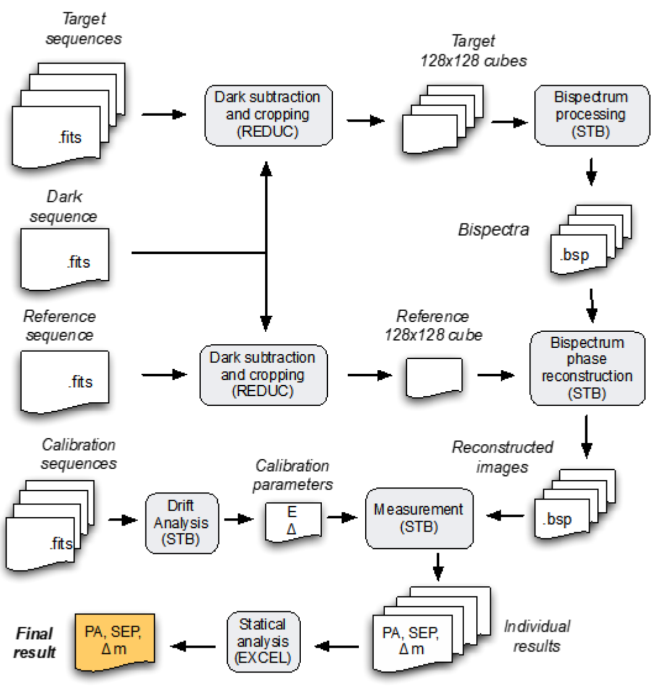

Figure 1. Processing pipeline

small size of the population from which the standard deviation is computed, here set, rather arbitrarily, to 2.

The estimation of Δm obtained using BS-based reduction must be taken with care because it can biased in several manners. First, the iterative image reconstruction process does not always succeed in completely removing the secondary peak. The reconstructed flux of the secondary component is then likely to be distributed between the two peaks and hence the derived Δm value biased. Second, when the companion sits on the diffraction rings of the primary, the correct way to perform aperture photometry is not well defined. This issue is discussed in detail in [6] (section 7). Because we currently have no definite solution to these problems, we have chosen not to report Δm values when they occur.

4. Results

The reported measurements have been obtained during 16 nights, between 2018-04-06 and 2018-10-22.

Figures 1, 2, and 3 show the distribution of these measurements according to the separation of the components, the magnitude of the secondary component and the date of the last measurement recorded in the WDS catalog [7] at the date of our observation.

The measures themselves are listed in Table 1. In this table, columns 1-11 respectively give

- the discoverer code of the pair
- its identifier in the WDS catalog

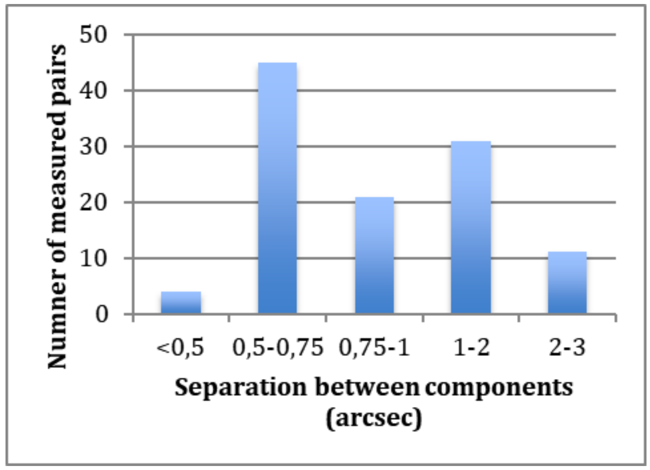

Figure 1. Distribution of measurements according to the separation of components

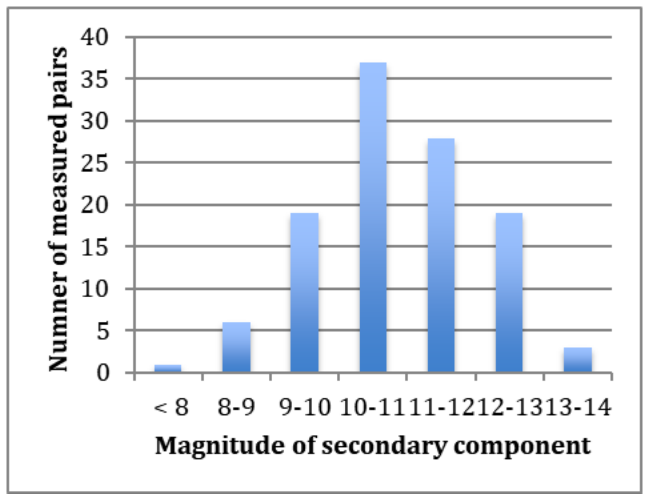

Figure 2. Distribution of measurements according to the magnitude of the secondary component

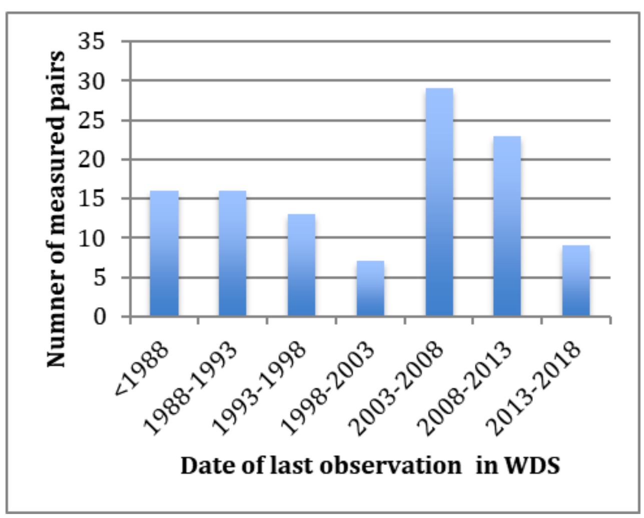

Figure 3. Distribution of measurements according to the date of the last observation recorded in the WDS

† At th
‡ Our c

Measurements of Visual Binary Stars: 2018 Report

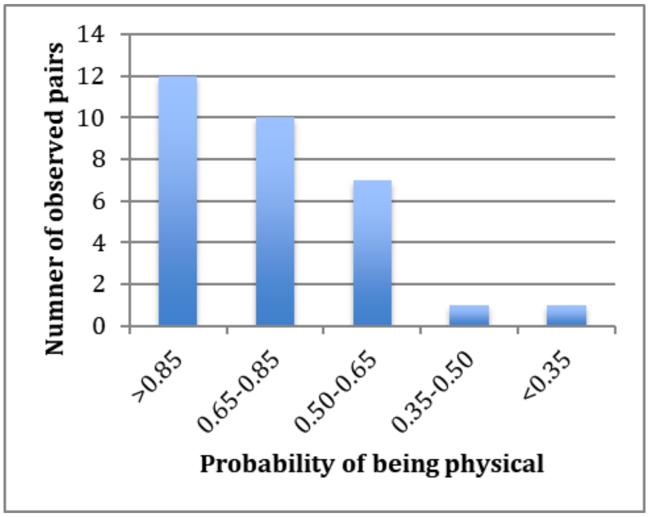

Figure 4. Distribution of observed binaries according to the ''physicality score'' defined in [9]

- the magnitudes of the primary and secondary component, as reported in the WDS catalog
- the date of the last measurement recorded in the WDS catalog†
- the final PA and SEP measurement (in degree and arcsec, resp.) with estimated error when available
- the estimated difference of magnitude, when it can be reliably estimated (see Sec. 3), with estimated error when available,
- the date of the measurement (computed as AAAA.FFF where AAAA is the current year and FFF is obtained by dividing the number of days since Jan 1, 2018 by 366)
- the number of individual measurements,
- an index φ related to the estimated probability for the pair of being physical (see below)
- additionnal notes, to be detailed after the table.

The mean standard error is 0.027 arcsec for SEP and 0.91° (resp. 1.93°) for PA when SEP>1 (resp. <1 arcsec).

The index reported in column φ is derived from the classification given by Harshaw in [9]. Pairs with index 1, 2, 3, 4 and 5 are those having respectively a "physicality score"

above 0.85 (class "Y" in [9]‡)
between 0.85 and 0.65 (class "Y?" in [9])
between 0.65 and 0.50 (class "Maybe" in [9])
between 0.50 and 0.35 (class "??" in [9])
under 0.35 (class "No" in [9])

Pairs listed with class "Uknown" in [9] are given an index φ=0.

As described in in [9], the "physicality score" is computed as a weighted sum of four factors, all derived from data extracted from the Gaia Data Release 2 [10]. These factors include the distance of the components (computed from their parallaxes), their relative motion through space, an R2 fit to trend lines in the data, and the relative radial velocities vis a vis system escape velocity. According to Harshaw, binaries with a score > 0.85 have a high probability of being physical, and those with a score between 0.65 and 0.85 a "medium to high" probability. Binaries with a score between 0.5 and 0.65 "might be" physical, those with score between 0.35 and 0.50 are "questionable" and those under 0.35 are almost certainly not. Among our observations, only 31 binaries have a score in [9]. The repartition of these scores for the corresponding stars is given in Figure 4. It is interesting to see that 22 of the observed binaries are very likely to be physical and only two are probably not.

A few pairs were viewed as simple or perceived as binaries but cannot be reliably measured because their separation was too close (< 0.4 arcsec typically). These pairs are listed in Table 2.

For pairs having a known orbit, Table 3 gives the O-C residuals, computed from the ephemerides published in the 6th Catalog of Orbits [8]. For A 2157 (11162+3136), the large O-C value for PA seems to be related to an incorrect orbit estimation. The two last measurements (Worley, 1979 and Gili, 2008) give PA=2.4° and 1.1° respectively).

Table 4 lists the stars that were last observed before 1988, giving in columns 3-6 respectively, the date of the last observation (as recorded in the WDS), the total number of measurements in the WDS and the variation in PA and SEP between the last WDS measurement and ours. Interestingly, six of these neglected binaries (A 3083, A 1787, COU 192, HU 351, HO 584 and A 1674CD) have a medium to high probability of being physical, justifying *a posteriori* our observation.

Acknowledgments

This research has made use of the Washington Double Star and 6th Orbit catalogs maintained at the U.S. Naval Observatory. Data reduction was carried out using the SpeckleToolbox software (v 1.13) developed and maintained by D. Rowe and the Reduc software (v 5.3) developed and maintained by F. Losse. The "physicality" score reported in Table 1 were extracted from data provided online by R. Harshaw. History of measurements for some pairs listed in Table 1 and 3 have been kindly provided by B. Mason.

(Text continues on page 321)

† At the date of our observation
‡ Our observations were carried out before the publication of Harshaw's paper.

Measurements of Visual Binary Stars: 2018 Report

Table 1. Measurements

NAME	WDS	M1	M2	DATE2	PA(°)	SEP (arcsec)	Δm	DATE	N	φ	NOTE
A 1502	00220+4033	10.3	10.3	2008	245.6 ± 0.1	0.94 ± 0.007	0.2 ± 0.00	2018.734	3	3	
A 912BC	00336+4509	9.7	12.9	2008	334.5 ± 2.8	0.58 ± 0.033		2018.734	2	0	
A 913	00364+5621	9.9	10.3	2008	90.2 ± 0.4	0.74 ± 0.002	0.7 ± 0.00	2018.734	3	0	
A 915	00378+3031	10.4	10.5	2008	129.5 ± 0.4	0.96 ± 0.002	0.3 ± 0.00	2018.734	3	2	
A 1507AB	00423+4015	10	10.4	2008	225.5 ± 0.5	0.7 ± 0.002	1.4 ± 0.10	2018.805	4	0	
A 1258	00544+5432	9.7	9.9	2008	202.3 ± 0.6	0.6 ± 0.012	1.1 ± 0.00	2018.734	3	0	
A 1510	00549+3827	10	10.3	2008	103.7 ± 0.0	0.62 ± 0.001	0.4 ± 0.00	2018.734	3	0	
A 656BC	01133+4426	10.1	12.4	2008	120.5 ± 0.4	0.72 ± 0.025	1.4 ± 0.50	2018.805	4	0	2
A 936	01172+5708	9.8	12.3	2008	241.3 ± 0.2	0.96 ± 0.007	2.2 ± 0.10	2018.805	4	1	
A 940	01280+5821	10.1	10.2	2008	86.1 ± 0.7	0.61 ± 0.013		2018.805	4	0	
A 943	01348+4656	9.6	11.9	1979	218.1 ± 0.9	0.56 ± 0.028	2.8 ± 0.10	2018.805	4	0	
A 2556	09181+0245	9.9	10.6	1991	353.7 ± 0.6	0.95 ± 0.023		2018.260	4	0	
A 344	09521+2916	9.6	9.9	1997	68.3 ± 1.3	0.67 ± 0.010		2018.260	4	0	
COU 169Aa.Ab	10140+2227	10.7	10.9	2014	321.7 ± 0.7	0.54 ± 0.006		2018.288	4	0	1
POP 117	10184+4346	8.3	9.6	2003	258.7 ± 1.8	0.77 ± 0.011	0 ± 0.00	2018.260	4	0	
STF1423	10192+2034	9.4	10	2010	308.3 ± 0.3	0.71 ± 0.002	1 ± 0.10	2018.288	4	0	1
STF1426AB	10205+0626	7.9	8.3	2015	313.4 ± 0.1	0.91 ± 0.001	0.4 ± 0.00	2018.288	4	0	1
A 2569	10261+0802	8.9	12.9	1987	305.4 ± 0.3	1.99 ± 0.077	5 ± 0.20	2018.296	4	0	
HU 1130	10262+6038	10.1	10.8	1991	137.8 ± 1.2	1.04 ± 0.052		2018.260	4	3	
COU2092	10382+4558	9.7	9.7	2003	279.5 ± 1.7	0.61 ± 0.020		2018.260	4	0	
STT 224AB	10397+0851	7.8	8.9	2014	127.5 ± 0.9	0.49 ± 0.019	1.5 ± 0.10	2018.288	4	0	1
A 2768	10426+0335	6.9	8.4	2015	240.9 ± 1.1	0.67 ± 0.006	1.4 ± 0.30	2018.288	4	0	1
A 2771	10446+0530	9.1	9.7	2013	111.7 ± 0.3	0.59 ± 0.009	0.9 ± 0.10	2018.288	4	0	1
A 2772AB	10520+0904	8.2	11.4	1991	97.4 ± 0.1	2.65 ± 0.009	3.5 ± 0.00	2018.296	4	2	
A 2375	10585+1711	10.4	10	2010	168.7 ± 0.7	0.54 ± 0.011		2018.288	4	0	1
A 2774	10596+0956	7.2	12	2003	109 ± 0.6	1.85 ± 0.015	4.5 ± 0.20	2018.296	4	1	
A 2775	11098+1009	8.5	9.8	2008	303 ± 1.8	0.62 ± 0.024	2 ± 0.20	2018.288	4	0	
A 2157	11162+3136	9.2	12.2	2008	2.9 ± 1.0	1.41 ± 0.001	4.4 ± 0.28	2018.301	2	0	1
A 3083	11189+1014	10	12.2	1988	249.8 ± 0.3	1.68 ± 0.006	2.4 ± 0.00	2018.301	2	2	
A 1846	11206+4324	8.8	11.8	1991	165.3 ± 0.5	1.88 ± 0.005	3.4 ± 0.00	2018.296	4	0	
A 2574	11244+0155	9.2	11.2	2010	66.2 ± 0.3	1.98 ± 0.025	3.3 ± 0.10	2018.301	4	3	
A 1354	11272+5513	7.8	11.2	1991	125.7 ± 0.2	1.28 ± 0.017	3.7 ± 0.10	2018.296	4	1	
A 1355	11282+5540	7.7	11.5	1999	359 ± 1.3	1.34 ± 0.024	4 ± 0.20	2018.296	4	0	
A 559	11312+2732	8.3	12.5	1987	152.5 ± 0.2	2.43 ± 0.020		2018.296	4	0	
A 678	11395+2518	7.9	11.1	1996	228.6 ± 0.5	1.19 ± 0.006	2.8 ± 0.10	2018.288	4	0	
A 2486	11574+1823	9.9	11.1	2010	240.9 ± 0.7	1.14 ± 0.023	1.6 ± 0.00	2018.301	4	1	
A 680	11579+2458	10.4	10.3	2008	322.1 ± 1.2	0.52 ± 0.019	2.3 ± 0.10	2018.288	4	0	
A 1779	12010+4347	9.8	11.4	2010	22.1 ± 0.5	0.6 ± 0.014	2 ± 0.10	2018.340	4	0	
A 1594	12050+5113	10.9	12.1	2010	129 ± 0.1	1.62 ± 0.009		2018.301	4	1	
A 2056	12093+1525	9.9	10.2	2010	306 ± 0.9	0.64 ± 0.010	2.2 ± 0.10	2018.288	4	0	
A 1596	12158+5351	9.2	12.4	1991	240.5 ± 0.2	2.81 ± 0.005	3.6 ± 0.10	2018.296	4	1	
A 2487	12171+0143	8.9	12.4	1991	176.8 ± 0.5	1.96 ± 0.022	3.9 ± 0.10	2018.296	4	2	
A 2059	12194+1744	8.3	10.2	2010	42.6 ± 1.5	0.49 ± 0.025	2.1 ± 0.10	2018.288	4	0	1
A 1597	12197+0533	9.2	11.9	1991	282.7 ± 0.8	1.43 ± 0.030	3.3 ± 0.00	2018.288	4	0	
A 1090	12281+0920	9.8	11.2	2001	92.4 ± 0.3	1.87 ± 0.003		2018.301	4	2	
STF1670AB	12417-0127	3.4	3.5	2016	0.5 ± 0.4	2.78 ± 0.016		2018.296	4	0	1
A 1602	12429+0516	8.7	10.1	2014	27.9 ± 0.8	0.68 ± 0.004	1.5 ± 0.00	2018.340	4	0	1
A 1603AB	12440+0356	9	11.6	1995	128.6 ± 0.8	1.22 ± 0.011	2.9 ± 0.00	2018.340	4	0	
A 2061	12461+1715	9.8	12.2	2007	194 ± 0.4	1.19 ± 0.050	2.7 ± 0.10	2018.340	4	0	
A 2000	12563+4300	9.7	10.2	2010	47.3 ± 0.2	1.03 ± 0.001	0.8 ± 0.00	2018.288	4	0	
A 564	13001+2343	9.4	11.3	2009	321.6 ± 0.3	1.73 ± 0.007	2.8 ± 0.00	2018.340	4	2	
A 1784	13041+0511	8.9	12.1	1991	314.2 ± 0.4	1.73 ± 0.028	3.8 ± 0.10	2018.296	4	0	

Table 1 continues on the next page.

Measurements of Visual Binary Stars: 2018 Report

Table 1 (continued). Measurements

NAME	WDS	M1	M2	DATE2	PA(°)	SEP (arcsec)	Δm	DATE	N	φ	NOTE
A 1605	13069+5200	10.7	10.7	2010	349.2 ± 0.4	1.1 ± 0.006		2018.301	4	1	
A 1360	13177+5845	8.2	10.8	1991	143.2 ± 1.4	0.78 ± 0.015	2.5 ± 0.10	2018.340	4	0	
A 2585AB	13189+0030	9.1	9.3	2012	215.8 ± 0.6	0.83 ± 0.006		2018.340	4	3	
A 1787	13196+0942	7.9	11.2	1944	354.7 ± 1.5	2.12 ± 0.102	4.9 ± 0.40	2018.296	4	3	
A 2489	13237-0043	9.4	9.8	2010	189.9 ± 0.2	0.99 ± 0.011	0.9 ± 0.00	2018.340	4	0	1
A 2490	13283+0214	7.5	10	1991	90.7 ± 0.9	1.26 ± 0.018	3.1 ± 0.20	2018.301	4	0	
A 567	13328+2421	6.2	9.7	2007	253.5 ± 0.4	1.39 ± 0.020		2018.296	4	0	
A 1611	13368+0650	8.9	9	2015	121.1 ± 0.2	0.88 ± 0.002	0.4 ± 0.00	2018.340	4	0	
A 1612	13455+0330	8.4	10.2	2015	344.8 ± 0.6	1.67 ± 0.008	2.4 ± 0.00	2018.340	4	0	
A 1795	14109+0424	8.5	11.4	1995	185.8 ± 0.5	1.37 ± 0.013	3.1 ± 0.10	2018.340	4	0	
A 147	14171+5100	8.7	10	2010	109 ± 1.3	0.65 ± 0.012	1.1 ± 0.20	2018.340	4	0	
A 148	14220+5107	8.3	8.9	2015	193.5 ± 0.4	0.52 ± 0.002	0.4 ± 0.00	2018.340	4	0	
A 1620AB	14288+5430	9.4	12.9	2010	226.3 ± 0.3	1.35 ± 0.008	2.8 ± 0.10	2018.340	4	2	
A 2075	15319+1623	9.3	10.1	2010	95.2 ± 0.5	0.48 ± 0.014	1.4 ± 0.10	2018.466	4	0	
A 2077	15468+1905	9.6	10.1	2010	222.7 ± 0.2	0.56 ± 0.005	1.2 ± 0.00	2018.466	4	0	
COU 192	15474+1851	8	14	1967	189.2	1.2	5.22	2018.466	1	3	3
A 1137	16192+5736	9.1	9.7	1997	203.7 ± 0.4	0.61 ± 0.006		2018.466	4	0	
A 1138	16311+5756	10.7	11.7	2010	172.9 ± 0.7	0.58 ± 0.004		2018.466	4	0	
A 1643	16376+4510	10.3	10.6	2008	150.7 ± 0.3	0.76 ± 0.002		2018.466	4	0	
A 349	16413+3006	10.6	10.9	2010	126.5 ± 0.3	0.7 ± 0.001	0.9 ± 0.00	2018.466	4	0	1
HDS2368	16414+3016	7.6	10.9	2010	156.9 ± 1.4	0.83 ± 0.020	3 ± 0.10	2018.466	4	0	
A 1149	17251+0716	9.6	10.3	2010	125.7 ± 0.2	1.03 ± 0.010	1.2 ± 0.00	2018.466	4	0	
A 2093	18054+1624	9	9.8	2008	230.7 ± 0.3	0.64 ± 0.004	0.8 ± 0.00	2018.526	4	0	
A 577	18173+4355	10.4	10.5	2008	303.7 ± 0.8	0.72 ± 0.005	2.1 ± 0.12	2018.479	3	1	
HEI 565	18565+1020	10.8	11.2	1996	96 ± 0.5	0.86 ± 0.019		2018.526	4	5	
A 590	19107+4136	9.8	10	2008	164.9 ± 2.2	0.51 ± 0.022		2018.479	4	0	
A 265AB	19143+2840	10.8	10.8	2008	16.6 ± 0.2	0.93 ± 0.008		2018.479	3	4	
COU2200	19166+3903	11	11.5	1984	121.6 ± 1.9	0.61 ± 0.023		2018.526	4	0	
POP 33	19268+3457	10.6	10.9	1996	230.8 ± 0.4	0.85 ± 0.006		2018.526	3	1	
HEI 812	19272+0312	10	10.1	1995	72.2 ± 0.4	0.69 ± 0.006		2018.526	3	0	
A 715	19335+6002	10.1	10.2	2008	356.4 ± 1.3	0.51 ± 0.027	1.3 ± 0.30	2018.479	4	0	
COU2206	19355+3641	10	11.7	1996	317.4 ± 1.1	0.64 ± 0.009	2.2 ± 0.10	2018.526	4	0	
COU 210	19364+1938	9.7	12	1967	211.3 ± 5.5	0.68 ± 0.010		2018.668	4	1	
HEI 876	19421+0545	9.8	10.2	1996	145.7 ± 0.2	0.76 ± 0.003		2018.526	3	0	
DA 13AB	19447+4456	7.4	11.6	1946	273.8 ± 0.3	2.03 ± 0.002	3.7 ± 0.00	2018.674	3	1	
FOX 89	19456+4147	10.1	11	1991	208.5 ± 0.3	0.89 ± 0.009	1.4 ± 0.00	2018.668	4	0	
BU 1301BC	19464+0418	9.5	9.5	1983	334.6 ± 1.3	0.69 ± 0.023		2018.668	4	0	
MLR 606	19508+5633	10.5	10.6	1991	205.4 ± 0.6	0.57 ± 0.009		2018.526	4	0	
HDS2830	19516+3932	8.3	11.2	1991	204.3 ± 3.4	0.74 ± 0.019	2.9 ± 0.10	2018.668	4	0	
HU 351	19522+1951	8.2	12.4	1977	157.8 ± 0.1	2.04 ± 0.007	3.7 ± 0.12	2018.674	3	2	
A 1660AB.C	19529+1425	10.2	10.3	2008	203.3 ± 1.0	0.68 ± 0.005		2018.479	3	0	
MLR 587	19545+5727	10.7	10.7	1995	347.9 ± 0.4	1.02 ± 0.001		2018.526	3	3	
A 2791	19583+2218	9.5	12.5	2008	136.2 ± 2.3	0.52 ± 0.005	2.4 ± 0.10	2018.479	4	0	
A 276	19594+2636	9.6	11.8	2008	332.4 ± 1.0	0.94 ± 0.011	2.4 ± 0.10	2018.479	4	0	
HO 584	20003+2611	6.6	12.1	1975	226.9 ± 0.3	2.38 ± 0.001	5.3 ± 0.14	2018.674	2	2	
A 2278AB	20068+0157	10	10.5	1991	213.7 ± 0.6	0.93 ± 0.013	1 ± 0.12	2018.490	3	0	
BAR 11AB	20180+3311	7.9	9	2000	198.6 ± 4.8	0.47 ± 0.010	3 ± 0.20	2018.674	4	0	
HO 592AB.C	20180+3311	7.6	11.9	1991	254.6 ± 0.1	3.05 ± 0.007	4.5 ± 0.30	2018.674	4	0	
A 1674AB	20275+1454	9.8	13.1	1977	14.1 ± 1.2	0.92 ± 0.006	2.6 ± 0.10	2018.526	4	1	
A 1674CD	20275+1454	12.5	13.5	1932	171.2 ± 1.7	1.28 ± 0.015	0.7 ± 0.00	2018.668	3	0	
BU 987AB	20302+1925	6.8	11.1	1986	127.5 ± 0.1	2.52 ± 0.002	4 ± 0.10	2018.674	4	0	

Table 1 concludes on the next page.

Measurements of Visual Binary Stars: 2018 Report

Table 1 (conclusion). Measurements

NAME	WDS	M1	M2	DATE2	PA(°)	SEP (arcsec)	Δm	DATE	N	φ	NOTE
A 395	20316+0530	10.1	11.9	1981	159.5 ± 1.5	0.69 ± 0.011	1.6 ± 0.10	2018.490	4	0	
BU 1302AB	20448+2311	8.8	12.9	1999	137.7 ± 0.1	2.28 ± 0.002	3.9 ± 0.00	2018.674	3	2	
A 876	20454+0023	10.1	10	1995	68.1 ± 1.0	0.58 ± 0.020		2018.490	4	0	
COU2431Aa.Ab	20599+4016	6.6	10.8	2012	205.4 ± 0.1	2.23 ± 0.008	4.1 ± 0.10	2018.674	4	0	
A 763	21202+6038	7.6	10.8	1994	214.4 ± 1.0	1.3 ± 0.044	3.7 ± 0.10	2018.674	4	0	
A 766	21249+5734	9.7	11.2	2008	225.1 ± 1.3	0.55 ± 0.031		2018.674	4	0	
A 891	21577-0038	9.5	9.5	2008	77.7 ± 0.3	0.65 ± 0.005	-0.2 ± 0.00	2018.668	4	0	
A 624	22107+5830	10.1	12.3	2008	10.6 ± 0.6	0.79 ± 0.007	1.6 ± 0.10	2018.668	4	0	
A 2495AB	22128+4048	8.4	10.5	2008	251.7 ± 1.8	0.69 ± 0.012	2.8 ± 0.10	2018.668	4	0	
A 1490	23335+5210	8.6	12.6	2008	192.6 ± 0.6	0.74 ± 0.008	2.6 ± 0.00	2018.734	4	0	

Notes for Table 1

1. Pair with an entry in 6th Catalog of Orbits. See Table 3 for O-C
2. AB=HJ2027
3. Only one measurement. Hence no estimation of standard errors

Table 2 – Pairs observed but for which no measure was obtained

NAME	WDS	M1	M2	DATE	NOTE
A 1523	01472+4212	10	9.3	2018.805	2
A 2770	10446+0402	8.7	11.8	2018.260	2
A 1104	14231+0729	9.8	9.4	2018.340	2
HU 252	18477+0916	9.2	9.7	2018.526	1
MLR 540	19393+5802	10	12.4	2018.668	1
COU1804DE	19466+3253	9.6	11.1	2018.674	1
HO 114AB	19466+3253	6.3	11.8	2018.674	1
A 866Ba,Bb	20055+5800	9.9	10.3	2018.490	1
A 1491	23363+5428	8.8	10.3	2018.734	1

Notes for Table 2

1. Viewed as simple
2. Viewed as elongated but too close to be measured.

Table 3 – O-C residuals for pairs having a known orbit

NAME	WDS	DATE	O-C PA(°)	O-C SEP (arcsec)	GRADE	REF
COU 169Aa,Ab	10140+2227	2018.288	-7.1	0.05	5	Cou1999b
STF1423	10192+2034	2018.288	3.7	0.11	3	WSI2004a
STF1426AB	10205+0626	2018.288	-0.1	0.01	4	Nov2006
STT 224AB	10397+0851	2018.288	-2.9	0.01	3	Hrt2010a
A 2768	10426+0335	2018.288	0.4	0.05	3	Tok2015c
A 2771	10446+0530	2018.288	-1.2	0.06	4	Tok2014a
A 2375	10585+1711	2018.288	1.3	0.04	3	Doc2009g
A 2157	11162+3136	2018.301	-229.3	0.34	5	Pop1996b
A 2059	12194+1744	2018.288	-0.3	0.06	5	Lin2017a
STF1670AB	12417-0127	2018.296	1.5	0.05	2	Sca2007c
A 1602	12429+0516	2018.340	1.5	0.06	5	Doc2015d
A 2489	13237-0043	2018.340	-1.5	0.01	5	WSI2004a
A 349	16413+3006	2018.466	-1.9	0.04	3	Hrt2014b

Measurements of Visual Binary Stars: 2018 Report

Table 4 – Binaries not observed since 1988

NAME	WDS	DATE2	NOBS	ΔPA	ΔSEP
A 943	01348+4656	1979	6	0.1	0.06
A 2569	10261+0802	1987	4	4.6	0.11
A 3083	11189+1014	1988	12	2.8	0.22
A 559	11312+2732	1987	4	0.5	0.03
A 1787	13196+0942	1944	4	3.3	0.42
COU 192	15474+1851	1967	1	4.2	0.31
COU2200	19166+3903	1984	1	9.4	0.11
COU 210	19364+1938	1967	1	9.7	0.02
DA 13AB	19447+4456	1946	13	1.8	0.23
BU 1301BC	19464+0418	1983	5	5.4	0.19
HU 351	19522+1951	1977	7	2.8	0.24
HO 584	20003+2611	1975	5	0.1	0.02
A 1674CD	20275+1454	1932	3	0.8	0.28
A 1674AB	20275+1454	1977	7	3.1	0.22
BU 987AB	20302+1925	1986	11	1.5	0.08
A 395	20316+0530	1981	7	8.5	0.01

(Continued from page 317)

This paper is dedicated to the memory of the great double star observer René Gili (d. 2018).

References

[1] Sérot, J., "Measurements of 208 Aitken Visual Binary Stars with a 280 mm Reflector", *JDSO*, **13**(3), 433-443, 2017.

[2] Sérot, J., "Measurements of Aitken Visual Binary Stars: 2017 Report", *JDSO*, **14**(3), 527-537, 2018.

[3] http://genicapture.com

[4] Harshaw R., Rowe D., Genet R., "The Speckle Toolbox: A Powerful Data Reduction Tool for CCD Astrometry", *JDSO*, **13**(1), 52-67, 2017.

[5] Losse, F. Reduc, http://www.astrosurf.com/hfosaf

[6] Sérot J., Wasson R., Rowe D., Genet R, "Bispectrum-based Measurements of Close Large-Differential-Magnitude Visual Double Stars", *JDSO*, **12**(5), 268-284, 2016.

[7] Mason, D.B., Wycoff G.L., Hartkopf, W.I., Washington Double Stars Catalog, USNO, 2015, http://www.usno.navy.mil/USNO/astrometry/optical-IR-prod/wds/WDS

[8] Hartkopf, W.I., Mason, D.B. Sixth Catalog of Orbits of Visual Binary Stars, USNO, 2009, http://www.usno.navy.mil/USNO/astrometry/optical-IR-prod/wds/orb6

[9] Harshaw R, "Gaia DR2 and the Washington Double Star Catalog: A Tale of Two Databases", *JDSO*, **14** (4), 734-740, 2018.

[10] ESA, 2018, http://sci.esa.int/gaia

Jonckheere Double Star Photometry – Part XIII: Peg

Wilfried R.A. Knapp

Vienna, Austria
wilfried.knapp@gmail.com

John Nanson

Star Splitters Double Star Blog
Manzanita, Oregon
jnanson@nehalemtel.net

Abstract: If any double star discoverer is in urgent need of photometry then it is Jonckheere. There are over 3000 Jonckheere objects listed in the WDS catalog and a good part of them with magnitudes obviously far too bright. This report covers the Jonckheere objects in the constellation Pegasus. At least one image per object was taken with V-filter to allow for visual magnitude measurement by differential photometry. All objects were additionally checked for potential gravitational relationship and 11 qualify indeed as potential physical pairs.

Preamble: This report in no way intends to belittle the work of Jonckheere – on the contrary: He was obviously a very dedicated and able double star observer fighting with a lot of obstacles including equipment destroyed in World War I. It seems that the basic double star parameters, RA/Dec coordinates and separation as well as position angle were his main concern and the estimation of magnitudes was rather a side aspect to him. The often crass over estimation of magnitudes may also be a side effect of his obviously extraordinary eyesight.

Introduction

As follow up to the reports on J-objects photometry beginning with Knapp/Nanson 2016 we selected this time the J-objects in Pegasus (Peg). 175 J-objects in Peg is quite a large number and weather conditions did often not allow for taking images of good quality so an unusual number of imaging sessions were required to get images of acceptable quality for photometry. But even images of good quality were often less than perfect for plate solving due to the lack of a sufficient population of well suited reference stars in some Peg areas. Due to these problems we did this time not look for other WDS objects in the existing image material.

Results of Photometry and Catalog Checking

With a few exceptions, for all selected J-objects one single image was taken with iTelescope iT24 with V-filter and 3s exposure. While for the mentioned image quality issues the astrometry results have to be taken with caution beyond the given error range the effects seem less significant for the V-filter measured magnitudes as a magnitude error of ~0.1 or even a bit larger seems negligible in comparison with those for the Jonckheere objects, which often have given magnitude errors in the range of up to 2 or more magnitudes. With the availability of precise GAIA positions for most of the listed components the value of astrometry results from processing of CCD images taken with traditional earth-bound telescopes seems anyway a bit questionable.

Several objects were too faint to be resolved with a 3s exposure time – additional images with longer exposure time were taken for these and stacked with AAVSO VPhot. The images were then plate solved with Astrometrica using the URAT1 catalog with reference stars in the Vmag range of 8.5 to 14.5 giving not only RA/Dec coordinates but also photometry results for all reference stars used including an average dVmag error. The J-objects were then located in the center of the image and astrometry/photometry was then done by the rather comfortable Astrometrica procedure with point and click at the components delivering RA/Dec coordinates and Vmag measurements based on all reference stars used for plate solving.

A subset of the measurement results for the first 10 objects is given in table 1 below. The full data set including the parameters listed in parenthesis is available for download from the JDSO website as fixed format text file "Jonckheere Peg Results" with the following structure:

- First row gives the WDS data as of April 2018:
    - WDS ID
    - Comp gives the components
    - J gives the number of the J-object
    - RA/Dec gives the position in the HH:MM:SS/DD:MM:SS format for the primary
    - Sep, PA, M1, M1, pmRA and pmDec give the WDS catalog data for this object
    - Date gives the year of the last observation
    - Notes gives additional comments listed below Table 1
- Data rows give data from GAIA DR2:
    - (RA and Dec give the J2015.5 coordinates in degrees for the primary)
    - Sep gives the calculated separation in arcseconds if coordinates for both components are available
    - (e_Sep gives the separation error)
    - PA gives the calculated position angle in degrees if coordinates for both components are available
    - (e_PA gives the position angle error)
    - M1 and M2 give GIA DR2 Gmags
    - (e_M1/2 give the magnitude error)
    - Plx1 and Plx2 give the parallax for both components if available
    - pmRA/pmDE give the proper motion data for both components if available
    - Ap and Me give aperture and used observation method
    - CPMR gives the common proper motion rating based on the available PM data according to the description in Appendix A
    - CPMS gives an estimated probability for being a physical pair based on proper motion data (see Appendix A)
    - PlxR gives the distance rating based on the available parallax data according to the description in Appendix A
    - PlxS gives an estimated probability for being a physical pair based on parallax (see Appendix A)
    - Notes gives additional comments listed below Table 1
- Measurement row gives the results from processing of own images:
    - (RA/Dec gives the position in degrees for the primary)
    - Sep gives the calculated separation in arcseconds for resolved pairs
    - (e_Sep gives the separation error)
    - PA gives the calculated position angle in degrees for resolved pairs
    - (e_PA gives the position angle error)
    - M1 and M1 give Vmags for both components measured by differential photometry
    - (e_M1/2 give the magnitude error)
    - Date gives the Julian observation epoch
    - Notes gives additional comments listed below Table 1

Summary

124 of the 175 J-objects in Peg show the expected magnitude difference larger than 0.5 compared with the WDS catalog data. Further about 39 of these objects qualify as solid or at least good CPM candidates based on a rating scheme using GAIA DR2 proper motion data if available for both components with the caveat of rather small proper motion values for a few of them. Further 11 objects have parallaxes and angular separations allowing for a higher than 50% likelihood for a distance between the components of less than 200,000 AU suggesting potential gravitational relationship between the components.

Acknowledgements

The following tools and resources have been used for this research:

- Washington Double Star Catalog
- CDS VizieR and X-Match
- GAIA DR2 catalog
- 2MASS images
- DSS images
- Aladin Sky Atlas v10.0
- iTelescope
    - iT24: 610mm CDK with 3962mm focal length. Resolution 0.625 arcsec/pixel. V-filter. No transformation coefficients available. Located in Auberry, California. Elevation 1405m
- AAVSO VPhot
- Astrometrica v4.10.0.427
- URAT1 and UCAC4 catalog
- AstroPlanner v2.2
- MaxIm DL6 v6.08

(Continued on page 326)

Jonckheere Double Star Photometry – Part XIII: Peg

WDS	Comp	J	Sep	PA	M1	M2	Plx1	Plx2	pmRA1	pmDec1	pmRA2	pmDec2	Ap	Me	Date	CPMR	CPMS	PlxR	PlxS	Notes
21551+1908		2	3.5	36	11.5	11.5			8	-41					2015					
			3.46732	35.996	10.776	10.899	5.4202	5.3973	53.798	31.832	53.609	29.951	0.96	Hg	2015.50000	BBAA	64	BA	80	1)
			3.32774	33.028	10.626	10.875							0.62	C	2015.84310					2)3)
00060+1315		143	2.5	86	11.3	11.6			-76	-32	15	-25			2015					
			2.53563	85.983	10.932	11.557	3.9741	3.9645	-12.456	-27.592	-12.841	-27.450	0.96	Hg	2015.50000	AAAA	100	BA	80	1)
			2.16635	86.030	10.933	11.355							0.62	C	2015.84311					2)4)
21212+1841		160	3.2	290	12.2	12.4			-3	-8					2016					
			3.22270	289.774	11.546	11.400	0.6267	0.1919	-4.264	-6.690	-2.730	-7.015	0.96	Hg	2015.50000	DDAB	0	DC	1	1)
			3.14631	289.302	11.646	13.031							0.62	C	2015.91146					2)3)5)
21288+1341		162	2.7	59	10.9	12.2			28	-34					2015					
			2.68405	59.022	10.196	11.758	5.4086	5.7380	29.718	-31.125	32.081	-34.060	0.96	Hg	2015.50000	ADAA	5	DA	1	1)
			2.66294	58.029	10.363	11.279							0.62	C	2015.84313					2)4)
21458+1419		164	5.1	301	9.4	11.0			-4	-13					2017					
			5.05090	300.182	10.878	12.397	1.5347	1.7322	-8.235	-11.563	-9.697	-11.375	0.96	Hg	2015.50000	DDAB	0	DA	1	1)
			4.96115	299.195	10.937	12.620							0.62	C	2015.84314					2)
22379+1131		165	2.0	137	10.6	11.0			33	3	33	3			2001					
			2.06893	137.189	10.281	10.810	4.8313	4.9578	36.615	6.002	36.779	2.683	0.96	Hg	2015.50000	DAAA	1	CA	20	1)
			2.39318	142.554	10.148	10.627							0.62	C	2015.84314					2)4)
23282+1701		166	4.8	351	10.6	12.6			17	2	26	10			2015					
			4.79536	350.916	10.366	12.089	4.6133	4.5091	15.738	8.616	16.001	9.254	0.96	Hg	2015.50000	BCAB	31	CA	20	1)
			4.63804	350.926	10.483	12.165							0.62	C	2015.91148					2)
21309+1141		178	2.9	186	10.8	11.1			-12	-25					2015					
			2.86029	185.654	11.186	11.805	4.7304	4.7031	-14.144	-36.939	-13.601	-35.497	0.96	Hg	2015.50000	ADAA	5	CA	20	1)
			2.41541	183.836	11.185	11.276							0.62	C	2015.91148					2)3)
22193+0800		179	3.8	311	11.2	11.4			-25	-17	-64	1			2016					
			3.77917	311.437	10.404	11.840			-28.417	-11.819	-29.875	-11.676	0.96	Hg	2015.50000	BDAB	4			1)
			3.55072	311.872	10.565	12.047							0.62	C	2015.91149					2)3)
22282+0910	AB,C	180	5.8	308	9.6	12.3			3	-40	-27	-2			2010					
																				6)
			5.74549	308.415	9.968	12.745							0.62	C	2015.91149					2)

Jonckheere Double Star Photometry – Part XIII: Peg

Content of the Notes column:

1. Source GAIA DR2 catalog. M1 and M2 are GAIA DR2 Gmags
2. iT24 1x3s: Image taken with iTelescope T24 with V-filter and 3 seconds exposure time
3. Touching star disks: Indicates that the rims of the star disks are touching and that the measurement results might be a bit less precise than with clearly separated star disks
4. Overlapping star disks: Indicates that the star disks overlap to the degree of an elongation and that the measurement results is probably less precise than with clearly separated star disks
5. Vmags confirmed by counter-checking with GAIA GBR-mags based estimation
6. AB resolved in GAIA DR2, for this reason no match with AB
7. iT24 5x3s: Five stacked images taken with iTelescope T24 with 5 filter and 3 seconds exposure time
8. No resolution
9. No Plx and PM listed in GAIA DR2 for secondary (or primary)
10. Image quality questionable: Rather large average errors for the reference stars used for plate solving and photometry for different reasons (mostly atmospheric influences). But this is at least to some degree already included in the calculation of the error range estimation
11. Small number of reference stars. Plate solved with UCAC4
12. SNR <20: Indicates that the measurement result might be a bit less precise than desired due to a low SNR value but this is already included in the calculation of the magnitude error range estimation
13. Source GAIA DR2 catalog. M1 is GAIA DR2 Gmag. No object at WDS location for C
14. No resolution of C, bogus assumed
15. Hint of elongation but no serious resolution. Combined magnitude suggests components about 0.4mag fainter than WDS
16. Hint of elongation but no serious resolution. Combined magnitude corresponds with WDS mags
17. SNR <10: Indicates that the measurement result might be much less precise than desired due to a low SNR value but this is at least to some degree already included in the calculation of the magnitude error range estimation
18. Hint of elongation but no resolution. Combined magnitude suggests fainter than WDS mags
19. B probably 0.5mag fainter
20. WDS position wrong. Correct position is 23:46:07.82 +30:26:25.4
21. Hint of elongation but no serious resolution. Combined magnitude suggests components being brighter than WDS listed
22. No resolution of A nor B. Both have to be fainter than 13.5mag
23. WDS J2000 position wrong. Correct position is 22 10 47.62 +21 52 41.7
24. iT24 5x4s: Five stacked images taken with iTelescope T24 with V filter and 4 seconds exposure time
25. iT24 5x6s: Five stacked images taken with iTelescope T24 with V filter and 6 seconds exposure time
26. PM for B is slightly different than above for the AB pair
27. B brighter than A
28. No object for the primary in GAIA DR2 although it exists in DR1
29. No secondary at this position. Wrong position or bogus
30. WDS J2000 position wrong. Correct coordinates are 22 34 58.65 +29 51 48.5
31. SNR <5: Indicates that the measurement result might indeed be much less precise than desired due to a low SNR value but this is at least to some degree already included in the calculation of the magnitude error range estimation
32. No such object at this position. WDS X-coded
33. iT24 1x4s: One image taken with iTelescope T24 with V filter and 4 seconds exposure time
34. WDS code “V” for common proper motion suggested
35. WDS code “T” for common parallax suggested

(Continued from page 323)

References

Knapp, Wilfried R. A.; Nanson, John, 2016, "Jonckheere Double Star Photometry – Part I: Cyg", *JDSO*, **12**(2), 168-179.

Knapp, Wilfried R. A.; Nanson, John, 2017, "A New Concept for Counter-Checking of Assumed CPM Pairs", *JDSO*, **13**(1), 31-51.

Knapp, Wilfried R. A., 2018, "A New Concept for counter-Checking of Assumed Binaries", *JDSO*, **14** (3), 487-491.

Knapp, Wilfried R. A.; Nanson, John, 2018, "Estimating Visual Magnitudes for Wide Double Stars", *JDSO*, **14**(3), 503-520 .

Appendix A

Description of the CPM rating procedure (according Knapp and Nanson 2017 and Knapp 2018):

- Four rating factors are used: Proper motion vector direction, proper motion vector length, size of position error in relation to proper motion vector length and relation separation to proper motion speed
- Proper motion vector direction ratings: "A" for within the error range of identical direction, "B" for similar direction within the double error range, "C" for direction within the triple error range and "D" for outside
- Proper motion vector length ratings: "A" for identical length within the error range, "B" for similar length within the double error range, "C" for length within the triple error range and "D" for outside
- Error size ratings: "A" for error size of less than 5% of the proper motion vector length, "B" for less than 10%, "C" for less than 15% and "D" for a larger error size
- Relation separation to proper motion speed: "A" for less than 100 years, "B" for less than 1000 years, "C" or less than 10000 years and "D" for above

To compensate for the extremely small proper motion GAIA DR2 errors resulting in a worse than "A" rating despite only very small deviations an absolute lower limit is applied regardless of calculated error size:

- - Proper motion vector direction: Max. 1° difference for an "A"
- - Proper motion vector length: Max. 1% difference for an "A"

The letter based scoring is then transformed into an estimated probability and a verbal assessment for being CPM

Description of the Plx rating procedure (according to Knapp 2018):

- Two rating factors are used: Distance between the components in AU and relationship Plx error to Plx value. The distance between the components is calculated from the inverted GAIA DR2 parallax data (if positive and Plx>3*e_Plx) and the angular separation using the law of cosine. Realistic case is based on the given Plx values and the best and worst case scenario uses the given e_Plx data on the Plx values to estimate a smallest and largest possible distance
- "A" for worst case distance, "B" for realistic case distance and "C" for best case distance less than 200,000 AU (means touching Oort clouds for two stars with Sun-like mass) and "D" for above
- "A" for Plx error less than 5% of Plx, "B" for less than 10%, "C" for less than 15% and "D" for above

The letter based scoring is then transformed into an estimated probability for being potentially gravitationally bound.

Recovery of "Very" Neglected WDS Objects in Gaia DR2

Wilfried R.A. Knapp
Vienna, Austria
wilfried.knapp@gmail.com

Abstract: The USNO WDS catalog website lists also 3 sets of neglected objects selected by different criteria (mainly "Not observed in 20 years") to point out double stars in need of new observations. To concentrate on "very" neglected double stars not observed in 60 years all objects with a last observation date before the year 1958 were selected directly from the WDS catalog and 3,149 such objects remained after elimination of all pairs with data not suitable for cross-matching with GAIA DR2. After a drill down process in several steps 1,473 pairs were successfully matched with GAIA DR2 objects – a recovery rate of about 47 percent. For the rest most not recovered objects are either bogus (or lost due to wrong J2000 positions) or simply not resolved in DR2 mostly with separations below 1 arcsecond.

1. Selection of the objects

Selecting all WDS objects with last observation year smaller than 2000 with CDS TAP-VizieR resulted per end of December 2018 in 36,459 neglected double stars with the X-coded bogus objects already eliminated. Several discoverer IDs are rather prominently present: Alone TDS/TDT (Tycho Double Stars) objects represent with a number of 12,661 about one third of the total number of neglected double stars, next comes RST (Rossiter) with 4,452 objects, then B (van den Bos) with 2,071 objects, A (Aitken) with 1,087 objects, I (Innes) with 1,063 objects, OCC (for doubles found by different discoverers during occultation observations) with 1,003 objects, BRT (Barton) with 918 objects, DON (Donner) with 872 objects, COU (Couteau) with 754 objects and so on.

In the next step all objects with separation or position angle "-1" for unknown were deleted due to missing data necessary for cross-matching as well as all objects with separation smaller than 0.4 arcseconds as this is the declared resolution limit for GAIA DR2 (Arenou et al. 2018) but also all objects with separation "999.9" indicating an unspecific separation larger than 1000 arcseconds. This reduced the number of neglected double stars suited for cross-matching with GAIA DR2 to 31,383 – a number still far too large for serious manual counter-checking. Besides I had already a look at TDS/TDT objects in a separate report (Knapp 2019) rendering any attempt in this direction redundant so I decided to concentrate on the 3,149 "very neglected" double stars with last observation year smaller than 1958. Interestingly 85% of these objects are with Dec values below zero located in the southern hemisphere suggesting a general neglect of double stars in the southern skies.

2. Recovery of selected objects in GAIA DR2

The next steps were straight forward:

- Cross-matching the list of 3,149 objects with GAIA DR2 for primary and secondary with 5" search radius using the CDS X-Match tool
- Eliminating all self-matches for objects with a separation less than 5 arcseconds
- Eliminating all matches with a delta in separation larger than 100% of the WDS separation and delta in position position angle larger than 40 degrees. These are rather generous thresholds for cross-matches but considering the huge time delta to the last recorded WDS observation still several correct matches might have been eliminated by this step
- Eliminating all pairs with magnitude delta differences (comparing GAIA DR2 Gmag deltas with WDS mag deltas) larger than 2.5 as well as all pairs with difference between WDS magnitude and GAIA DR2 Gmag for primary or secondary larger than 2.5mag. Considering the often questionable reliability of WDS magnitudes and the fact that in some cases the delta between Vmag and Gmag might be larger than 2.5 this might

Recovery of "Very" Neglected WDS Objects in Gaia DR2

again mean eliminating a few correct matches.

Next came the manual counter-check of all matched objects with delta separation >20% and delta position angle >20 degrees using AstroPlanner and Aladin with the consequence of deleting several obvious mismatches especially for components of multiples mostly based on magnitude issues. A surprisingly large part of these matches was found to be correct despite such large deltas in separation or position angle probably due to changes caused by proper motion but maybe also caused by poor quality of earlier measurements often over 100 years old.

Side results of the manual counter-checks:

- RST3185: J2000 measurement for RST3185AB seems to be in error - probably AC measurement
- RST2406: AB might be bogus
- ES 694 AB: TDT3959 Aa;Ab probably bogus
- ES 2350 BC: Probably bogus, B has same WDS position as A
- SEI 975: Probably bogus as there is no 11.7 secondary at the given location
- RST1515: TDS7211 Aa;Ab not resolved - bogus?
- RST1578 AC: Very different proper motion
- KUI 85: Curious object - no such bright stars at this position. Jump in separation from 0.2 to 3.1" from first to last observation despite rather slow proper motion seems curious
- I 1152/RMC 136/DAW 189/HJ 3796/: Of in total about 70 objects (members of the 30 Dor cluster in Large Magellanic Cloud) only 2 could be recovered due to the overly dense star field. Why such objects should be listed as double stars remains unclear as neither Plx nor PM suggest any physical relationship.

3. Results of Cross-Matching

After eliminating all obviously suspect matches 1,473 objects remain

- 364 objects of these come without proper motion and parallax data making assessment for common proper motion and potential gravitational relationship impossible
- 194 objects qualify as common proper motion pairs
- 80 objects qualify for potential gravitational relationship
- Only 26 objects qualify for both
- Several matched GAIA DR2 objects have "duplicated_source" issues or a number of "visibility_periods_used" of less than 9 – this might indicate data precision issues but in the given task using such data seems the better choice than just keep the WDS neglected pair status.

Table 1 lists a subset of the data for the first 20 of the recovered 1,473 WDS objects not observed longer than 60 years. The full table is abailable for download from the JDSO website as fixed format flat text file "WDS very neglected XX DR2".

4. Summary

With 47% a surprisingly large part of the more than 60 years not observed WDS objects could be recovered in GAIA DR2. In many cases this required a manual counter-check to overcome differences in separation and position angle due to the long time delta between observations larger than usually accepted for software based cross-matching.

The reasons for 53% negative cross-matching results are according to a random sample:

- No DR2 object for the secondary mostly in cases with a separation of less than 1 arcsecond like for example
  - DON1056
  - RST1183
  - RST2229
- although in some cases this might simply suggest a bogus like for example for B 631
- Deltas in parameters too large for a positive match at least with the in this report applied cut values as for example LDS2080 or RST1179 with a clear positive recovery with a pure manual procedure
- Missing objects in DR2 for the primary as for example for RST3341 (interestingly despite an existing object in DR1) or POU5868
- Obviously bogus or lost due to wrong J2000 positions as for example
  - WG 1
  - DOO 1
  - BRT1578
  - BRT 528
  - LDS2064
  - ES 1355
  - ARA 314
  - FEN 44
  - BRT 526
  - J 299
- Not obviously bogus but at least very doubtful like for example
  - BRT 527
  - FEN 43

(Text continues on page 330)

Recovery of "Very" Neglected WDS Objects in Gaia DR2

Table 1: Subset of the data for the first 20 of the recovered 1,473 WDS objects not observed longer than 60 years

WDS	Disc	Comp	PA	Sep	Gmag1	Gmag2	Plx1	Plx2	pmRA1	pmDE1	pmRA2	pmDE2	CPMR	CPMS	PlxR	PlxS
00010-4920	RST1178		294.511	2.01869	9.598	12.577	1.9870	1.8757	6.531	-5.899	6.914	-5.779	CCAB	8	DA	1
00025-5654	B 1022		127.414	2.96263	9.798	12.273	2.9743	2.8526	21.247	28.690	21.448	28.527	AAAA	100	DA	1
00068-4055	RST1179		106.157	1.32607	8.764	12.132	1.8570	0.1978	13.892	6.715	14.427	-1.910	DDBA	0	DD	1
00089-1107	RST3342		301.826	1.55661	9.465	13.094	4.0414	4.1751	33.405	6.798	32.745	5.135	BCAA	32	CA	20
00091+4051	BU 483	AB	34.045	2.06759	6.689	11.107	16.7115	16.5777	126.532	-171.143	119.707	-178.928	CBAA	16	BA	80
00108-3452	RST2236		98.298	1.97939	6.635	11.288	5.6522		85.667	-0.872						
00136-4340	DON 1		248.701	2.08249	10.175	13.199	5.3159	5.3392	-12.837	5.230	-11.399	2.939	DDAB	0	BA	80
00170-2803	RST1184		60.851	3.52453	9.380	13.389	5.4261	5.3560	-8.419	-47.453	-9.558	-46.697	BBAA	64	CA	20
00185-4606	RST 3		131.147	2.22547	11.396	12.705	5.7267	5.4746	18.232	14.927	17.518	13.799	BDAA	4	DA	1
00262+3815	A 1503		304.855	2.02759	9.413	11.923	2.7519	2.6771	-5.423	-6.493	-5.456	-6.668	ABAB	78	CA	20
00281-2512	B 5	AB	222.478	1.29337	9.281	11.982	9.9580		-42.269	-75.819						
00289-3931	RST1188		18.354	1.87420	10.407	13.008	3.5322	3.4424	10.690	2.932	10.756	2.923	AAAB	97	CA	20
00310-0850	RST4149		154.936	2.05516	9.386	13.080	5.8203	5.8466	57.852	36.186	63.046	37.264	BDAA	4	BA	80
00316-3721	JSP 6		206.381	1.63575	11.465	12.630	2.9213	3.0335	35.978	12.942	36.575	13.556	ABAA	80	DA	1
00341-3217	RST2247		340.923	1.06089	6.973	10.628	2.4756		15.212	3.291						
00397-2205	DON 9		172.725	1.63034	11.163	12.894	2.6687	2.7129	55.053	1.033	54.589	-0.121	BAAA	80	CA	20
00420-2457	RST2250	BC	313.024	0.77609	11.088	12.288	5.1102		11.703	-7.839						
00456-2055	HU 1204		267.370	1.45443	9.582	11.996	1.8576	-1.0790	20.517	-1.269	17.436	-24.176	DDBA	0	DD	1
00525-3138	JSP 14		216.171	3.24964	9.478	12.797	3.0822	3.1024	22.484	-4.651	20.859	-3.688	BDAB	4	CA	20
00529-5123	RST 22		17.959	1.51524	10.714	12.164	3.9347	3.9290	36.812	-16.526	36.620	-16.871	AAAA	100	BA	80

Description of the table content (all values per epoch 2015.5, values in parentheses only in download file):

WDS = WDS ID
Disc = Discoverer code
Comp = Components
PA = Position angle calculated from the GAIA DR2 coordinates
(e_PA = Error position angle)
Sep = Separation in arcseconds calculated from the GAIA DR2 coordinates
(e_Sep = Error separation)
Gmag1 = GAIA DR2 Gmag primary
(e_Gmag1 = Error Gmag1)
Gmag2 = GAIA DR2 Gmag secondary
(e_Gmag2 = Error Gmag2)
Plx1 = Parallax primary in mas
(e_Plx1 = Error Plx1)
Plx2 = Parallax secondary in mas
(e_Plx2 = Error Plx2)
pmRA1 = Proper motion RA primary in mas/yr
(e_pmRA1 = Error pmRA1)
pmDE1 = Proper motion DE primary in mas/yr
(e_pmDE1 = Error pmDE1)
pmRA2 = Proper motion RA secondary in mas/yr
(e_pmRA2 = Error pmRA2)
pmDE2 = Proper motion DE secondary in mas/yr
(e_pmDE2 = Error pmDE2)
CPMR = Common proper motion rating letter based
CPMS = Common proper motion estimated probability
(BCD_1_2 = Best case distance between primary and secondary in AU)
(RCD_1_2 = Realistic case distance between primary and secondary in AU)
(WCD_1_2= Worst case distance between primary and secondary in AU)
PlxR = Rating for potential gravitational relationship
PlxS = Estimated probability for gravitational relationship

Recovery of "Very" Neglected WDS Objects in Gaia DR2

(Continued from page 328)

Overall it seems that most not recovered objects are either bogus (or simply lost due to wrong J2000 positions) or not resolved in DR2 because of separations below 1 arcsecond.

5. References

F. Arenou, X. Luri, C. Babusiaux, C. Fabricius, A. Helmi, T. Muraveva, A. C. Robin, F. Spoto, A. Vallenari, T. Antoja, T. Cantat-Gaudin, C. Jordi, N. Leclerc, C. Reylé, M. Romero-Gómez, I-C. Shih, S. Soria, C. Barache, D. Bossini, A. Bragaglia, M. A. Breddels, M. Fabrizio, S. Lambert, P.M. Marrese, D. Massari, A. Moitinho, N. Robichon, L. Ruiz-Dern, R. Sordo, J. Veljanoski, P. Di Matteo, L. Eyer, G. Jasniewicz, E. Pancino, C. Soubiran, A. Spagna, P. Tanga, C. Turon, C. Zurbach, 2018, "Gaia Data Release 2: Catalogue validation', *Astronomy & Astrophysics*, **616**, A17.

Knapp, Wilfried R. A. and Nanson, John, 2017, A New Concept for Counter-Checking of Assumed CPM Pairs", *JDSO*, **13**(1), 31.

Knapp, Wilfried R. A., 2018, "A New Concept for Counter-Checking of Assumed Binaries", *JDSO*, **14**(3), 487.

Knapp, Wilfried R. A., 2019, "Cross-Match of WDS TDS/TDT Objects with Gaia DR2", *JDSO*, **15**(1), 168.

6. Acknowledgements

The following tools and resources have been used for this research:

- 2MASS images
- DSS2 images
- PS1 images
- PS1 catalog
- Aladin Sky Atlas v10.0
- GAIA DR2 and DR1 catalogs
- TAP-VizieR
- CDS X-Match
- VizieR
- Washington Double Star Catalog

Appendix A

Description of the CPM rating procedure (according Knapp and Nanson 2017 and Knapp 2018):

- Four rating factors are used: Proper motion vector direction, proper motion vector length, size of position error in relation to proper motion vector length and relation separation to proper motion speed
- Proper motion vector direction ratings: “A” for within the error range of identical direction, “B” for similar direction within the double error range, “C” for direction within the triple error range and "D" for outside
- Proper motion vector length ratings: “A” for identical length within the error range, “B” for similar length within the double error range, "C" for length within the triple error range and "D" for outside
- Error size ratings: “A” for error size of less than 5% of the proper motion vector length, “B” for less than 10%, “C” for less than 15% and "D" for a larger error size
- Relation separation to proper motion speed: "A" for less than 100 years, "B" for less than 1000 years, "C" or less than 10000 years and "D" for above

To compensate for the extremely small proper motion GAIA DR2 errors resulting in a worse than “A” rating despite only very small deviations an absolute lower limit is applied regardless of calculated error size:

- Proper motion vector direction: Max. 1° difference for an “A”
- Proper motion vector length: Max. 1% difference for an “A"

The letter based scoring is then transformed into an estimated probability and a verbal assessment for being CPM

Description of the Plx rating procedure (according to Knapp 2018):

- Two rating factors are used: Distance between the components in AU and relationship Plx error to Plx value. The distance between the components is calculated from the inverted GAIA DR2 parallax data (if positive and Plx>3*e_Plx) and the angular separation using the law of cosine. Realistic case is based on the given Plx values and the best and worst case scenario uses the given e_Plx data on the Plx values to estimate a smallest and largest possible distance
- "A" for worst case distance, "B" for realistic case distance and "C" for best case distance less than 200,000 AU (means touching Oort clouds for two stars with Sun-like mass) and “D” for above
- "A" for Plx error less than 5% of Plx, "B" for less than 10%, "C" for less than 15% and “D” for above

The letter based scoring is then transformed into an estimated likelihood for being potentially gravitationally bound.

A Plx Score of

- less than 10 means a likelihood of or near zero
- less than 50 means a likelihood lower than 50%
- larger than 50 means a likelihood larger than 50%
- equal 100 means a likelihood of 100%

for a distance between the components smaller than 200,000 AU.

These likelihoods are based on the assumption that RA and DEC coordinates as well as parallaxes are normal distributed measurements with the given error range as standard deviation.

Astrometric Measurements of Star System WDS 06571+5438

Alex Hewett[1], Mikila Tuchscher[1], Marie Yokers[1], Alexander Beltzer-Sweeney[1], Irena Stojimirovic[1], Pat Boyce[2], and Grady Boyce[2]

1 San Diego Mesa College, San Diego, California
2 Boyce Research Initiatives and Education Foundation (BRIEF), California

Abstract: We report CCD astrometric measurements of the double star system WDS 06571+5438 (HJ 2350) obtained using Las Cumbres Observatory (LCO) sites and AstroImageJ (AIJ) software. We found a mean position angle of 195.76° ± 0.4° and a mean separation distance of 6.24" ± 0.04". Calculations found for distance between the stars using Gaia Parallax data suggest that the system is an optical double.

Introduction

The goal of this study was to select a double star system to research and observe using CCD imaging in order to determine whether the system is binary or not. A comparison of data listed by the Washington Double Star Catalog (WDS), the Stelle Doppie Double Star Database (Stelle Doppie), and Dave Rowe's WDSGaiaDR2 V2 (Harshaw 2018) excel spreadsheet lead to the selection of this star system. Candidate systems for our research were chosen based on the following specifications: being positioned between 00-08H of Right Ascension (RA) and a Declination (DEC) between +35 and +50 degrees to optimize imaging potential. Other qualifications required that the primary star (*a*) had a magnitude between 7 and 12 and a secondary star (*b*) a magnitude between 7 and 13; and a delta magnitude no larger than 3. Selecting systems with these magnitudes, as well as ones with a angular separation (ρ) of at least 5" to ensure both stars within the system were easily distinguishable.

The observed star system WDS 06571+5438 HJ 2350 (hereinafter HJ 2350) fit these qualifications. HJ 2350, discovered by John Herschel in 1831, is located in Lynx (Stelle 2018). The spectral class of *a* is F8 (Stelle 2018) and *b* is determined to be F9 using the GAIA Archival Data (GAIA 2018), which is graphed on the HR Diagram in Figure 1. The difference in magnitude (Δmag) between the stars is 2.03, with *a* having a magnitude of 9.47 and B with a magnitude of 11.50. There have been 13 observations since 1831; the most recent being in 2016. When first observed, its position angle (θ) was documented as 225° with a rho (ρ) of 10" (arcseconds) and the last observation, 2016, found it to have a θ of 197° with a ρ of 6.3" (WDS 2018).

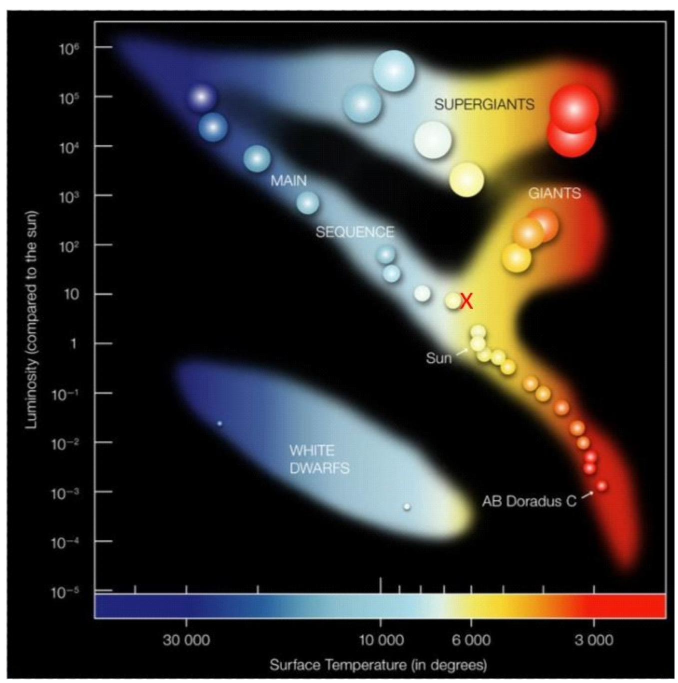

Figure 1. HR Diagram with graphed b star with effective temperature of 6185.5K and a solar luminosity of 9.591 L⊙

Astrometric Measurements of Star System WDS 06571+5438

Equipment and Procedures

The system has an RA of 06h 15m 06.99s and DEC of +44° 09' 35.7" (Stelle 2018). Based on the DEC of the system, it was deemed most appropriate to utilize one of the northern hemisphere Las Cumbres Observatory (LCO) sites, which range in DEC approximately +20 to +30. Each site utilizes an LCO developed 0.4m telescope, Figure 2, equipped with an SBIG STX6303 CCD camera. The camera has a resolution of 0.57" arcseconds making it sufficient for resolving the approximate separation of 6.3". A total of 58 images were ordered: fifteen of these images utilized the Pan-STARRS W filter which comprises a wavelength center of 6250Å and wavelength width of 4416Å with an exposure time of 1 second. The remaining 43 images utilized the SDSS R' filter which comprises a wavelength center of 6215Å and a wavelength width of 1390Å with exposure times of 0.5 seconds, 1 second, and 1.5 seconds. The Our Solar Siblings (OSS) pipeline processed all images and exported them as FITS files (Fitzgerald 2018).

The program AstroImageJ (AIJ) was utilized to take measurements of the θ, ρ, and Δmag of the star system by first approximating the centroids of both components and fine-tuning based on the aperture selection (Collins 2018). These results for each image were exported as an excel spreadsheet that included the mean, standard deviation, and standard error calculations for comparison with the historical data received from WDS (Mason 2018).

Figure 2. 0.4 m diameter telescopes equipped with SBIG STX6303 camera and mounted at the Cassegrain Focus. These telescopes use CCD imaging with a total field of view of 19 x 29 arcminutes (LCO 2018)

Data & Measurements

Listed below are the historical data points as reported by the WDS (Table 1) in comparison with the data acquired in this observation (Table 2).

Table 1. Listed above are the historical observations provided by WDS

Observation Date (year)	Position Angle (θ)	Separation Distance (ρ)
1831.11	224.5°	10.0"
1903.08	213.9°	10.364"
1909.076	213.9°	9.92"
1913.10	217.5°	9.992"
1915.60	220.9°	10.0"
1918.11	224.0°	9.752 "
1988.17	206.0°	7.05"
1999.01	200.5°	6.88"
2003.21	200.1°	6.716"
2003.77	200.1°	6.677"
2011.62	198.01°	6.35"
2011.823	197.77°	6.42"
2015	196.817°	6.363"
2016.1	196.57°	6.32"

Table 2. Listed above are the averages of the Mean, Standard Deviation, and the Standard Error of the Mean from all 58 images taken through LCO.

Astrometric Results for HJ 2350		
SBIG 6303 0.4-meter		
(58) Images		
Filters: (43) R, (15) w		
Epoch 2018.832	**θ (°)**	**ρ (")**
Mean	195.76	6.24
Standard Deviation	0.4	0.04
Standard Error of Mean	0.05	0.005

Astrometric Measurements of Star System WDS 06571+5438

Table 3. Shows a breakdown of filter-types, and exposure times with the p and theta averages

Astrometric Results by Filter for HJ 2350		
SBIG 6303 0.4-meter (58) Images		
Epoch 2018.832	θ (°)	ρ (")
(15) rp , 0.5s	195.87	6.25
(14) rp, 1.0s	195.71	6.23
(14) rp, 1.5s	195.73	6.25
(15) w, 1.0s	195.71	6.24

Discussion

As Figure 3 indicates, the separation angle measured in this observation falls within the trend in the historical data displayed in Table 1, with a calculated standard deviation of 0.04", as seen in Table 2. The distance between *a* and *b* was determined by using the stellar parallax, from GAIA (2018), with the formula:

$$d = \frac{1}{p} \times 10^3$$

This calculation is with distance in parsecs (pc) and parallax in milliarcseconds (mas), thus requiring the scalar to convert to arcseconds (Williams College). The parallax for *a* was 2.662 ± 0.030 mas and *b* was 3.880 ± 0.032 mas (ESA, 2018). The result is a mean distance of 257.7 ± 8.299 pc to star *a* and 375.7 ± 11.27 pc to star *b*, implying a minimum distance of 117.9 pc between *a* and *b*.

Conclusion

We obtained measurements for the position angle and separation of the system HJ 2350, which were in line with the trend observed from the WDS historical data. However, from calculating distance between the stars from GAIA parallax data indicates that there would be a minimum of 117.87 pc between the stars. Therefore, we would we suggest a classification be appended from uncertain double to visual double.

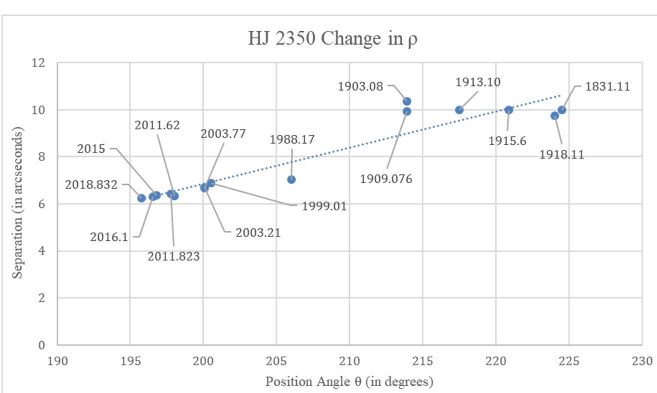

Figure 3. The change in ρ over time with the inclusion of the observations made in this study.

Acknowledgments

We would like to thank Pat and Grady Boyce for their guidance, support, and expertise throughout this process. We would also like to thank Alex Beltzer-Sweeney and Irena Stojimirovic for their mentorship and guidance. This work has made use of data from the European Space Agency (ESA) mission Gaia (https://www.cosmos.esa.int/gaia), processed by the Gaia Data Processing and Analysis Consortium (DPAC, https://www.cosmos.esa.int/web/gaia/dpac/consortium). Funding for the DPAC has been provided by national institutions, in particular the institutions participating in the Gaia Multilateral Agreement.

References

Collins, K. A., Kielkopf, J. F., Stassun, K. G., and Hessman, F. V., 2018, "AstroImageJ: image processing and photometric extraction for ultra-precise astronomical light curves", *The Astronomical Journal*, **153**(2), 77.

Fitzgerald, M., 2018, "The Our Solar Siblings Pipeline: Tackling the data issues of the scaling problem for robotic telescope based astronomy education projects, *Robotic Telescopes, Student Research, and Education Proceedings*, Fitzgerald, M. T., James, C. R., Buxner, S., and White, S., editors, pp 347–358.

Harshaw, Richard W., 2018, "Gaia DR2 and the Washington Double Star Catalog: A Tale of Two Databases ", *Journal of Double Star Observations*, **14**, 734-740.

J. R. North, J. Davis, J. G. Robertson, T. R. Bedding, H. Bruntt, M. J. Ireland, A. P. Jacob, S. Lacour, J. W. O'Byrne, S. M. Owens, D. Stello, W. J. Tango, P. G. Tuthill; *Monthly Notices of the Royal Astronomical Society*, Volume 393, Issue 1, 11 February 2009, Pages 245–252, https://doi.org/10.1111/j.1365-2966.2008.14216.x

Las Cumbres Observatory Filters. (2018, October 15). Retrieved from Las Cumbres Observatory: https://lco.global/observatory/filters/

Mason, B., "The Washington Double Star Catalog", 2018, Astrometry Department, U.S. Naval Observatory. http://ad.usno.navy.mil/wds/Webtextfiles/wdsnewframe2.html

Astrometric Measurements of Star System WDS 06571+5438

Stelle Doppie. 06571+5438 HJ2350., 2018, https://www.stelledoppie.it/index2.php?menu=29&iddoppia=29419

Williams College (n.d.). *Distances in Astronomy.* Williams College. Retrieved from https://web.williams.edu/Astronomy/Course-Pages/330/images/distances.pdf

Double Star Measurements at the Southern Sky with a 50 cm Reflector in 2017

Rainer Anton

Altenholz/Kiel, Germany
e-mail: rainer.anton"at"ki.comcity.de

Abstract: A 50 cm Ritchey-Chrétien reflector was used in October 2017 for recordings of double stars with a CCD webcam, which were analyzed with "lucky imaging". Data from the Gaia catalogs DR1 and DR2 were used for calibration of the image scale. Also, parallax and proper motion data were checked for estimating the probability of physical relation for some systems with doubtful status. About one third of the 92 pairs investigated here are not resolved or not listed in Gaia, either because of too close separations and/or too bright components. For several binaries, deviations from currently assumed orbits were found. Some images of noteworthy systems are also presented.

Introduction

"Lucky imaging" is an alternative method to speckle interferometry for beating the seeing, and is especially suitable for small to medium sized telescopes. By using short exposure times, and selection of only the best images for stacking, one can obtain virtually diffraction limited images. More details of this technique are described, for example, in reference [1]. The accuracy of position measurements depends on mainly three factors: the seeing, the size and resolution of the telescope, and the calibration factor of the image scale. This applies equally well for speckle and lucky imaging, only the method of image analyzing differs. In fact, given the telescope, the precision of position measurements should be the same. As in earlier work, a rather accurate calibration was obtained with data from the Gaia satellite mission, which delivered highly accurate star positions [2].

Instrumental

The 50 cm Ritchey-Chrétien telescope is located at the "*Internationale Amateursternwarte*" on a guest farm in Namibia [3], which I have already used in 2014 and 2016 for double star work [4]. The primary focal length of 4.1 m was extended by a 2x Barlow lens, resulting in an f-ratio of about f/16. Series of 1000 to 2000 images were taken with a b/w-CMOS camera of type "QHY 5 III 178" with exposure times ranging from less than a millisecond to several tenths of a second, depending on the star brightness, on the filter being used, and on the seeing. Recordings were made with a red or near infrared filter, which reduce effects from atmospheric dispersion, seeing, as well as from chromatic aberrations of the Barlow lens. Only the best frames, typically several tens and up to more than 100, were selected, registered, and stacked. The pixel size of 2.4 µm square results in a nominal resolution of 0.061 arc sec/pixel. A more accurate value was obtained with reference systems, as was already indicated above, and as will be explained in more detail below. In any case, the accuracy of position measurements is typically better by more than one order of magnitude. Images were re-sampled before stacking, as registering can be done with sub-pixel accuracy, which results in smoothening of the intensity profiles, and better definition of the peak centroids. Position angles were obtained by recording star trails with the telescope drive switched off, from which the east-west direction was determined. Statistical analysis resulted in an s.d. of about ± 0.1 degrees.

Calibration

The image scale was adjusted by using data from the Gaia DR1 and DR2 catalogs, which were released in 2016 and 2018, respectively. For 59 pairs out of the total of 92 investigated here, values for right ascension and declination of the components were found, with error margins typically smaller than 0.001 arc sec, from which separations and position angles were calculated. These are marked in table 1 below with shaded lines. Star positions in DR1 and DR2 refer to the epoch 2015.0 and 2015.5, respectively, and were extrapolated

Double Star Measurements at the Southern Sky with a 50 cm Reflector in 2017

to the epoch of my own recordings. However, in several cases, this turned out as ambiguous, mostly due to large scatter of other literature data. Also, in cases, where one or both components are close doubles, which are not resolved by Gaia, their positions are deemed as less accurate (see below). In total, 47 pairs were found suitable for reference. These are indicated with darker shading. The image scale was adjusted by statistical evaluation of the residuals of the reference systems, such that the mean value and the standard deviation (s.d.) were minimized. As a result, the range of residuals extended from -0.008 to +0.009 arc sec (this can be seen in Figure 1), the mean was less than 0.0001 arc sec, the s.d. was ± 0.005 arc sec, and the scale factor became 0.06488 arc sec/pixel with an estimated error of less than ± 0.1 per cent.

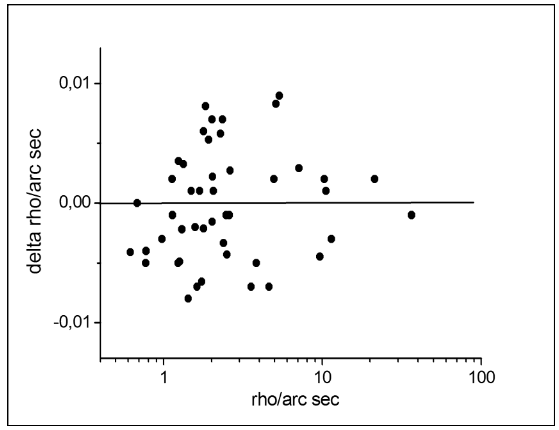

Figure 1. Plot of the residuals delta rho vs. rho of the reference systems used for calibration of the image scale. The mean value for the 47 pairs is less than 0.001 arc sec, and the standard deviation amounts to ± 0.005 arc sec.

Results

All measurements are listed in Table 1. Names, nominal positions, and magnitudes are adopted from the WDS [5]. Residuals refer to extrapolated literature data, mainly from the so-called “speckle catalog” [6], as well as from Gaia, and for binaries, to ephemeris data from the Sixth Catalog of Orbits of Visual Binary Stars [7]. In several cases, no reasonable residuals could be given, because of too few literature data and/or too large a scatter. The table is followed by individual notes, which are numbered with RA values. There are several pairs with unclear physical status, either truly binary or merely optical. These were checked with parallax and proper motion data from Gaia, and are commented in the notes.

(Text continues on page 343)

Table 1: List of measurements. Position angles (PA) are in degrees, separations (rho) in arc seconds. N is the number of recordings. Shaded lines indicate pairs, for which data have been found in Gaia DR1 and/or DR2. Darker shadings mark pairs used for calibration of the image scale. Residuals (delta PA, delta rho) are given, when reasonable. Asterisks in column “Pair” refer to figures shown below.

Pair	RA & Dec	Mags	PA	rho	Date	N	delta PA	delta rho
BU 391 AB	00 09.4 -27 59	6.13 6.24	258.2	1.328	2017.791	1	~0	0.003
* LCL 119 AC	00 31.5 -62 57	4.28 4.51	167.8	27.15	2017.797	2	-0.4	0.150
* I 260 CD	„	4.60 6.54	347.0	0.350	„	2	-2.5	0.035
HDO 182	00 42.7 -38 28	6.60 7.01	23.7	0.665	2017.792	1	1.3	-0.017
HJ 3416 AB	01 03.3 -60 06	7.58 7.67	129.1	5.115	2017.797	1	0.1	0.008
* SLR 1 AB	01 06.1 -46 43	4.10 4.19	79.3	0.573	2017.795	3	-0.8	-0.046
HJ 3423 AB	01 15.8 -68 53	5.00 7.74	315.1	4.601	2017.792	2	-0.4	-0.007
STF 113 AB	01 19.8 -00 31	6.45 6.99	21.3	1.613	2017.792	2	~0	-0.007
HJ 2036	01 20.0 -15 49	7.40 7.61	337.4	2.373	2017.792	1	0.5	-0.003
* I 264 AB	01 31.6 -53 22	8.36 8.84	25.8	0.793	2017.789	1	-1.5	-0.101
STF 138 AB	01 36.0 +07 39	5.97 7.35	60.0	1.727	2017.795	1	0.3	-0.007
DUN 4	01 38.8 -53 26	7.15 8.49	104.5	10.300	2017.800	1	0.1	0.002
DUN 5	01 39.8 -56 12	5.78 5.90	186.3	11.410	2017.800	2	~0	-0.003
HJ 3461 AB	01 45.6 -25 03	5.38 8.50	17.9	4.957	2017.789	1	~0	0,002
HJ 3475	01 55.3 -60 19	7.18 7.23	78.3	2.481	2017.800	2	-0.5	-0.001
* STF 186	01 55.9 +01 51	6.79 6.84	71.5	0.655	2017.792	1	-1.1	-0.034

Table 1 continues on the next page.

Double Star Measurements at the Southern Sky with a 50 cm Reflector in 2017

Table 1 (continued). List of measurements. Position angles (PA) are in degrees, separations (rho) in arc seconds. N is the number of recordings. Shaded lines indicate pairs, for which data have been found in Gaia DR1 and/or DR2. Darker shadings mark pairs used for calibration of the image scale. Residuals (delta PA, delta rho) are given, when reasonable. Asterisks in column "Pair" refer to figures shown below.

Pair	RA & Dec	Mags	PA	rho	Date	N	delta PA	delta rho
STF 202 AB	02 02.0 +02 46	4.10 5.17	262.1	1.842	2017.795	1	-0.1	0.008
HTG 1	02 15.8 -18 14	8.49 9.25	166.0	2.022	2017.794	1	-0.3	0.007
BU 738	02 23.2 -29 52	7.60 7.97	211.6	2.017	2017.792	1	-0.2	-0.002
DAW 1 AB	02 27.9 -58 08	8.04 8.45	208.2	1.246	2017.800	2	0.2	0.008
HJ 3503 AC	„	8.04 9.61	298.7	17.570	2017.800	2	~0	-0.15
DUN 7 A,BC	02 39.7 -59 34	7.67 7.69	97.0	36.519	2017.800	1	0.1	-0.001
I 386 BC	„	8.02 8.94	18.2	0.445	2017.800	1	?	?
BU 741 AB	02 57.2 -24 58	8.06 8.20	351.9	0.459	2017.789	1	0.3	0.045
S 423 AC	„	8.06 7.86	225.7	29.226	„	1	?	?
HJ 3555	03 12.1 -28 59	3.98 7.19	301.1	5.369	2017.792	1	0.5	0.009
* JC 8 AB	03 12.4 -44 25	6.42 7.36	143.1	0.414	2017.792	1	-2.5	0
* HJ 3556 AC	„	6.42 8.76	187.8	3.667	„	1	?	?
AC 2 AB	03 18.4 -00 56	5.60 7.97	261.7	1.173	2017.792	1	2.0	-0.012
BU 1004 AB	04 02.1 -34 29	7.26 7.94	50.8	1.127	2017.792	2	0.1	-0.008
* I 152 A,BC	04 04.9 -35 27	8.37 8.65	75.2	0.983	2017.790	1	?	?
* CHR 224 BC	„	8.65 10.3	~110	~0.23	„	1	?	?
I 153	04 08.3 -32 51	8.14 8.16	348.0	1.206	2017.789	1	?	?
* BU 311	04 26.9 -24 05	6.67 7.09	161.1	0.428	2017.792	1	2.1	~0
BU 184	04 27.9 -21 30	7.40 7.70	247.7	1.924	2017.792	1	-0.1	0.005
HJ 3683 AB	04 40.3 -58 57	7.33 7.45	89.9	3.831	2017.792	1	0.3	-0.005
STF 590	04 43.6 -08 48	6.74 6.78	317.9	9.343	2017.792	2	~0	?
BU 314 AB	04 59.0 -16 23	5.92 7.50	318.6	0.792	2017.827	2	0.4	-0.004
* STT 98	05 07.9 +08 30	5.76 6.67	287.1	0.955	2017.793	1	0.6	-0.007
* STT 517 AB	05 13.5 +01 58	6.79 6.99	240.8	0.699	2017.793	2	-0.1	-0.002
STF 668 A-BC	05 14.5 -08 12	0.3 6.8	201.7	~9.67	2017.827	1	?	?
BU 320 AB	05 28.2 -20 46	2.90 7.50	10.1	2.696	2017.798	1	0.3	0.006
STF 728	05 30.8 +05 57	4.44 5.75	44.0	1.302	2017.792	2	0.1	-0.002
STF 774 AB	05 40.7 -01 57	1.88 3.70	166.6	2.432	2017.792	1	?	?
STF 795	05 48.0 +06 27	5.29 6.03	220.0	0.988	2017.792	1	0.0	0.005
DUN 23	06 04.8 -48 28	7.30 7.69	128.8	2.589	2017.798	1	0.3	-0.001
STF 919 AB	06 28.8 -07 02	4.62 5.00	132.8	7.109	2017.787	1	0.1	0.003
AC	„	4.62 5.39	125.6	9.918	„	1	0.1	0.013
BC	„	5.00 5.32	108.3	2.996	„	1	0.2	0.003
R 65 AB	06 29.8 -50 14	5.97 6.15	248.5	0.341	2017.798	2	-0.6	0.006
HDO 195 CD	„	7.98 8.73	196.5	0.415	„	2	-3.3	0.018
DUN 30 AC	„	5.97 7.98	312.1	11.744	„	1	?	?
I 7	07 17.5 -46 59	7.10 8.35	201.7	0.618	2017.800	1	0.9	0.009
STF 1104 AB	07 29.4 -15 00	6.39 7.60	38.6	1.783	2017.800	1	-0.9	-0.002
DUN 65 AB	08 09.5 -47 20	1.79 4.14	220.6	41.177	2017.789	1	?	?
HJ 4073	08 18.2 -37 22	7.18 7.83	177.2	2.032	2017.800	1	~0	0.002

Table 1 concludes on the next page.

Double Star Measurements at the Southern Sky with a 50 cm Reflector in 2017

Table 1 (conclusion). List of measurements. Position angles (PA) are in degrees, separations (rho) in arc seconds. N is the number of recordings. Shaded lines indicate pairs, for which data have been found in Gaia DR1 and/or DR2. Darker shadings mark pairs used for calibration of the image scale. Residuals (delta PA, delta rho) are given, when reasonable. Asterisks in column "Pair" refer to figures shown below.

Pair	RA & Dec	Mags	PA	rho	Date	N	delta PA	delta rho
* RST 4888 AB	08 25.0 -42 46	6.59 6.81	103.6	0.512	2017.800	1	0.8?	-0.16?
* BU 205 AB	08 33.1 -24 36	7.14 6.84	283.9	0.543	2017.800	1	2.8	-0.048
I 13 AB	10 09.5 -68 41	6.63 6.47	105.8	0.565	2017.789	2	2.2	-0.003
RHD 1 AB	14 39.6 -60 50	-0.01 1.33	325.1	4.388	2017.799	3	0.7	-0.002
BSO 13 AB	17 19.1 -46 38	5.61 8.88	258.2	10.591	2017.800	1	-0.1	0.001
STF 2262 AB	18 03.1 -08 11	5.27 5.86	289.1	1.503	2017.794	1	~0	0.001
HJ 5014	18 06.8 -43 25	5.65 5.68	0.9	1.796	2017.800	2	~0	0.006
BU 132 AB	18 11.2 -12 51	7.01 7.13	187.4	1.417	2017.892	1	0.2	-0.008
BU 133	18 27.7 -26 38	6.59 8.48	229.5	0.615	2017.802	1	-0.9	-0.004
ARN 52 AB	18 32.5 -18 58	7.14 9.63	261.5	69.965	2017.800	1	-0.2	0.036
AC		7.14 ~10	255.6	65.823	„	1	-0.1	0.076
BC		9.63 ~10	138.2	8.172	„	1	-0.1	-0.084
DUN 222	18 33.4 -38 44	5.58 6.16	358.4	21.347	2017.800	1	-0.1	0.002
STN 62	18 34.5 -34 49	7.57 7.77	132.0	2.282	2017.800	1	-0.4	0.006
HDO 150 AB	19 02.6 -29 53	3.27 3.48	245.6	0.545	2017.802	1	~0	~0
H 5 78 AB,C	„	2.60 10.68	301.6	72.28	„	1	?	?
I 253 AB	19 19.0 -33 17	8.77 7.25	141.5	0.498	2017.794	1	0.2	0.065
SCJ 22	19 28.2 -12 09	8.12 8.69	291.8	1.120	2017.794	1	-0.4	0.002
HDO 294	20 01.2 -38 35	8.08 9.11	33.9	1.254	2017.803	1	0.6	-0.005
STF 2613 AB	20 01.4 +10 45	7.48 8.02	354.9	3.548	2017.827	1	0.1	-0.007
STF 2644	20 12.6 +00 52	6.92 7.06	205.5	2.623	2017.827	1	-0.3	0.003
DUN 230	20 17.8 -40 11	7.42 7.72	117.6	9.641	2017.802	1	0.1	-0.004
R 321	20 26.9 -37 24	6.58 8.09	123.8	1.579	2017.802	1	-1.2	-0.002
SHJ 323 AB	20 28.9 -17 49	4.97 6.88	189.6	1.684	2017.797	2	~0	0.001
* HU 200 AB	20 39.3 -14 57	5.38 7.31	121.9	0.341	2017.794	1	-0.9	0.021
STF 2729	20 51.4 -05 38	6.40 7.43	30.8	0.765	2017.792	1	-0.3	-0.005
RMK 26	20 51.6 -62 26	6.23 6.58	79.8	2.444	2017.797	1	-0.4	0.003
STF 2744 AB	21 03.1 +01 32	6.76 7.33	109.3	1.242	2017.827	2	0.2	-0.005
* BU 766 AB	21 24.4 -41 00	6.24 6.88	177.1	~0.28	2017.794	1	3.1	?
STF 2862	22 07.1 +00 34	8.04 8.41	95.9	2.499	2017.827	1	0.1	-0.004
HJ 5319	22 12.0 -38 18	7.65 7.66	315.7	2.059	2017.795	1	0.3	0.001
STF 2909 AB	22 28.8 -00 01	4.34 4.49	161.1	2.340	2017.827	2	-0.3	0.007
* I 22 AB	22 55.3 -48 28	7.29 8.91	177.5	0.560	2017.788	2	1.4	-0.28
* I 22 AB-CD	„	7.14 6.71	180.8	93.88	„	1	-0.1	0.09
SEE 492 AB	23 35.7 -27 29	6.84 9.18	35.7	0.637	2017.789	1	2.5	-0.049
SLR 14 Phe	23 50.6 -51 42	8.28 8.59	56.0	0.973	2017.792	1	-0.2	-0.003

Double Star Measurements at the Southern Sky with a 50 cm Reflector in 2017

Notes: Term “relfix” is adopted from Burnham [8], distances are given in light years (ly).

00 09.4: BU 391, kappa Sculptoris, PA and rho decreasing. According to Gaia DR2, proper motions of the components and their directions are rather similar, while the nominal parallax values result in a separation of about 10 ly. Thus, although the error margins overlap, a binary status does not appear very likely. See table 3.

00 31.5: LCL 119 AC, beta Tucanae, few data, optical, component B (~13.5 mag) was not detected. I 260 CD close binary, P = 44.7 y. Difficult, as dim component D interferes with diffraction ring of C. CD not resolved by Gaia. Separation of AC may be influenced by (CD). Parallax values for A and (CD) given by Gaia significantly differ, which excludes that this system is physical. See fig. 3.

00 42.7: HDO 182, lambda Sculptoris, close pair, PA increasing, rho decreasing.

01 03.3: HJ 3416 AB, in Tucana, few data with large scatter. Nominal parallax values of the components from Gaia are very similar, and the error margins overlap. Also, virtually identical values of the proper motions, their directions, as well as their radial velocities, respectively, let this pair appear as binary. See table 3.

01 06.1: SLR 1 AB, beta Phoenicis, binary, P = 168 y. Residuals refer to ephemeris. See fig. 2 c.

01 15.8: HJ 3423 AB, kappa Tucanae, binary, P = 857 y, significant deviation from currently assumed ephemeris (Sca2005), in accordance with trend of literature data, including Gaia. See fig. 6.

01 19.8: STF 113, 42 Ceti, PA increasing, recent rho data exhibit some scatter. Parallax values of the components from Gaia give a separation of more than 19 ly, far too large for a binary.

01 20.0: HJ 2036, in Cetus. PA decreasing, rho increasing. An orbit has been calculated (Ole2003) with P = 1443 y, although only a rather small portion is documented with measurements. However, parallax data from Gaia result in a separation of the components of 9.7 (±2.6) ly, which would exclude that this pair is a binary at all.

01 31.6: I 264 AB, in Eridanus, binary, P = 250 y, rho data markedly deviate from ephemeris (USN2002), in accordance with recent literature data. See fig.2 d.

01 36.0: STF 138 AB, in Pisces, PA & rho increasing. Gaia: The ranges of parallax values of the components overlap, and their proper motions are rather similar, which suggests that this pair is physical. See table 3.

01 38.8: DUN 4, in Eridanus, few data. Gaia data for proper motions of A and B are about similar, but the large difference of the distances (~ 6 ly), and not overlapping error margins, indicate that this pair is not physical.

01 39.8: DUN 5, p Eridani, binary, P = 484 y.

01 45.6 HJ 3461 AB, epsilon Sculptoris, binary, P = 1122 y (?). PA decreasing. Only small portion of orbit covered with data. Measured position, as well as from Gaia, deviate from ephemeris.

01 55.3: HJ 3475, in Hydrus, few data. PA increasing. Gaia: Nominal parallax values of the components result in a separation of only 0.3 (±0.7) ly. Also, proper motions are roughly similar. Thus, this pair seems to be physical. See table 3.

01 55.9: STF 186 in Cetus, binary, P = 165.7 y. See fig. 2 c.

02 02.0: STF 202 AB, alpha Piscium, many speckle data, binary, P = 3267 y (?), only small arc on orbit covered with measurements.

02 15.8: HTG 1, in Cetus, binary, P = 296 y (?), rho measures deviate from currently assumed ephemeris (Tok2015), in accordance with Gaia data.

02 23.2: BU 738, in Fornax, binary, P = 560 y, orbit highly inclined.

02 27.9: DAW 1, in Horologium, few data, PA of AB and AC decreasing, rho(AB) increasing. Gaia: Proper motions of all three components are roughly similar, but the parallax of B significantly differs from A and C, while their parallax values are about similar, with overlapping error margins. Thus, A and C possibly form a binary, but B is excluded. See table 3.

02 39.7: DUN 7 A, BC, in Horologium, tripel, few data, BC close pair, not resolved by Gaia. Physical status of A,BC unclear, as parallax and proper motion data of only one component are given by Gaia. See fig. 5.

02 57.2: BU 741 AB,C, in Fornax AB binary, P = 149.9 y, few data for AC.

03 12.1: HJ 3555, alpha Fornacis, binary, P = 269 y.

03 12.4: JC 8, in Eridanus, AB binary, P = 45.2 y, many speckle data, not resolved by Gaia. Few data for HJ 3556 AB, C, extrapolation ambiguous. See fig. 2 a.

03 18.4: AC 2 AB, 95 Ceti, binary, P = 282.4 y, residuals refer to ephemeris.

04 02.1: BU 1004 AB, in Eridanus, binary, P = 410 y, recent measures of rho tend to deviate from ephemeris, including from Gaia.

04 04.9: I 152 A, BC/CHR 224 BC, in Eridanus. Positions of A and B (BC not resolved) are listed in Gaia DR1 and DR2. Nevertheless, extrapolation is ambiguous because other data exhibit large scatter. The pair AB probably is not physical, as the difference of the parallax values correspond to a separation of about 15 ly, and the error margins, although being quite large, do not overlap. BC is not resolved here, but the image appears elongated, so that PA and rho values are estimated only. See fig. 2 d.

04 08.3: I 153, in Eridanus. Few data with some scatter. PA and rho increasing. Extrapolation ambiguous. Significant difference of parallax data for A and B from Gaia excludes that this pair is physical, at a nominal separation of 43 ly, despite roughly similar proper motions.

04 26.9: BU 311, in Eridanus, binary, P = 596 y. See fig. 2 b.

04 27.9: BU 184, in Eridanus, PA decreasing, rho increasing. Parallax data from Gaia yield a separation of 0.5 ly, with widely overlapping error margins. Also, proper motions are rather similar. Further, PA is decreasing in a curve since 1860. In all, this pair seems to be physical. See table 3.

04 40.3: HJ 3683 AB, in Dorado, binary, P = 326.2 y, orbit highly inclined, rho increasing, slightly off ephemeris.

04 43.6: STF 590, 55 Eridani, few data, extrapolation ambiguous. Gaia: Proper motions and directions of the components are very similar, while the nominal difference of the parallax values would give a separation of 4.9 ly. However, the error margins widely overlap, so this pair may well be a binary. See table 3.

04 59.0: BU 314 AB, in Lepus, binary, P = 55 y, recent PA and rho data deviate from ephemeris, in accordance with Gaia. See fig. 7.

05 07.9: STT 98, 14 Orionis, binary, P = 197.5 y, many speckle data.

05 13.5: STT 517 AB, in Orion, binary, P = 987 y (?), many speckle data, residuals refer to ephemeris (Tok 2014). See fig. 2 c.

05 14.5: STF 668 A-BC, beta Orionis, few data, residuals ambiguous. Measurement difficult, because of large difference of brightness. BC not resolved.

05 28.2: BU 320 AB, beta Leporis, few data, PA and rho increasing. Large differences of parallax and proper motion data from Gaia let this pair appear as not physical.

05 30.8: STF 728, 32 Orionis, binary questionable. While the decrease of PA, and the increase of rho seem to be about linear, an orbit has been calculated with period P = 613.7 y, which is highly inclined and elongated. Taking parallax data from Gaia for A and B at face values, their difference would give a separation of more than 5 ly, which would be too large for a physical binary. However, the unusually large error margins widely overlap. While the proper motion data significantly differ, the last word does not seem to be spoken. See table 3.

05 40.7: STF 774, zeta Orionis, binary ?, premature orbit questionable (Hop1967). PA slowly increasing. Not listed in Gaia.

05 48.0: STF 795, 52 Orionis, PA increasing, rho decreasing. Not listed in Gaia DR2.

06 04.8: DUN 23, in Puppis, binary, P = 915 y (?), recent rho data, including from Gaia, deviate from ephemeris.

06 28.8: STF 919, beta Monocerotis, famous optical tripel, although all three components are listed in Gaia DR2, extrapolation of positions is somewhat ambiguous, due to large scatter of other recent literature data.

06 29.8: R 65 AB, HDO 195 CD, two close binaries in Puppis, with periods P =53.1 y, and P = 99.2 y, respectively, separated by about 11.7 arc sec. Few data for DUN 30 AC. Not listed in Gaia DR2.

07 17.5: I 7, in Puppis, close binary, P = 85 y, residuals refer to ephemeris.

07 29.4: STF 1104 AB, in Puppis, binary, P = 729 y, residuals refer to ephemeris.

08 09.5: DUN 65 AB, gamma Velorum, few data, main star too bright for Gaia.

08 18.2: HJ 4073, in Puppis. PA slowly decreasing, rho slowly increasing. Although few data, positions from Gaia DR1 and DR2 allow reasonable extrapolation. Large difference of parallaxes excludes that this pair is physical.

08 25.0: RST 4888 AB, in Puppis. Literature data exhibit some scatter. Extrapolation ambiguous. See fig. 2 b.

08 33.1: BU 205 AB, in Pyxis, binary, P = 142.9 y (?). Residuals refer to ephemeris, significant deviation of recent rho measures. See fig. 2 b.

10 09.5: I 13 AB, in Carina. Few data, PA and rho decreasing.

14 39.6: RHD 1, alpha Centauri, famous binary, P = 79.9 y.

17 19.1: BSO 13 AB, in Ara, binary, P = 953 y. Gaia position close to ephemeris.

18 03.1: STF 2262 AB, tau Ophiuchi, binary, P = 257 y, many speckle data.

18 06.8: HJ 5014, in Corona Australis, binary, P = 450 y, residuals refer to extrapolated trend of literature data, including Gaia. Significant deviation from currently assumed orbit.

18 11.2: BU 132 AB, in Sagittarius. PA is decreasing, rho increasing. Parallax data from Gaia DR2 result in a separation of more than 1.5 ly, but the error margins overlap. Although the actual data of proper motion of A and B significantly differ, it may not be excluded that the pair is physical. See table 3.

18 27.7: BU 133, in Sagittarius, PA and rho decreasing.

18 32.5: ARN 52 AB, few data, a third component C is found near B, which is not listed in the WDS, but appears in Gaia DR2. According to Gaia, C is even brighter than B in the red (~8.2 mag vs. ~9.2 mag), while magnitudes are about the same in the green. A is listed with ~5.6 mag in the red. Residuals refer to Gaia DR2. Neither pair seems to be physical, as parallax and/or proper motion data of all three components significantly differ.

18 33.4: DUN 222, kappa Coronae Australis, denoted as “relfix”, but PA is decreasing. Few data, extrapolation ambiguous. Parallax data of A and B from Gaia would result in a separation of more than 4 ly, but the error margins, being quite large, widely overlap. While the proper motion values are rather similar, the physical nature of the pair is not quite clear. See table 3.

18 34.5: STN 62, in Sagittarius, few data, but extrapolation appears trustworthy. PA decreasing, rho increasing. Nominal parallax values of the components from Gaia result in a separation of 4.3 ly, but the error margins overlap. So it may not be excluded that this pair is physical. See table 3.

19 02.6: HDO 150 AB: short period binary, P = 21.0 y. H 5 78 AB, C: zeta Sagittarii, few data, residuals ambiguous.

19 19.0: I 253 AB, in Sagittarius, binary, P = 60 y, orbit highly inclined. Measured PA close to ephemeris (B__1954), but rho significantly deviates, in accordance with recent literature data.

19 28.2: SCJ 22, in Sagittarius, binary, P = 170.2 y, many speckle data.

20 01.2: HDO 294, in Sagittarius, binary, P = 4484.5 y (?), „premature“ orbit (Dom1978), only short arc documented, significant deviation of recent measurements, including Gaia, from ephemeris.

20 01.4: STF 2613 AB, in Aquila, binary, P = 2352 y (?), “premature” orbit (Hop1937), highly inclined. Only short arc documented, but many recent speckle data. Residuals refer to trend, including results from Gaia. Significant deviation from ephemeris.

20 12.6: STF 2644, in Aquila, “relfix”, many speckle data, but with large scatter. PA and rho slowly decreasing. Residuals ambiguous. Gaia: Nominal parallax values of the components result in a separation of 2.9 ly, but the error margins widely overlap. Proper motions differ by only 2.3 km/s, their directions by about 10 degrees. In all, this pair might be physical. See table 3.

20 17.8: DUN 230, in Sagittarius, PA increasing, rho decreasing, few data, but extrapolation with data from Gaia appears reasonable.

20 26.9: R 321, in Sagittarius, binary, P = 177.5 y, measure of rho close to ephemeris, while PA deviates, in accordance with recent speckle and Gaia data.

20 28.9: SHJ 323 AB, rho Capricorni, binary, P = 278 y, orbit highly inclined. Trend of recent speckle data, and from Gaia, deviates from ephemeris, for both PA and rho.

20 39.3: HU 200 AB, tau Capricorni, close binary, P = 420 y, many speckle data, but with considerable scatter. Residuals refer to ephemeris. Near the resolution limit. See fig. 2 a.

20 51.4: STF 2729 AB, 4 Aquarii, binary, P = 200.7 y, many speckle data.

20 51.6: RMK 26, in Pavo, few data, PA decreasing.

21 03.1: STF 2744, in Aquarius, binary, P = 1532 y (?), “premature” orbit, many speckle data, rho data exhibit considerable scatter.

21 24.4: BU 766, in Microscopium, very close pair, at the resolution limit, PA rapidly decreasing, rho passing a minimum? Image at the resolution limit. See fig. 2 a.

22 07.1: STF 2862, in Aquarius, “relfix”, speckle data show some scatter, in particular in the 1990ties. While the proper motion

values and directions of the components from Gaia are quite similar, their parallaxes would result in a separation of the components of more than 4.3 (± 1.8) ly. Thus, the pair probably is not physical.

22 12.0: HJ 5319, in Grus, few data. PA has been about linearly increasing since the 1880ies, while rho, after increasing, seems to have passed a maximum in the 1980ies, and is now decreasing. Nominal parallax data for A and B from Gaia result in a separation of about 4.7 (±3.3) ly. Also, the directions of proper motions are rather different. Thus, this pair does not seem to be physical.

22 28.8: STF 2909 AB, zeta Aquarii, binary, P = 540 y. An unseen companion causes a wobble on the orbit of AB with period P ~ 26 y (Tok2016).

22 55.3: I 22, tau2 Gruis, AB binary, not resolved by Gaia, P = 198 y, orbit highly inclined, B seems to have turned around earlier than expected. Large residual of rho, referred to ephemeris. Close pair B 2506 CD not resolved. (Last entry for 2015 in the speckle catalog reads < 0.1 arc sec.) Separation of AB-C is possibly influenced by binary movement of AB, and/or large proper motion of (AB). The system AB,CD is referred to in the Sixth Catalog of Visual Binary Stars [6] as probably being physical. However, no data for parallax and proper motion are listed in Gaia DR2 for (CD), so the question remains open. See fig. 4.

23 35.7: SEE 492 AB, in Sculptor, binary, P = 77.8 y. PA and rho increasing, residuals refer to ephemeris.

23 50.6: SLR 14, in Phoenix, binary, P = 118.9 y.

(Continued from page 337)

Discussion

Compared to Gaia DR1, many more doubles could be found in DR2, yielding over 60 per cent in this work, for stars down to about 11th mag, and separations down to the resolution limit of the telescope of about 0.23 arc sec, whereas Gaia is limited to stars hardly brighter than about 4th mag, and separations of doubles greater than about 0.4 arc sec. Figures 2 a – d show a number of close doubles, which are mostly not resolved by Gaia.

Several wide doubles were found, which turned out as not suitable for calibration, as one or both components are close doubles themselves, which, however, are not resolved by Gaia. Their positions are deemed as less accurate, because they may be influenced by asymmetric intensity profiles, or by movements of the components. Examples are the systems LCL 119AC/I 260CD (β Tucanae, see Figure 3), I 22AB-CD (τ^2 Gruis, see Figure 4). Another case is DUN 7 AB/I 386BC (in Horologium, see Figure 5): The close pair BC is not resolved by Gaia, but its position angle is about perpendicular to that of AB. Therefore, the separation of AB is less affected, but the apparent position angle may be disturbed.

Binaries with Deviations from Ephemeris

As was already indicated above, residuals were generally obtained by plotting PA and rho *vs.* time, and by analyzing the trend of all available observational data, including from Gaia. For several binaries, this revealed deviations from currently assumed orbits. The most significant cases are listed in Table 2. For two examples, HJ 3423 AB (κ Tuc) and BU 314 AB (in Lep), the evolution with time of the separation is plotted in Figures. 6 and 7, respectively.

Table 2: List of binaries with significant deviations from currently assumed orbits. In most cases, deviations are confirmed by Gaia, except for I 264AB, BU 205AB, I 253AB, and I 22AB, which are not listed, incomplete, or not resolved in Gaia. See also corresponding TAble 1 notes.

Pair/Name	RA+Dec
HJ 3423 AB (κ Tuc)	01 15.8 -68 53
I 264 AB (in Eri)	01 31.6 -53 22
HJ 3461 AB (ε Scl)	01 45.6 -25 03
HTG 1 (in Cet)	02 15.8 -18 14
BU 1004 AB (in Eri)	04 02.1 -34 29
HJ 3683 AB (in Dor)	04 40.3 -58 57
BU 314 AB (in Lep)	04 59.0 -16 23
DUN 23 (in Puppis)	06 04.8 -48 28
BU 205 AB (in Lepus)	08 33.1 -24 36
HJ 5014 (in CrA)	18 06.8 -43 25
I 253 AB (in Sgr)	19 19.0 -33 17
HDO 294 (in Sgr)	20 01.2 -38 35
STF 2613 AB (in Aql)	20 01.4 +10 45
R 321 (in Sgr)	20 26.9 -37 24
SHJ 323 AB (rho Cap)	20 28.9 -17 49
I 22 AB (τ^2 Gruis)	22 55.3 -48 28

(Text continues on page 346)

Double Star Measurements at the Southern Sky with a 50 cm Reflector in 2017

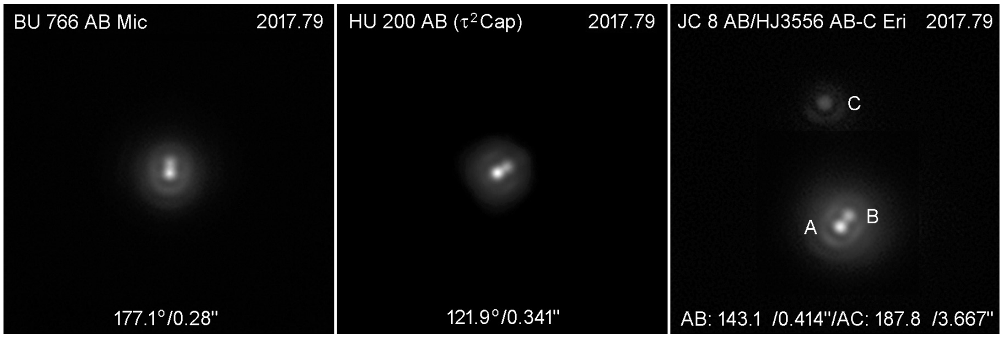

Figure 2 a. Collection of close doubles. Pairs BU 766, HU 200, JC 8 AB are listed in Gaia, but not resolved. HJ 3556 (AB)-C is listed, but position accuracy may be influenced by AB. See notes 21 24.4, 20 39.3, and 03 12.4. North is down, east is right, as in all images.

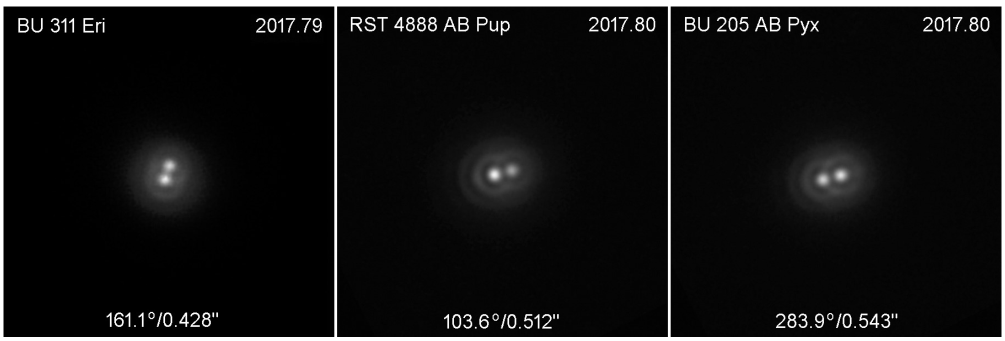

Figure 2 b. Collection of close doubles continued. All three are not listed in Gaia. See notes 04 26.9, 08 25.0, and 08 33.1.

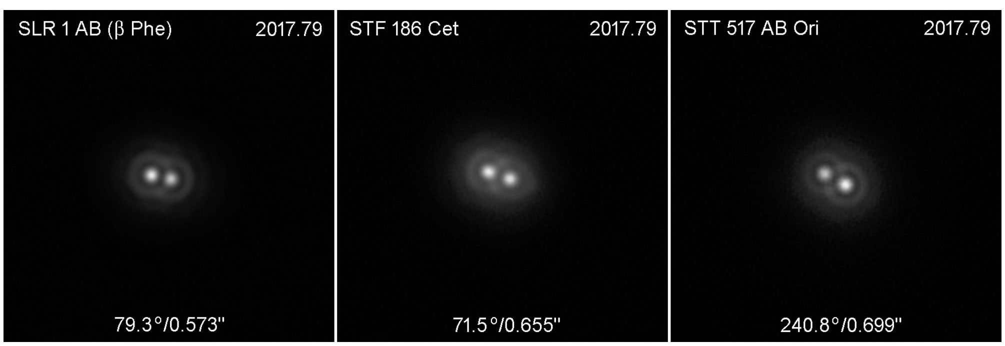

Figure 2 c. Collection of close doubles continued. SLR 1 is too bright, STF 186 and STT 517 are not resolved by Gaia. See also notes 01 06.1, 01 55.9, and 05 13.5.

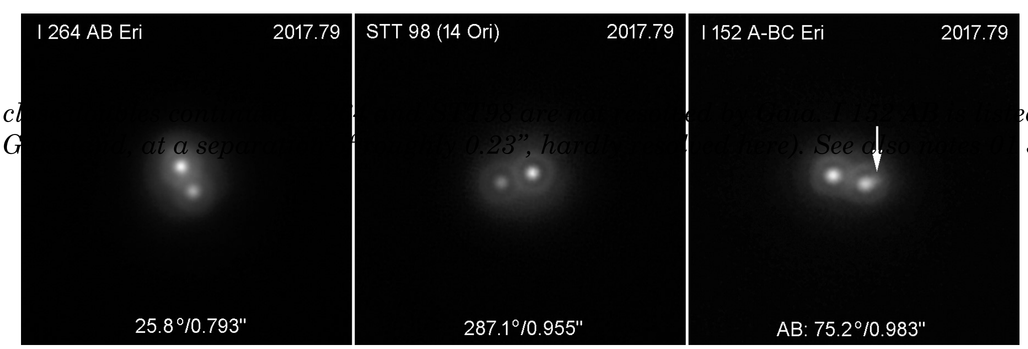

Figure 2 d. Collection of close doubles continued. I 264 and STT98 are not resolved by Gaia. I 152 AB is listed, but CHR 224 BC (arrow) is not resolved by Gaia (and, at a separation of roughly 0.23", hardly resolved here). See also notes 01 31.6, 05 07.9, and 04 04.9.

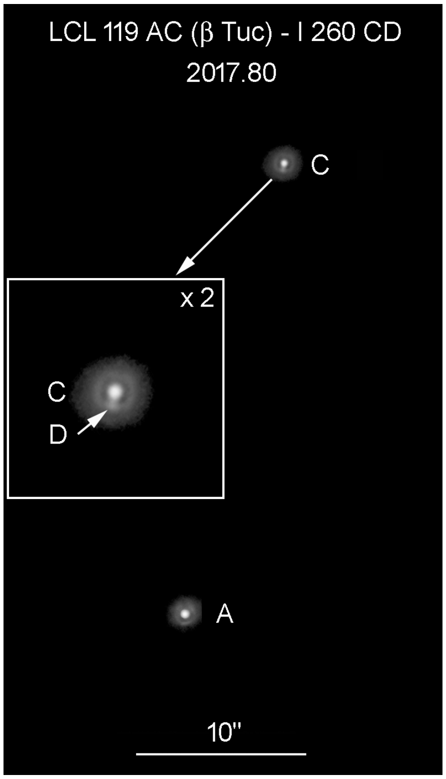

Figure 3. The triple LCL 119 AC/I 260 CD (beta Tucanae). In Gaia DR2, position data are only listed for AC, while the close pair CD is not resolved, and is close to the resolution limit in this image (see inset). The position angles of AC and CD are roughly in parallel. Thus, the separation AC given by Gaia may be influenced by D, which would explain the relatively large residual in Table 1. See also note 00 31.5.

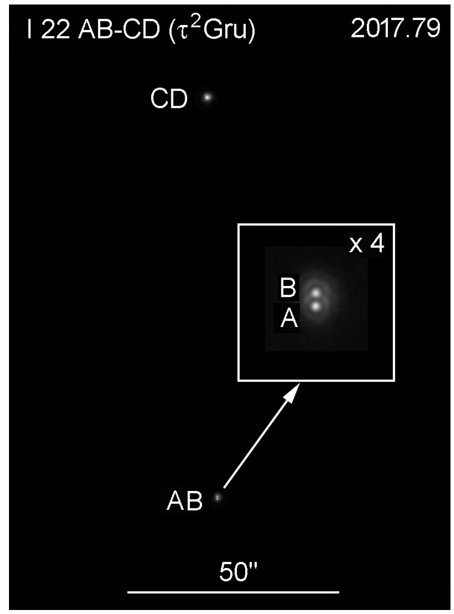

Figure 4. The system I 22AB-CD (τ^2 Gruis). The close binary AB is not resolved by Gaia. The position angles of AB and AB-CD are roughly in parallel. Thus, the separation of AB-C given by Gaia may be affected by movements of A and B. CD is not resolved by Gaia, neither here. See also note 22 55.3.

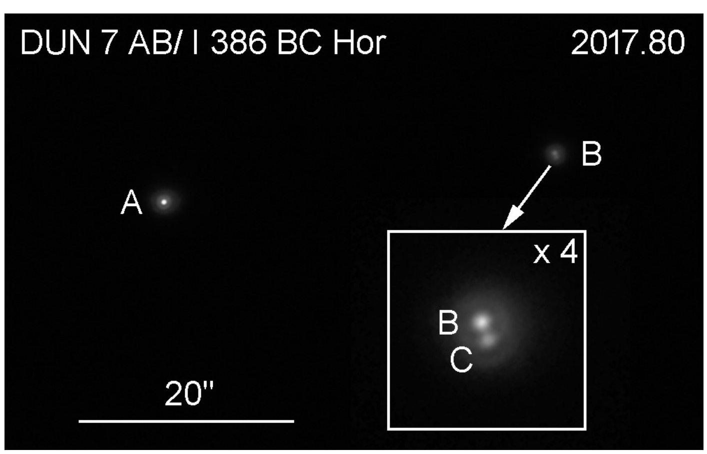

Figure 5. DUN 7 AB/I 386BC (in Horologium). The close pair BC is not resolved by Gaia. This may affect the position angle of AB, as given by Gaia. See also note 02 39.7.

Double Star Measurements at the Southern Sky with a 50 cm Reflector in 2017

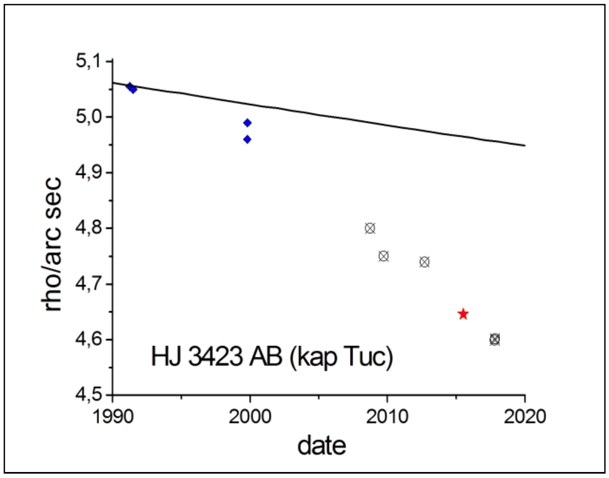

Figure 6. Plot of the separation rho vs. time for the binary kappa Tucanae. The solid line is the ephemeris, blue rhombs are data from the speckle catalog, crossed circles are own measurements, and the red star is from Gaia DR2.

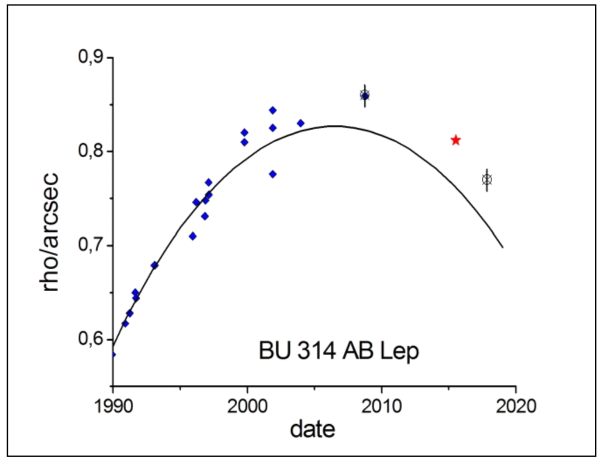

Figure 7. Plot of the separation rho vs. time for the binary BU 314 AB in Tucana. The meaning of the symbols is as in Figure 6. Error margins of own measurements are indicated with vertical lines.

(Continued from page 343)

Binary candidates

As was noted above, a number of pairs with unclear status, being physical or not, were checked with parallax and proper motion data from Gaia. In Table 3 is a list of pairs with about similar values, respectively, which may be candidates for binaries. This is mainly concluded from overlapping error margins of the parallax values of the components, and more or less similar proper motions. There are many uncertainties, but it is expected that they will be reduced in future issues of Gaia catalogs, and of course, by observations. See also the notes following Table 1.

Summary

For 59 of the 92 systems investigated here, position data were found in the recent Gaia Data Release 2. For 12 systems, however, the accuracy was less reliable, in particular because one of the components was a close double, which was not resolved by Gaia. The remaining 47 pairs were found suitable for calibration of the image scale. Statistical analysis resulted in a scale factor of 0.06488 arc sec per original pixel, with an estimated

Table 3. List of possible binaries according to parallax and proper motion data from Gaia DR2. Parallax data are in milliarcsec (mas), and are rounded. From the differences, separations in the line of sight were calculated in light years.

Pair/name	RA+Dec	Parallax A/mas	Parallax B(C)/mas	Separation/ly
BU 391 AB/κ Scl	00 09.4 -27 59	14.5122 ± 0.1464	13.9054 ± 0.6000	9.80 ± 12.8
HJ 3416 AB	01 03.3 -60 06	11.3409 ± 0.0311	11.3661 ± 0.0326	0.64 ± 1.61
STF 138 AB	01 36.0 +07 39	11.8799 ± 0.0642	11.9114 ± 0.0643	0.73 ± 2.96
HJ 3475	01 55.3 -60 19	17.5854 ± 0.0342	17.5539 ± 0.0316	0.33 ± 0.70
DAW 1 AC	02 27.9 -58 08	9.0123 ± 0.0393	9.0470 ± 0.0316	1.39 ± 2.84
BU 184	04 27.9 -21 30	8.2919 ± 0.0333	8.2814 ± 0.0394	0.50 ± 3.45
STF 590/55 Eri	04 43.6 -08 48	7.0374 ± 0.0454	6.9640 ± 0.0482	4.88 ± 6.23
STF 728/32 Ori	05 30.8 +05 57	9.2261 ± 0.6985	9.0883 ± 0.7614	5.36 ± 57.2
BU 132 AB	18 11.2 -12 51	9.0478 ± 0.0546	9.0861 ± 0.0583	1.52 ± 4.47
DUN 222/κ CrA	18 33.4 -38 44	4.6899 ± 0.1270	4.7197 ± 0.1248	4.39 ± 37.1
STN 62	18 34.5 -34 49	9.3565 ± 0.0450	9.2414 ± 0.0504	4.34 ± 5.08
STF 2644	20 12.6 +00 52	6.4257 ± 0.0664	6.4628 ± 0.0577	2.91 ± 9.76

error of less than ± 0.1 per cent. The standard deviation of separation measurements amounts to about ± 0.005 arc sec, which is more than one order of magnitude below the nominal resolution of the telescope of about 0.23 arc sec. A similar analysis of measurements of the position angle (PA) resulted in an s.d. of about ± 0.1 degrees.

Residuals of own measurements were evaluated by referring to the trend of literature data, mainly from the speckle catalog, as well as from Gaia. For a number of systems, no residuals are given, because of too few data, or too large a scatter, as to allow reasonable extrapolations to the date of own measurements. Sometimes, even accurate data from Gaia did not help. In case of binaries, residuals refer to the ephemeris, if not otherwise stated. In several cases, more or less significant deviations were found, mostly in accordance with trends of recent speckle data, and confirmed by Gaia data. This may sooner or later lead to some revisions of orbit calculations.

For a number of doubles with unclear status, parallax and proper motion data were analyzed in order to estimate the probability of being physical or optical. While in several cases the difference of the parallax values of the components were too large, 12 systems were found with overlapping error margins, and proper motions being not too different. At least for some of them, a binary nature appears likely.

The remaining 33 pairs are either not listed or not resolved by Gaia, in particular because of too bright components, and/or too close separations. This means that earth bound observations are still not obsolete, especially of such systems. As a conclusion, the present work may help to improve the knowledge about their status.

Acknowledgements

This work has made use of data from the double star catalogs provided by the United States Naval Observatory, as well as data from the Gaia satellite mission, which were recently published by the ESA consortium.

References

[1] Anton, R., Lucky Imaging, in *Observing and Measuring Visual Double Stars*, 2nd edition, Robert Argyle, ed., Springer New York 2012.

[2] Gaia Archive, Data Release 1 and 2 (2016/2018): http://esac.esa.int/archive/.

[3] IAS, http://www.ias-observatory.org.

[4] Anton, R., 2017, *Journal of Double Star Observations*, **13**(4), 495-505.

[5] Mason, B.D. et al., *The Washington Double Star Catalog (WDS)*, U.S. Naval Observatory, online access Dec. 2018.

[6] Hartkopf, W.I. et al., *Fourth Catalog of Interferometric Measurements of Binary Stars*, U.S. Naval Observatory, online access Dec. 2018.

[7] Hartkopf, W.I. et al., *Sixth Catalog of Orbits of Visual Binary Stars*, U.S. Naval Observatory, online access Dec. 2018.

[8] R. Burnham, *Burnham´s Celestial Handbook*, Dover Publications, New York 1978.

A New Double Star Observed During Lunar Occultation: S 763A

Dave Gault (DG)

Kuriwa Observatory MPC-E28; Hawkesbury Heights; Australia
Western Sydney Amateur Astronomy Group (WSAAG)
International Occultation Timing Association (IOTA)
davegault@bigpond.com

Dave Herald (DH)

Murrumbateman MPC-E07; Australia
Canberra Astronomical Society (CAS)
International Occultation Timing Association (IOTA)
drherald@bigpond.com

Abstract: A lunar occultation observation observed at two separate sites in November 2018 detected a new, previously unknown companion to S 763A (HIP 102685).

Circumstances

On 2018 November 14, a lunar occultation disappearance of S 763A was observed at two separate stations, 208km apart. Both stations used video recording equipment operating at 25 frames/sec, using a 40cm telescope at one site (DH) and a 30cm telescope at the other site (DG).

The waxing moon was 39% illuminated. The star was 20 degrees above the western horizon.

Observation

The light curves that were recordedare shown in Figure 1.

The brighter star was occulted first, leaving the fainter star in view for 1.08 seconds (DH) and 1.2 seconds (DG), before it too was occulted by the moon.

The measured magnitude for the new star is 10.9 ± 0.3.

The events were seen to occur at the lunar position angle of 74.291 degrees (DH) and 73.213 degrees

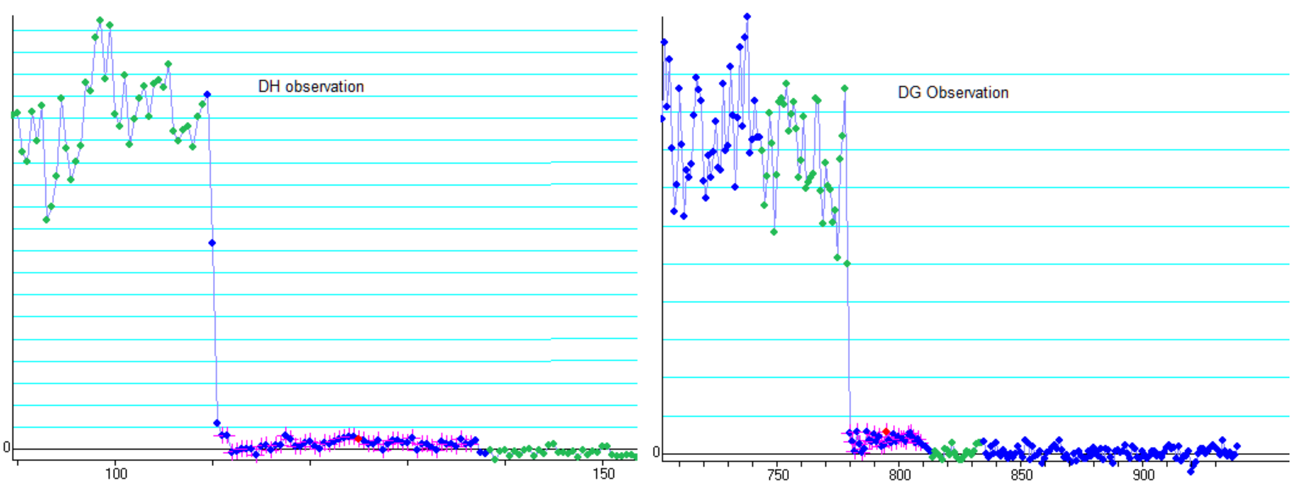

Figure 1. Recorded light curves. Relative brightness on the y-axis, frame number on the x-axis. Dots in green represent sample measures before the occultation when both stars are clear of the lunar limb, and after the occultation. Dot in purple represent measures when only the fainter star was visible.

(DG), however this is too close to produce a good PA and Separation for the new star.

The apparent radial velocity of the star-moon at those PAs was 0.4650"/s (DH) and 0.4721"/s (DG), so the separation of the new star from S 763A is at least 0.50".

S 763

The lunar occultation historic record showed several video observations of this star and the observers were contacted (including author DG) to see if they might have missed this faint star in previous analysis, but this line of enquiry was not successful.

Star	HIP 102685 =HD 198063 =SAO 163895
Coord. (J2000)	20h 48m 25.98, -18º 12' 06.18"
Spectral type	K1

Derived double data:

Mag A	7.24 ±0.1 (V)
Mag B	10.9 ±0.3 (V)
Epoch	2018.87
Separation	>0.50"
PA at epoch	between 13º and 133º

References

Lunar Occultation Archive: VizieR Catalogue number VI/132A

The Southern Double Stars of James Dunlop I: History and Description of the First Published Catalogue Dedicated to Southern Double Stars

Roderick R. Letchford[1], Graeme L. White[2], Allan D. Ernest[3]

1. Vianney College Seminary, Wagga Wagga, NSW 2650, Australia, rodvianney@yahoo.com.au
2. Centre for Astronomy, University of Southern Queensland, Toowoomba, Australia QLD 4350, graemewhiteau@gmail.com
3. Charles Sturt University, Wagga Wagga, NSW 2650, Australia, aernest@csu.edu.au

Abstract: The first dedicated catalogue of southern double stars was published in 1829 by James Dunlop. Basing our work solely on the published data, we describe this catalogue, give a biography of Dunlop and a history of the catalogue and look at the data presented. Of the 253 doubles presented, Dunlop himself described one as single and 14 as triples. The smallest separation claimed was ~2 arcsec and limiting magnitudes were ~7 and ~8.5 for each of the two telescopes used. All observations were across the sky and approximately south of the Tropic of Capricorn.

1. Introduction

The Dunlop papers follow three papers (Rümker Papers I, II, and III) previously published in this journal on the double star work of another of the Parramatta astronomers, Carl Rümker (Letchford, White, and Ernest 2017; Letchford, White, and Ernest 2018a; Letchford, White, and Ernest 2018b).

In this Paper we look at the history and description of the first double star catalogue dedicated to the southern sky, namely that of James Dunlop published in 1829 (Dunlop 1829b).

The finding, cataloguing, and astrometric study of double stars dominated the astronomy of the 19th century. In the southern sky, the pioneering double stars work of Sir John Herschel (JH) between 1834 and 1838 is recognized for its accuracy and completeness.

However, some two decades prior to the work of JH, a small but well equipped privately owned observatory was established in the fledgling British Colony of New South Wales (now the State of New South Wales within the Australian Commonwealth) by Sir Thomas Makdougall Brisbane, the 6th Governor of the Colony. For about a decade, the Parramatta Observatory reigned supreme in the southern hemisphere, systematically exploring the deep southern skies for the first time.

The Parramatta Observatory was constructed by Sir Thomas Brisbane (1773-1860), and staffed by two astronomers; Carl Rümker (1788-1862) and James Dunlop (1793-1848). From Parramatta Observatory came dedicated catalogues of stars (Richardson 1835), double stars (Rümker 1832; Dunlop 1829a) and non-stellar objects (Dunlop 1828), as well as numerous other papers on diverse subjects.

2. Brief Biography of James Dunlop

James Dunlop (1793-1848) was born 1793, October 31, to John, a weaver, and Janet née Boyle in Dalry, Ayrshire, Scotland, a small poor rural community (Figure 1). Fourth of seven children, at the age of 14 he started work at a nearby textile factory in Beith owned and operated by a cousin. He resided with an uncle, and at the same time attended night-school. Despite very little formal education, by the time he was 17 he had built his own reflecting telescope. At the age of 22 he married his cousin Jean Service on 1816 June 25. There were no children.

Through mutual acquaintances, while living near Beith, James got to know Sir Thomas Brisbane from Largs, in the same county. This meeting was fortuitous and life-changing for both James and Jean. Brisbane was an aristocrat, educated in astronomy and mathe-

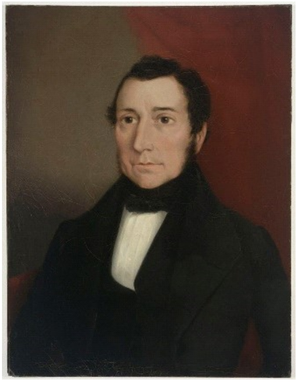

Figure 1: James Dunlop, from Wikipedia (by Joseph Blackler, c. 1843). Held by the Mitchell Library, State Library of New South Wales.

matics at the University of Edinburgh. He had a distinguished career in the Army serving in numerous campaigns under the Duke of Wellington.

In 1821, the year after Dunlop and Brisbane met, Brisbane was appointed Governor of the penal colony of New South Wales on the recommendation of the Duke of Wellington. The southern sky, at least that south of -30 degrees declination, was virtually unexplored and Brisbane decided to set up his own private observatory in the grounds of Government House, Parramatta, about 26 km west of Sydney. Because he knew his official duties would not leave him much time for astronomy, he chose the well-known astronomer Carl Rümker to run the Parramatta Observatory and James Dunlop to maintain the instruments.

James was charged with packing Brisbane's instruments at his Observatory at Largs, and he and his wife travelled with the Brisbane family and Rümker out to Sydney, arriving 1821 November 7. The Parramatta Observatory was completed, and observations commenced 1822 May 2 (Letchford, White, and Ernest 2017). Dunlop learnt the art of astronomical observation from Rümker and Brisbane. Exactly one month after the opening, Dunlop was the first person in the world to sight the return of Enke's comet (Rümker having previously calculated its return position).

The main goal of Brisbane was to publish a catalogue of stars in the southern sky. Rümker and Dunlop set about doing this, with occasional help, as time permitted, from the Governor. This was finally published in 1835 as A Catalogue of 7385 Stars: Chiefly in the Southern Hemisphere, Prepared from Observations Made in the Years 1822, 1823, 1824, 1825, and 1826, at the Observatory at Paramatta, New South Wales, Founded by Lieutenant General Sir Thomas Makdougall Brisbane (Richardson 1835, but known as the "Brisbane Catalogue"). The reductions were completed by William Richardson of Greenwich Observatory.

For reasons which are not entirely clear, Rümker fell out with Brisbane and left the Observatory on 1823 June 16, leaving Dunlop with the bulk of the work. Brisbane and Dunlop became close friends and the Governor rewarded him with a grant of 5,000 acres of land near Gosford, NSW, known as Borra Borra†.

Brisbane was re-called by the British Government and vacated his Governorship on 1825 December 1, to be replaced by Ralph Darling. Because the Observatory was on Government land, Dunlop moved his observing to a small cottage in Parramatta, returning to the Observatory in 1826 March.

Dunlop returned to Scotland in 1827 February 4. The Parramatta Observatory moved into Government hands and Rümker returned to work at the observatory, and on 1827 December 21 Rümker was appointed as Government Astronomer.

Dunlop moved to Brisbane's estate at Makerstoun in the council area of The Scottish Borders, which Brisbane had inherited by marriage to his wife, Anna. Brisbane had built an observatory at Makerstoun. Dunlop continued to work with Brisbane, publishing numerous papers. On 1827 December 20 his paper A Catalogue of Nebulae and Clusters of Stars in the Southern Hemisphere, Observed at Paramatta in New South Wales (Dunlop 1828; Cozens, Walsh, and Orchiston 2010) was read before the Royal Astronomical Society (RAS) by no less a person than John F. W. Herschel. For this major work, Dunlop was awarded the Gold Medal of the RAS on 1828 February 8.

On 1828 May 9 Dunlop's paper Approximate Places of Double Stars in the Southern Hemisphere, observed at Paramatta in New South Wales was read to the RAS and published the following year (Dunlop 1829a). Approximate Places is the subject of this paper. An image of the first nine entries in the Catalogue is presented in Figure 2.

Meanwhile, Rümker was dismissed from his position on 1830 June 18. Dunlop was offered and accepted the position of Superintendent of Parramatta Observatory, and returned there as the sole astronomer. A residence attached to the Observatory was built for him and Jean in 1832.

The state of the Observatory was poor, as is illustrated by this report by Dunlop himself: "Sunday morning between 8 and 9 o'clock, about four or five yards of ceiling fell and broke the table. No other damage." A simple entry in his notebook for 1835 March 17.

Between 1838 and 1847, while still in Government employment, Dunlop failed to submit any reports. According to a letter written by his wife 1837 July 20,

† see http://www.environment.nsw.gov.au/heritageapp/ViewHeritageItemDetails.aspx?ID=1620196.

Dunlop had contracted dysentery two years previously and had only recently become infected with tetanus.

A Commission of Enquiry called and asked to see Dunlop's records. Much of it had been literally white anted, including the Observatory itself. The recommendation of the Commission was that the Observatory be closed and the instruments and remaining library packed up by Dunlop and put into storage.

James and Jean retired to Borra Borra in 1847 August and he died on 1848 September 22 aged 44. His body is buried in the churchyard of St Paul's Anglican Church, Kincumber NSW.

Dunlop was awarded numerous accolades. Apart from the Gold Medal of the RAS, he was elected Fellow of the Royal Society in about 1830. He was awarded medals for his work by the King of Denmark in 1833, and the Institut Royal de France in 1835, and elected Fellow of the Royal Society of Edinburgh in 1832, his proposer being Sir Thomas Makdougall Brisbane.

The Catalogue of Scientific Papers, a 19th and early 20th century catalogue of all published scientific papers (Csiszar 2017), listed 9 papers authored by Dunlop; one co-authored with Brisbane, and one with T. Henderson (White and Morley 1868). The main biographies of James Dunlop, from which the above was taken, are those of: John Service (1890), Harley Wood (1966), Elizabeth Brenchley (1980), Cozens & White (2001), and Sharon Rutledge (2009).

3. History of Dunlop's Published Catalogue

Dunlop's double star observations were made from the later part of 1825 until his departure to Scotland on 1827 February 4. Their reduction took place while he was at Makerstoun.

3.1 Telescopes and clocks used and their location

For his double star work, Dunlop used two telescopes: a 46 inch focal length, 3¼ inch achromatic refractor equatorially mounted, made by Banks of London, and housed in the southern dome of the Observatory; and a 9 foot focal length, 9 inch speculum Newtonian reflector made by Dunlop himself which he used at his home in Parramatta. With the Observatory telescope he had the use of filar micrometers which he himself had made, but with his own telescope the positions and distances were "only estimations while passing through the field". Observations with the speculum 9 inch were made at the cottage in Parramatta "about 2s of time east of the Brisbane observatory" (Dunlop 1829a).

The double stars marked with an asterisk in the Catalogue are those measured with the Banks telescope, those without were made with the Dunlop telescope. We continue this nomenclature in the present paper.

123 pairs were "discovered" using the 3¼ inch refractor and 120 were discovered with the 9 inch reflector.

There were two main clocks in the Observatory for right ascension: a sidereal clock by Hardy of England near the 3¼ inch in the southern dome and a mean time clock by Breguet in the north dome. For his double star work, which Dunlop largely did alone, he used the nearby sidereal clock. The clock he used at home in Parramatta along with his 9 inch, is unknown. It is possible, even likely, that he borrowed one of two other Observatory clocks, one by Barraud and another by Grimaldi†. For a description of the Observatory, see Rumker Paper I (Letchford, White, and Ernest 2017).

3.2 Contemporary Reactions

John Herschel was, at first, effusive in his praise of the work:

"Mr Dunlop has amassed a copious and valuable collection of Southern Double Stars which he is at present occupied in reducing and arranging; and a variety of interesting and curious particulars relative to the magnitudes, colours, and other peculiarities, of all the more conspicuous single ones." (Herschel 1828).

However, after his own observations at the Cape, he wrote:

"[I]n comparing my observations with [Dunlop's Catalogue] I have found a star to be double in a different sense from that which caused it to be registered as double therein, - or when, with agreeing places, I have met with such discordances in the descriptions or measures, that it is impossible to suppose the same star to be intended by both observers, - a number has been affixed. … A great many mistakes appear to have been committed in the Catalogue alluded to either in the places, descriptions, or measures of the objects set down in it." (Herschel 1847)

To be fair to Dunlop, Herschel had far superior equipment, was better trained and had more money, to say nothing of his family heritage in astronomy. Also, Dunlop, by his own admission, stated that his double star work was not a high priority. In fact he only observed double stars deliberately during less than ideal weather and in the presence of moonlight:

"The nebulae being a primary object to me, I devoted the whole of the favourable weather in the absence of the moon to that department, and moonlight, in general, was allotted to the observations of double stars" (Dunlop 1829a).

In passing, we also note that Dunlop's A Catalogue of Nebulae and Clusters of Stars in the Southern Hemisphere, Observed at Paramatta in New South Wales (Dunlop 1828) also suffered considerable, and similar,

† *http://www.austehc.unimelb.edu.au/fam/1545.html*

No.	Name of Star.	Approximate Æ.	Declination.	Angle of Pos.	Quadrant.	Distance.	Δ Æ.	Δ Declin.	Magnitudes.	Remarks.
		h m s	° ′	° ′		″	s	″		
1	β^1 β^2 Toucani *	0 23 16	63 56	84 5	*np*		0,607	24,86	4,4	Double. L. C.
2	λ Toucani *	0 44 50	70 28		*sf*			6,62	6,7	
3	Anonym.	1 19 43	33 31						7	A very singular star of the 7th magnitude, of an uncommon red purple colour, very dusky and ill-defined; 3 obs. on this star; a small star preceding, and another following.
4	100 Phœnicis *	1 32 11	54 18	17 27	*sf*	15,809			6,8	
5	6 Eridani *	1 33 24	57 4	73 6	*nf*	2,5			6·7,6·7	Very nearly equal. Pretty d. star.
6	φ Eridani	2 10 12	52 20	50 0	*sp*	90			4,12	
7	Anonym.	2 34 57	60 21	20 0	*np*	35			8,8	
8	41 App. Chemici *	2 50 37	25 40	49 6	*sp*				7,7	
9	θ Eridani *	2 51 19	41 0	1 37	*nf*	10,81			4,6	

Figure 2. Image of the first nine entries in Dunlop's Approximate Places (Double Star Catalogue). An explanation of the meaning of each column is given in Table 2.

criticism from John Herschel after Herschel's detailed examination of the southern skies from the Cape. Discussion of the validity of the criticism of the non-stellar catalogue is covered in Cozens et al. (2010).

4. Description of the Published Catalogue

Dunlop's Approximate Places of Double Stars in the Southern Hemisphere, observed at Paramatta in New South Wales of 1829 presents the positions, and double-star data for 253 pairs mostly south of declination -27 degrees. An image of the first nine entries is given in Figure 2.

Although extensive observational notes made by Dunlop do exist, we have chosen to describe only the data as presented by Dunlop himself for publication. To the best of our knowledge, a dedicated description of the catalogue has never been published. As the first published dedicated catalogue of southern double stars, it deserves wider acknowledgement.

4.1 Equinox of Catalogue and Epochs of Observations

Like Rümker, Dunlop did not publish the equinox or the epoch of any measures in his catalogue. It is impossible to be conclusive without recourse to an extensive inspection of the unpublished notes, but there are two possibilities; either the positions and measures given are equinox of epoch (date) or there is a catalogue equinox.

We do know that Dunlop had a large hand in observing and recording data for the Brisbane Catalogue, A Catalogue of 7385 Stars, published in 1835. Although the reductions for that catalogue were completed by William Richardson of Greenwich Observatory, it would be odd for Richardson to choose, as he did, the Equinox of the Catalogue as B1825.0, some 10 years prior to its publication, unless the data was presented to him with that equinox or at least with that equinox in mind.

We therefore suspect that, if there is indeed a catalogue Equinox for Dunlop's double star catalogue, it is B1825.0.

4.2. Column Headings

Dunlop published data on 253 doubles using 11 columns (see Figure 2). Columns 1-4 are complete (except for a missing declination for DUN 50); columns 5-11 frequently contain incomplete or missing information. Column descriptions are in Table 1.

4.3 Names of the doubles (Column 2)

Table 2 presents statistics on the names (Column 2) Dunlop gave to his doubles.

Table 2: Statistics on the number of different designation types

Name	3 ¼ inch	9 inch
Anonym.	32	89
Bayer-type (e.g. λ Toucani)	41	22
Flamsteed-type (e.g. 100 Phoenicis)	48	21

Table 1: Descriptions of Column Headings in Dunlop's Published Catalogue (see also Figure 2).

Column	Heading	Information
1	No.	General number (1 to 253)
2	Name of Star.	Number or character of the star in Bode's Catalogue with or without an asterisk (*). See section 4.3 for more on Bode's Catalogue.
3	Approximate AR.	Approximate Right Ascension (RA), in hours, minutes, seconds
4	Declination.	Approximate Declination (DE), in degrees, minutes
5	Angle of Posn.	Angle formed by sweeping from the small circle parallel to the equator running through the primary to the an arc of a great circle from the primary to the secondary, in degrees and minutes.
6	Quadrant.	Quadrant of the secondary with respect to the primary. "nf" north following = Quadrant I; "sf" south following = Quadrant II; "sp" south preceding = Quadrant III; "np" north preceding = Quadrant IV; "n" north; "s" south; "e" east; "w" west. For DUN 108, 194 and 211, two quadrants are given since they are triple stars. For our purposes, we chose only the first quadrant given in each case.
7	Distance.	Observed or estimated separation, in arcseconds (")
8	Δ AR.	Observed or estimated difference in RA, in seconds of time
9	Δ Declin.	Observed or estimated difference in DE, in arcseconds (")
10	Magnitudes.	Estimated magnitudes of the stars
11	Remarks.	Dunlop's own comments on selected doubles

For the Bayer-type (Greek letter + Latin name) and the Flamsteed-type (Number + Latin name) designations, Dunlop claimed to have obtained these from "Bode's Catalogue". Johann Elert Bode (1747-1826), a German astronomer, published two editions of his Vorstellung der Gestirne "Catalogue of the Stars"; one in 1782 and a revised and enlarged edition in 1805 (Bode 1782; Bode 1805). Dunlop did not specify which edition he was using, but it was likely the second edition, as it contains stars observed by Nicholas-Louis de Lacaille (1713-1762), a French Catholic permanent Deacon, which Dunlop sometimes noted in his "Remarks" (Column 11).

4.4 Distribution in the Southern Sky (Columns 3 & 4)

Figure 2 shows the distribution of the Dunlop doubles in the Southern sky. Observations cover all Right Ascensions (Column 3), and are south of declination ~-23o (Declinations in Column 4). In keeping with Dun-

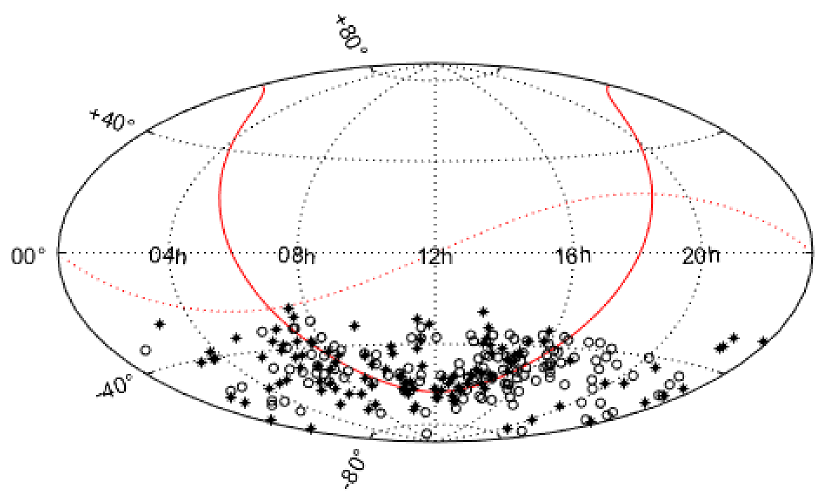

Figure 2. Hammer-Aitoff projection of the whole sky. The symbol '' represents the position of primaries observed with the 3¼ inch refractor, 'o' those observed with the 9 inch reflector at Equinox of Epoch 1825.0. The red dotted line is the ecliptic and the red solid line is the galactic plane.*

Table 3: Ways of calculating Position Angles from Dunlop's Catalogue.

Method	Columns used (see Table 1)	3 ¼ inch (out of possible 110)	9 inch (out of possible 85)	Example (DUN 18*)
1	5, 6	96	81	~ 59.9°
2	4, 6, 8, 9	62	7	~ 56.6°
3	4, 6, 7, 8	21	1	~ 53.5°
4	4, 6, 7, 9	34	1	~ 58.0°
			Mean	~57.0°

lop's own notation, pairs observed with the 31/4-inch refractor are shown as '*' and those observed with the 9-inch reflector are shown as 'o'.

4.5 Position Angles and Quadrants (Columns 5, 6, 7, 8, 9)

Position angles (PAs) in the modern form (measured from N through E, 0° to 360°) were not explicitly recorded by Dunlop. Rather he recorded information such that a modern position angle could be determined in up to four different ways, depending on the information presented for each double. These ways are summarized in Table 3 which should be read in conjunction with Dunlop's Catalogue (Dunlop 1829a). In the following section (section 4.5.1) we explain each method.

PAs were able to be calculated in at least one way for 110 (out of the 121 pairs) for the 3 ¼ inch; and 85 (out of the 132 pairs) for the 9 inch.

4.5.1 How to determine Position Angles from Dunlop's Catalogue

DUN 18* has information recorded in all relevant columns (5, 6, 7, 8, 9) and so we use it as an example. Please refer to Table 1, section 4.2 for explanation of terms.

4.5.1.1 PA Method 1

For DUN 18*, Angle of Posn. = 30° 4', and Quadrant = nf. Therefore:

PA = 90 - 30° 4' ≈ 59.9°.

4.5.1.2 PA Method 2

For DUN 18*, Declination = -53° 46', Quadrant = nf, Δ AR. = 1.137s, and Δ Declin. = 6.659". Therefore:

ΔRA" = 15*cos(-53° 46')*1.137 ≈ 10.08"

Angle of Posn = atan(Δ Declin./ΔRA").180/π ≈ 33.45°.

PA = 90 – 33.45 ≈ 56.6°.

4.5.1.3 PA Method 3

For DUN 18*, Declination = -53° 46', Quadrant = nf, Distance = 12.547", and Δ AR. = 1.137s. Therefore:

ΔRA" = 15*cos(-53° 46')*1.137 ≈ 10.08"

Angle of Posn. = acos(ΔRA"/Distance).180/ π ≈ 36.55°

PA = 90 – 36.55 ≈ 53.5°.

4.5.1.3 PA Method 4

For DUN 18*, Declination = -53° 46', Quadrant = nf, Distance = 12.547", and Δ Declin. = 6.659". Therefore:

ΔRA" = 15*cos(-53° 46')*1.137 ≈ 10.08"

Angle of Posn. = asin(Δ Declin/Distance).180/ π ≈ 32.05°

PA = 90 – 32.05 ≈ 58.0°.

4.5.2 Dunlop's Mean Position Angles

Histograms of Dunlop's mean PAs are given in Figures 3 and 4. In each case the PA represented is the average of the possible PA's for each pair. For example, from Table 3, the Dunlop PA for DUN 18∗ is ~57.0°. As expected, the PAs for both telescopes cover the domain 0° < PA < 360°, though we note from Figure 4 a decrease in the number of PAs as the value of the PA

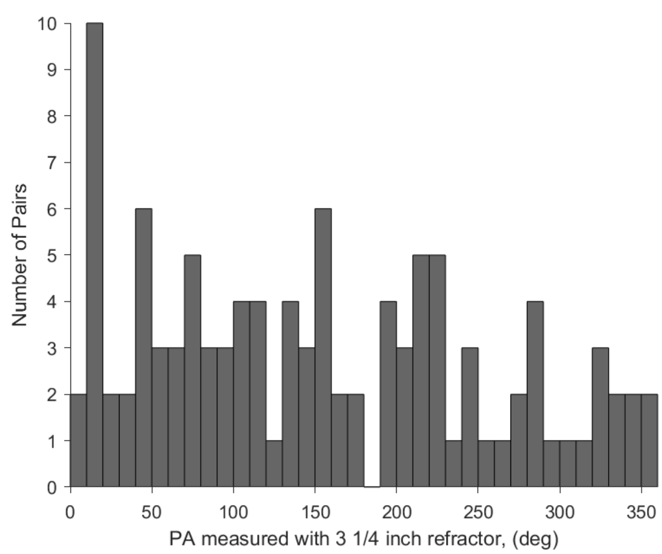

Figure 4: PA measured with the 3 ¼ inch refractor. PAs were calculated using the mean result for each pair taken from the available methods in Table 3.

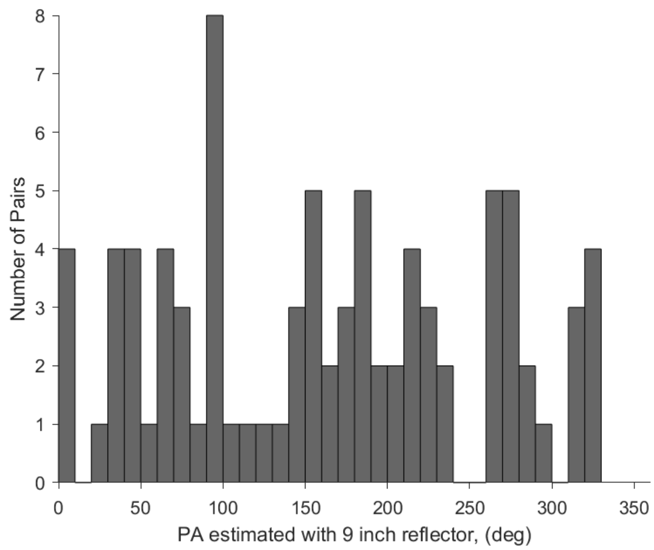

Figure 4. PA measured with the 9 inch reflector. PAs were calculated using the average result for each pair taken from the available methods in Table 3.

increases, for the 3 ¼ inch refractor; and, we suggest, a possible quadrant ambiguity in some values of PA between 10°-20° and 180°-190°.

4.6 Separation and Telescope Resolution (Columns 5, 7, 8, 9)

Separations (Seps) in the modern form (measured in arcseconds) were recorded in column 7 "Distance". However, not all separations were recorded this way. Like the PAs, separation information can be extracted by a combination of other columns. These ways are summarized in Table 4 which should be read in conjunction with Dunlop's Catalogue (Dunlop 1829a). In the following section (section 4.6.1) we explain each method.

Column 7 "Distance" of DUN 17*, 181, 183*, 215 contain two distances separated by an "and"; DUN 141* by an "or". In each case (except for 141*), three stars are involved. For the histograms in Figures 5 and 6, we have used the larger of the two distances to calculate the mean separations of doubles.

4.6.1 How to determine Position Angles from Dunlop's Catalogue

DUN 18* has information recorded in all relevant columns (5, 6, 7, 8, 9) and so we use it as an example. Please refer to Table 1, section 4.2 for explanation of terms.

4.6.1.1 Separation Method 1

For DUN 18*, Distance = 12.547". Therefore:

Sep = 12.547".

4.6.1.2 Separation Method 2

For DUN 18*, Declination = -53° 46', Δ AR. = 1.137s, and Δ Declin. = 6.659". Therefore:

ΔRA" = 15*cos(-53° 46')*1.137 ≈ 10.08"

Sep = √(ΔRA"^2 + Δ Declin.^2) ≈ 12.1"

4.6.1.3 Separation Method 3

For DUN 18*, Declination = -53° 46', Angle of Posn. = 30° 4', and Δ AR. = 1.137s. Therefore:

ΔRA" = 15*cos(-53° 46')*1.137 ≈ 10.08"

Sep = ΔRA"/cos(Angle of Posn.) ≈ 11.6"

4.6.1.3 Separation Method 4

For DUN 18*, Angle of Posn. = 30° 4', and Δ Declin. = 6.659". Therefore:

Sep = Δ Declin./sin(Angle of Posn.) ≈ 13.3"

The smallest separation published by Dunlop was 2 arcsec (DUN 24, 33, 50, 84*, 132*, 170 and 173) for both telescopes. For comparison, the largest mean separations were DUN 125* at ~ 440.0" for the 3 ¼ inch and DUN 72 at ~136.6" for the 9 inch. The theoretical resolution for two stars of equal brightness is 1.4" and 0.5" for a modern $3^1/_4$ inch refractor and the 9 inch reflector respectively.

(Text continues on page 358)

Table 4: Ways of calculating Separations (Seps) from Dunlop's Catalogue.

Method	Columns used (see Table 1)	3 ¼ inch (# possible Seps)	9 inch (# possible Seps)	Example (DUN 18*)
1	7	60	77	= 12.547"
2	4, 8, 9	66	9	~12.1"
3	4, 5, 8	54	4	~11.6"
4	5, 9	69	5	~13.3"
			Mean	~12.4"

The Southern Double Stars of James Dunlop I: History and Description of the First Published Catalogue ...

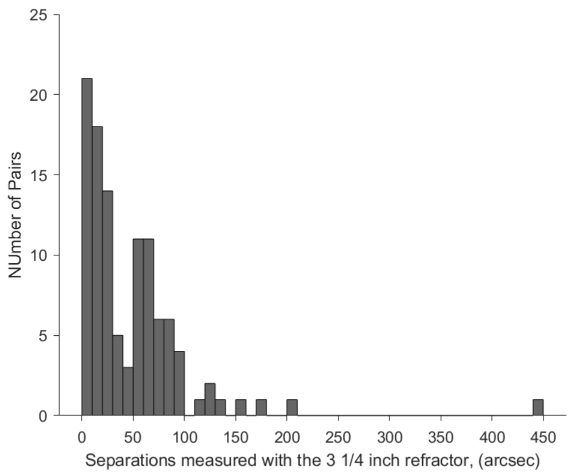

Figure 5. Mean separation measured with the 3 1/4 inch refractor. The smallest separation is ~2.0", the largest ~440.0". Median Separation is ~32".

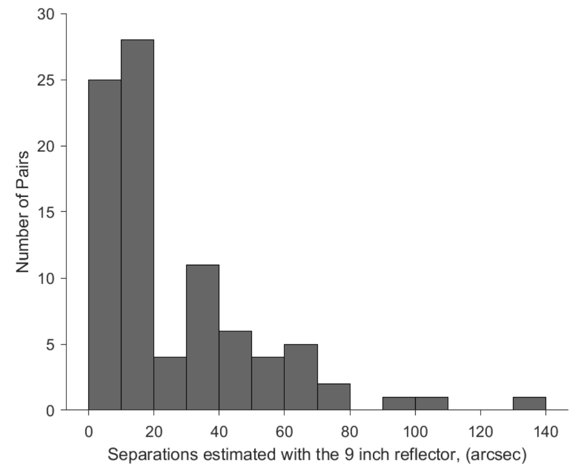

Figure 6. Mean Separation measured with the 9 inch reflector. The smallest Separation is ~2.0", the largest ~136.6". Median Separation is ~14".

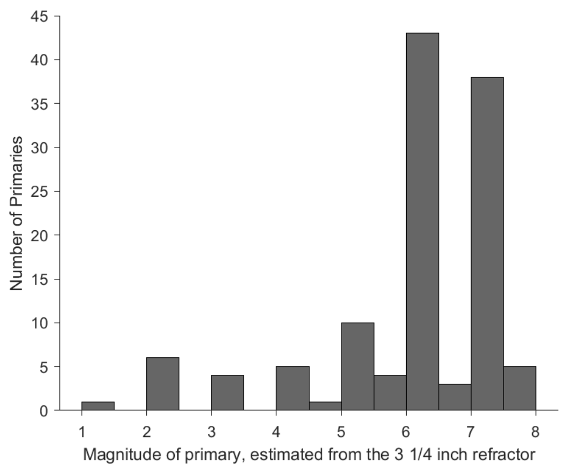

Figure 7. Estimates of magnitudes of primaries through the 3 1/4 inch refractor.

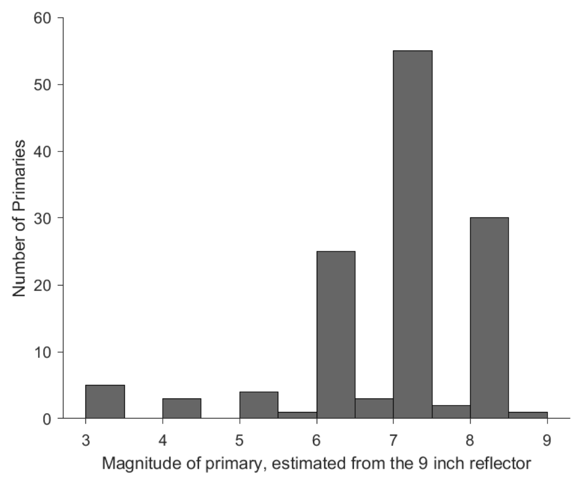

Figure 8. Estimates of magnitudes of secondaries through the 3 1/4 inch refractor.

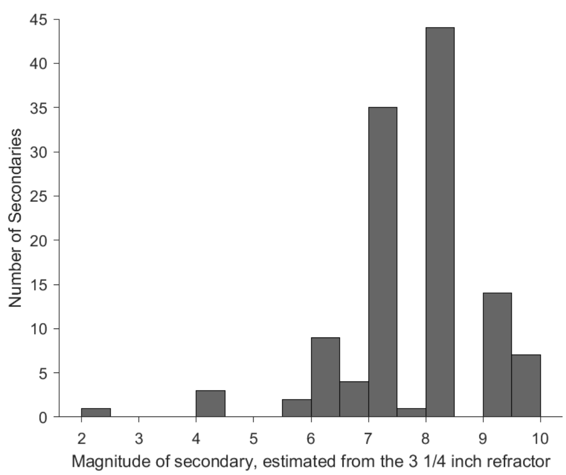

Figure 9. Estimates of magnitudes of primaries through the 9 inch reflector.

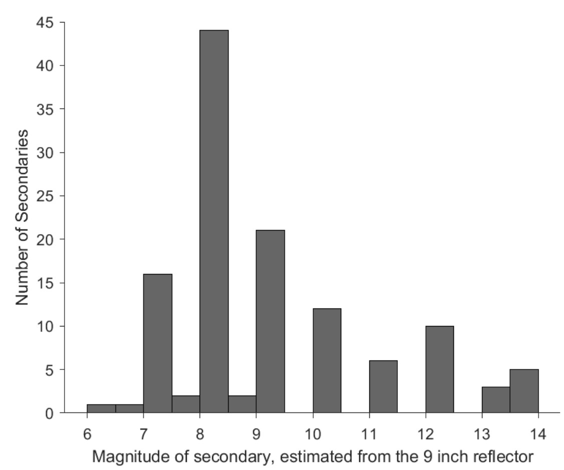

Figure 10. Estimates of magnitudes of secondaries through the 9 inch reflector.

(Continued from page 356)

4.7 Magnitudes (Column 10)

Column 10 contains magnitude estimates for up to three stars. Magnitude statistics are summarized in Table 5. Histograms for primary and secondary magnitudes estimated through the 3 ¼ inch and 9 inch are presented in Figures 7 - 10.

The faintest primary star catalogued with the 3¼ inch was (reported to be) magnitude 10 (on Dunlop's estimation) and the faintest secondary reported with the 9 inch was magnitude 14.

These magnitudes are, in the opinion of the authors, too faint for the period 3¼ inch refractor and the home-made 9 inch speculum. There is debate, especially amongst amateur astronomers, about the magnitude limit that modern telescopes can reach, and this has been studied by many (e.g. Schaefer, 1990). An experienced young observer using a modern 80 mm refractor and 230 mm reflector at 100 magnifications may 'see' magnitude 13.5 and 15.1 respectively. However, measuring the position of a faint star is a very different thing to 'glimpsing' it in the eyepiece. These modern seeing limits are very much overestimated and the instruments at Parramatta observatory were not "modern", and the reflector contained a speculum metal mirror, the reflectance of which was perhaps 70% at best. Magnitude estimates by early telescopic observers are notoriously overestimated, and it was not until 1905 that the modern rational Pogson scale became standard (Jones 1968).

Given these caveats, the magnitude estimates by Dunlop should be treated with considerable care. Nevertheless, the limiting completeness magnitudes of ~7 and ~8.5 for the 3 ¼ and 9 inch respectively, are readily acceptable.

4.8 Remarks (Column 11)

Brief notes are given for 36 pairs from the 3 ¼ inch and 43 from the 9 inch. Some statistics on recurring themes in the Remarks Column are summarised in Table 6.

Table 5: Statistics on magnitude information.

Component	3 ¼ inch (# measures)	9 inch (# measures)
Primary	120	129
Secondary	120	123
Tertiary	2	8

From Table 6 it is noteworthy that Dunlop chose to inject subjective remarks into his catalogue with words such as "pretty" and "beautiful". More importantly, he included one single star (DUN 3) in what was supposedly a double star catalogue.

5. Conclusion

There can be no question that Dunlop's publication of the first dedicated catalogue of southern double stars is a major achievement and should be acknowledged as such. Nevertheless its production was not rigorous by today's standards. There are large amounts of missing or incomplete data, subjective comments on some pairs, and even the deliberate inclusion of a single star. Most disappointing were the discrepancies in recording measures from which position angles and separations for each double can be made (in up to four ways each) - none of them agreed - and so averages were used for analysis. Of the 253 doubles presented, 120 were observed from the Paramatta's Observatory's own 3 ¼ inch refractor; 132 from Dunlop's own self-made 9 inch reflector. The smallest separation claimed was ~2 arcsec. As for Herschel's criticisms, they may be justified in some cases, but were unfair considering he had access at the Cape to a telescope much superior to any Dunlop used, to say nothing of his own skills and resources.

Acknowledgements

Pawlowicz, R., 2018. "M_Map: A mapping package for MATLAB", version 1.4j, [Computer software], available online at www.eoas.ubc.ca/~rich/map.html.

Table 6: Statistics on the Remarks (Column 11)

Contents of Remarks	3 ¼ inch (num of Remarks)	9 inch (num of Remarks)
Number of Remarks	36 (out of possible 121)	43 (out of possible 132)
"L. C." (de Lacaille)	15	5
"pretty"	4	8
"beautiful"	3	1
"triple", "triangle", "three"	4	10

References

Bode, Johann Elert. 1782, Vorstellung Der Gestirne Auf XXXIV Kupfertafeln Nach Der Pariser Ausgabe Des Flamsteadschen Himmels Atlas. Berlin: Lange. http://adsabs.harvard.edu/abs/1782vgkp.book.....B.

———. 1805, Vorstellung Der Gestirne Auf Vier Und Dreyssig Kupfertafeln: Nebst Einer Anweisung Zum Gebrauch Und Einem Verzeichnisse von 5877 Sternen, Nebelflecken Und Sternhaufen. 2nd ed. Berlin ; Stralund: Lange. http://adsabs.harvard.edu/abs/1805vgvd.book.....B.

Brenchley, Elizabeth, 1980, Parramatta Observatory Old Government House Parramatta: The Case for Archaeological Investigation. http://dx.doi.org/10.4227/11/54D02928F133E.

Cozens, Glendyn J, Andrew Walsh, and Wayne Orchiston, 2010, "James Dunlop's Historical Catalogue of Southern Nebulae and Clusters", *Journal of Astronomical History and Heritage*, **13**, 59–73. http://adsabs.harvard.edu/abs/2010JAHH...13...59C.

Cozens, Glendyn J, and Graeme L White, 2001, "James Dunlop: Messier of the Southern Sky", *Sky & Telescope*, June, 112–16. http://adsabs.harvard.edu/abs/2001S%26T...101f.112C.

Csiszar, Alex, 2017, "How Lives Became Lists and Scientific Papers Became Data: Cataloguing Authorship during the Nineteenth Century", *British Journal for the History of Science*, **50** (1). England: 23–60. https://doi.org/10.1017/S0007087417000012.

Dunlop, James, 1828, "A Catalogue of Nebulae and Clusters of Stars in the Southern Hemisphere, Observed at Paramatta in New South Wales", *Royal Society of London Philosophical Transactions (Series I)*, **118** (1), 113–51. http://adsabs.harvard.edu/abs/1828RSPT..118..113D.

———, 1829a, "Approximate Places of Double Stars in the Southern Hemisphere, Observed at Paramatta in New South Wales," *Memoirs of the Royal Astronomical Society*, **3** (1), 257–75. http://adsabs.harvard.edu/abs/1827MmRAS...3..267D.

———, 1829b, "Description of Some Remarkable Nebulae and Clusters of Stars in the Southern Hemisphere, Observed at Paramatta, in New South Wales", *Edinburgh Journal of Science*, **10** (20), 282–94. http://archive.org/details/edinburghjournal10edinuoft.

Herschel, John F W., 1828, "The Society's Medal to Mr. Dunlop", *Monthly Notices of the Royal Astronomical Society*, **1** (9), 60–62. http://adsabs.harvard.edu/abs/1828MNRAS...1...60.

———, 1847, "Results of Astronomical Observations Made During the Years 1834, 1835, 1836, 1837, 1838, at the Cape of Good Hope; Being the Completion of a Telescopic Survey of the Whole Surface of the Visible Heavens, Commenced in 1825", London: Smith, Elder & Co. http://adsabs.harvard.edu/abs/1847raom.book.....H.

Jones, Derek, 1968, "Norman Pogson and the Definition of Stellar Magnitude", *Astronomical Society of the Pacific Leaflets*, **10** (469), 145–52. http://adsabs.harvard.edu/abs/1968ASPL...10..145J.

Letchford, Roderick R, Graeme L White, and Allan D Ernest, 2017. "The Southern Double Stars of Carl Rümker I: History, Identification, Accuracy." *JDSO*, **13** (2), 220–32. http://www.jdso.org/volume13/number2/Letchford_220-232.pdf.

———, 2018a, "The Southern Double Stars of Carl Rümker II: Their Relative Rectilinear Motion." *JDSO*, **14** (2), 208–22. http://www.jdso.org/volume14/number2/Letchford_208_222.pdf.

———, 2018b, "The Southern Double Stars of Carl Rümker III: Quantified Probability of Boundedness and Preliminary Grade 5 Orbits for Some Very Long Period Doubles", *JDSO*, **14** (4), 761–70. http://www.jdso.org/volume14/number4/Letchford_761_770.pdf.

Richardson, William, 1835, *A Catalogue of 7385 Stars: Chiefly in the Southern Hemisphere, Prepared from Observations Made in the Years 1822, 1823, 1824, 1825, and 1826, at the Observatory at Paramatta, New South Wales, Founded by Lieutenant General Sir Thomas Makdougall Brisbane*, London: William Clowes and Sons. http://adsabs.harvard.edu/abs/1835acos.book.....R.

Rümker, Carl, 1832, *Preliminary Catalogue of Fixed Stars: Intended for a Prospectus of a Catalogue of the Stars of the Southern Hemisphere Included Within the Tropic of Capricorn : Now Reducing from the Observations Made in the Observatory at Paramatta*, Hamburg: Perthes and Besser. http://adsabs.harvard.edu/abs/1833AN.....10..377R.

Rutledge, Sharon, 2009, "For Further Consideration: Mr James Dunlop, Esq." *Journal and Proceedings of the Royal Society of New South Wales*, **142**, 17–28. http://nsw.royalsoc.org.au/publications/journal_2000_on/142_p1,2_rutledge.pdf.

Schaefer, Bradley E., 1990, "Telescopic Limiting Magnitudes", *Publications of the Astronomical Society of the Pacific*, **102** (February), 212. doi:10.1086/132629.

Service, John, 1890, "A Biographical Sketch of James Dunlop, Esq.", *In Thir Notandums : Being the Literary Recreations of Laird Canticarl of Mongrynen of Kittle Memory*, 128–222. Edinburgh ; Sydney: Young J. Pentland ; Angus & Robertson. http://library.sl.nsw.gov.au/record=b1729860~S2.

White, Henry, and Herbert F Morley, 1868, "Catalogue of Scientific Papers (1800-1900): 1st Ser., 1800-1863", Volume II. Royal Society of London. https://archive.org/stream/cataloguescient01unkngoog.

Wood, Harley W., 1966, "James Dunlop (1793-1848).", *Australian Dictionary of Biography: Volume I 1788 - 1850 A-H*, edited by Douglas Pike, 338. Melbourne University Press. http://adb.anu.edu.au/biography/dunlop-james-2008.

The Southern Double Stars of James Dunlop II: Modern Identification of the First Dedicated Published Catalogue of Southern Double Stars

Roderick R. Letchford[1], Graeme L. White[2], Allan D. Ernest[3]

1. Vianney College Seminary, Wagga Wagga, NSW 2650, Australia, rodvianney@yahoo.com.au
2. Centre for Astronomy, University of Southern Queensland, Toowoomba, Australia QLD 4350, graemewhiteau@gmail.com
3. Charles Sturt University, Wagga Wagga, NSW 2650, Australia, aernest@csu.edu.au

Abstract: The first dedicated catalogue of southern double stars was published in 1829 by James Dunlop. Basing our work solely on the published data, we present modern designations of the doubles listed by Dunlop in the *Appendix*. We find that of the 253 listed; 168 have discoverer codes in the WDS under "DUN"; 31 are listed under another discoverer code; 27 remain unidentified; 11 are single stars; 8 are double stars not in the WDS and 8 are multiple systems.

1. Introduction

This paper (Dunlop Paper II) continues a series of papers on the double stars of James Dunlop, one of three astronomers who worked at the privately-owned observatory in Parramatta, NSW Australia in the 1820's. The Parramatta Observatory was the venture of Sir Thomas Makdougll Brisbane (1773-1860) the 6th British Governor of the Colony of NSW from 1822 to 1825.

In Dunlop Paper I (Letchford, White and Ernest, this issue) we presented a history and description of the first published dedicated catalogue of southern double stars, by James Dunlop (1793-1848) and issued in 1829 as *Approximate Places of Double Stars in the Southern Hemisphere*, observed at Paramatta in New South Wales (Dunlop, 1829).

The Dunlop papers follow three papers (Rümker Papers I, II, and III) previously published in this journal on the double star work of another of the Parramatta astronomers, Carl Rümker (Letchford, White, & Ernest, 2017, 2018a, 2018b).

In this paper (Dunlop Paper II), we present modern designations of the pairs in Dunlop's original catalogue.

2. Modern Identification of the Dunlop Doubles

We identified the stars in the original catalogue using the same method as presented in our paper on the southern doubles of Carl Rümker (Letchford, White, & Ernest, 2017, Rümker Paper I). In addition, we compared our identifications with those of Andrew James who has written excellent and extensive notes on many (not all) of the individual doubles of Dunlop and has them available on the web. We agree with James' identifications except where he suggests possible candidates for some of those we classify as "unidentified". In such cases (e.g. DUN 50 which has a missing declination in the original published catalogue, which James identifies as RST 2482), we have chosen only to identify those we are more confident about.

The Table of Identification for the Dunlop pairs is given in the Appendix of this paper.

Dunlop's catalogue of 1829 is a real assortment of data. As detailed in Dunlop Paper I, it consists of discoveries made with two different telescopes; the Parramatta Observatory's 3¼ inch refracting telescope (measures from this telescope Dunlop designated with an asterisk, ∗) and Dunlop's homemade 9 inch speculum mirrored reflector. Statistics on the observations are summarized in Table 1.

We note from Table 1 that the number of confirmed doubles found with the 3¼ inch is 121, and 132 for the 9 inch, and that the number of doubles either unidentified or in which only one star was found by the

Table 1: Statistics of Modern Identifications

	3¼ inch refractor (*)	9 inch reflector
Telescope	121	132
In WDS as "DUN"	83	85
In WDS as another discoverer	21	12
"unidentified"	5	11
"one"	5	10
"two"	7	6
"three", "four", "five"	0	8

authors are 10 and 21 respectively. This suggests that Dunlop did his best work with the 3¼ inch, which might be expected given its superior build quality (Letchford, White and Ernest, Dunlop Paper I, IN PRINT).

Except for DUN 58, it is not obvious from Dunlop's published catalogue which pair should be taken as the Dunlop double in those entries marked with a "three", "four", or "five" in Column 2. In such cases only the brightest star was inserted into the Modern Identification of the Appendix.

2.1 Notes on Some Individual Pairs

DUN 3 is described as a single star by Dunlop, but is the double LDS 2199 (01270-3233).

The single star DUN 54* is part of the open cluster NGC 2451 which in fact is two open clusters NGC 2451A and NGC 2451B aligned along the same line of sight.

DUN 64* and DUN 65* are a group of stars associated with γ Argus, now γ Velorum. The identification of these pairs is made difficult by the fact that Dunlop recorded both as having the same RA and DE. We base our identification on his magnitude estimates: 2.3 and 8 for DUN 64* and 2.3 and 6 for DUN 65*. Thus: DUN 64 AC and DUN 65 AB are the respective discoverer and component codes.

DUN 122* and DUN 123* are listed in the WDS as DUN 252AC and DUN 252AB respectively, i.e. *alf01 Cru (α Crucis), both with WDS 12266-6306.

DUN 252AB* is listed in the WDS with 12266-6306 (otherwise DUN 122* and 123*). We identify it as two stars (HR 8996 and HD 222830) not previously categorized as double.

DUN 253AB* is listed in the WDS as 14067-3622, but is identified here as LAL 192, WDS 23544-2703.

2.2 Omissions in the WDS

In the course of our investigation, we identified 13 apparent doubles first discovered by Dunlop but which are not in the WDS, namely those indicated by a "two" in Column 2 of the Appendix: 35*, 37, 100, 107, 112*, 118, 119*, 149*, 153*, 164*, 167, 198, 252*.

3. Format of the Appendix "Identification of Dunlop's Double Stars"

We present in the Appendix a detailed cross identification of Dunlop (1829). The column details are given in Table 2.

4. Conclusion

Basing our work solely on the published data, we present modern designations of the double stars listed by Dunlop. We find that of the 253 listed; 168 have dis-

Table 2: Explanation of Columns in "Identification of Dunlop's Double Stars", Appendix

Column	Name	Data
1	DUN	A running catalogue entry corresponding to the entries of Dunlop, 1829. An asterisk '*' indicates that Dunlop observed this pair with the 3 1/4 refractor; without, with the 9 inch reflector.
2	WDS	Washington Double Star Catalog (WDS) designation. "one" indicates that only one star could be found. "two" indicates that two stars were found that are not recorded as double stars in the current WDS. So for "three", "four" and "five". "Unidentified" means that the pair remains unidentified.
3	DisC	Discoverer Code as it appears in the WDS
4	Comp	Component as and only if it appears in the WDS
5	SIMBAD	Main SIMBAD name of star: Primary on first line; secondary on second
6	ASCC	All-sky Compiled Catalogue of 2.5 million stars, 3rd version, identification number: Primary on first line; secondary on second
7	GAIA DR2	Gaia data release 2, Source ID: Primary on first line; secondary on second

coverer codes in the WDS with "DUN"; 33 are listed under another discoverer code; 31 remain unidentified or are single stars; 13 are double stars not in the WDS and 8 (9 if 54* is included here) are members of multiple systems.

The Table of Identification for the Dunlop pairs is given in the Appendix accompanying this paper.

5. Acknowledgements

Simbad database, operated at CDS, Strasbourg, France (SIMBAD).

The Aladin sky atlas developed at CDS, Strasbourg Observatory, France.

The Washington Double Star Catalog maintained by the USNO (WDS).

All-sky Compiled Catalogue of 2.5 million stars, 3rd version (ASCC).

The Gaia Catalogue (Gaia DR2, Gaia Collaboration, 2018), from VizieR (GAIA DR2).

6. References

Dunlop, J., 1829, “Approximate Places of Double Stars in the Southern Hemisphere, observed at Paramatta in New South Wales”, *Memoirs of the Royal Astronomical Society*, **3**(1), 257–275. Retrieved from http://adsabs.harvard.edu/abs/1827MmRAS...3..267D

Letchford, R. R., White, G. L., & Ernest, A. D., 2017, “The Southern Double Stars of Carl Rümker I: History, Identification, Accuracy”, *Journal of Double Star Observations*, **13**(2), 220–232. Retrieved from http://www.jdso.org/volume13/number2/Letchford_220-232.pdf

Letchford, R. R., White, G. L., & Ernest, A. D., 2018a, “The Southern Double Stars of Carl Rümker II: Their Relative Rectilinear Motion”, *JDSO*, **14**(2), 208–222. Retrieved from http://www.jdso.org/volume14/number2/Letchford_208_222.pdf

Letchford, R. R., White, G. L., & Ernest, A. D., 2018b, “The Southern Double Stars of Carl Rümker III: Quantified Probability of Boundedness and Preliminary Grade 5 Orbits for Some Very Long Period Doubles”, *JDSO*, **14**(4), 761–770. Retrieved from http://www.jdso.org/volume14/number4/Letchford_761_770.pdf

Letchford, R. R., White, G. L., & Ernest, A. D., 2019, “The Southern Double Stars of James Dunlop I: History and Description of the first Published Catalogue dedicated to Southern Double Stars”, *JDSO*, **15**(3), 350-360. This issue.

http://simbad.u-strasbg.fr/simbad/

https://aladin.u-strasbg.fr

https://ad.usno.navy.mil/wds

http://vizier.u-strasbg.fr/viz-bin/VizieR-3?-source=I/280B/ascc

http://vizier.u-strasbg.fr/viz-bin/VizieR-3?-source=I/345/gaia2

Appendix

Identification of Dunlop's Double Stars

(see Table 2, Section 3, for explanation of columns)

DUN	WDS	DisC	Comp	SIMBAD	ASCC	GAIA DR2
1*	00315-6257	LCL 119	AC	*bet01 Tuc	2292377	4900927434176620160
				*bet02 Tuc	2292378	4900926678262376704
2*	00524-6930	DUN 2		*lam01 Tuc	2373287	4691995692046507520
				HD 5208	2373289	4691996001284152576
3	01270-3233	LDS 2199		V* R Scl	1716249	5016138145186249088
				CCDM J01270-3233B		
4*	01388-5327	DUN 4		HD 10241	2103580	4912810337375316992
				CPD-54 358B	2103581	4912810337375317632
5*	01398-5612	DUN 5		*p Eri A	2199057	4911306239828325632
				*p Eri B	2199056	4911306239828325760
6	02165-5131	DUN 6	AB	*phi Eri	2104402	4936685751335824896
				CD-52 465	2104399	4936685716976087552
7	02397-5934	DUN 7	A,BC	HD 16852	2200322	4726060211542143616
				HD 16853	2200329	4726066018337928192
8*	02572-2458	S 423	AB,C	HD 18455A	1525490	
				HD 18445	1525486	5076269164798852864
9*	02583-4018	PZ 2		*tet01 Eri	1909803	5044368071869592832
				*tet02 Eri	1909804	5044368071868204160
10	03046-5119	DUN 10	AB	HD 19330	2105363	4747692278185293312
				CD-51 706	2105365	4747693686934567040
11	unidentified					
12	03152-6427	DUN 12	A,BC	HD 20586	2295352	4672336699019592320
				CCDM J03152-6427BC	2295353	4672336694724418560
13*	unidentified					
14	03382-5947	DUN 14		HD 22989	2201630	4728825002249947904
				HD 22960	2201628	4728825036609672576
15*	03398-4022	DUN 15		HD 22986A	1910857	4849246401941883264
				HD 22986B	1910855	4849246397645456000
16*	03486-3737	DUN 16		HD 24072	1817423	4856719713756945664
				HD 24071	1817421	4856719713756946176
17*	04010-5424	DUN 17	AB	HD 25590	2106767	4779816503255644672
				HD 25591	2106768	4779816297097214336
18*	04509-5328	DUN 18	AB	*iot Pic A	2108254	4777112872882315648
				*iot Pic B	2108256	4777112872882315264

Appendix: Identification of Dunlop's Double Stars continued

DUN	WDS	DisC	Comp	SIMBAD	ASCC	GAIA DR2
19*	one			HD 34496	1724040	4826073060516094080
20*	05248-5219	DUN 20	AB,C	* tet Pic	2109422	4771835629385988992
				HD 35859	2109419	4771835595026248832
21	05302-4705	DUN 21	AD	HD 36553	2012117	4798709239757160320
				HD 36520	2012100	4798709067958473216
22*	05312-4219	DUN 22		HD 36648	1915227	4806195676992118784
				CD-42 1975B	1915228	4806195299034996864
23	06048-4828	DUN 23		V* V575 Pup	2013728	5554191685020871424
				TYC 8105-1651-2	2013729	5554191685019290368
24	one			*del Pic	2111224	5499415974230271488
25	06189-3212	JSP 96		TYC 7077-705-1	1728092	2892904187481797504
				TYC 7077-705-2	1728093	2892904187482208128
26*	06122-6532	DUN 26	AB	HD 43618	2379551	5476519984615508224
				HD 43639	2379552	5476521251625953152
27*	06163-5913	DUN 27	AB	HD 44120	2206307	5482551183847322752
				HD 44105	2206304	5482551183847322496
28*	06240-3642	DUN 28	AC	HD 45145	1824828	5575351648860045312
				HD 45158	1824835	5575351545780828032
29*	06291-4022	DUN 29		HD 46039	1918620	5570747993673945984
				HD 46040	1918630	5570747890594733568
30	06298-5014	DUN 30	AB,CD	HR 2384	2112078	
				TYC 8111-2008-2	2112074	
31*	06386-4813	DUN 31		HD 47973	2015711	5551248086235237248
				CD-48 2416	2015712	5551248292393667200
32*	06423-3824	DUN 32		HD 48543A	1826228	5576835955197352192
				HD 48543B	1826226	5576836023916828288
33	one			HD 49319	1826535	5575933531029392896
34*	06442-5442	DUN 34		HD 49219	2112826	5497185992850609152
				HD 49192	2112821	5497185133857153920
35*	two			HD 49942	1920145	5562241106570387584
				HD 49850	1920113	5562253407356693120
36*	06504-3142	H 5 108	A,BC	V* HZC Ma	1730756	5583324035874959360
				CD-31 3719	1730759	5583323314320455936
37	two			HD 53142	**2113773**	5505040697762533760
				HD 53348	**2113809**	5505041728554364928

Appendix: Identification of Dunlop's Double Stars continued

DUN	WDS	DisC	Comp	SIMBAD	ASCC	GAIA DR2
38*	07040-4337	DUN 38	AB	HD 53705	1921369	5559265690666326016
				HD 53706	1921372	5559265690666327168
39*	07033-5911	DUN 39		HD 53921A	2208454	5480486644608749696
				HD 53921B	2208456	5480486640313882880
40*	07092-5622	DUN 40		HD 55327	2208793	5490000787442758144
				HD 55352	2208795	5490000787442760576
41	07104-5536	RMK 5		HD 55598	2208862	5490328648067150720
				CD-55 1708	2208857	5490328648067151104
42*	07087-7030	DUN 42		*gam02 Vol	2445952	5267405895348357120
				*gam01 Vol	2445949	5267405964069463680
43*	07171-3706	DUN 43	AB	*pi. Pup Aa	1829087	5589311357724458368
				HD 56856	1829080	5589305477912168192
44	unidentified	RMK 6		HD 57852	2114933	5492026740697659648
				HD57853	2114936	5492026740697659264
45*	07214-4832	DUN 45		HD 58017	2018751	5506905297684851584
				HD 58018	2018756	5506905228965376768
46	unidentified					
47	07247-3149	DUN 47	A,CD	HD 58535	1734969	5592885801315568768
				HD 58534	1734962	5592886110552963968
48*	unidentified					
49	07289-3151	DUN 49		HD 59499	1735664	5593011729755869696
				HD 59500	1735667	5593011832835083008
50	unidentified					
51	07292-4318	DUN 51		*sig Pup	1923547	5512070906388269568
				*sig Pup B	1923553	5512071009471894912
52*	07343-2328	H N 19		*n Pup A	1550714	5618420137803147008
				*n Pup B	1550719	5618420137803146240
53*	07388-2648	H 3 27	AB	*k02 Pup	1645677	5612323414549657728
				*k01 Pup	1645672	5612323414549657984
54*	one			* c Pup	1831780	5538814190271704960
55*	07442-5027	DUN 55	AC	HD 63008	2116430	5493209501673364736
				CD-50 2948	2116437	5493209437253410432
56*	07471-4130	DUN 56		HD 63425	1925301	5535916496103849088
				V* V394 Pup	1925303	5535916393024640896

Appendix: Identification of Dunlop's Double Stars continued

DUN	WDS	DisC	Comp	SIMBAD	ASCC	GAIA DR2
57	07418-7236	DUN 57		*zet Vol	2447249	5263150888430032256
				*zet Vol B	2447251	5263150888430032384
58	three			HD 65013	1926351	5531438838080560384
				HD 65037	1926359	5531438558901143680
59	07592-4959	DUN 59	AB	HD 66005	2022196	5514090400016110976
				HD 66006	2022202	5514090434376720512
60	08014-5431	DUN 60		V* V461 Car	2117504	5320234267972369152
				CD-54 2029	2117508	5320234057513080320
61	08069-2707	DUN 61		HD 67409	1652760	5694066331642125824
				CD-26 5531	1652767	5694066709599229568
62*	08047-6250	DUN 62		HD 67536	2304263	5289522090708710656
				CD-62 329	2304251	5289516936747952768
63*	08098-4238	DUN 63		HD 68242A	1928607	5533290621824556672
				HD 68242B	1928610	5533290621824555264
64*	08095-4720	DUN 65	AC	*gam02 Vel	2023562	
				CD-46 3848	2023566	5519219999721187968
65*	08095-4720	DUN 65	AB	*gam02 Vel	2023562	
				*gam01 Vel	2023557	5519266900766220800
66*	08079-6837	RMK 7		*eps Vol A	2383172	5270986008289935232
				*eps Vol B	2383174	5270986008289935488
67	08140-3619	DUN 67		HD 69081	1835488	5541637564345383808
				HD 69082	1835490	5541624335846120192
68	08136-3621	DUN 68		HD 68944	1835397	5541636739711787264
				HD 68962	1835404	5541636945870181632
69	08255-5144	DUN 69	AB	HD 71510	2118943	5322244690627583104
				CD-51 3003	2118941	5322244690627585280
70*	08295-4443	DUN 70		HD 72127A	1931221	5522979294390810752
				HD 72127B	1931220	5522979294390810624
71	08306-4031	DUN 71		HD 72318	1931403	5527782446519946880
				HD 72317	1931411	5527782480879666816
72	08404-4223	DUN 72	A,BC	HD 74105	1932766	5525075856907721216
				HD 74104	1932764	5525076548400146688
73*	08562-5532	DUN 73	AB	HD 76824	2215700	5305072895992630784
				HD 76823	2215701	5305073136510805760
74*	08570-5914	DUN 74		*b01 Car	2215750	5303286052150068352
				CD-58 2350	2215754	5303286017790332416
75	09179-6948	RMK 10		HD80807	2386328	5222647212228907136
				CPD-691035B	2386329	5222650171466372480

Appendix: Identification of Dunlop's Double Stars continued

DUN	WDS	DisC	Comp	SIMBAD	ASCC	GAIA DR2
76*	09286-4530	DUN 76	AC	HD 82109	2032680	5423001668454182656
				HD 82121	2032690	5423001462295754368
77	09293-4432	DUN 77	AB	HD 82207	1938548	5423340970868485504
				HD 82241	1938560	5423346674585062144
78*	09308-3153	DUN 78		*zet01 Ant A	1753443	5632038276500794496
				*zet01 Ant B	1753440	5632038276500795648
79*	09336-4945	DUN 79		HD 82965	2033099	5409197334336573056
				HD 82986	2033117	5409197437415809024
80	09450-4929	DUN 80	AB	HD 84627	2034180	5409029212137818368
				HD 84612	2034174	5409029212137815808
81	09543-4517	DUN 81		HD 85980	2035254	5411771119252271872
				HD 85980B	2035252	5411771119252271360
82	09333-8601	DUN 82		HD 85300	2453141	5189985016733501440
				CPD-85 210B	2453130	5189985021031273472
83	10021-5459	DUN 83		HD 87254	2130673	5260124688857959040
				HD 87221	2224417	5260124345260563200
84*	10032-5203	HJ 4282		HD 87364	2130814	5404964317652126336
				HD 298817	2130810	5404964283292384384
85	10288-6235	DUN 85		HD 91027	2316921	5252242702326780160
				HD 91026	2316914	5252242667967046016
86*	10312-4214	DUN 86	AB	HD 91239	1945198	5368269388368281600
				HD 91223	1945183	5368269285289064832
87*	10307-6121	DUN 87		HD 91270	2317155	5253945227372557312
				HD 91269	2317146	5253948354108765696
88*	10320-4504	PZ 3		HD 91355	2039586	5367389229311297280
				HD 91356	2039582	5367389229311295872
89*	10333-5523	DUN 89	AB	HD 300791	2230402	5352404294598481920
				HD 91593	2230408	5352404397648913152
90	unidentified					
91*	10319-7207	DUN 91		HD 91601	2456738	5229628256374245248
				CPD-71 1045B	2456739	5229628256374246528
92*	one			*p Car	2317331	5253796346588022656
93*	10349-6408	DUN 93	AB	HD 91906	2317750	5251822104760873344
				HD 307860	2317757	5251822139120626432
94*	10387-5911	DUN 94		HD 92397	2231436	5350588691654540544
				HD 92398	2231442	5350588691654545792

Appendix: Identification of Dunlop's Double Stars continued

DUN	WDS	DisC	Comp	SIMBAD	ASCC	GAIA DR2
95*	10393-5536	DUN 95	AB	*x Vel	2231547	5352174702825907840
				HD 92463	2231572	5352174805905137920
96*	one			HD 92964	2232192	5350406619413548032
97	10432-6110	DUN 97	AB	HD 93010	2318912	5254068613204875264
				CPD-60 2203B	2318913	5254068613204866432
98*	10451-5941	DUN 98	AH	*eta Car	2232700	5350358580171706624
				HD 303308	2232708	5350358683250920704
99*	10443-7052	DUN 99	AB	HD 93344	2457524	5231271579581900800
				HD 93359	2457533	5231271476495341952
100	two			HD 93540	2319277	5239810318189195776
				HD 93600	2319318	5239808668922019584
101	10510-5957	HJ 4378		HD 94173	2233856	5338305738062716544
				CPD-59 2783	2233851	5338305841141942272
102*	10535-5851	DUN 102	AB	*u Car	2234363	5338833263115792512
				HD 94491	2234336	5338832919518362752
103*	10535-5851	DUN 103	AC	*u Car	2234363	5338833263115792512
				CPD-58 2836	2234366	5338833297475543936
104	three			HD 95429	2138437	5359955053246566144
105*	11049-6103	DUN 105		HD 96264	2321918	5337284326102045568
				HIP 54171	2321912	5337283948144897664
106	one			HD 98161	1855147	5397046115926029056
107	two			HD 98537	2459375	5226029103836945280
				HD 98486	2459352	5226076112259827968
108	four			HD 98897	2239471	5339606563379239040
109*	11286-4240	BSO 6		HD 99803	1949977	5382258371728407680
				CD-41 6565B	1949980	5382258371728407040
110	three			HD 100015	2240660	5343376445138829824
111*	11323-2916	H 3 96		*17 Crt A	1670309	3482326708703712896
				*17 Crt B	1670306	3482326708703712640
112*	two			HD 100838	2143041	5369911474631774080
				HD 100786	2142996	5369911058009191424
113*	11370-3858	DUN 113		HD 100954	1856216	5384606275726561792
				HD 100965	1856220	5384603045914957952

Appendix: Identification of Dunlop's Double Stars continued

DUN	WDS	DisC	Comp	SIMBAD	ASCC	GAIA DR2
114	11400-3806	DUN 114		HD 101406	1856371	5385035016545554560
				SAO 202691	1856373	5385035016545554688
115	11400-3327	I 232		HD 101387	1762657	3477249370166290048
				TYC 7220-1242-2	1762658	
116*	11567-3216	DUN 116	AB	HD 103743	1763493	3466924200065405824
				HD 103742	1763490	3466924200065405184
117*	12048-6200	DUN 117	AB	HD 104901	2330777	6057680496326765184
				V* BY Cru	2330784	6057680423278480512
118	two			HD 106132	2246408	6058972663008775808
				HD 106145	2246421	6058971941454265216
119*	two			HD 106344	2397544	5860530296185991552
				HD 106362	2397555	5860530399265248512
120*	unidentified					
121	unidentified					
122*	12266-6306	DUN 252	AC	*alf01 Cru	2333718	
				HD 108250	2333711	6053807844582485248
123*	12266-6306	DUN 252	AB	*alf01 Cru	2333718	
				*alf02 Cru	2333721	
124*	12312-5707	DUN 124	AB	*gam Cru	2248482	
				HD 108925	2248502	6071671369457586688
125*	12477-5941	DUN 125	AC	*bet Cru	2250231	
				HD 111160	2250260	6056724299185776512
126*	12546-5711	DUN 126	AB	*mu.01 Cru	2250896	6060547163653418112
				*mu.02 Cru	2250898	6060547331128876928
127*	12598-5555	DUN 127		HD 112764	2251414	6061478965373623680
				HD 112781	2251416	6061478209476557696
128	13069-4954	DUN 128		*ksi02 Cen	2052802	6081542475600377472
				V* V1261 Cen	2052804	6081530720270030208
129*	13081-6518	RMK 16	AB	*tet Mus A	2401910	5858915766471945984
				*tet Mus B	2401908	5858915766471941248
130	unidentified					
131*	13152-6754	DUN 131	AC	*eta Mus A	2402372	5845487808865581568
				*eta Mus C	2402368	5845487911944804864
132*	unidentified					

Appendix: Identification of Dunlop's Double Stars continued

DUN	WDS	DisC	Comp	SIMBAD	ASCC	GAIA DR2
133*	13226-6059	DUN 133	AB,C	*J Cen	2339008	5869474548409857024
				HD 116072	2339002	5869474617129630976
134	one			*iot Cen	1862167	6165699748415726848
135	five			HD 116119	2339037	5868514605999645696
136	13310-3924	SEE 179		*d Cen	1862827	6161403234933132032
				HD 117425	1862820	6161399867678728960
137*	13321-6303	DUN 137		HD 117460	2340319	5865249812400697472
				CD-62 732B	2340318	5865249812400694272
138*	13368-2630	H N 69	AB	HD 118349A	1675685	6188997162858447360
				HD 118349B	1675683	6188994207920947328
139	three			HD 118258	2255294	6064406277664894208
140	13458-7159	DUN 140		CPD-71 1507	2468095	5839923627169745664
				CPD-71 1507B	2468099	5839923622864522112
141*	13417-5434	DUN 141		*Q Cen A	2154813	6065381024758288128
				*Q Cen B	2154815	6065381029065308416
142*	13440-5914	DUN 142		HD 119283	2256060	5870795061866221952
				HD 119312	2256069	5870795096225959808
143	13492-6206	DUN 143		HD 120112	2342940	5865546577434035712
				HD 120113	2342944	5865546680492798976
144	13496-4722	DUN 144		HD 120275A	2056192	6095002662584749056
				HD 120275B	2056190	6095002623922974080
145	13546-6654	DUN 145		HD 120891	2404962	5850667092761177856
				CD-66 1486	2404966	5850667092761180416
146*	13493-4031	DUN 146		HD 120272	1959103	6113942884244624384
				HD 120287	1959109	6113945804822385408
147*	13521-5249	RMK 18		HD 120642	2155481	6065984557860591360
				HD 120641	2155477	6065984179910876032
148*	13518-3300	H 3 101		V* V983 Cen	1769687	6170485544575679104
				* 3 Cen B	1769689	6170485544575678592
149*	two			HD 120974	1864369	6115338095775994880
				HD 120957	1864353	6115337546020644480
150	13575-5743	DUN 150	AB	V* V412 Cen	2257485	5871308465073102720
				HD 121506	2257470	5871311316931389312
151	13573-5602	DUN 151		HD 121504	2257462	5872266689452551552
				CPD-55 5793	2257469	5872266723812297216

The Southern Double Stars of James Dunlop II: Modern Identification of the First Dedicated ...

Appendix: Identification of Dunlop's Double Stars continued

DUN	WDS	DisC	Comp	SIMBAD	ASCC	GAIA DR2
152	one			*ups02 Cen	2057267	6097035006747824768
153*	two			*chi Cen	1960483	6110115278109271808
				HD 123021	1960490	6110115621706655616
154	14055-3633	DUN 154		HD 122917	1865200	6120853555338661888
				CD-35 9249B	1865203	6120853555338661248
155*	14077-5341	DUN 155		CPD-53 5879	2156705	5896839777864869120
				HD 123186	2156706	5896839846584347264
156	14067-3622	DUN 253	AB	*tet Cen	1865291	
157	14096-5130	HJ 4651		V* V869 Cen	2156835	6089748096519831296
				HD 123530	2156844	6089747340605583616
158	unidentified					
159*	14226-5828	DUN 159	AB	HD 125628A	2260099	5891112112577938816
				HD 125628B	2260102	5891112112577932800
160*	14261-4513	DUN 160		*tau01 Lup	2059445	6099307559838681216
				CD-44 9321	2059437	6099307181888632960
161	one			HD 124580	2058511	6096524382383054720
162	14339-4628	DUN 162		HD 127629	2060207	6098217909463037440
163*	14380-5431	DUN 163		HD 128291	2159018	5894221187876054656
				HD 128306	2159023	5894221119156564352
164*	two			*eta Cen	1962822	6103094140452223872
				HD 127992	1962835	6103093865574313216
165*	14396-6050	RHD 1	AB	*alf Cen A	2348879	
				*alf Cen B	2348875	
166	14425-6459	DUN 166	AB	*alf Cir	2349085	5849837854817580672
				*alf Cir B		5849837820492182272
167	two			HD 128974	1867812	6202874511432521600
				HD 128975	1867814	6202873686798792704
168	14428-5511	DUN 168		HD 129107	2262002	5893460978673615104
				CPD-54 6120B	2262001	5893460978673614336
169*	14452-5536	DUN 169		V* BU Cir	2262258	5893392327911628928
				HD 129578	2262269	5893392362271368192
170	unidentified					

Appendix: Identification of Dunlop's Double Stars continued

DUN	WDS	DisC	Comp	SIMBAD	ASCC	GAIA DR2
171	14534-4551	DUN 171	AB	HD 131168	2062279	5907676972474481920
				CD-45 9492B	2062275	5907676976779709312
172	one			*zet Cir	2408966	5848760573954755968
173	14529-3748	SHT 57		HR 5543	1868661	6198599507144514432
174*	one			HD 131464	2062468	5906831108744751616
175	15019-5155	HJ 4723	AB	HD 132606A	2161181	5900200263369385728
				HD 132606B	2161182	5900200263369382272
176*	15123-5206	DUN 176		*zet Lup	2162355	5888394463418285312
				HD 134483	2162342	5888394257280681856
177*	15119-4844	DUN 177		*kap Lup	2064147	5902489309143933056
				*kap02 Lup	2064151	5902489102985502208
178*	15116-4517	DUN 178	AC	HD 134444	2064113	5904208906640444928
				HD 134443	2064106	5904209082753017600
179*	15145-4323	DUN 179		HD 135034	1966427	6003544598199761408
				HD 135034B	1966431	6003544632559500288
180*	15185-4753	DUN 180	AC	*mu.02 Lup	2064815	
				HD 135748	2064822	5902970620350884736
181	15202-3823	DUN 181	AB	HD 136125	1870909	6006932605834289792
				CPD-37 6455	1870908	6006932635892069248
182*	15227-4441	DUN 182	AC	*eps Lup	1967246	6000130236633865856
				*eps Lup C		6000130236647036288
183*	15253-3844	DUN 183	AB	*k Lup	1871257	6006429373106563712
				HD 137059	1871250	6006429235667604096
184	15263-4252	DUN 184		HD 137214	1967615	6000758641901550720
				CD-42 10392	1967618	6000758573181780736
185	15285-5136	SEE 234		HD 137465	2164420	5888999332297729024
186	15331-5812	DUN 186		HD 138168	2266206	5882204934544123264
				HD 138181	2266209	5882204934544118528
187	15336-4732	DUN 187		HD 138362	2066357	5986870951058297728
				CPD-47 7206	2066352	5986870916698555136
188	15367-6619	DUN 188		*eps Tr A	2412057	5823955832118781184
				HD 138510	2412046	5823955694698562816
189	15388-5222	DUN 189	AB	HD 139129	2165954	5886050373367262080
				CD-51 9323	2165944	5886050437749100800

The Southern Double Stars of James Dunlop II: Modern Identification of the First Dedicated ...

Appendix: Identification of Dunlop's Double Stars continued

DUN	WDS	DisC	Comp	SIMBAD	ASCC	GAIA DR2
190	15430-5807	DUN 190	AB	V* V359 Nor	2266975	5882323574372973952
				TYC 8704-2534-1	2266976	5882323578753114624
191	15453-5841	DUN 191	AB,C	HIP 77160	2267183	
				HD 140177	2267181	5834232658151618304
192	15471-3531	DUN 192	AB,C	HD 140817	1872803	6011560759514133760
				HD 140840	1872805	6011549008483608192
193	15511-5503	DUN 193		HD 141318	2267782	5884607985911748224
				SAO 243045	2267783	5884608088990966528
194	15549-6045	DUN 194	AC	HD 141913	2354178	5832716255424187392
				CD-60 5919	2354188	5832716362853215104
195	15548-5020	DUN 195	AB	HD 142080	2168121	5982530525830998016
				CD-49 10123	2168122	5982530525831001344
196*	15569-3358	PZ 4		* ksi01 Lup	1777138	6012174802400278016
				* ksi02 Lup	1777140	6012174836760016512
197*	16001-3824	RMK 21	AC	*eta Lup	1873533	5998019895872140800
				HD 143099	1873521	5998065285088239360
198	two			V* QY Nor	2169105	5932866131031997696
				CD-53 6383	2169101	5932864657931055744
199	16086-3906	DUN 199	AC	V * V1027 Sco	1874042	5997082115537645696
				V * V856 Sco	1874040	5997082081177906048
200	16225-4355	DUN 200		HD 147225	1972315	5992149225369945344
				CD-43 10723	1972313	5992149191010199168
201	16280-6403	DUN 201		*iot Tr A	2357385	5828317422956035072
				TYC9 045-2914-1	2357386	5828317422956037376
202	16317-4149	DUN 202	AC	HD 148688	1973070	5968761680983851776
				CPD-41 7500C	1973071	5968761582230644992
203	16331-6054	DUN 203		V* NP Tr A	2357806	5830447000863289344
				HD 148628	2357801	5830447005197478400
204	one			HD 149274	1874980	6020514769906985728
205	unidentified					
206	16413-4846	DUN 206	A,C	HD 150136	2073934	5940954177259978880
				HD 150135	2073931	5940954898814487168
207	16444-4224	DUN 207		HD 150674	1973850	5967756491149042304
				HD 150673	1973849	5967756491149041024
208	one			HD 150500	2074201	5942647283393791232

The Southern Double Stars of James Dunlop II: Modern Identification of the First Dedicated ...

Appendix: Identification of Dunlop's Double Stars continued

DUN	WDS	DisC	Comp	SIMBAD	ASCC	GAIA DR2
209	16482-3653	DUN 209		HD 151315	1875678	5971596329361239808
				HD 151316	1875680	5971596260664472704
210	16487-5526	DUN 210	AB	HD 151163	2274180	5929426381963737344
				HD 151162	2274176	5929426416323498112
211	16475-4819	DUN 211	BC	HD 151115	2074679	5939444375994517376
				HD 151116	2074676	5939444272915289216
212	17040-5105	DUN 212	AB	HD 153772	2176845	5937998243333786112
				HD 153771	2176843	5937998243333788416
213	17103-4644	DUN 213		CCDM J17103-4644AB	2076679	5950941488064653056
				CD-46 11258B	2076681	5950941488064651136
214	17133-6712	DUN 214	AB	HD 154903	2418812	5814757008599356928
				TYC 9064-3629-1	2418813	5814757008599360896
215	17193-5323	DUN 215	AB	HD 156239	2178088	5923327700182691840
				HD 156260	2178095	5923327356584965760
216*	17269-4551	DUN 216	AC	HD 157661A	2078475	5951986642593137408
				HD 157649	2078460	5951987398507431808
217	17290-4358	DUN 217		HD 158042	1978893	5958561447264080768
				CD-43 11741B	1978895	5958561447264078208
218	17336-3706	DUN 218	AC	*lam Sco	1880898	
				CD-36 11635	1880889	5962581880247644288
219	17589-3652	DUN 219	AB	HD 163652	1884115	4037358426191922688
				HD 163651	1884101	4037358597990619264
220	18222-5534	DUN 220		V* QW Tel	2280785	6649398690418063232
				CD-55 7677	2280786	6649398690418059392
221	18243-4407	DUN 221		HD 168905	1986993	6721718444965335936
				CD-44 12570	1986998	6721718170088625664
222	18334-3844	DUN 222		*kap02 Cr A	1889607	6726876327040339712
				*kap01 Cr A	1889606	6726876327040344576
223	unidentified					
224	18540-4716	DUN 224	AC	HD 174691	2088578	6710469826831780736
				HD 174713	2088587	6710469655033078016
225	19124-5148	DUN 225	AB	HD 178734	2187130	6656986282721029120
				HD 178710	2187123	6656985939123649920
226	19226-4428	DUN 226		*bet01 Sgr	1992514	6664464851575462016
				HD 181484	1992517	6664464851575461120
227	19526-5458	DUN 227		HD 187420	2189330	6641186850384256896
				HD 187421	2189331	6641186850384254848

Appendix: Identification of Dunlop's Double Stars continued

DUN	WDS	DisC	Comp	SIMBAD	ASCC	GAIA DR2
228*	unidentified					
229*	19583-5154	DUN 229		HD 188557	2189635	6666516540271227904
				HD 188534	2189627	6666516505911492224
230	20178-4011	DUN 230		HD 192724A	1995385	6692595444253828480
				HD 192724B	1995387	6692595547333043456
231*	20366-7104	DUN 231		HD 195459	2494845	6374497315769911296
				CD-71 1627	2494836	6374497384489388800
232*	20417-7521	DUN 232		*mu.02 Oct	2495054	6369544118965772416
				HD 196068	2495055	6369544118966055296
233	one			*phi01 Pav	2367957	6454999399628150016
234	20376-4717	HJ 5209	AB	*alf Ind	2094623	6674382927491854848
235*	20450-5029	DUN 235	AC	CCDM J20451-5030AB	2191473	6480764633558584704
				HD 197341	2191478	6480763877644331904
236*	21022-4300	DUN 236		HD 200011	1997452	6484888042680733824
				HD 200026	1997457	6484888008320993152
237	four			V* BT Ind	2288078	6458506566841143040
238	22259-7501	DUN 238	AB	HD 212168	2498785	6357835694518769408
				CPD-75 1748B	2498787	6357835488360338560
239	22298-4345	DUN 239		*del02 Gru	2000590	6520955322607576320
				CD-44 14934	2000587	6520953845138827264
240*	22315-3221	PZ 7	AC	*bet Ps A	1808438	6601750220152445440
				CD-32 17127	1808439	6601750151432831104
241*	22366-3140	DUN 241		HD 214122	1808592	6601132054099267456
				HD 214121	1808596	6607136899415399680
242*	22397-2820	H 6 119	AB	HD 214599	1711391	6608821179430481408
				CD-28 17874B	1711392	6608821076351265024
243	three			*bet Gru	2099216	
244	23023-6418	DUN 244		HD 217488	2371330	6393362255241691648
				CPD-64 4310	2371332	6393362358320906368
245	23086-5944	DUN 245		HD 218392	2290627	6490761943032664960
				CPD-60 7635B	2290626	6490761943032665344
246	23072-5041	DUN 246		HD 218269	2195694	6502570319958250496
				HD 218268	2195691	6502570319958250624

Appendix: Identification of Dunlop's Double Stars continued

DUN	WDS	DisC	Comp	SIMBAD	ASCC	GAIA DR2
247	23180-6100	DUN 247		HD 219631	2371641	6490359006380772480
				HD 219621	2371639	6490359075100249856
248	23208-5018	DUN 248	AB,C	HD 220003A	2196066	6502030631546224512
				CD-50 13947	2196064	6502030631547502720
249*	23239-5349	DUN 249		V* DQ Gru	2196130	6499534465274954496
				HD 220391	2196129	6499534465274949376
250*	23272-5017	DUN 250		HD 220803	2196210	6525816229153083776
				HD 220815	2196212	6525816332232298112
251*	23395-4638	DUN 251		*tet Phe A	2100751	6525488231089676800
				*tet Phe B	2100750	6525488226794240256
252*	two	DUN 252	AB	HR 8996	2372143	6485678866417832704
				HD 222830	2372146	6485685051170731648
253*	23544-2703	LAL 192		HD 223991A	1713655	2334419836112293120
				HD 223991B	1713654	2334419797455932160

The Southern Double Stars of James Dunlop III: Modern Version and Analysis of Accuracy of the First Dedicated Published Catalogue of Southern Double Stars

Roderick R. Letchford[1], Graeme L. White[2], Allan D. Ernest[3]

1. Vianney College Seminary, Wagga Wagga, NSW 2650, Australia, rodvianney@yahoo.com.au
2. Centre for Astronomy, University of Southern Queensland, Toowoomba, Australia QLD 4350, graemewhiteau@gmail.com
3. Charles Sturt University, Wagga Wagga, NSW 2650, Australia, aernest@csu.edu.au

Abstract: The first dedicated catalogue of southern double stars was published in 1829 by James Dunlop. Basing our work solely on the published data, we present a modern version of the catalogue with data from GAIA DR2 and, where unavailable, data from the ASCC in the *Appendix*. We also compare this modern data precessed back to B1825.0 with that of Dunlop's original catalogue and estimate the accuracy of his main parameters.

1. Introduction

This paper (Dunlop Paper III) continues a series of papers on the double stars of James Dunlop, one of three astronomers who worked at the privately owned observatory in Parramatta, NSW Australia in the 1820's. The Parramatta Observatory was the venture of Sir Thomas Makdougll Brisbane (1773-1860) the 6th British Governor of the Colony of NSW from 1822 to 1825.

In Dunlop Paper I (Letchford, White and Ernest, IN PRINT) we presented a history and description of the first published dedicated catalogue of southern double stars, by James Dunlop (1793-1848) and issued in 1829 as Approximate Places of Double Stars in the Southern Hemisphere, observed at Paramatta in New South Wales (Dunlop 1829). In Dunlop Paper II (Letchford, White and Ernest, IN PRINT) we presented modern designations of the pairs in Dunlop's original catalogue.

The Dunlop papers follow three papers (Rümker Papers I, II, and III) previously published in this journal on the double star work of another of the Parramatta astronomers, Carl Rümker (Letchford, White, and Ernest 2017; Letchford, White, and Ernest 2018a; Letchford, White, and Ernest 2018b).

In this paper (Dunlop Paper III), we present a modern version of the catalogue with data from The Gaia Catalogue Data Release 2 (GAIA DR2) and, where unavailable, data from the All-sky Compiled Catalogue of 2.5 million stars, 3rd version (ASCC). We also compare this modern data precessed back to B1825.0 (with proper motions taken into account) with that of Dunlop's original catalogue and estimate the accuracy of his main parameters.

2. Format of the Appendix "Modern Version of the Dunlop Catalogue"

We present in the Appendix a modern version of the Dunlop Catalogue based on online data using the Appendix from Dunlop Paper II (Letchford, White and Ernest, IN PRINT). All positions are ICRS, epoch J2000.0. The column details are given in Table 1.

3. Accuracy Analysis

All of the Dunlop doubles are considered slow moving (prior to further study) and so a comparison between Dunlop's published data and modern precessed values (with proper motion taken into account) should not differ significantly from those when Dunlop made his observations. Hence reasonable estimation of the accuracy of his various measures is possible.

(Text continues on page 380)

Table 1: Explanation of Columns in "Modern Version of the Dunlop Catalogue" (Appendix)

Column	**Name**	**Data**
1	DUN	A running catalogue entry corresponding to the entries of Dunlop, 1829. An asterisk (*) indicates that Dunlop observed this pair with the 3 1/4 refractor; without an asterisk, with the 9 inch reflector.
2	RA (h:m:s)	The Right Ascension (RA) of the primary star (the brighter of the pair or grouping) at ICRS, epoch J2000.0. Taken from the GAIA DR2 release unless marked by an "A", in which case, data was not available from GAIA DR2 and was taken from ASCC.
3	DE (d:m:s)	The Declination (DE) of the primary star (the brighter of the pair or grouping) at ICRS, epoch J2000.0. Taken from the GAIA DR2 release unless marked by an "A", in which case, data was not available from GAIA DR2 and was taken from ASCC.
4	WDS	Washington Double Star Catalog (WDS) designation. "one" indicates that only one star could be found. "two" indicates that two stars were found that are not recorded as double stars in the current WDS. So for "three", "four" and "five". "Unidentified" means that the pair remains unidentified.
5	Disc	The discoverer and component code following the WDS.
6	PA (deg)	The Position Angle of the secondary relative to the primary at ICRS, epoch J2000 in units of degrees, computed from positions obtained from the GAIA DR2 release (unless positions taken from ASCC).
7	Sep (as)	The separation of the secondary from the primary in units of arcseconds ("), computed from position obtained from the GAIA DR2 release (unless positions taken from ASCC).
8	Vmag1	The visual magnitude of the primary star taken from ASCC.
9	Vmag2	The visual magnitude of the secondary star taken from ASCC.
10	SpType1	The spectral type of the primary star, taken from ASCC.
11	SpType2	The spectral type of the secondary star, taken from ASCC.
12	pmRA1 (mas/yr)	The Right Ascension component of the proper motion of the primary star in units of milli-arcseconds per year. Taken from the GAIA DR2 release unless marked by an "A", in which case, data was not available from GAIA DR2 and was taken from ASCC.
13	pmDE1 (mas/yr)	The Declination component of the proper motion of the primary star in units of milli-arcseconds per year. Taken from the GAIA DR2 release unless marked by an "A", in which case, data was not available from GAIA DR2 and was taken from ASCC.
14	pmRA2 (mas/yr)	The Right Ascension component of the proper motion of the secondary star in units of milli-arcseconds per year. Taken from the GAIA DR2 release unless marked by an "A", in which case, data was not available from GAIA DR2 and was taken from ASCC.
15	pmDE2 (mas/yr)	The Declination component of the proper motion of the secondary star in units of milli-arcseconds per year. Taken from the GAIA DR2 release unless marked by an "A", in which case, data was not available from GAIA DR2 and was taken from ASCC.

(Continued from page 378)

3.1 Equinox of Catalogue and Epochs of Observations

Like Rümker, Dunlop did not publish the equinox or the epoch of any measures in his catalogue. Following the method pioneered in Rümker Paper I (Letchford, White, & Ernest, 2017), we find the most likely equinox from the difference in the catalogues positions and the precessed positions of the primary star, as a function of equinox (see Figure 1). The best fit of these data corresponds to the likely date of the equinox of the Catalogue. For the sake of analysis we assume the epoch of each observation to be also this equinox date.

In this paper we refine the technique using a more detailed stellar reduction as detailed in The Astronomical Almanac for the Year 2018, pages B51-55,73-74 (Nautical Almanac Office 2017). Here we use high precision, including nutation and frame bias, and take into account parallax data available from GAIA DR2. The results are depicted in Figure 1. The effect of precession is given by the U-shaped curve and the effect of nutation by the wavy line.

It is clear from Figure 1 that the Equinox with the lowest total separation is J1825.1 (marked by the red circle). There is very little difference between J1825.1 and B1825.0, so we say with some confidence that Dunlop's Catalogue Equinox was B1825.0.

3.2 Accuracy of Position of Primaries

Utilizing the new identifications and modern positions and proper motions, it is now possible to determine the accuracy of the position of the primary stars as

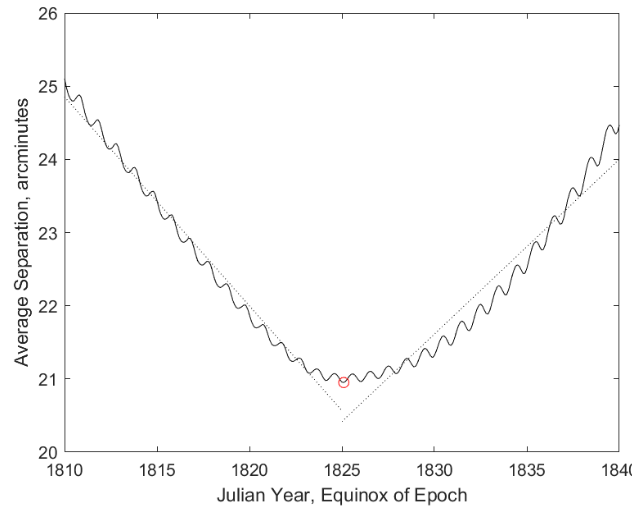

Figure 1. The average separation in arcminutes between the catalogued positions of the primary stars in Dunlop's catalogue and the precessed modern positions of these stars as a function of date. The wavy nature of the curve results from the inclusion of nutation in the formal calculation. Dotted lines are extrapolations of the precession effect.

reported by Dunlop using the same method as detailed in Rümker Paper I. Figure 2 is the target diagram for all DUN numbers for which sufficient data is currently available (see *Appendix* for modern star positions and proper motions).

All offsets in this paper are in this sense: 'Modern – Dunlop'. For example in Figure 2, the target diagram,

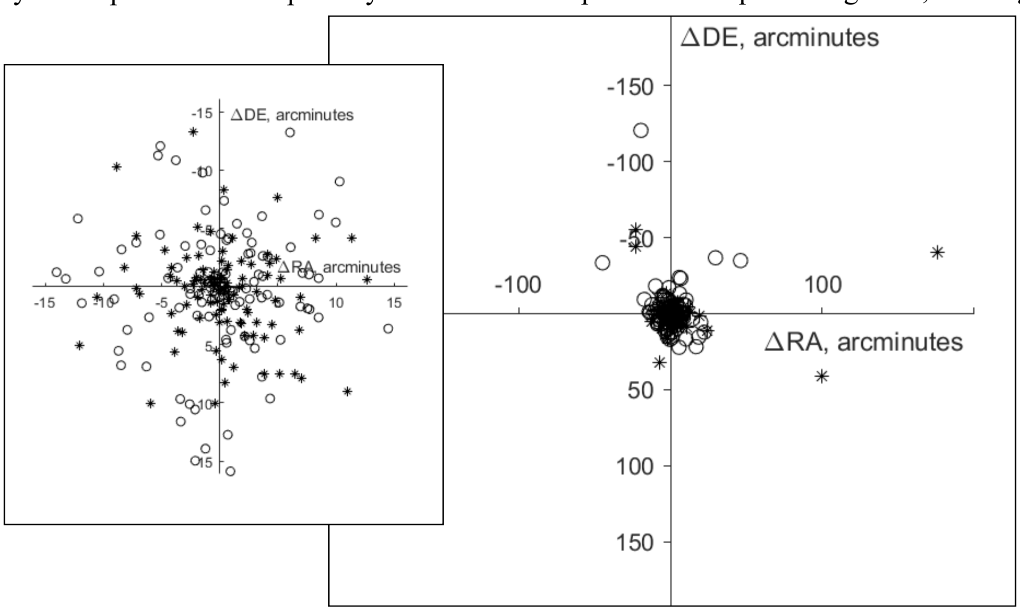

Figure 2. Target Diagram for all DUN numbers with sufficient data. Here '' represents the offset of primaries observed with the 3¼ inch refractor, 'o' those observed with the 9 inch reflector. Positions are compared at B1825.0 (Modern – Dunlop). The insert is the target diagram limited to 15 arcmin square.*

The Southern Double Stars of James Dunlop III: Modern Version and Analysis of Accuracy ...

'Modern' are modern positions (RA and DE) precessed to B1825.0, taking into account proper motions, and 'Dunlop' is the position as presented in his published Catalogue.

From Figure 2, the outliers can be immediately seen. We suggest that some of these are probably due to typographical errors or quadrant errors in the original catalogue. The vast majority of offsets fall within 15 arcminutes of the center in both ΔRA and ΔDE (as in inset of Figure 2). Confining our attention to this range, we present four histograms in Figures 3-6.

An analysis of the differences between the modern-but-precessed positions and those of Dunlop shows that there is no overall bias in the Dunlop positions. The mean differences in right ascension are 3 ± 2 arcmin for the 3 ¼ inch telescope and 12 ± 12 arcmin for 9 inch. The declination differences are 0.2 ± 1 arcmin and -4 ± 6 arcmin for the two instruments respectively. These estimates are from 115 pairs observed with the 3 ¼ inch and 122 pairs for the 9 inch, out of a possible 121 and 132 respectively.

Given the instruments at hand, we propose that Dunlop did a fine job and note that Herschel's criticisms (Letchford, White, Ernest, Paper I, in print) do not apply to Dunlop's positions of the primaries but rather to the accuracy of pair identification (for which see Letchford, White and Ernest, Dunlop Paper II, IN PRINT).

3.3 Accuracy of Position Angles

Precessing modern positions back to 1825.0 using modern proper motions and parallax, enabled us to compare Dunlop's published position angles with modern equivalents (see beginning of Section 3). Results of offsetting the position angles (modern PA (precessed to B1825.0) – average of Dunlop's PA) are given in Figures 7-8. It should be noted that Dunlop recorded data that enables position angles to be determined in up to four different ways (see Letchford, White and Ernest, Paper I, in print) and hence we take the average where available.

Of Dunlop's 121 pairs from the 3 ¼ inch, 98 had PA data that could be compared to modern precessed values. Of the 132 pairs from the 9 inch, 68 had sufficient data. The poorer quality work from the 9 inch is clearly indicated in the mean ΔPA° of ~ +2.5° as opposed to just ~ -0.9° for the 3¼ inch. Although there is much variation, Dunlop tended to over-measure his PAs from the 3 ¼ inch and over-estimate those from the 9 inch.

The doubles with the most extreme differences in PA were DUN 99* (extreme left of Figure 7) and DUN 78* (extreme right of Figure 7) for the 3 ¼ inch and DUN 115 (extreme left of Figure 8) and DUN 7 (extreme right of Figure 8) for the 9 inch. They and oth-

(Continued on page 384)

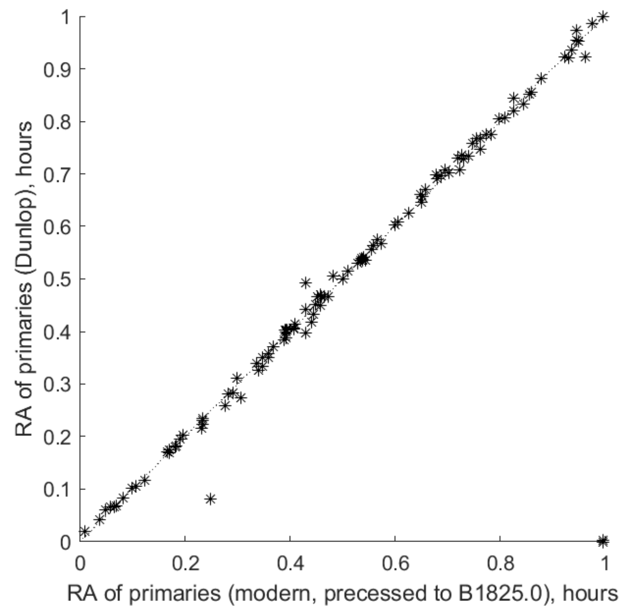

Figure 3. Cross plot of modern RA (precessed to B1825.0) and Dunlop's RA as published of primaries observed with the 31/4 inch refractor, at Equinox of Epoch B1825.0. RA whole hours have been truncated to better reflect the spread. Histogram inset is offset in Right Ascension limited to ± 15 arcmin fitted with a single peak Gaussian curve.

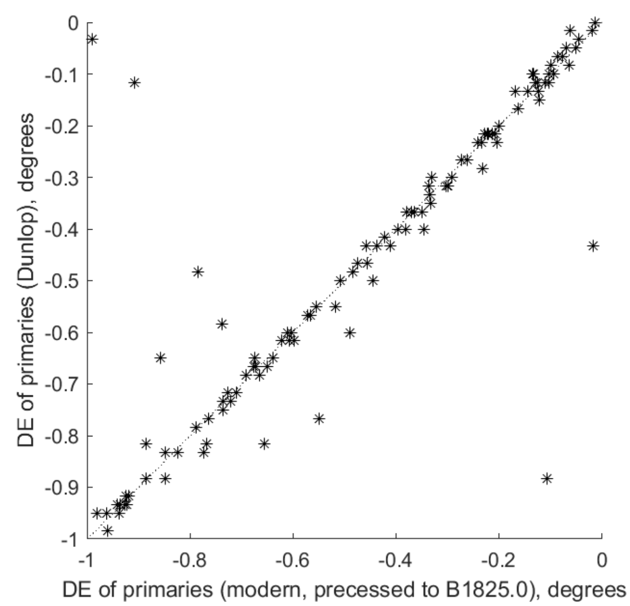

Figure 4. Cross plot of modern DE (precessed to B1825.0) and Dunlop's RA as published of primaries observed with the 31/4 inch refractor, at Equinox of Epoch B1825.0. DE whole degrees have been truncated to better reflect the spread. Histogram inset is offset in Declination limited to ± 15 arcmin fitted with a single peak Gaussian curve.

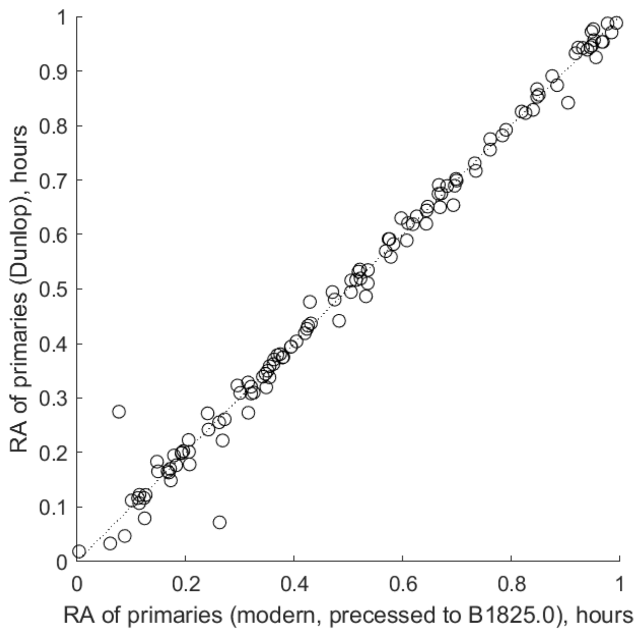

Figure 4. Cross plot of modern DE (precessed to B1825.0) and Dunlop's RA as published of primaries observed with the 31/4 inch refractor, at Equinox of Epoch B1825.0. DE whole degrees have been truncated to better reflect the spread. Histogram inset is offset in Declination limited to ± 15 arcmin fitted with a single peak Gaussian curve.

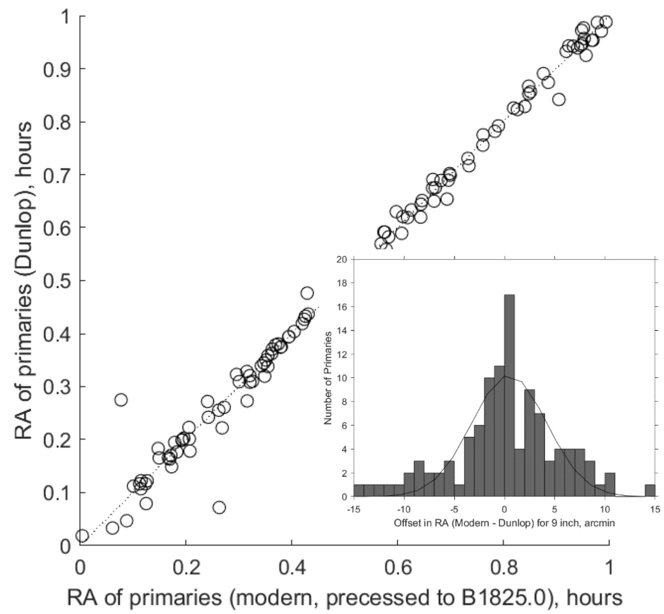

Figure 5. Cross plot of modern RA (precessed to B1825.0) and Dunlop's RA as published of primaries observed with the 9 inch reflector, at Equinox of Epoch B1825.0. RA whole hours have been truncated to better reflect the spread. Histogram inset is offset in Right Ascension limited to ± 15 arcmin fitted with a single peak Gaussian curve.

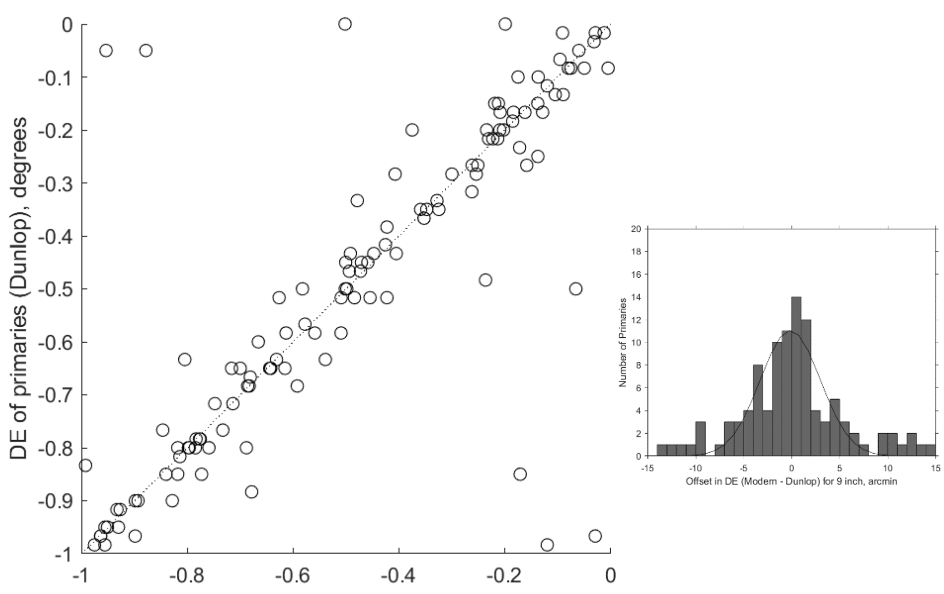

Figure 6. Cross plot of modern DE (precessed to B1825.0) and Dunlop's RA as published of primaries observed with the 9 inch reflector, at Equinox of Epoch B1825.0. DE whole degrees have been truncated to better reflect the spread. Histogram inset is offset in Declination limited to ± 15 arcmin fitted with a single peak Gaussian curve.

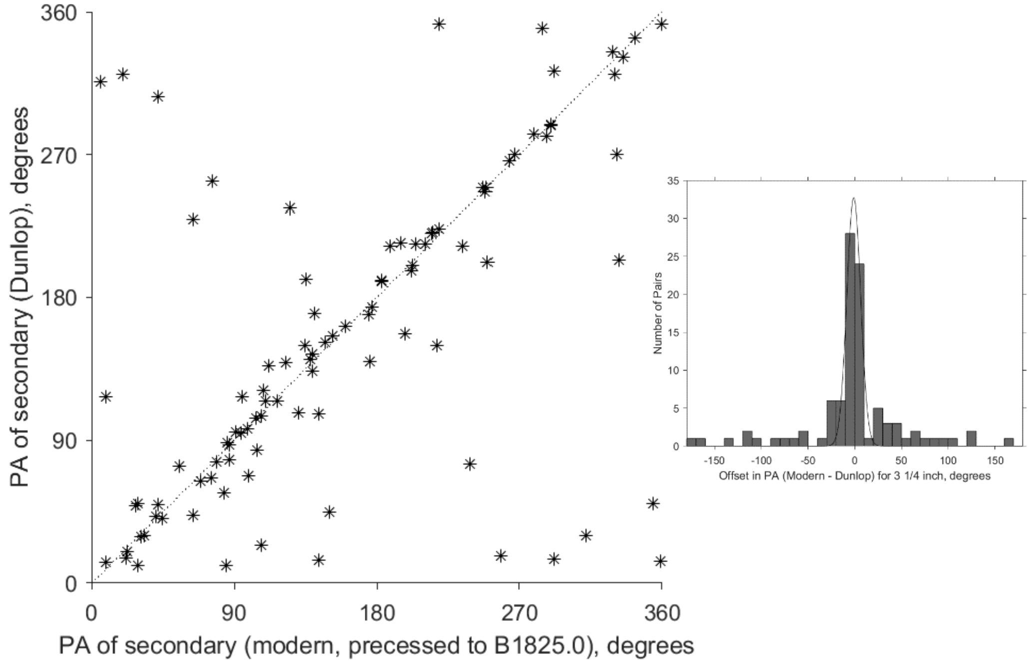

Figure 7. Cross plot of modern PA (precessed to B1825.0) and Dunlop's PA as published of pairs observed with the 3 ¼ inch refractor, at Equinox of Epoch B1825.0. Histogram inset is PA offset fitted with a single peak Gaussian curve.

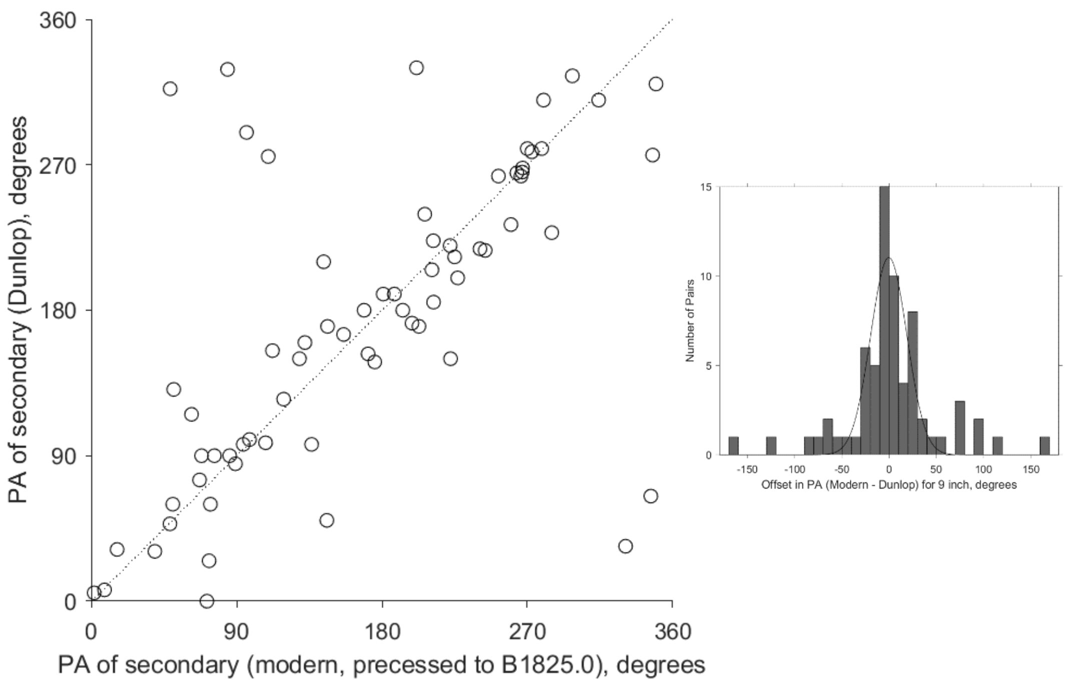

Figure 8. Cross plot of modern PA (precessed to B1825.0) and Dunlop's PA as published of pairs observed with the 9 inch reflector, at Equinox of Epoch B1825.0. Histogram inset is PA offset fitted with a single peak Gaussian curve.

The Southern Double Stars of James Dunlop III: Modern Version and Analysis of Accuracy ...

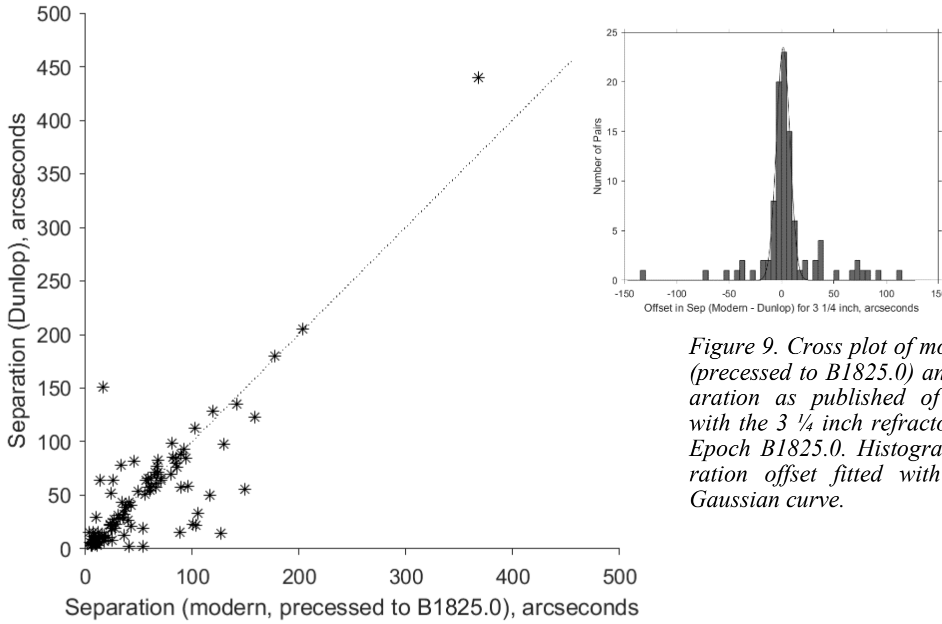

Figure 9. Cross plot of modern Separation (precessed to B1825.0) and Dunlop's Separation as published of pairs observed with the 3 ¼ inch refractor, at Equinox of Epoch B1825.0. Histogram inset is Separation offset fitted with a single peak Gaussian curve.

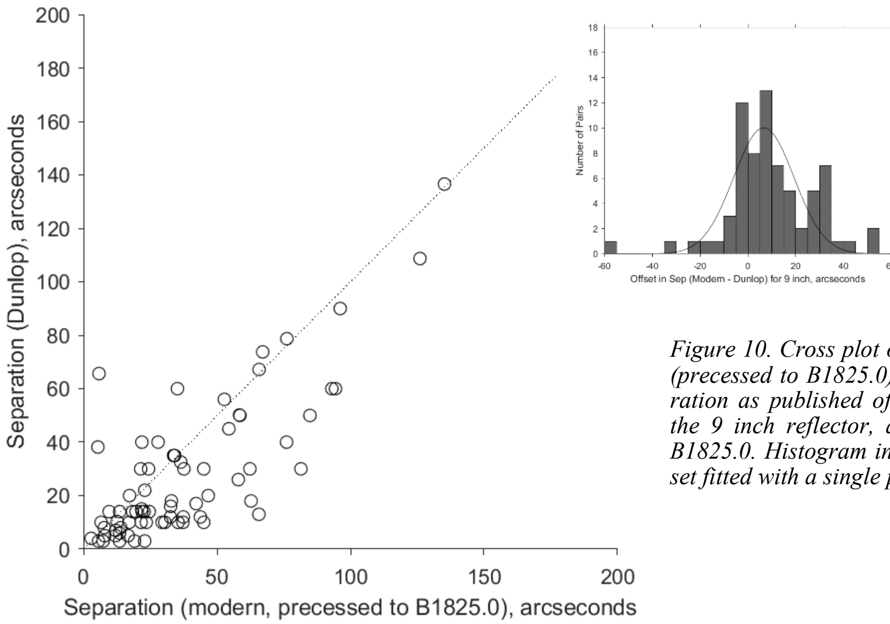

Figure 10. Cross plot of modern Separation (precessed to B1825.0) and Dunlop's Separation as published of pairs observed with the 9 inch reflector, at Equinox of Epoch B1825.0. Histogram inset is Separation offset fitted with a single peak Gaussian curve.

(Continued from page 381)

ers are probably due to quadrant errors on the part of Dunlop. For example, in Dunlop's Catalogue, DUN 1* has the quadrant at "np" but should be "sf"; which explains in large part its PA offset of -133.4°.

3.4 Accuracy of Separations

Precessing modern positions back to 1825.0 using modern proper motions and parallax, enabled us to compare Dunlop's published separations (Sep) with modern equivalents. Results of offsetting the separations (modern Sep (precessed to B1825.0) – average of Dunlop's Sep) are given in Figures 9-10 and Table 4. It should be noted that Dunlop recorded data that enables separations to be determined in up to four different ways (see Letchford, White and Ernest, Dunlop Paper I, IN PRINT) and hence we take the average where available.

Of Dunlop's 121 pairs from the 3 ¼ inch, 100 had separation (Sep) data that could be compared to modern precessed values. Of the 132 pairs from the 9 inch, just 71 had sufficient data. The poorer quality work from

The Southern Double Stars of James Dunlop III: Modern Version and Analysis of Accuracy ...

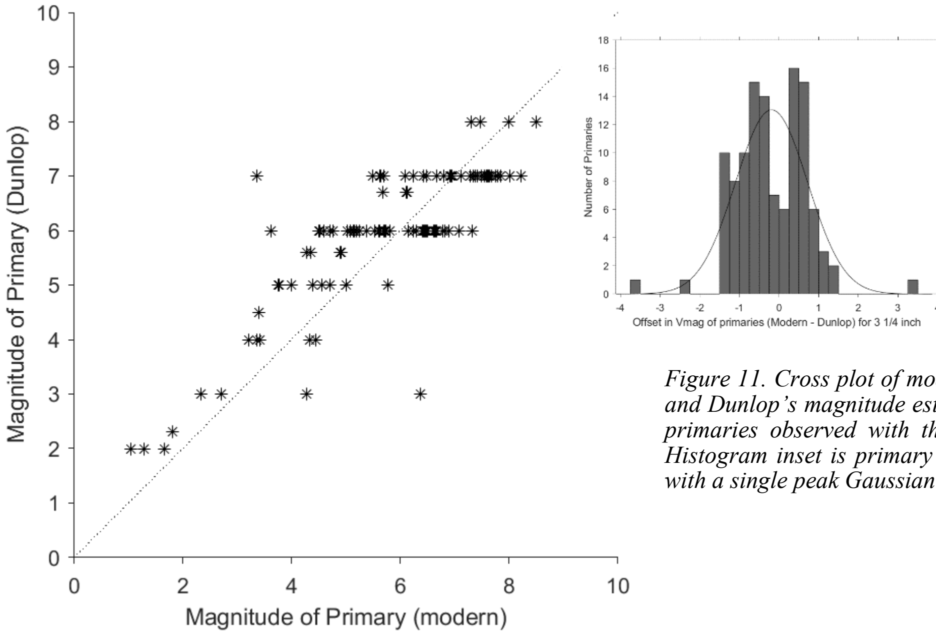

Figure 11. Cross plot of modern visual magnitudes and Dunlop's magnitude estimates as published, of primaries observed with the 3 ¼ inch refractor. Histogram inset is primary magnitude offset fitted with a single peak Gaussian curve.

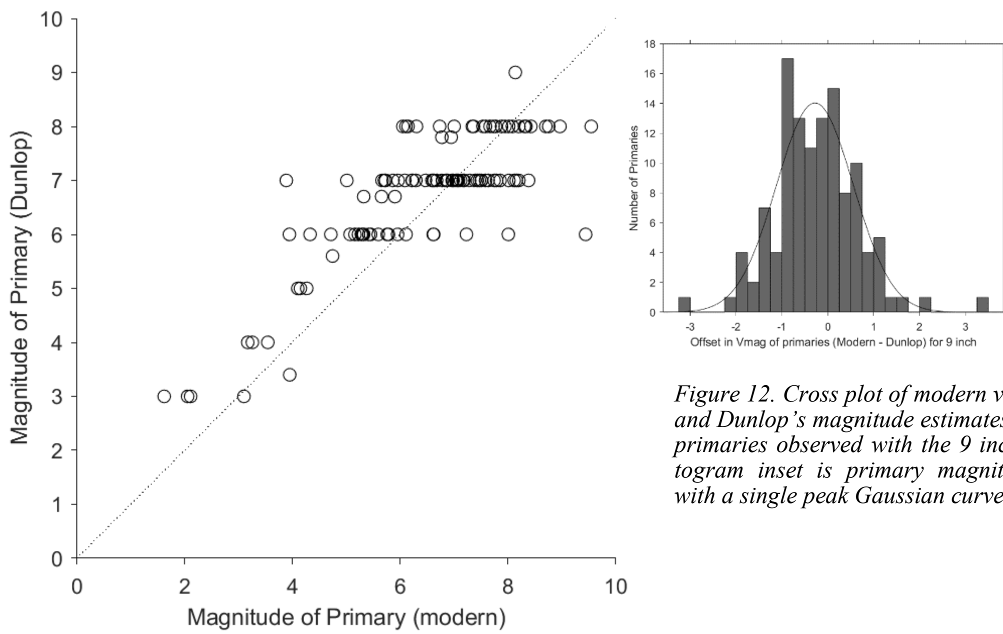

Figure 12. Cross plot of modern visual magnitudes and Dunlop's magnitude estimates as published, of primaries observed with the 9 inch reflector. Histogram inset is primary magnitude offset fitted with a single peak Gaussian curve.

the 9 inch is clearly indicated in the bias spread of ~12.7" as opposed to just ~6.5" for the 3¼ inch. Again, Dunlop did better at measuring separations with the 3 ¼ inch. Although with wide variation, Dunlop had a tendency to underestimate separations, especially with the 9 inch.

DUN 109* is unusual. The published Catalogue recorded one estimate of the separation as 2' 49.3" or 169.3" (the other estimate was calculated to be 132.8"). The correct quadrant is recorded, also the magnitude estimates are approximately correct, but the modern precessed separation is only ~16.7". There is no star with the right magnitude at ~169" from the primary. Dunlop's average PA for DUN 109* is ~106.6° the modern precessed value is ~143.3°.

3.5 Accuracy of Visual Magnitudes

Dunlop visually estimated the magnitudes of the stars at each telescope. Results of offsetting the visual magnitudes (modern Vmag (precessed to B1825.0) – average of Dunlop's magnitudes) of the primaries are given in Figures 11-12; those for the secondaries in Figures 13-14.

On average, Dunlop over-estimated the visual magnitude of the primaries by ~0.2 for both telescopes.

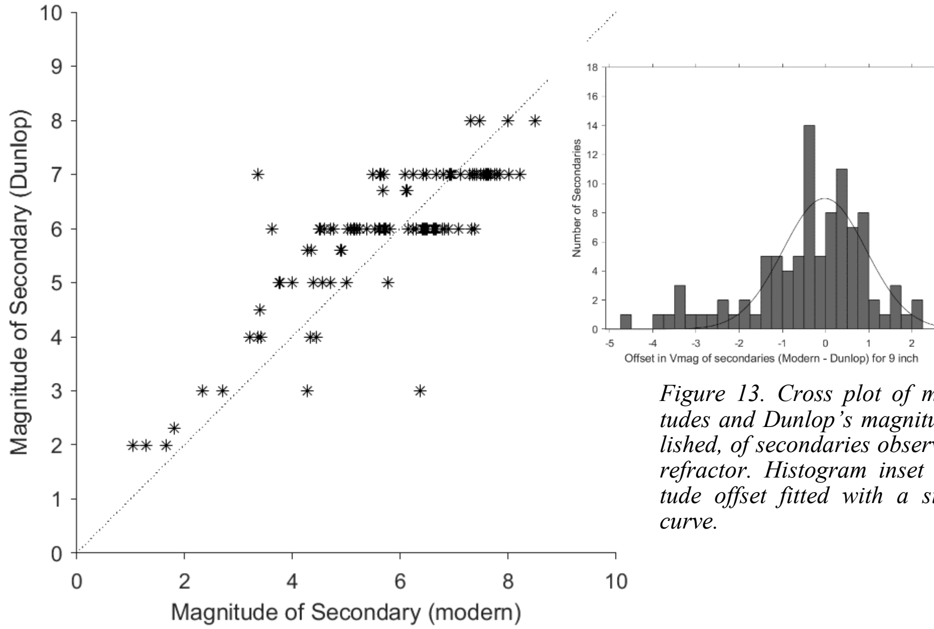

Figure 13. Cross plot of modern visual magnitudes and Dunlop's magnitude estimates as published, of secondaries observed with the 3 ¼ inch refractor. Histogram inset is secondary magnitude offset fitted with a single peak Gaussian curve.

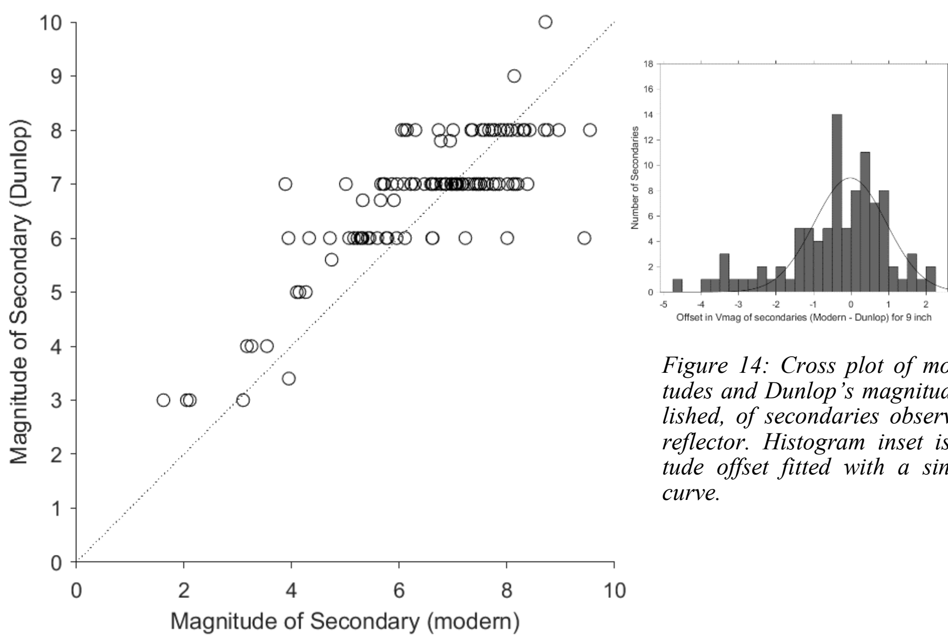

Figure 14: Cross plot of modern visual magnitudes and Dunlop's magnitude estimates as published, of secondaries observed with the 9 inch reflector. Histogram inset is secondary magnitude offset fitted with a single peak Gaussian curve.

Though the bias is relatively small, its uncertainties for both telescopes indicate that Dunlop was often up to 1 magnitude out, and frequently more. For further discussion on Dunlop's magnitude estimates, see Dunlop Paper I (Letchford, White and Ernest, Paper I, IN PRINT).

On average, Dunlop over-estimated the visual magnitude of the secondaries by ~0.3 for the 3 ¼ inch and ~0.4 for the 9 inch, more than for the primaries. The bias for both is also larger, meaning that, as for the primaries, Dunlop had a clear tendency for overestimation of the secondary magnitudes of up to 1 magnitude and often more.

4. Limiting Completeness Magnitudes

Using modern (ASCC) measures of magnitudes, and considering the primary and secondary magnitudes together, Figures 15 and 16 are histograms of the magnitudes measured with the 3 ¼ inch reflector and 9 inch refactor, respectively. They indicate a limiting completeness magnitude for Dunlop of ~7.5 through the 3

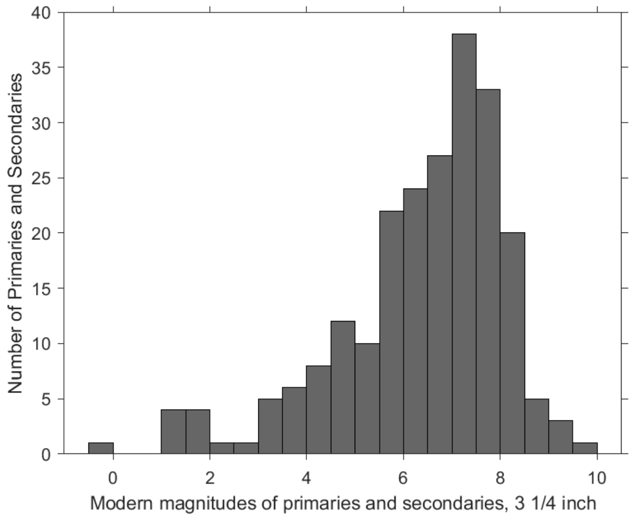

Figure 15: Histogram of modern magnitude measures of primary and secondary components observed with the 3 ¼ inch refractor. Limiting completeness magnitude ~7.5.

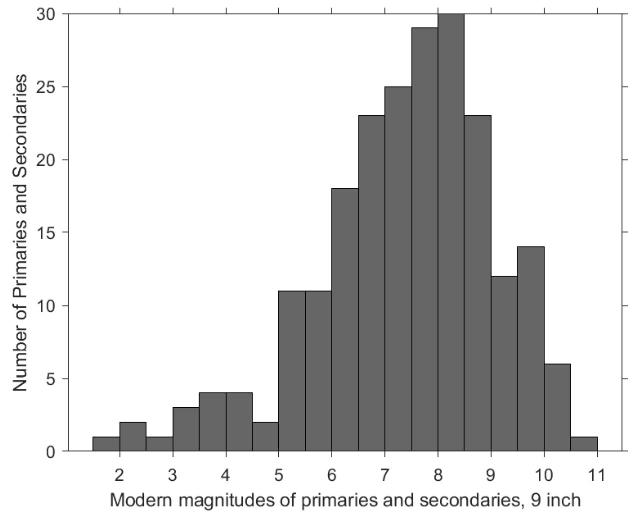

Figure 16: Histogram of modern magnitude measures of primary and secondary components observed with 9 inch reflector. Limiting completeness magnitude ~8.

¼ inch refractor and ~8 through the 9 inch reflector. We of course use the word "completeness" cautiously. There is no suggestion that Dunlop either intended to or wanted to find every southern double star brighter than ~8.

5. Omissions in the WDS

In the course of our investigation, we identified 13 real doubles first discovered by Dunlop but are not in the WDS, namely those indicated by "two" in Column 2 of the Appendix: 35*, 37, 100, 107, 112*, 118, 119*, 149*, 153*, 164*, 167, 198, 252*. See Dunlop Paper II (Letchford, White and Ernest, Paper II, IN PRINT). We offer the data on these pairs in our Appendix for possible inclusion in a future edition of the WDS.

6. Conclusion

A summary of our accuracy estimations for Dunlop are given in the appropriate sections above. The Appendix of this paper (Dunlop Paper III) contains a modern Catalogue of the Dunlop doubles. The Appendix associated with Dunlop Paper II contains modern Identifications of the Dunlop doubles.

Our analysis shows that Herschel's criticisms of Dunlop's Double Star Catalogue Dunlop Paper I (Letchford, White and Ernest, Paper I, IN PRINT) were unjustified, except when it came to separation and perhaps to his magnitude estimates.

7. Acknowledgements

We acknowledge the following:-

- The Aladin sky atlas developed at CDS, Strasbourg Observatory, France.
- The Washington Double Star Catalog maintained by the USNO. (WDS)
- All-sky Compiled Catalogue of 2.5 million stars, 3rd version (ASCC)
- The Gaia Catalogue (Gaia DR2, Gaia Collaboration, 2018), from VizieR (GAIA DR2).

8. References

Dunlop, James, 1829, "Approximate Places of Double Stars in the Southern Hemisphere, Observed at Paramatta in New South Wales", *Memoirs of the Royal Astronomical Society*, **3** (1): 257–75. http://adsabs.harvard.edu/abs/1827MmRAS...3..267D.

Letchford, Roderick R, Graeme L White, and Allan D Ernest, 2017, "The Southern Double Stars of Carl Rümker I: History, Identification, Accuracy", *Journal of Double Star Observations*, **13** (2): 220–32. http://www.jdso.org/volume13/number2/Letchford_220-232.pdf.

———, 2018a, "The Southern Double Stars of Carl Rümker II: Their Relative Rectilinear Motion", *JDSO*, **14** (2): 208–22. http://www.jdso.org/volume14/number2/Letchford_208_222.pdf.

———, 2018b, "The Southern Double Stars of Carl Rümker III: Quantified Probability of Boundedness and Preliminary Grade 5 Orbits for Some Very Long Period Doubles", *JDSO*, **14** (4): 761–70.

http://www.jdso.org/volume14/number4/Letchford_761_770.pdf.

Nautical Almanac Office, USNO. 2017, *Astronomical Almanac for the Year 2018*, Edited by Marc C. Eckardt and John Humphrey, Washington, D. C. https://books.google.com/books?id=0dLWSt24CEoC.

Letchford, Roderick R, Graeme L White, and Allan D Ernest, 2019, "The Southern Double Stars of James Dunlop I: History, Identification, Accuracy", *JDSO*, **15** (3), 350-360. This issue.

Letchford, Roderick R, Graeme L White, and Allan D Ernest, 2019, "The Southern Double Stars of James Dunlop II: Modern Identification of the first dedicated Published Catalogue of Southern Double Stars", *JDSO*, **19** (3), 361-377. This issue.

Appendix
Modern Version of the Dunlop Catalogue
(See Table 1 Section 2, for explanation of columns)

DUN	RA h:m:s	DE d:m:s	WDS	Disc	PA deg	Sep as	Vmag1	Vmag2	SpType1	SpType2	pmRA1 mas/yr	pmDE1 mas/yr	pmRA2 mas/yr	pmDE2 mas/yr
1*	00 31 32.664	-62 57 29.52	00315-6257	LCL 119AC	168.877	27.150	4.329	4.504	B9V	A2V	-54.577	-54.577	105.607	-48.057
2*	00 52 24.528	-69 30 13.68	00524-6930	DUN 2	80.817	20.303	6.646	7.317	F7IV/V	G1V	-67.462	-67.462	9.966	-79.096
3	01 26 58.104	-32 32 35.52	01270-3233	LDS 2199			6.681		C6.5II		-30.900	-30.900		
4*	01 38 48.552	-53 26 20.04	01388-5327	DUN 4	104.038	10.389	7.092	8.425	F5IV/V	F5	-48.180	-48.180	-8.577	-46.990
5*	01 39 47.808	-56 11 35.88	01398-5612	DUN 5	190.175	11.338	5.682	5.835	K0V	K0V	15.333	15.333	309.102	10.686
6	02 16 30.600	-51 30 43.92	02165-5131	DUN 6AB	223.979	89.051	3.546	9.338	B8IV-V		-22.854	-22.854	-0.643	12.013
7	02 39 39.840	-59 34 03.00	02397-5934	DUN 7A,BC	96.722	36.906	7.587	7.665	G8/K0III	A9IV	0.287	0.287	19.15 A	-0.2 A
8*	02 57 14.688 A	-24 58 09.84 A	02572-2458	S 423AB,C	224.598	28.818	7.613	7.795	K1/K2V	K2V	33.47 A	-36.31 A	1.073	-40.460
9*	02 58 15.672	-40 18 16.92	02583-4018	PZ 2	90.000	8.511	3.211	4.278	A4III+...	A1V	23.503	23.503	-51.661	16.178
10	03 04 33.144	-51 19 19.56	03046-5119	DUN 10AB	69.397	39.898	7.540	8.498	G1V	K0	71.856	71.856	86.5 A	71.72 A
11			unidentified											
12	03 15 11.040	-64 26 38.04	03152-6427	DUN 12A,BC	105.378	19.006	6.617	8.887	F5M	F5	-57.011	-57.011	-24.461	-60.221
13*			unidentified											
14	03 38 10.248	-59 46 35.04	03382-5947	DUN 14	271.795	57.473	6.951	8.302	F3V	F5V	43.356	43.356	25.698	44.655
15*	03 39 45.480	-40 21 07.92	03398-4022	DUN 15	327.582	7.676	6.901	7.752	A3V		18.996	18.996	21.711	10.570
16*	03 48 35.880	-37 37 12.72	03486-3737	DUN 16	216.799	8.093	4.709	5.300	B8	A1V	-5.007	-5.007	63.251	-8.658
17*	04 00 59.376	-54 23 31.56	04010-5424	DUN 17AB	141.883	64.518	7.677	8.173	A3V	A9III/IV	17.142	17.142	29.236	-6.599
18*	04 50 55.320	-53 27 41.40	04509-5328	DUN 18AB	58.325	12.340	5.606	6.342	F0IV...	F0IV	66.139	66.139	-80.769	85.658
19*	05 16 23.832	-33 32 16.08	one				6.947		K0III		-14.998	-14.998		
20*	05 24 46.272	-52 18 59.04	05248-5219	DUN 20AB,C	288.734	38.110	6.234	6.761	A0V	A2V	-5.23 A	-27.93 A	-7.188	-28.139
21	05 30 09.480	-47 04 39.72	05302-4705	DUN 21AD	271.461	197.665	5.455	6.638	G3IV	F2V	-132.345	-132.345	28.157	-0.165
22*	05 31 10.440	-42 17 59.28	05312-4219	DUN 22	167.489	7.375	6.131	7.789	A5	A7/F0V+(F	59.768	59.768	31.348	66.174
23	06 04 46.680	-48 27 29.88	06048-4828	DUN 23	121.097	2.788	6.969	7.570	G6V		-22.693	-22.693	-117.386	-39.041
24	06 10 17.904	-54 58 06.96	one				4.717		B0.5IV		7.634	7.634		
25	06 18 53.184	-32 12 06.12	06189-3212	JSP 96	9.605	1.826	9.446	10.159	K0		9.365	9.365	11.079	8.378
26*	06 12 11.232	-65 31 52.32	06122-6532	DUN 26AB	119.394	20.537	6.800	8.071	F6V	F7IV	154.474	154.474	18.163	143.919
27*	06 16 18.792	-59 12 48.60	06163-5913	DUN 27AB	232.931	34.640	6.421	7.638	G1V	F3/F5V	-316.585	-316.585	26.814	-209.198
28*	06 24 01.008	-36 42 28.08	06240-3642	DUN 28AC	74.229	63.579	5.617	6.822	K1II/III	G6/G8III	55.014	55.014	-25.344	-5.049
29*	06 29 07.104	-40 22 18.84	06291-4022	DUN 29	117.927	64.567	7.556	7.862	K2IV/V	K0PBA	25.845	25.845	-11.053	1.190
30	06 29 49.128 A	-50 14 20.40 A	06298-5014	DUN 30AB,CD	312.678	12.215	5.297	9.173	F2V		-53.31 A	-60.9 A	-67 A	-52.4 A

Modern Version of the Dunlop Catalogue (continued)
(See Table 1 Section 2, for explanation of columns)

DUN	RA h:m:s	DE d:m:s	WDS	Disc	PA deg	Sep as	Vmag1	Vmag2	SpType1	SpType2	pmRA1 mas/yr	pmDE1 mas/yr	pmRA2 mas/yr	pmDE2 mas/yr
31*	06 38 37.632	-48 13 12.72	06386-4813	DUN 31	321.026	12.966	5.027		G8III		20.104	20.104	5.297	18.934
32*	06 42 16.392	-38 23 55.68	06423-3824	DUN 32	277.785	7.973	6.501	5.762	A3V+...	A3	3.682	3.682	-13.959	2.181
33	06 46 03.216	-39 32 25.08	one				6.626		B4Vne		8.125	8.125		
34*	06 44 12.792	-54 41 43.80	06442-5442	DUN 34	191.598	129.361	6.473	6.672	B5/B6V	B8/B9V	5.979	5.979	-8.861	14.066
35*	06 48 43.128	-43 48 05.40	two		270.535	269.972	7.328	7.407	B8V	A4V	10.642	10.642	-13.571	41.058
36*	06 50 23.352	-31 42 21.96	06504-3142	H 5 108A,BC	65.605	42.710	5.735	7.735	B3V	F3	15.219	15.219	-2.053	14.232
37	07 01 18.288	-50 28 00.12	two		74.081	483.010	7.234	7.592	B8III	B9V	3.492	3.492	-5.041	1.900
38*	07 03 57.312	-43 36 28.80	07040-4337	DUN 38AB	125.024	21.327	5.534	6.691	G3V...	K0V	389.550	389.550	-101.764	382.276
39*	07 03 15.096	-59 10 41.16	07033-5911	DUN 39	90.000	1.476	5.697	6.789	B9IV		12.429	12.429	-17.013	10.128
40*	07 09 13.800	-56 21 36.36	07092-5622	DUN 40	142.548	36.732	8.010	8.439	G8/K0III	F0III	3.274	3.274	-9.964	1.587
41	07 10 24.480	-55 35 15.72	07104-5536	RMK 5	225.262	7.160	7.590	7.725	G8/K0III+G/K		-11.968	-11.968	0.404	-11.671
42*	07 08 44.856	-70 29 56.04	07087-7030	DUN 42	297.632	13.972	3.756	5.548	G8IIIvar	F0/3	106.881	106.881	5.938	112.927
43*	07 17 08.568	-37 05 51.00	07171-3706	DUN 43AB	213.346	68.952	2.710	7.921	K3Ib	B9/A0(V)	2.283	2.283	-9.960	6.374
44	07 20 21.432	-52 18 41.40	unidentified	RMK 6	25.569	9.179	5.965	6.534	F0-2IV-V	F9Ve+K3V+	148.387	148.387	-34.085	137.956
45*	07 21 22.152	-48 31 37.56	07214-4832	DUN 45	157.097	22.667	6.787	7.862	B9V	B8IV/V+...	23.524	23.524	-10.307	24.127
46			unidentified											
47	07 24 43.848	-31 48 32.04	07247-3149	DUN 47A,CD	343.044	98.607	5.328	7.584	K1III	B8V	9.185	9.185	-7.720	5.415
48*			unidentified											
49	07 28 51.144	-31 50 54.24	07289-3151	DUN 49	53.655	9.112	6.372	7.044	B3V+...	B4V	4.058	4.058	-10.264	5.200
50			unidentified											
51	07 29 13.848	-43 18 05.04	07292-4318	DUN 51	73.723	21.835	3.260	9.491	K5IIISB	G5V	174.579	174.579	-63.322	189.489
52*	07 34 18.624	-23 28 25.32	07343-2328	H N 19	116.711	9.611	5.771	5.816	F6V	F5/7V	-0.739	-0.739	-87.414	-11.691
53*	07 38 49.872	-26 48 13.68	07388-2648	H 3 27AB	316.857	9.868	4.441	4.651	B5IV	B6V	21.357	21.357	-22.705	12.708
54*	07 45 15.288	-37 58 06.96	one				3.621		K4III		4.903	4.903		
55*	07 44 12.504	-50 27 24.12	07442-5027	DUN 55AC	133.302	51.965	6.629	7.528	F8V	G0	143.459	143.459	-111.783	142.603
56*	07 47 07.200	-41 30 13.32	07471-4130	DUN 56	178.135	49.706	6.916	7.692	B1/B2Ib/II	K7III	5.205	5.205	-6.212	3.664
57	07 41 49.272	-72 36 21.96	07418-7236	DUN 57	118.244	16.736	3.947	9.307	K0III		16.213	16.213	27.817	28.001
58	07 54 44.736	-44 21 20.88	three		159.506	84.551	7.171	7.842	B8II/III	B8II	4.445	4.445	-5.367	4.836
59	07 59 12.312	-49 58 36.84	07592-4959	DUN 59AB	47.169	16.416	6.296	6.318	B2IV-V	B2IV-V	8.398	8.398	-5.623	7.875
60	08 01 23.040	-54 30 55.80	08014-5431	DUN 60	162.251	40.445	6.113	7.986	B2IV-V	A8	6.417	6.417	-3.302	5.025
61	08 06 51.528	-27 06 51.48	08069-2707	DUN 61	34.767	69.679	7.051	8.925	B7III	K0	1.606	1.606	-17.806	-5.395
62*	08 04 42.936	-62 50 10.68	08047-6250	DUN 62	259.185	86.339	6.244	7.677	B2.5Vn	M	11.960	11.960	11.144	-46.039
63*	08 09 47.688	-42 38 26.88	08098-4238	DUN 63	82.623	5.608	6.477	7.473	B7V		5.598	5.598	-10.314	7.716
64*	08 09 31.944 A	-47 20 11.76 A	08095-4720	DUN 65AC	152.008	62.377	1.812	7.288	WC8+O9I	F0	-5.94 A	13.19 A	-6.725	9.203
65*	08 09 31.944 A	-47 20 11.76 A	08095-4720	DUN 65AB	220.333	41.087	1.812	4.199	WC8+O9I	B2III*	-5.94 A	13.19 A	-6.706	10.775
66*	08 07 55.800	-68 37 01.56	08079-6837	RMK 7	23.411	6.277	4.390	7.296	B6IV		29.553	29.553	-30.036	29.584
67	08 13 58.320	-36 19 20.28	08140-3619	DUN 67	176.014	66.761	5.074	6.073	B2V:	B2IV/V	7.093	7.093	-6.904	7.598
68	08 13 18.192	-36 20 30.12	08136-3621	DUN 68	25.579	124.924	7.294	7.322	B5V	B2/B3V	7.279	7.279	-7.425	7.218
69	08 25 31.320	-51 43 38.64	08255-5144	DUN 69AB	218.143	25.634	5.165	9.626	B2V		17.555	17.555	-6.649	7.502
70*	08 29 27.480	-44 43 29.28	08295-4443	DUN 70	350.689	4.742	5.162	6.972	B3Vn		8.166	8.166	-6.480	7.339
71	08 30 34.416	-40 30 42.12	08306-4031	DUN 71	51.516	63.636	7.034	7.500	B8V	K4III	5.500	5.500	4.444	-11.887
72	08 40 21.120	-42 23 21.12	08404-4223	DUN 72A,BC	359.765	129.601	6.863	7.704	A3V	(G)	37.681	37.681	0.751	6.163
73*	08 56 11.256	-55 31 41.88	08562-5532	DUN 73AB	0.177	65.880	7.689	8.152	K0	K0	6.848	6.848	1.675	6.021
74*	08 56 58.416	-59 13 45.48	08570-5914	DUN 74	75.957	40.059	4.897	6.692	B2IV-V	B9.5V	8.421	8.421	-10.283	8.077
75	09 17 54.984	-69 48 16.92	09179-6948	RMK 10	18.412	10.624	8.142	8.515	A0V:	A0	6.229	6.229	-7.509	6.167

Modern Version of the Dunlop Catalogue (continued)
(See Table 1 Section 2, for explanation of columns)

DUN	RA h:m:s	DE d:m:s	WDS	Disc	PA deg	Sep as	Vmag1	Vmag2	SpType1	SpType2	pmRA1 mas/yr	pmDE1 mas/yr	pmRA2 mas/yr	pmDE2 mas/yr
76*	09 28 34.176	-45 29 51.72	09286-4530	DUN 76AC	99.232	60.589	7.125	7.594	B6Vnn	B5IV/V	-2.923	-2.923	-9.745	-0.649
77	09 29 18.672	-44 32 20.40	09293-4432	DUN 77AB	77.363	108.606	7.006	6.968	G0V...	F8V	8.244	8.244	-113.311	16.341
78*	09 30 46.104	-31 53 21.12	09308-3153	DUN 78	212.031	8.068	6.155	6.879	A1V	A1V	-22.448	-22.448	20.756	-21.530
79*	09 33 38.688	-49 45 28.44	09336-4945	DUN 79	33.023	140.401	7.340	7.522	K0III	G6IV	-34.944	-34.944	53.565	-1.471
80	09 45 03.672	-49 29 07.44	09450-4929	DUN 80AB	249.970	18.919	8.020	8.111	F8/G0V	G0/G1IV/V	98.409	98.409	-23.581	97.158
81	09 54 17.664	-45 17 00.60	09543-4517	DUN 81	239.103	5.609	5.787	8.220	B4V	B9V	5.356	5.356	-15.021	2.722
82	09 33 17.640	-86 00 36.36	09333-8601	DUN 82	275.093	16.221	7.083	7.554	F3/F5IV+...	F2	-23.253	-23.253	-50.4 A	-19.98 A
83	10 02 05.736	-54 58 53.76	10021-5459	DUN 83	226.680	113.864	7.748	7.896	K2III	B8/B9V	-12.832	-12.832	-13.764	0.217
84*	10 03 10.440	-52 02 46.68	10032-5203	HJ 4282	194.518	49.459	7.346	8.345	A4/5IV/V	B9	38.332	38.332	-15.952	0.794
85	10 28 48.504	-62 35 02.40	10288-6235	DUN 85	220.392	21.743	8.310	8.770	B6V	B5/7	4.159	4.159	-14.348	4.276
86*	10 31 13.320	-42 13 45.84	10312-4214	DUN 86AB	291.461	83.636	7.343	8.015	APEUCR (SR)	A1V	-7.451	-7.451	-13.416	-5.012
87*	10 30 39.240	-61 21 23.40	10307-6121	DUN 87	331.134	82.215	6.427	7.558	M2III	B4:V:ne	12.591	12.591	-8.881	3.456
88*	10 31 57.432	-45 04 00.12	10320-4504	PZ 3	217.844	13.676	5.701	6.052	B6II	B8II	-1.435	-1.435	-15.865	-2.876
89*	10 33 15.144	-55 23 12.84	10333-5523	DUN 89AB	30.385	25.874	6.676	7.722	G5	A1V	-0.886	-0.886	-13.670	-3.012
90			unidentified											
91*	10 31 55.368	-72 06 38.16	10319-7207	DUN 91	61.822	9.911	8.512	8.810	B8/9V		2.594	2.594	-5.986	2.320
92*	10 32 01.464	-61 41 07.08	one				3.359		B4Vne		7.607	7.607		
93*	10 34 56.472	-64 08 02.40	10349-6408	DUN 93AB	39.427	24.235	7.425	8.338	A0V	A9III	11.672	11.672	-17.395	2.221
94*	10 38 45.000	-59 10 58.80	10387-5911	DUN 94	20.681	14.622	4.702	7.464	K4/K5III:	B9II/III	1.117	1.117	-14.380	0.932
95*	10 39 18.384	-55 36 11.88	10393-5536	DUN 95AB	105.293	51.866	4.276	6.179	G2II	B8V	4.880	4.880	-19.178	5.524
96*	10 42 40.560	-59 12 56.88	one				5.392		B2.5Ia		2.484	2.484		
97	10 43 09.432	-61 10 06.60	10432-6110	DUN 97AB	174.491	12.658	6.592	7.909	B3III	A0III:	2.907	2.907	-14.740	3.370
98*	10 45 03.528	-59 41 04.20	10451-5941	DUN 98AH	17.143	61.032	6.369	8.123	PECULI-ARE	O3V	-10.86 A	3.86 A	-6.547	2.145
99*	10 44 20.016	-70 51 34.92	10443-7052	DUN 99AB	75.341	62.591	6.237	6.441	A5IV/V	A6IV	-0.080	-0.080	-47.578	0.999
100	10 46 16.536	-64 30 52.56	two		157.027	396.093	5.327	8.414	B7:V	F7V	10.854	10.854	-84.929	20.375
101	10 50 58.632	-59 57 26.28	10510-5957	HJ 4378	346.914	31.046	6.787	10.173	B8/B9IV		-0.965	-0.965	-6.335	1.880
102*	10 53 29.664	-58 51 11.52	10535-5851	DUN 102AB	204.434	159.352	3.776	6.244	K0III-IV...	B5V	39.426	39.426	-15.284	2.841
103*	10 53 29.664	-58 51 11.52	10535-5851	DUN 103AC	6.994	56.581	3.776	7.842	K0III-IV...		39.426	39.426	19.485	-14.069
104	11 00 08.280	-51 49 04.08	three				6.150		A3III/IV		1.694	1.694		
105*	11 04 55.512	-61 03 05.76	11049-6103	DUN 105	221.378	23.988	7.597	9.819	O9V		1.404	1.404	-6.582	1.574
106	11 17 12.000	-38 00 51.84	one				6.231		A1V		8.975	8.975		
107	11 18 41.688	-74 11 26.16	two		299.644	123.005	7.730	8.562	F7IV/V	APSI	-14.419	-14.419	-13.052	1.635
108	11 22 15.576	-58 23 09.60	four				6.631		G8III		-47.996	-47.996		
109*	11 28 35.088	-42 40 27.12	11286-4240	BSO 6	169.585	13.177	5.131	7.513	B9V	A3V	9.153	9.153	-34.534	12.493
110	11 29 54.960	-55 19 07.68	three				7.775		K2/4		-4.802	-4.802		
111*	11 32 16.416	-29 15 39.60	11323-2916	H 3 96	211.253	9.686	5.619	5.723	F8V	F3/5	144.524	144.524	-22.025	139.982
112*	11 35 58.920	-50 44 32.64	two		288.907	209.980	7.791	8.121	F0/F2V	A5V	11.378	11.378	-28.678	-1.658
113*	11 36 58.008	-38 57 34.20	11370-3858	DUN 113	149.285	149.072	6.941	7.465	A0/A1V	K2III	-2.705	-2.705	50.376	-17.133
114	11 39 58.488	-38 06 30.24	11400-3806	DUN 114	94.843	17.057	6.618	8.168	G8III	K5	-18.768	-18.768	-51.558	-17.676
115	11 39 57.024	-33 26 59.64	11400-3327	I 232	146.277	2.164	6.875	10.034	K1III		-26.794	-26.794	-48.15 A	-27.04 A
116*	11 56 43.776	-32 16 02.64	11567-3216	DUN 116AB	261.184	18.791	7.749	7.697	G3V	G3V	-6.668	-6.668	-171.610	-8.250
117*	12 04 46.968	-61 59 48.48	12048-6200	DUN 117AB	149.500	22.980	7.380	7.631	B8Ib-II...	F0Ib-II	-0.065	-0.065	-6.532	0.151
118	12 12 52.104	-59 39 19.08	two		125.565	58.801	7.054	8.479	K0III	K0III	0.265	0.265	-8.491	-0.107
119*	12 14 17.040	-66 32 55.32	two		32.176	102.503	7.119	7.433	B5V	B0.5Ib	0.312	0.312	-5.490	-0.532
120*			unidentified											

The Southern Double Stars of James Dunlop III: Modern Version and Analysis of Accuracy ...

Modern Version of the Dunlop Catalogue (continued)
(See Table 1 Section 2, for explanation of columns)

DUN	RA h:m:s	DE d:m:s	WDS	Disc	PA deg	Sep as	Vmag1	Vmag2	SpType1	SpType2	pmRA1 mas/yr	pmDE1 mas/yr	pmRA2 mas/yr	pmDE2 mas/yr
121			unidentified											
122*	12 26 35.952 A	-63 05 56.76 A	12266-6306	DUN 252AC	202.454	89.982	1.039	4.795	B0.5IV	B3/5V	-35.56 A	-13.9 A	-39.591	-14.537
123*	12 26 35.952 A	-63 05 56.76 A	12266-6306	DUN 252AB	111.026	4.014	1.039	1.570	B0.5IV	B1V	-35.56 A	-13.9 A	-42.52 A	-7.67 A
124*	12 31 09.936 A	-57 06 45.36 A	12312-5707	DUN 124AB	26.149	125.527	1.656	6.402	M4III	A3V	26.55 A	-263.85 A	2.317	-21.349
125*	12 47 43.320 A	-59 41 19.32 A	12477-5941	DUN 125AC	22.836	372.650	1.294	7.177	B0.5III	B7II	-47.77 A	-12.97 A	-10.676	-2.082
126*	12 54 35.616	-57 10 40.44	12546-5711	DUN 126AB	17.341	34.697	3.993	5.096	B2IV-V	B5Vne	-14.510	-14.510	-28.155	-10.343
127*	12 59 48.312	-55 54 44.28	12598-5555	DUN 127	125.717	16.650	8.222	8.942	B7IV/V	B9	-4.565	-4.565	-15.511	-4.833
128	13 06 54.648	-49 54 22.68	13069-4954	DUN 128	99.153	24.894	4.269	10.012	B1.5V	F5V	-10.580	-10.580	-27.853	-12.561
129*	13 08 07.152	-65 18 21.60	13081-6518	RMK 16AB	186.357	5.433	5.649	7.552	WC6+O9.5I	O9.5II	-1.649	-1.649	-3.926	-1.944
130			unidentified											
131*	13 15 14.928	-67 53 40.56	13152-6754	DUN 131AC	331.252	58.307	4.775	7.250	B8V	F0	-9.652	-9.652	-30.949	-11.420
132*			unidentified											
133*	13 22 37.920	-60 59 18.24	13226-6059	DUN 133AB,C	345.647	60.571	4.508	6.185	B3V	B4Vn	-23.842	-23.842	-10.259	-9.996
134	13 20 35.808	-36 42 44.28	one				2.743		A2V		-82.181	-82.181		
135	13 22 55.632	-62 00 43.92	five				7.953		A0Ia		-1.713	-1.713		
136	13 31 02.640	-39 24 26.64	13310-3924	SEE 179	188.949	573.987	3.890	8.192	G8II/III	M2III	-14.71 A	-11.52 A	-3.130	-10.911
137*	13 32 03.912	-63 02 30.84	13321-6303	DUN 137	357.640	15.853	7.478	8.484	B0.5III:		-1.999	-1.999	-3.534	-2.895
138*	13 36 48.456	-26 29 42.72	13368-2630	H N 69AB	190.856	10.264	5.714	6.578	A7V+...	A2	16.448	16.448	-84.974	14.125
139	13 36 54.840	-56 09 24.48	three				8.012		G6V		-44.774	-44.774		
140	13 45 47.280	-71 59 04.92	13458-7159	DUN 140	72.798	10.956	8.708	9.656			-8.391	-8.391	-14.223	-7.738
141*	13 41 44.760	-54 33 33.84	13417-5434	DUN 141	162.815	5.652	5.193	6.511	B8Vn+...	A0V	-24.437	-24.437	-42.883	-27.608
142*	13 43 57.336	-59 14 09.60	13440-5914	DUN 142	90.000	33.330	6.487	7.702	B8V	B9V	-10.603	-10.603	-31.023	-10.321
143	13 49 14.256	-62 06 11.88	13492-6206	DUN 143	37.173	13.102	7.508	7.986	K2/K3II/III	B2II:	-6.595	-6.595	-5.477	-2.875
144	13 49 34.392	-47 22 09.48	13496-4722	DUN 144	256.175	9.039	8.208	8.954	F6V+F7/G0		6.117	6.117	52.444	5.605
145	13 54 37.512	-66 54 03.96	13546-6654	DUN 145	48.327	23.824	7.796	8.906	B9V	F0	-22.574	-22.574	-13.657	-12.284
146*	13 49 16.488	-40 30 59.04	13493-4031	DUN 146	86.606	66.895	6.920	7.316	F3V	M1III	2.347	2.347	-0.203	-1.343
147*	13 52 04.872	-52 48 41.40	13521-5249	RMK 18	288.525	18.130	5.250	7.469	B9Vn	B8V	-27.426	-27.426	-40.104	-27.611
148*	13 51 49.608	-32 59 38.76	13518-3300	H 3 101	105.968	7.852	4.528	5.974	B5III	B8V	-27.909	-27.909	-36.737	-23.774
149*	13 53 32.712	-38 15 57.60	two		216.219	179.384	7.636	8.286	A4III/IV	K1III/IV	-24.703	-24.703	-66.165	-10.121
150	13 57 28.080	-57 42 39.96	13575-5743	DUN 150AB	265.774	58.621	7.367	8.767	M3Iab/Ib	B7III	-1.534	-1.534	-2.879	-3.765
151	13 57 17.232	-56 02 24.00	13573-5602	DUN 151	54.766	36.192	7.515	8.934	G2V	A2	-84.789	-84.789	-16.026	-0.664
152	14 01 43.512	-45 36 12.24	one				4.331		F6II		-26.805	-26.805		
153*	14 06 02.760	-41 10 46.56	two		78.065	85.298	4.348	8.482	B2V	A1Vn	-20.186	-20.186	-23.419	-21.649
154	14 05 30.336	-36 32 42.72	14055-3633	DUN 154	129.942	20.747	8.208	9.880	A9V		-7.915	-7.915	-14.112	-7.548
155*	14 07 44.568	-53 41 27.96	14077-5341	DUN 155	6.623	18.483	7.849	8.397	F2	F0V+...	-2.392	-2.392	-54.572	-18.304
156	14 06 41.328 A	-36 22 07.32 A	14067-3622	DUN 253AB			2.058		K0IIIb		-519.66 A	-518.73 A		
157	14 09 35.040	-51 30 16.92	14096-5130	HJ 4651	130.526	64.267	5.956	8.722	B9IV	K2III	-12.572	-12.572	-14.853	-3.199
158			unidentified											
159*	14 22 37.008	-58 27 32.40	14226-5828	DUN 159AB	155.406	9.502	4.914	7.151	G8/K1+F/G		-46.45 A	31.37 A	-39.632	24.115
160*	14 26 08.232	-45 13 17.04	14261-4513	DUN 160	204.036	156.883	4.552	8.928	B2IV		-14.308	-14.308	-15.266	0.872
161	14 15 38.688	-45 00 02.88	one				6.306		F9V		-137.455	-137.455		
162	14 33 51.696	-46 27 53.64	14339-4628	DUN 162			7.188		G6/G8III		-35.452	-35.452		
163*	14 38 00.576	-54 30 40.68	14380-5431	DUN 163	103.290	64.209	7.991	8.364	F0III	B8III	-34.664	-34.664	-6.285	-7.422
164*	14 35 30.384	-42 09 28.80	two		141.555	129.621	2.328	9.192	B1Vn+A	A5V	-35.29 A	-34.59 A	4.847	-1.749
165*	14 39 40.896 A	-60 50 06.36 A	14396-6050	RHD 1AB	214.906	19.315	-0.008	1.348	G2V	K1V	-3678.16 A	481.82 A	-3600.35 A	952.09 A

The Southern Double Stars of James Dunlop III: Modern Version and Analysis of Accuracy ...

Modern Version of the Dunlop Catalogue (continued)
(See Table 1 Section 2, for explanation of columns)

DUN	RA h:m:s	DE d:m:s	WDS	Disc	PA deg	Sep as	Vmag1	Vmag2	SpType1	SpType2	pmRA1 mas/yr	pmDE1 mas/yr	pmRA2 mas/yr	pmDE2 mas/yr
166	14 42 30.408	-64 58 30.36	14425-6459	DUN 166AB	226.218	15.609	3.174		F1Vp		-232.614	-232.614	-170.705	-250.314
167	14 41 01.392	-36 08 05.64	two		148.149	82.644	5.659	9.331	APSI	F0V	-6.363	-6.363	-31.616	-8.199
168	14 42 46.512	-55 10 54.48	14428-5511	DUN 168	200.839	5.778	8.430	8.659	F3+FIII		-13.473	-13.473	6.736	-13.343
169*	14 45 10.968	-55 36 05.76	14452-5536	DUN 169	105.433	68.993	6.090	7.486	B2III	K2III	-7.221	-7.221	2.470	-6.707
170			unidentified											
171	14 53 22.128	-45 51 20.88	14534-4551	DUN 171AB	228.203	17.825	7.086	9.496	B3Ve	B8	-2.830	-2.830	-10.654	-0.452
172	14 54 42.576	-65 59 27.96	one				6.074		B3Vn		-8.510	-8.510		
173	14 52 51.072	-37 48 11.52	14529-3748	SHT 57			5.014		B7II/III		-20.118	-20.118		
174*	14 55 18.960	-46 37 52.68	one				7.296		G6III		-25.563	-25.563		
175	15 01 56.928	-51 55 05.88	15019-5155	HJ 4723AB	168.382	5.513	7.436	9.937	G8/K0III		-21.908	-21.908	-35.634	-21.738
176*	15 12 17.088	-52 05 57.12	15123-5206	DUN 176	248.789	71.640	3.398	6.670	G8III	F8V	-72.951	-72.951	-111.478	-69.076
177*	15 11 56.088	-48 44 16.08	15119-4844	DUN 177	143.582	26.395	3.848	5.613	B9V	A3IV	-51.638	-51.638	-98.451	-43.845
178*	15 11 34.800	-45 16 39.00	15116-4517	DUN 178AC	258.524	30.760	6.415	7.293	K1III	K0III	14.346	14.346	34.467	-47.458
179*	15 14 30.984	-43 23 13.20	15145-4323	DUN 179	46.499	10.460	7.301	8.477	A1V+B/A		-15.529	-15.529	-6.984	-15.199
180*	15 18 31.968 A	-47 52 30.00 A	15185-4753	DUN 180AC	130.523	23.825	5.005	6.619	B8	A2/A3V:	-26.54 A	-44.34 A	-18.595	-24.721
181	15 20 14.112	-38 22 43.32	15202-3823	DUN 181AB	350.769	29.907	9.550	10.109	B9V		-6.713	-6.713	7.027	-0.474
182*	15 22 40.872	-44 41 22.56	15227-4441	DUN 182AC	168.829	26.421	3.369		B2IV-V		-24.139	-24.139	-6.461	-13.865
183*	15 25 20.208	-38 44 00.96	15253-3844	DUN 183AB	203.821	92.478	4.597	9.286	A0V	G5V	-24.603	-24.603	-39.517	-43.507
184	15 26 15.264	-42 51 44.28	15263-4252	DUN 184	96.807	21.260	8.388	9.432	G0V		-29.764	-29.764	-6.436	-6.703
185	15 28 27.216	-51 35 52.44	15285-5136	SEE 234			6.090		G2Ib		-5.219	-5.219		
186	15 33 04.800	-58 11 38.76	15331-5812	DUN 186	114.903	39.327	8.762	8.682	F3IV	F3/F5V	-62.513	-62.513	-42.649	-61.069
187	15 33 33.264	-47 32 16.08	15336-4732	DUN 187	218.746	24.464	7.126	9.347	F0IV		-69.183	-69.183	26.510	-70.857
188	15 36 43.224	-66 19 01.20	15367-6619	DUN 188	219.956	82.187	4.102	9.295	K0III	A8/F0IV/V	-55.113	-55.113	-10.660	-11.821
189	15 38 49.464	-52 22 21.72	15388-5222	DUN 189AB	278.958	53.178	5.421	10.564	B9V		-31.787	-31.787	-34.663	-31.194
190	15 42 58.248	-58 06 52.92	15430-5807	DUN 190AB	90.000	4.944	7.859	9.694	M3III+...	B8/A0(III)	-2.815	-2.815	-5.770	-4.106
191	15 45 16.224 A	-58 41 13.56 A	15453-5841	DUN 191AB,C	296.260	32.546	7.672	8.079	G6III+...	A4V	9.84 A	2.05 A	8.914	1.473
192	15 47 04.464	-35 30 37.08	15471-3531	DUN 192AB,C	143.109	34.660	6.848	7.309	A0V	B9.5V	-25.639	-25.639	-18.870	-24.999
193	15 51 06.816	-55 03 19.80	15511-5503	DUN 193	11.766	16.180	5.763	8.932	B2II		-3.891	-3.891	-28.427	-36.475
194	15 54 52.632	-60 44 37.32	15549-6045	DUN 194AC	47.413	44.687	6.227	9.956	B9II		-3.844	-3.844	-3.699	-6.224
195	15 54 50.472	-50 20 17.88	15548-5020	DUN 195AB	8.796	12.021	6.777	7.480	A3/5V+B/A		-40.644	-40.644	-37.997	-39.871
196*	15 56 53.496	-33 57 57.96	15569-3358	PZ 4	50.147	10.112	5.087	5.568	A3V	B9V	-37.981	-37.981	10.821	-41.299
197*	16 00 07.320	-38 23 48.12	16001-3824	RMK 21AC	247.730	114.942	3.414	9.319	B2.5IV	G0V	-28.463	-28.463	-18.187	-26.577
198	16 04 21.312	-53 42 37.44	two		190.814	80.632	6.474	9.734	B9II/IIIp..	A2	-11.037	-11.037	-4.952	-7.694
199	16 08 34.560	-39 05 34.44	16086-3906	DUN 199AC	184.003	44.027	6.632	7.084	A1/A2III	A7IVe	-19.959	-19.959	-8.950	-23.007
200	16 22 29.064	-43 54 43.56	16225-4355	DUN 200	194.980	39.130	5.907	9.541	G2Ib		-12.758	-12.758	1.414	0.848
201	16 27 57.336	-64 03 28.44	16280-6403	DUN 201	2.178	16.572	5.283	9.649	F4IV		26.065	26.065	-1.072	-4.837
202	16 31 41.760	-41 49 01.56	16317-4149	DUN 202AC	178.674	57.976	5.316	9.595	B1Ia		-2.340	-2.340	2.735	-2.578
203	16 33 05.160	-60 54 12.96	16331-6054	DUN 203	277.439	22.245	7.886	8.157	A3III	F8/G0V	-22.679	-22.679	58.938	79.868
204	16 35 13.848	-35 43 28.56	one				6.627		B9V		-25.699	-25.699		
205			unidentified											
206	16 41 20.424	-48 45 46.80	16413-4846	DUN 206A,C	265.768	9.756	5.668	6.755	O5V:+O6:	O7V	-4.439	-4.439	1.270	-3.724
207	16 44 25.584	-42 23 34.80	16444-4224	DUN 207	185.274	11.569	8.970	9.585	G8III/IV	A3/5	-46.216	-46.216	-13.169	-46.250
208	16 43 44.376	-47 06 20.52	one				7.064		APSI		-16.278	-16.278		
209	16 48 11.328	-36 53 02.40	16482-3653	DUN 209	138.658	23.975	7.473	8.347	A5IV/V	A0/1	0.613	0.613	6.192	9.153
210	16 48 42.816	-55 26 01.68	16487-5526	DUN 210AB	351.315	75.749	8.161	8.647	K	APSI	-16.215	-16.215	-2.430	-8.239

Modern Version of the Dunlop Catalogue (conclusion)
(See Table 1 Section 2, for explanation of columns)

DUN	RA h:m:s	DE d:m:s	WDS	Disc	PA deg	Sep as	Vmag1	Vmag2	SpType1	SpType2	pmRA1 mas/yr	pmDE1 mas/yr	pmRA2 mas/yr	pmDE2 mas/yr
211	16 47 36.864	-48 20 11.40	16475-4819	DUN 211BC	193.482	45.165	8.121	8.168	F3/8(III)	F2/3IV/V	-36.729	-36.729	-5.591	-37.335
212	17 04 01.224	-51 05 00.96	17040-5105	DUN 212AB	282.812	16.234	8.340	8.810	B2V	B3V	-2.641	-2.641	-1.042	-4.664
213	17 10 20.832	-46 44 18.24	17103-4644	DUN 213	166.006	8.162	6.883	8.270	B1Ib		-3.170	-3.170	0.542	-5.519
214	17 13 17.880	-67 11 47.76	17133-6712	DUN 214AB	14.005	37.474	5.872	8.746	K0III-IV		-89.998	-89.998	-9.949	-9.580
215	17 19 19.776	-53 23 08.88	17193-5323	DUN 215AB	43.082	61.612	8.317	8.925	K1III	F3/F5V	-176.351	-176.351	-46.609	-70.485
216*	17 26 51.984	-45 50 34.80	17269-4551	DUN 216AC	311.954	102.852	5.502	7.102	B8V	A0V	-28.278	-28.278	-5.906	-29.375
217	17 29 00.864	-43 58 26.04	17290-4358	DUN 217	167.924	13.621	6.293	8.503	B5III		-11.042	-11.042	-2.767	-8.684
218	17 33 36.528 A	-37 06 13.32 A	17336-3706	DUN 218AC	329.789	94.148	1.623	9.121	B1.5IV+...		-4.94 A	-29.7 A	-5.037	-31.096
219	17 58 55.680	-36 51 30.24	17589-3652	DUN 219AB	254.228	52.978	5.734	7.718	G8III	F0IV/V	13.942	13.942	-21.464	-45.722
220	18 22 09.912	-55 33 51.12	18222-5534	DUN 220	176.989	31.003	8.022	8.420	F8/G0		1.586	1.586	79.534	1.748
221	18 24 18.240	-44 06 37.08	18243-4407	DUN 221	161.666	73.954	5.229	10.098	B2.5Vn		-23.107	-23.107	16.144	-0.098
222	18 33 23.136	-38 43 33.60	18334-3844	DUN 222	358.485	21.247	5.598	6.260	B9V	B8	-20.368	-20.368	-0.145	-21.424
223			unidentified											
224	18 54 01.608	-47 16 27.84	18540-4716	DUN 224AC	62.269	86.649	6.987	7.289	F5V	A0IV/V	-38.288	-38.288	21.472	-22.312
225	19 12 24.120	-51 48 20.16	19124-5148	DUN 225AB	250.232	70.252	7.061	8.376	K5III	F6IV	-21.779	-21.779	0.381	-30.727
226	19 22 38.304	-44 27 32.40	19226-4428	DUN 226	76.029	28.332	3.953	7.111	B9V	A3	-11.929	-11.929	13.182	-14.984
227	19 52 37.728	-54 58 15.60	19526-5458	DUN 227	148.346	22.838	5.710	6.427	G8/K0III	A2V	3.509	3.509	19.910	2.370
228*			unidentified											
229*	19 58 15.288	-51 53 43.44	19583-5154	DUN 229	242.300	80.543	7.619	8.197	A9IV	F6V	-43.879	-43.879	45.758	-43.416
230	20 17 49.680	-40 11 05.28	20178-4011	DUN 230	116.871	9.558	7.342	7.622	F7/G0+F8/ G2		14.210	14.210	40.123	12.546
231*	20 36 35.952	-71 04 17.04	20366-7104	DUN 231	285.396	48.814	6.827	8.786	A0IV		-25.972	-25.972	91.473	-74.296
232*	20 41 44.112	-75 21 02.88	20417-7521	DUN 232	18.733	16.726	6.447	7.087	G1V	G5V	-162.079	-162.079	163.555	-171.231
233	20 35 34.848	-60 34 54.48	one				4.749		F1III		-184.963	-184.963		
234	20 37 34.032	-47 17 29.40	20376-4717	HJ 5209AB			3.104		K0III		67.590	67.590		
235*	20 44 57.576	-50 29 16.44	20450-5029	DUN 235AC	122.269	125.419	7.591	7.386	A0IV/V	K0III	-10.029	-10.029	28.227	-7.504
236*	21 02 12.744	-43 00 07.56	21022-4300	DUN 236	72.830	57.316	6.620	6.868	G3IV+...	K0IV	-121.947	-121.947	71.018	-111.224
237	21 32 00.744	-58 48 54.36	four				8.086		M3III:		-9.313	-9.313		
238	22 25 51.144	-75 00 56.52	22259-7501	DUN 238AB	78.395	21.475	6.111	8.718	G3IV	G0	12.925	12.925	30.613	-7.127
239	22 29 45.432	-43 44 57.12	22298-4345	DUN 239	210.661	60.684	4.151	9.684	M4.5IIIa		5.662	5.662	2.447	-6.740
240*	22 31 30.336	-32 20 45.96	22315-3221	PZ 7AC	172.462	30.140	4.283	7.123	A1V		-17.951	-17.951	56.838	-21.045
241*	22 36 35.448	-31 39 49.68	22366-3140	DUN 241	31.321	93.132	5.809	7.432	K2III	K2III	-40.126	-40.126	-8.840	-3.543
242*	22 39 44.184	-28 19 32.52	22397-2820	H 6 119AB	159.331	86.188	6.308	7.265	K0/K1III	F5V	-40.596	-40.596	96.340	-37.578
243	22 42 39.936 A	-46 53 04.56 A	three				2.114		M5III		135.16 A	-5.05 A		
244	23 02 16.032	-64 17 52.80	23023-6418	DUN 244	91.330	46.539	7.638	9.800	F3:IV/V+...		-48.390	-48.390	22.600	-7.841
245	23 08 37.608	-59 44 11.76	23086-5944	DUN 245	289.967	13.705	7.390	9.425	F5V		-63.923	-63.923	62.034	-67.227
246	23 07 14.784	-50 41 12.12	23072-5041	DUN 246	256.006	8.932	6.224	6.993	F6.5IV-V+..	F8/G2	-24.686	-24.686	-37.933	-30.367
247	23 18 00.792	-61 00 13.32	23180-6100	DUN 247	293.634	50.289	6.736	8.173	K1IIICN...	A6V	-90.261	-90.261	1.874	9.434
248	23 20 50.184	-50 18 23.76	23208-5018	DUN 248AB,C	211.911	16.964	6.054	8.723	FMDEL- TADEL	G4IV	-72.625	-72.625	42.769	-72.534
249*	23 23 54.528	-53 48 31.32	23239-5349	DUN 249	211.741	26.669	6.118	7.061	A4III	A3III	-34.465	-34.465	70.508	-27.565
250*	23 27 11.064	-50 16 46.92	23272-5017	DUN 250	82.691	28.297	7.491	8.385	K2III	K2/3	-35.168	-35.168	-14.629	-5.741
251*	23 39 27.936	-46 38 16.08	23395-4638	DUN 251	275.546	3.725	6.291	7.236	A8V+...		41.522	41.522	24.905	35.030
252*	23 44 12.048	-64 24 16.20	two	DUN 252AB	8.643	235.960	5.717	7.070	K3II	K1/K2III	34.864	34.864	31.237	-2.115
253*	23 54 21.408	-27 02 34.44	23544-2703	LAL 192	270.000	6.413	6.664	7.380	A2V+...	F2V	0.277	0.277	29.719	3.667

The Southern Double Stars of James Dunlop IV: Rectilinear and Orbital Motion of Some Very Slow Moving Doubles

Roderick R. Letchford[1], Graeme L. White[2], Allan D. Ernest[3]

1. Vianney College Seminary, Wagga Wagga, NSW 2650, Australia, rodvianney@yahoo.com.au
2. Centre for Astronomy, University of Southern Queensland, Toowoomba, Australia QLD 4350, graemewhiteau@gmail.com
3. Charles Sturt University, Wagga Wagga, NSW 2650, Australia, aernest@csu.edu.au

Abstract: We present rectilinear and orbital elements and their plots of some very slow moving doubles from the first published dedicated catalogue of southern double stars. Of the 12 Dunlop doubles analysed, DUN 4*, 42*, 138*, 251 probably are not binaries; DUN 38*, 52*, 111*, 116*, 168, 230, 246 have uncertain but possible binarity; and only DUN 5* is a confirmed binary. The orbital parameters for DUN 52*, 230 and 246 we consider to be grade 5. Of those grade 5 orbits, curvature was detected in the historical data for DUN 230, with a probability of binarity of ~50.5%.

1. Introduction

This paper (Dunlop Paper IV) concludes a series of papers on the double stars of James Dunlop, one of three astronomers who worked at the privately owned observatory in Parramatta, NSW Australia in the 1820's. The Parramatta Observatory was the venture of Sir Thomas Makdougll Brisbane (1773-1860) the 6th British Governor of the Colony of NSW from 1822 to 1825.

In Dunlop Paper I (Letchford, White and Ernest, IN PRINT) we presented a history and description of the first published dedicated catalogue of southern double stars, by James Dunlop (1793-1848) and issued in 1829 as Approximate Places of Double Stars in the Southern Hemisphere, observed at Paramatta in New South Wales (Dunlop 1829). In Dunlop Paper II (Letchford, White and Ernest, IN PRINT) we presented modern designations of the pairs in Dunlop's original catalogue. In Dunlop Paper III (Letchford, White and Ernest, IN PRINT) we gave a detailed analysis of the original catalogue, comparing Dunlop's measurement accuracy with modern precessed data, as well as presenting modern data on each double star.

The Dunlop papers follow three papers (Rümker Papers I, II, and III) previously published in this journal on the double star work of another of the Parramatta astronomers, Carl Rümker (Letchford, White, and Ernest 2017; Letchford, White, and Ernest 2018a; Letchford, White, and Ernest 2018b).

Using the methods detailed in Rümker Papers II and III, in this paper we calculate and compare the rectilinear and orbital elements of 12 wide southern binaries first discovered by James Dunlop in the 1820s. Such a comparison will enable the probability of their binarity to be quantified directly by comparing their relative motions as if they were optical doubles (rectilinear) and then as physical binaries (orbital).

Distinguishing between optical and physical doubles is one of the fundamental aims of double star study because it has important implications for stellar formation models (Guinan, Harmanec, and Hartkopf 2007). There has been renewed interest in wide binary systems (of which the Dunlop pairs may be considered a subset) because of their potential to distinguish between the mainstream-accepted WIMP-based hypothesis of dark matter, and Modified Newtonian Dynamics (Longhitano, Binggeli, and Zejda 2010; Németh et al. 2016; Chanamé and Gould 2004). Relatively slow moving doubles may be either chance alignments of unrelated stars or very long period bound pairs. A comparison of the best-fit rectilinear motion and curved orbital motion should result in a clear distinction between these two types, since it is the variations from linearity that allows a sensitive identification of a Keplerian system.

2. Method for finding Rectilinear Elements

White, Letchford, and Ernest (2018) have shown that the precision of historic ground observations of double stars has improved with time; from ~0.6 arcsec to 0.14 arcsec in ρ (separation), and 0.74 degree to 0.5 degree in PA, over our period of interest (~1820 to the present). These uncertainties are dwarfed by the precisions of the HIPPARCOS and GAIA spacecraft (milli-arcsecond and micro-arcsecond respectively), and the inclusion of historic ground data in the rectilinear analysis presented here would not contribute to the accuracy of that analysis.

To find non-subjective rectilinear elements, we follow the method detailed in our paper Letchford, White, and Ernest (2018a), except that we used the second data release from the GAIA spacecraft (GAIA DR2) instead of the first data release (GAIA DR1).

3. Rectilinear Results

Rectilinear elements are given in Table 1; associated plots are in the Appendix. An ephemeris, based on these elements is given in Table 3.

4. Method for finding Orbital Elements

To find non-subjective orbital elements, the probability of binarity, and the detection of curvature in the historical data, we follow the methods detailed in our paper, Rümker Paper III (Letchford, White, and Ernest, 2018b), except for the following improvements:

We used GAIA DR2 data instead of GAIA DR1.

We obtained better estimates of masses using the luminosity (L) data from GAIA DR2 (instead of estimates from spectral types) and employing the following

Table 1: Rectilinear Elements and their uncertainties, all ICRS (Equinox effectively = J2000.0)

DUN	x0 (DE) " +/-	xa (DE) "/yr +/-	y0 (RA) " +/-	ya (DE) "/yr +/-	t0 yr +/-	θ0 ° +/-	ρ0 " +/-
4*	2.865	0.001	1.936	-0.002	6990.235	34.048	3.458
	1.578	0.000	0.945	0.000	1882.256	19.559	1.411
5*	-10.723	-0.014	-3.319	0.045	1971.528	197.199	11.225
	0.010	0.000	0.006	0.000	15.192	0.033	0.010
38*	4.421	-0.008	10.661	0.003	-157.102	67.478	11.541
	1.695	0.001	1.611	0.001	231.210	8.356	1.623
42*	9.324	-0.003	-2.483	-0.011	1049.013	345.090	9.649
	0.329	0.000	0.265	0.000	84.445	1.602	0.325
52*	0.837	-0.011	8.261	0.001	1509.641	84.218	8.303
	0.069	0.000	0.067	0.000	50.434	0.475	0.067
111*	0.285	-0.005	-0.579	-0.002	165.241	296.242	0.645
	0.188	0.000	0.180	0.000	40.084	16.576	0.182
116*	-5.951	-0.001	-1.114	0.007	4348.536	190.600	6.054
	0.927	0.000	1.225	0.001	685.732	11.510	0.939
138*	-4.668	-0.002	-6.004	0.001	-831.590	232.134	7.605
	0.566	0.000	0.744	0.000	393.019	4.812	0.682
168	-4.716	0.000	0.956	0.002	3495.603	168.542	4.812
	0.145	0.000	0.139	0.000	396.499	1.653	0.145
230	-6.926	-0.002	3.205	-0.004	3509.310	155.167	7.632
	0.226	0.000	0.250	0.000	348.436	1.848	0.231
246	2.907	-0.006	-5.916	-0.003	1068.301	296.171	6.592
	0.146	0.000	0.097	0.000	76.607	1.199	0.109
251*	2.158	0.003	-2.210	0.003	2522.161	314.321	3.089
	0.069	0.000	0.054	0.000	163.319	1.158	0.062

mass-luminosity relationship (Duric 2004):

$$M_{star} = \begin{cases} \left(\frac{L_{star}}{0.23}\right)^{1/2.3} \\ \left(L_{star}\right)^{1/4} \text{ if } M_{star} > 0.43 \\ \left(\frac{L_{star}}{1.4}\right)^{1/3.5} \text{ if } M_{star} > 2 \end{cases}$$

Where the units are solar units. The mass constraint on the orbits was ±10% of the combined masses of the pair calculated as above.

In section 7 we discuss our probability of binarity for each pair. Our method of quantifying this is detailed in Rümker Paper III (Letchford, White, and Ernest, 2018b).

5. Orbital Results

Orbital elements are given in Table 2; associated plots are in the *Appendix*. An ephemeris, based on these elements is given in Table 3.

7. Notes on Each Double

DUN 4* (WDS 01388-5327, DUN 4) Our probability of binarity ~49.8%. A probability <= 50% means that curvature in the historical data was not detected (Letchford, White, and Ernest 2018b). Closing. Separation at 2015.5 ≈ 1.83 pc ≈ 377386 AU. Separation calculated by subtracting the parallax (from GAIA DR2) of each after converting to parsecs. Cannot be binary given our probability and a separation larger than ~1 pc ≈ 206265 AU. Harshaw's (2018) Supplemental Download rates the binary probability as 0.88, and physical relationship as "definitely physical".

DUN 5* (WDS 01398-5612, DUN 5) Our probability of binarity ~99.5%. A probability > 50% means that curvature in the historical data was detected. Widening. Separation at 2015.5 ≈ 0.01 pc ≈ 1081 AU. Binarity confirmed. Harshaw's (2018) Supplemental Download rates the binary probability as 0.00 and physical relationship as "unknown". At the time of writing the orbital elements in the 6th orbit catalogue for DUN 5* were (in the order and units presented in Table 2; no uncertainties recorded): 475.2, 7.826, 140.5, 13.7, 1811.90, 0.513, 18.6, Equinox 2000. DUN 5* has been

Table 2: Orbital Elements and their uncertainties, all ICRS (Equinox effectively = J2000.0)

DUN	P yrs +/-	a " +/-	i ° +/-	Ω ° +/-	T yr +/-	e +/-	ω ° +/-
4*	43597.01	15.92	108.63	98.21	4911.46	0.82	109.66
	5257.54	1.38	0.61	16.29	1779.57	0.01	45.78
5*	501.08	8.59	128.22	15.26	1803.09	0.37	27.13
	322.45	3.48	6.86	5.64	34.22	0.01	55.24
38*	34763.12	76.49	75.27	1.09	-1064.62	0.94	301.90
	52206.44	64.38	9.06	137.64	13585.65	0.45	182.72
42*	165670.81	122.85	111.60	104.37	1991.81	0.87	146.22
	31501.46	20.2	0.301	5.087	21.717	0.1	8.708
52*	44933.72	58.15	78.58	172.73	1929.16	0.28	276.56
	9733.39	8.54	0.59	0.11	355.68	0.06	4.89
111*	192603.07	163.67	91.11	31.42	1503.81	0.98	104.21
	1.11	26.83	0.37	0.92	71.38	0.01	11.90
116*	24679.17	29.50	105.29	84.23	3779.97	0.62	283.00
	16148.66	12.51	1.23	1.67	288.37	0.09	13.93
138*	195827.60	55.08	108.38	4.11	1993.19	0.81	160.43
	60072.53	12.09	0.07	0.02	3.68	0.07	0.07
168	73574.55	15.95	123.13	43.83	1998.33	0.58	218.30
	30197.20	3.48	1.66	12.32	20.67	0.00	14.44
230	55471.40	26.88	60.04	51.52	6199.20	0.67	183.75
	1508.32	0.15	2.27	7.11	448.80	0.12	19.96
246	88826.31	65.77	98.19	27.25	1945.37	0.30	97.07
	0.01	2.23	0.51	0.10	604.64	0.00	2.26
251*	10633.66	8.49	66.90	93.59	2192.45	0.56	215.63
	1709.50	1.00	0.80	0.23	33.10	0.07	4.58

included here to demonstrate the veracity of our brute force monte-carlo method of finding orbits for very slow wide binaries. Except for i and e, our uncertainties of the orbital elements encompass the values of the 6th orbit (and i, inclination, not by much). Our orbit could be improved using differential corrections (e.g. van den Bos (1937)) and/or the “grid-search” method of Hartkopf, McAlister, and Franz (1989).

DUN 38* (WDS 07040-4337, DUN 38AB) Our probability of binarity ~49.6%. A probability <= 50% means that curvature in the historical data was not detected. Widening Separation at 2015.5 ≈ 0.0004 pc ≈ 90 AU. Binarity uncertain but possible. Harshaw's (2018) Supplemental Download rates the binary probability as 0.00, and physical relationship as “unknown”.

DUN 42* (WDS 07087-7030, DUN 42) Our probability of binarity ~55.2%. A probability > 50% means that curvature in the historical data was detected. Widening. Separation at 2015.5 ≈ 2.71 pc ≈ 558334 AU. If separation at 2015.5 is approximately correct, pair cannot be binary despite our probability. Binarity uncertain but possible. Harshaw's (2018) Supplemental Download rates the binary probability as 0.83 and physical relationship as “highly likely to be physical”.

DUN 52* (WDS 07343-2328, H N 19) Our probability of binarity ~49.9%. A probability <= 50% means that curvature in the historical data was not detected. Widening. Separation at 2015.5 ≈ 0.06 pc ≈ 13080 AU. Binarity uncertain but possible. Harshaw's (2018) Supplemental Download rates the binary probability as 0.88 and physical relationship as “definitely physical”.

DUN 111* (WDS 11323-2916, H 3 96) Our probability of binarity ~50.6%. A probability > 50% means that curvature in the historical data was detected. Widening. Separation at 2015.5 ≈ 0.06 pc ≈ 12129 AU. Binarity uncertain but possible. Harshaw's (2018) Supplemental Download rates the binary probability as 0.89 and physical relationship as “definitely physical”.

DUN 116* (WDS 11567-3216, DUN 116AB) Our probability of binarity ~50.0%. A probability <= 50% means that curvature in the historical data was not detected. Closing. Separation at 2015.5 ≈ 0.02 pc ≈ 3,227 AU. Binarity uncertain but possible. Harshaw's (2018) Supplemental Download rates the binary probability as 0.89 and physical relationship as “definitely physical”.

DUN 138* (WDS 13368-2630, H N 69AB) Our probability of binarity ~50.1%. A probability > 50% means that curvature in the historical data was detected. Widening. Separation at 2015.5 ≈ 2.80 pc ≈ 576861 AU. Cannot be binary. Harshaw's (2018) Supplemental Download rates the binary probability as 0.88 and physical relationship as “definitely physical”.

DUN 168 (WDS 14428-5511, DUN 168) Our probability of binarity ~50.2%. A probability > 50% means that curvature in the historical data was detected. Closing. Separation at 2015.5 ≈ 0.68 pc ≈ 140947 AU. Binarity uncertain but possible. Harshaw's (2018) Supplemental Download rates the binary probability as 0.90 and physical relationship as “definitely physical”.

DUN 230 (WDS 20178-4011, DUN 230) Our probability of binarity ~50.5%. A probability > 50% means that curvature in the historical data was detected. Closing. Separation at 2015.5 ≈ 0.13 pc ≈ 26510 AU. Binarity uncertain but possible. Harshaw's (2018) Supplemental Download rates the binary probability as 0.89 and physical relationship as “definitely physical”.

DUN 246 (WDS 23072-5041, DUN 246) Our probability of binarity ~50.0%. A probability <= 50% means that curvature in the historical data was not detected. Widening. Separation at 2015.5 ≈ 0.03 pc ≈ 6809 AU. Binarity uncertain but possible. Harshaw's (2018) Supplemental Download rates the binary probability as 0.88 and physical relationship as “definitely physical”.

DUN 251* (WDS 23395-4638, DUN 251) Our probability of binarity ~52.1%. A probability > 50% means that curvature in the historical data is detected. Closing. Separation at 2015.5 ≈ 2.60 pc ≈ 536972 AU. Cannot be binary. Harshaw's (2018) Supplemental Download rates the binary probability as 0.85 and physical relationship as “definitely physical”.

8. Conclusion

Of the 12 Dunlop doubles whose possible rectilinear and orbital motions were analysed, only DUN 4* had a binarity probability of ≤ 50% and a 2015.5 separation ≥ 1pc making it very unlikely to be a physically bound pair. DUN 42*, 138* and 251* had a binary probability of ≥ 50% but a 2015.5 separation ≥ 1 pc, again making them unlikely to be physical pairs. DUN 38* and 52* had binary probabilities of < 50% and a 2015.5 separation < 1pc making them possible but unlikely binaries. DUN 5*, 111*, 116*, 168, 230 and 246 had a binary probability of ≥ 50% and a 2015.5 separation < 1pc making them possible binaries. Only DUN 5* is a confirmed binary. The orbital parameters for DUN 52*, 230 and 246 we consider to be grade 5 (on grade 5 orbits see Letchford, White, and Ernest 2018b). Of those grade 5 orbits, curvature was detected in the historical data for DUN 230, with a probability of binarity of ~50.5%.

9. Acknowledgements

We acknowledge the use of the following online data bases:

The Washington Double Star Catalogue maintained

by the USNO. (WDS)

All-sky Compiled Catalogue of 2.5 million stars, 3rd version (ASCC)

The Gaia Catalogue (Gaia DR2, Gaia Collaboration, 2018), from VizieR. (GAIA DR2)

10. References

Chanamé, Julio, and Andrew Gould, 2004, "Disk and Halo Wide Binaries from the Revised Luyten Catalog: Probes of Star Formation and MACHO Dark Matter", *The Astrophysical Journal*, **601**, 289–310. http://adsabs.harvard.edu/abs/2004ApJ...601..289C.

Dunlop, James, 1829, "Approximate Places of Double Stars in the Southern Hemisphere, Observed at Paramatta in New South Wales", *Memoirs of the Royal Astronomical Society*, **3** (1), 257–75. http://adsabs.harvard.edu/abs/1827MmRAS...3..267D

Duric, Neb, 2004, *Advanced Astrophysics. Advanced Astrophysics*, Cambridge, UK: Cambridge University Press. https://books.google.com.au/books?id=-ljdYMmI0EIC

Guinan, Edward F, Peter Harmanec, and William I Hartkopf, *2007*, "Introduction & Overview to Symposium 240: Binary Stars as Critical Tools and Tests in Contemporary Astrophysics", In *IAU Symposium 240: Binary Stars as Critical Tools and Tests in Contemporary Astrophysics*, edited by William I Hartkopf, Edward F Guinan, and Peter Harmanec, **240**, 5–16. Cambridge, UK: Cambridge University Press. http://adsabs.harvard.edu/abs/2007IAUS..240....5G

Harshaw, Richard, 2018, "Gaia DR2 and the Washington Double Star Catalog: A Tale of Two Databases", *Journal of Double Star Observations*, **14** (4), 734–40. http://www.jdso.org/volume14/number4/Harshaw_734_740.pdf

Hartkopf, William I, Harold A McAlister, and Otto G Franz, 1989, "Binary Star Orbits from Speckle Interferometry. II - Combined Visual-Speckle Orbits of 28 Close Systems", *The Astronomical Journal*, **98**, 1014–39. http://adsabs.harvard.edu/abs/1989AJ.....98.1014H

Letchford, Roderick R, Graeme L White, and Allan D Ernest, 2017, "The Southern Double Stars of Carl Rümker I: History, Identification, Accuracy", *JDSO,* **13** (2), 220–32. http://www.jdso.org/volume13/number2/Letchford_220-232.pdf

———, 2018a, "The Southern Double Stars of Carl Rümker II: Their Relative Rectilinear Motion", *JDSO*, **14** (2): 208–22. http://www.jdso.org/volume14/number2/Letchford_208_222.pdf

———, 2018b, "The Southern Double Stars of Carl Rümker III: Quantified Probability of Boundedness and Preliminary Grade 5 Orbits for Some Very Long Period Doubles", *JDSO*, **14** (4), 761–70. http://www.jdso.org/volume14/number4/Letchford_761_770.pdf

Longhitano, Marco, B Binggeli, and M Zejda, 2010, "The Widest Binary Stars: A Statistical Approach", In *ASP Conference Proceedings 435: Binaries - Key to Comprehension of the Universe*, edited by A Prša and M Zejda, **435**, 67–70. http://adsabs.harvard.edu/abs/2010ASPC..435...67L

Németh, Péter, Eva Ziegerer, Andreas Irrgang, Stephan Geier, Felix Fürst, Thomas Kupfer, and Ulrich Heber, 2016, "An Extremely Fast Halo Hot Subdwarf Star in a Wide Binary System", *The Astrophysical Journal Letters*, **821** (L13), 1–7. http://adsabs.harvard.edu/abs/2016ApJ...821L..13N

van den Bos, W.H., 1937, "Differential Correction of the Orbit of a Visual Binary", *Circular of the Union Observatory Johannesburg 98*. http://adsabs.harvard.edu/abs/1937CiUO...98..337V

White, Graeme L, Roderick R Letchford, and Allan D Ernest, 2018, "Uncertainties in Separation and Position Angle of Historic Measures - Alpha Centauri AB Case Study", *JDSO*, **14** (3): 432–42.

Letchford, Roderick R, Graeme L White, and Allan D Ernest, 2019, "The Southern Double Stars of James Dunlop I: History, Identification, Accuracy", JDSO, **15** (3), 350-360. This issue.

Letchford, Roderick R, Graeme L White, and Allan D Ernest, 2019, "The Southern Double Stars of James Dunlop II: Modern Identification of the first dedicated Published Catalogue of Southern Double Stars", *JDSO*, **19** (3), 361-377. This issue.

Letchford, Roderick R, Graeme L White, and Allan D Ernest, 2019, "The Southern Double Stars of James Dunlop III: Modern Version and Analysis of Accuracy of the first dedicated Published Catalogue of Southern Double Stars", *JDSO*, **19** (3), 378-393.

The Southern Double Stars of James Dunlop IV: Rectilinear and Orbital Motion of Some ...

Appendix

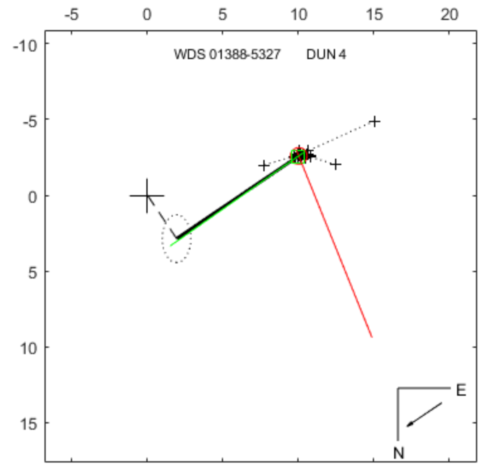

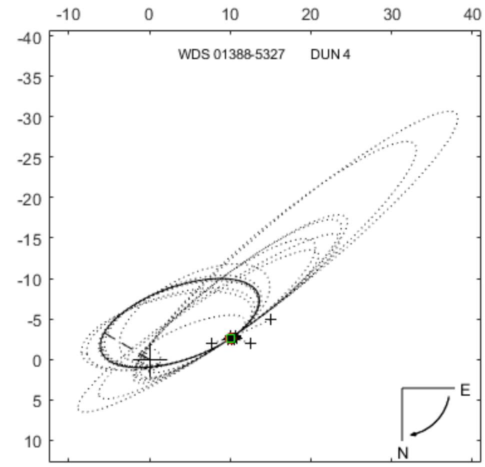

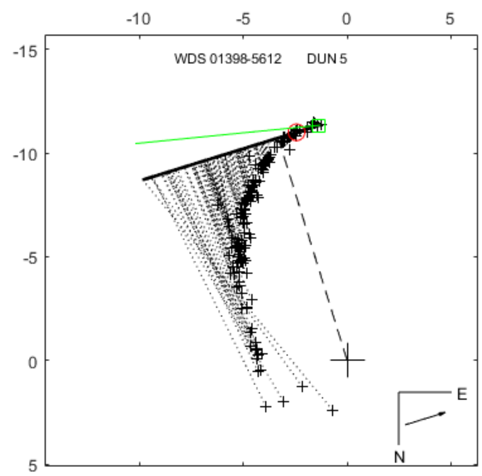

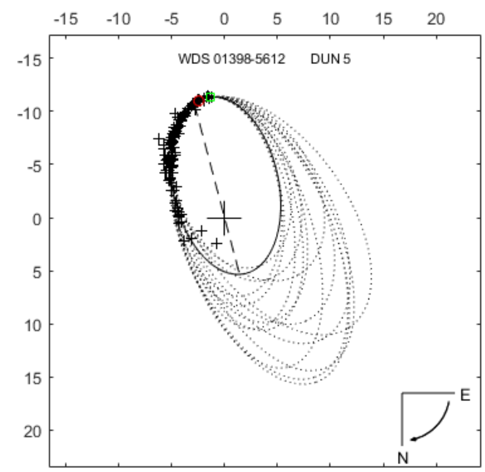

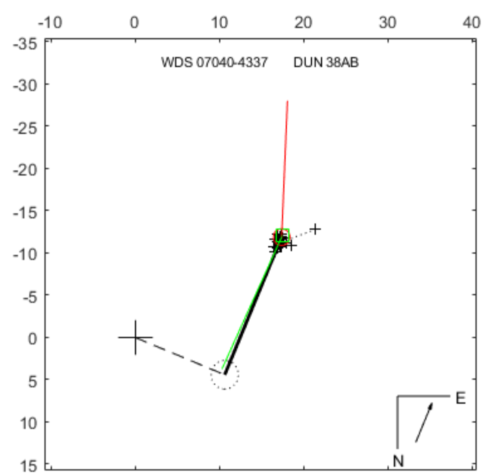

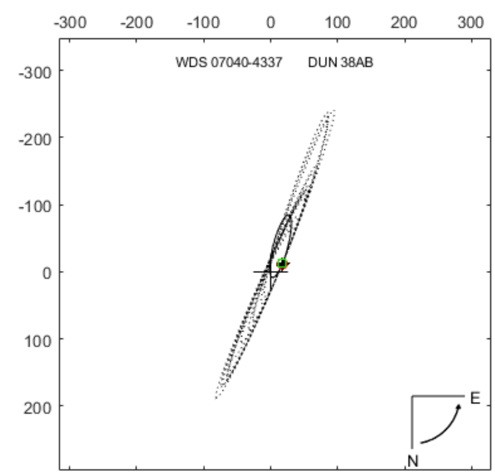

The Southern Double Stars of James Dunlop IV: Rectilinear and Orbital Motion of Some ...

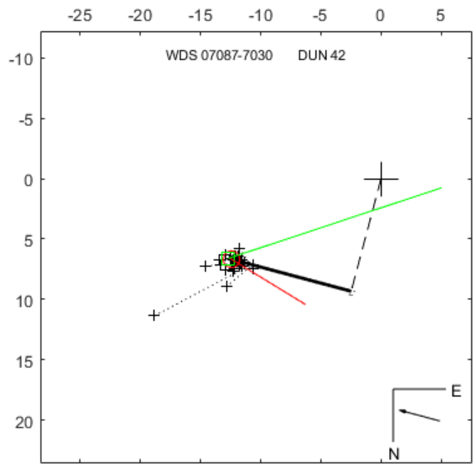

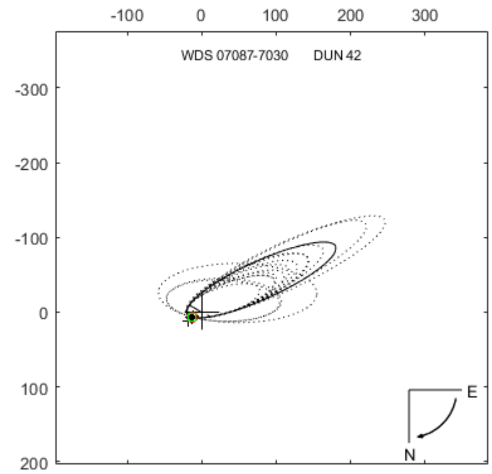

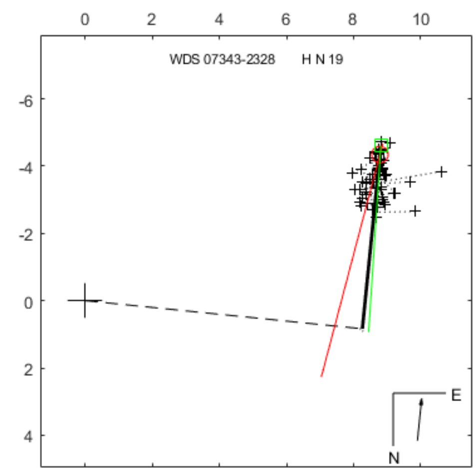

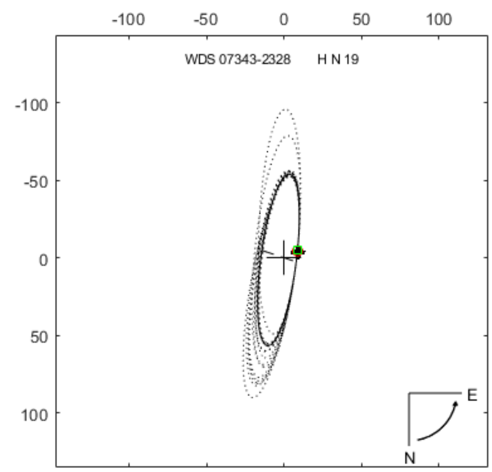

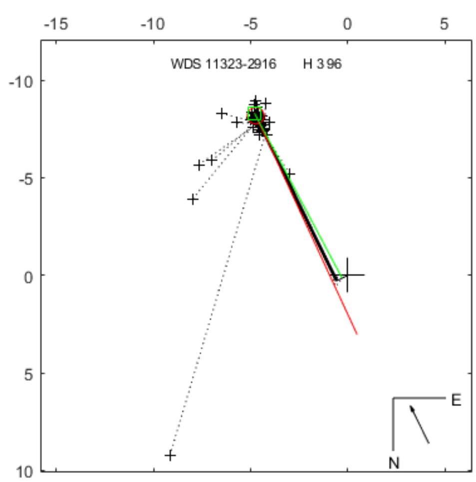

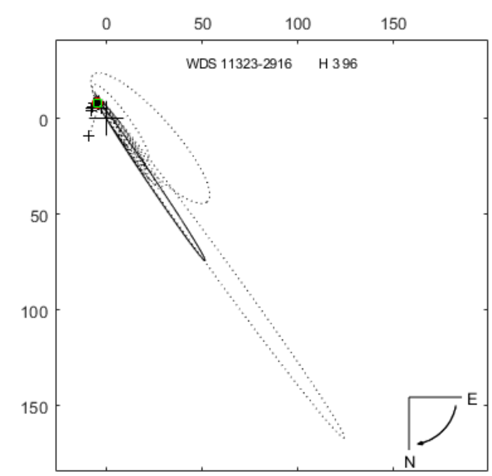

The Southern Double Stars of James Dunlop IV: Rectilinear and Orbital Motion of Some ...

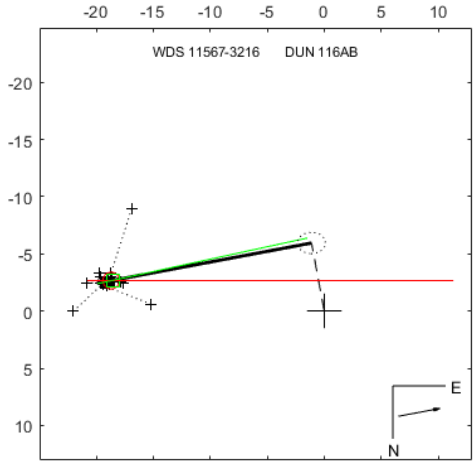

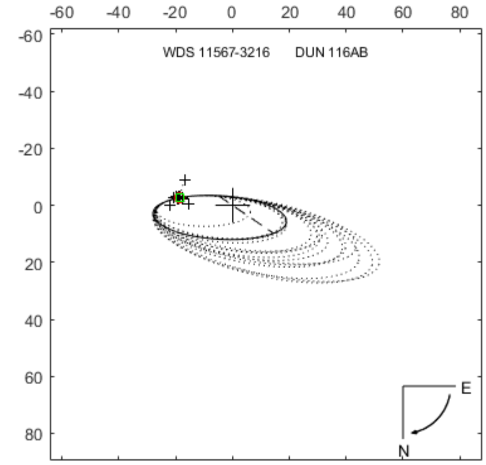

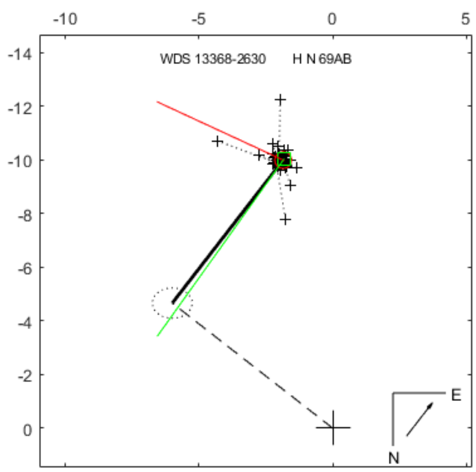

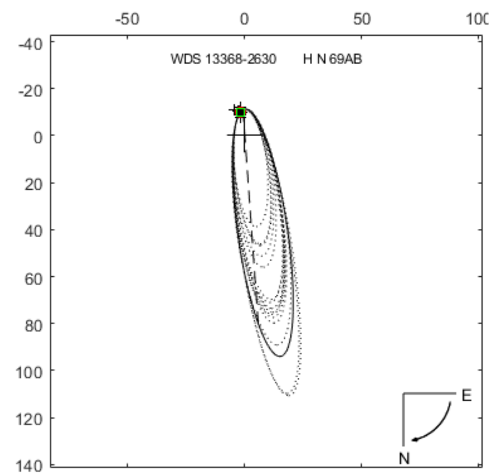

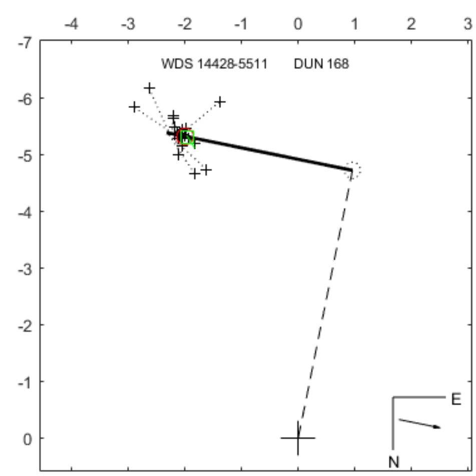

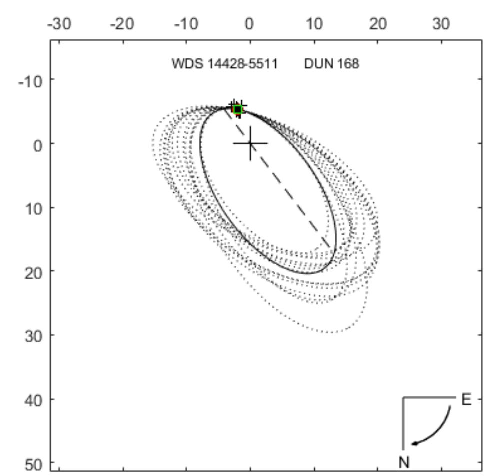

The Southern Double Stars of James Dunlop IV: Rectilinear and Orbital Motion of Some ...

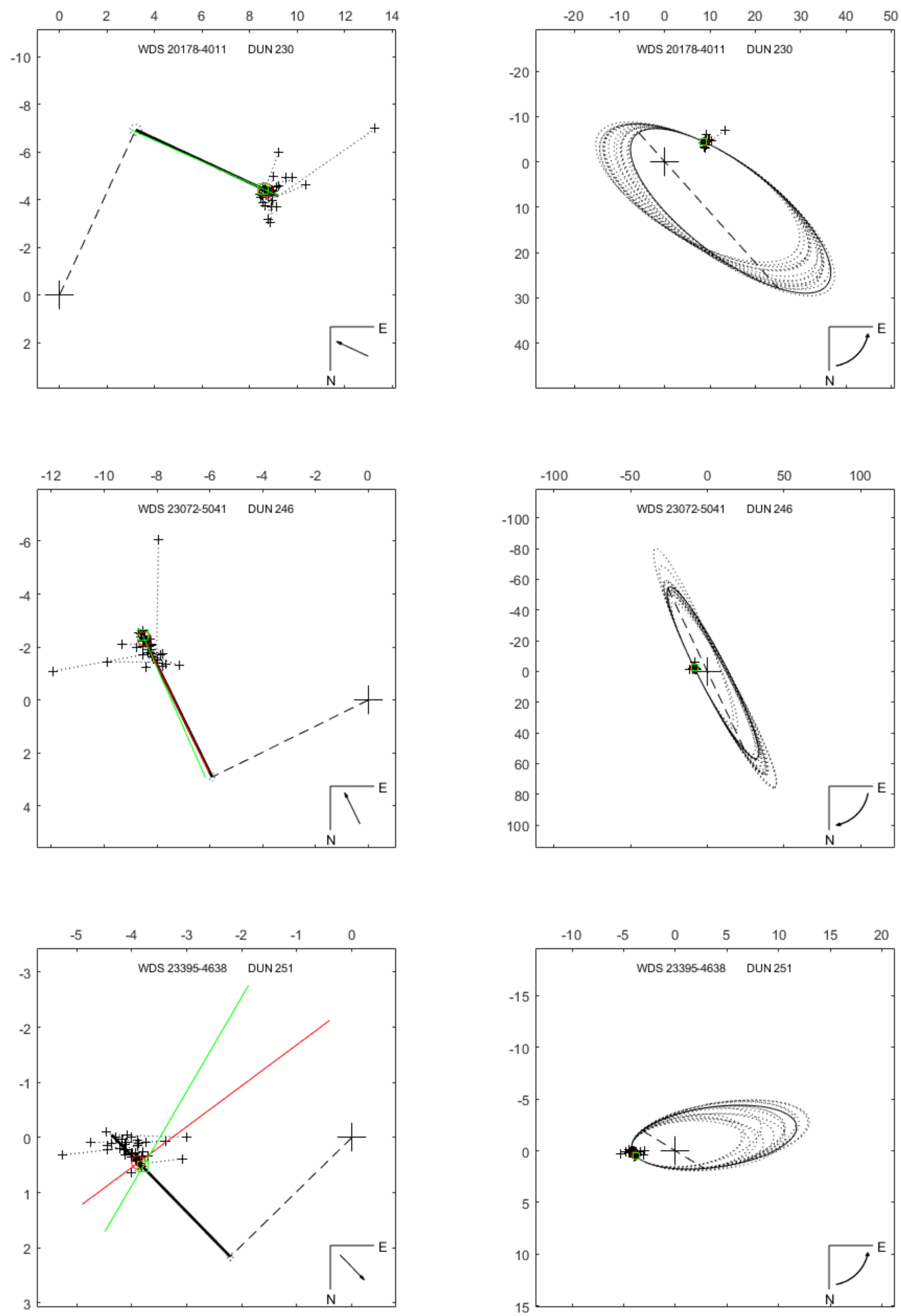

New Double Stars Within 25 Parsecs

George Gatewood and Carolyn Gatewood

Sirius Two Observatory
665 Forest Pine Drive
Ball Ground GA, 30107
Gatewood@pitt.edu

Abstract: We list coordinates, positions angles, separations magnitudes, proper motions, parallaxes, and radial velocities for new doubles stars we found in the Gaia Data Release II.

Introduction

We have been following the Gaia mission for some time. The precision greatly exceeds that of the Hipparcos mission and the magnitude limit exceeds that investigation by several magnitudes. The Gaia mission will provide answers to many of the questions that have fascinated us for decades, such as the motion of Barnard's star (Gatewood and Eichhorn, 1973), the distance and motion of Sirius B (Gatewood and Gatewood 1978), and the distance of the Pleiades cluster (Gatewood et al., 2000). One of our areas of interest concerns the population and characteristics of stars surrounding us in space. Stellar characteristics are usually determined from binary and multiple stars. Thus, the start of this, the third paper in this series (Gatewood and Gatewood 2012, 2016).

The ongoing Gaia project released their second preliminary set of results along with estimates of the errors and the number of observations of each object in early in 2018 (https://www.cosmos.esa.int/web/gaia/dr2). The data release is based on less than two full years of observations, but the estimates of the precision are already inviting. On the other hand, by releasing the data in stages they are inviting us to study the results before all the data has been collected and fully processed. The results are preliminary, and some of it will be modified considerably before the final publication. Thus, we are at a stage where conformation of results is most useful.

Available Data and Techniques

To obtain a large sample we set our original goal on a study of all of the stars within 50 parsecs of the Sun. Because parallax errors will cause more stars to fall out of distance-limited sample than into it, we chose 51 parsecs instead of 50 for our sample limit. With this parameter, the Gaia R2 yields 80,287 stars. This is not the total number of stars in that volume. As the Gaia mission continues this number may get significantly larger or even significantly smaller.

Facing this large data download, we were happy to learn that my crusty old Fortran programs could still be used, without alteration, using the Absoft compilers f77 and even f90. With a little review of my techniques I was able to write a program that matched pairs of stars by comparing their separation, relative parallax, and relative proper motions. Looking to increase the likelihood that each pair would form a binary system we made a short survey of the separations, relative proper motions, and relative parallaxes of known binary stars. We then applied these limitations to the selection of double stars from the Gaia down load. Gaia radial velocities are available for moderately bright stars, but not for bright, or for fainter objects. They are not generally available for both the primary and secondary in our sample so no attempt was made to use them in our selection process.

To find which of these stars were already known we used the USNO WDS Catalogue of 145,404 double stars with high precision coordinates, as of its 10/18/18 update. Gaia doubles that were 20.2 arc seconds or more from any star in the WDS Catalog were designated as new discoveries. Those within that limit were examined to determine if they were the Primary system, a known companion, or a new companion. While the algorithm was not fool proof, hand checking found few errors. In examining the results one is impressed with the quality of past surveys. None of the new discoveries include secondaries brighter than the 10th magnitude nor are there any new doubles within 10 parsecs.

Facing the development of new programs and the huge number of stars in the original Gaia download we decided to reduce our distance limit to just over one half. This would yield about an eight as many double stars for this document. Instead of a limiting parallax of 0.019 arcsec we chose 0.039 arcsec. Our initial download also included objects with Gaia, Gg, magnitudes in the range 18 through 20. After reviewing the statistics of these difficult objects we decided to limit our sample to primary stars with an apparent magnitude brighter than 18. Willem Luyten once showed us two plates he was measuring on his old hand repaired and operated blink machine. Although they were taken 10 degrees or more from the galactic disk, the field was filled with images, some overlapping and others almost touching. He said that field crowding would always set a limit to what could be observed near the disk in the direction of the galactic center. Perhaps the most interesting thing about Gaia's observation of stars within 25 parsecs is how rare these very faint objects are except in the direction of the galactic disk near the galactic center. This is evidence that astronomy has indeed established the bottom of the HR Diagram.

Many of us usually think of the photometric characteristics of stars in terms of the Johnson-Cousins UBVRI system (Bessell 1990). With over a billion stars measured, Gaia measurements and magnitudes will likely be the standards for some time. We will call the three Gaia photometric bands Gg, Bg, and Rg. Crudely speaking, the Gaia green, Gg, band pass is rather like that of an unfiltered reflector and a standard CCD. The Gg band spans almost 6,000 Angstroms, including the Johnson-Cousins B, V, R, and I, and is centered near the 6,400 Angstroms line of a red light laser. The Gaia blue, Bg, band includes the B and V bands as well as approximately half of the R band. The Gaia red, Rg, band includes the longer wave lengths of the R band, all of the I band, and a little that's even longer wave lenght than that. All of the available Gaia photometry for the new doubles is given in Table 1 and Table 2. Where a value is not available it is entered as 0.000.

The Bg-Rg values of the faintest stars can reach 4 and even higher. A high Gaia red value indicates a very cool star. In a distance limited sample, such as this, the fainter stars will generally be red, unless they are white dwarfs. In the Gaia photometric system, very faint white dwarfs, with absolute mg values as faint as +16 usually have Bg-Rg values that exceed 0.8 sometimes approaching 1.8 (http://sci.esa.int/gaia/60198.).

Results

Table 1 lists the new double's J2000 RA and Dec, the angle in degrees of the line from the assumed primary to the secondary and their separation in arc seconds followed by the Gaia green band pass magnitudes of the primary and secondary star. These are followed by their proper motion in RA and Dec in mas/yr. The last two values are the primary and secondary parallax in mas (milli arc seconds).

Table 2 contains the same stars, in the same order as Table 1, listing their X and Y values in arc seconds and estimates of their standard errors in mas as well as their Bg and Rg magnitudes and the Gaia radial velocities in kilometers per sec. The X and Y values are the Standard Coordinates of the secondary star in the plane of the sky in a coordinate system formed and centered at the primary star. X and Y are the coordinates that would have been observed with a calibrated CCD on 01/01/2000. Note that the errors in X and Y are not easily transformed into similar values in polar coordinates. While polar coordinates give a better visual impression of the orbital motion of a binary star, most modern measurement and reductions are done in X and Y.

Notice that there are no actual observation dates in the Gaia data. Instead, the data has all been reduced to, and is given for, 2015.5. The reader's observations confirming these new double stars should include the dates of each observation. Such new observations will mark the start of our continued observation of the systems. The Gaia satellite will complete its mission soon leaving the continue observation of many thousands of stars to us. A good time to start is while there is still a chance to overlap our results with those of Gaia. The high precision of the Gaia observations give us an extraordinary opportunity to test and refine our observing techniques in preparation for the task that lays ahead.

Acknowledgements

This work has made use of data from the European Space Agency (ESA) mission Gaia (https://www.cosmos.esa.int/gaia), processed by the Gaia Data Processing and Analysis Consortium (DPAC, https://www.cosmos.esa.int/web/gaia/dpac/consortium). Funding for the DPAC has been provided by national institutions, in particular the institutions participating in the Gaia Multilateral Agreement.

Thanks to Brian Mason and William Hartkopffor for answering numerous data requests. This research made extensive use of the Washington Double Star Catalog maintained at the U.S. Naval Observatory.

(Text continues on page 407)

New Double Stars Within 25 Parsecs

Table 1.

Dbl	Hr	Mn	Sec	Dg	Mr	Sec	Theta	Rho	Pri G	Sec G	P pm	P pm	S pm	S pm	P pi	P pi
1	0	33	17.361	34	19	11.04	174.6394	3.1469	13.3	13.43	100	-56	82	-59	40.6	40.5
2	3	54	25.621	-9	9	30.94	153.5023	3.1766	10.54	11.88	-95	110	-96	98	47.4	47.4
3	6	35	22.267	-57	37	35.18	57.0872	1.5206	10.29	14.33	-17	53	-40	49	42.8	44.1
4	7	11	16.923	-21	17	54.66	103.8248	2.1845	13.22	13.38	-103	-64	-124	-67	50.3	50.4
5	7	30	17.51	-3	40	24.47	75.2236	199.4488	9.73	15.84	-154	44	-154	45	40.8	41
6	7	49	50.936	-3	17	19.21	265.9078	1.9446	11.55	11.92	-174	-65	-139	-37	58.8	58.8
7	8	35	12.898	-69	26	33.40	339.0264	1.2149	15	15.34	-118	65	-119	79	43.3	43.3
8	10	9	36.277	-17	50	27.87	2.5907	123.1523	10.7	10.92	84	3	85	4	46.7	46.7
9	10	31	4.541	82	33	31.27	84.2879	13.5038	5.12	12.76	-65	12	-105	37	44	44.2
10	13	36	0.026	40	24	11.88	181.5033	145.9332	13.93	14.65	39	26	36	27	42.3	42.3
11	14	19	46.721	31	37	3.73	310.0895	8.8925	12.98	15.47	99	-25	104	-21	52.6	52.6
12	14	55	59.813	-21	58	5.63	307.2401	13.4168	12	12.92	-7	-59	-6	-66	42.2	42
13	15	47	29.806	-27	55	12.11	117.9975	1.2486	12.14	13.83	96	24	98	-4	40.3	40.4
14	15	47	29.806	-27	55	12.11	37.0654	111.8905	12.14	14.74	96	24	91	30	40.3	40.8
15	15	55	46.901	-31	57	41.38	222.4897	188.6164	11.59	12.49	-126	-87	-129	-89	46.2	45.9
16	16	56	42.671	-39	8	12.75	22.8977	169.3688	8.06	11.78	51	-108	47	-113	63.7	63.6
17	16	56	42.671	-39	8	12.75	23.9608	169.199	8.06	10.38	51	-108	56	-106	63.7	63.8
18	17	12	9.199	-43	14	21.12	128.7552	591.8311	3.11	10.4	20	-285	24	-288	46	44.6
19	17	26	22.214	-24	10	31.11	188.8418	18.0551	4.03	14.56	-2	-117	13	-116	40.2	39.3
20	17	33	40.635	-42	55	43.33	22.1979	0.8619	13.23	13.24	-11	68	-11	52	42.8	44.6
21	18	8	59.136	-35	46	44.96	32.3823	3.224	13.01	13.14	-83	-96	-86	-83	45.6	45.7
22	18	9	21.379	29	57	6.17	300.682	29.1715	6.65	13.14	71	61	66	74	41	40.9
23	18	45	23.818	-32	53	38.62	68.2107	4.5216	10.44	17.14	117	49	99	39	45.7	44.9
24	18	52	43.733	36	59	25.68	160.0909	8.6133	13.41	14.1	77	34	84	28	44.3	44.4
25	19	59	25.4	34	54	25.62	128.8793	1.3986	11.5	14.6	92	12	77	13	40.3	40.1
26	21	5	32.058	6	9	15.47	166.0123	5.0952	11.45	14.88	27	45	37	49	44.3	44.5
27	22	56	4.365	75	56	22.33	19.8557	242.3707	7.99	13.68	34	-36	34	-36	40.5	40.8
28	23	17	25.752	-58	14	8.71	110.1853	4.7167	3.81	12.03	-7	86	-35	57	42.3	41.1
29	23	36	18.274	-48	35	17.07	327.9683	334.691	9.46	14.93	-126	-24	-132	-24	39.9	40.5

New Double Stars Within 25 Parsecs

Table 2.

Dbl	X	Xe	Y	Ye	Bg P	Rg P	Bg S	Rg S	RV p	RV s
1	0.294	0.07191	-3.13313	0.07013	15.02	12.03	15.16	12.15	0	0
2	1.41728	0.04297	-2.8429	0.04166	11.68	9.502	13.32	10.69	2.306	0
3	1.27651	0.03137	0.82622	0.04177	11.29	9.318	0	0	31.21	0
4	2.12118	0.03246	-0.52198	0.04423	14.91	11.86	15.09	12.09	0	0
5	192.8528	0.05042	50.86893	0.04496	10.66	8.809	18.43	14.37	46	0
6	-1.93969	0.09782	-0.13877	0.07838	13.19	10.28	13.48	10.63	0	0
7	-0.43486	0.20189	1.13442	0.2115	16.87	13.19	0	0	0	0
8	5.56651	0.04968	123.0264	0.05162	11.85	9.667	12.14	9.867	-10.48	-11.26
9	13.43672	0.35732	1.34403	0.34515	5.366	4.828	14.37	11.52	0	0
10	-3.8286	0.04703	-145.883	0.05953	15.82	12.62	16.77	13.28	0	0
11	-6.80312	0.06193	5.72662	0.07306	14.65	11.74	18.19	14	0	0
12	-10.6812	0.07134	8.11927	0.05805	13.36	10.87	14.5	11.7	0	0
13	1.10245	0.14329	-0.58612	0.06667	13.4	10.94	0	0	0	0
14	67.43931	0.14329	89.28283	0.06667	13.4	10.94	17.01	13.35	0	0
15	-127.402	0.08003	-139.086	0.0423	12.96	10.47	14.17	11.25	0	0
16	65.89912	0.06886	156.0227	0.06209	8.758	7.297	13.49	10.53	-8.582	0
17	68.71371	0.06886	154.618	0.06209	8.758	7.297	11.77	9.248	-8.582	0
18	461.5264	0.57039	-370.483	0.5009	3.588	2.891	11.5	9.391	0	-22.88
19	-2.77519	0.39879	-17.8405	0.34169	4.253	3.864	16.25	13.21	0	0
20	0.32563	0.38997	0.79801	0.30349	14.24	11.33	14.23	11.34	0	7.986
21	1.72666	0.09509	2.72263	0.08443	14.49	11.81	14.63	11.94	0	0
22	-25.0879	0.02501	14.88541	0.03014	6.997	6.188	12.99	13.34	-14.55	0
23	4.19856	0.05678	1.67839	0.05783	11.54	9.433	18.11	15.41	-6.439	0
24	2.93309	0.03504	-8.09855	0.04228	14.82	12.25	15.73	12.87	0	0
25	1.08876	0.02586	-0.87787	0.03261	12.61	10.45	0	0	0	0
26	1.23158	0.06593	-4.94414	0.04708	12.88	10.31	17.07	13.48	0	0
27	82.32176	0.0378	227.9621	0.03607	8.497	7.372	15.38	12.42	-9.309	0
28	4.42701	0.2535	-1.62754	0.29814	4.144	3.543	11.29	10.48	0	0
29	-177.516	0.03075	283.736	0.04318	10.33	8.567	17.17	13.53	-0.782	0

(Continued from page 404)

References

Bessell, M. S. 1990, *PASP*, **102**, 1181.

Gatewood; Eichhorn, H. 1973, *AJ*, **78.**

Gatewood, G. D., & Gatewood, C. V. 1978, *ApJ*, **225**, 191.

Gatewood, G.D. and Gatewood, C.V. 2012, *JDSO*, **8**, 335-339.

Gatewood, G.D. and Gatewood, C.V. 2016, *JDSO*, **12**, 580-585.

Gatewood, G., de Jonge, J. K. & Han, I. 2000, *ApJ*, **533**, 938.

https://www.cosmos.esa.int/web/gaia/dr2

http://sci.esa.int/gaia/60198-gaia-hertzsprung-russell-diagram/

http://sci.esa.int/gaia/60198

The Human Element: Why Robotic Telescope Networks are not always Better, and Performing Backyard Research

Ryan Caputo
Stanford Online High School, Stanford, CA

Abstract: In some cases, backyard astronomy with amateur-grade telescopes, mounts, and cameras can yield results on par, or even better, than research-grade robotic telescopes. The "human element" gives more control over variables such as gain, dark frames, camera cooling, and tracking. Furthermore, being able to adjust variables on-the-fly allows a much greater control of an otherwise limited setup. For purposes of comparison, I took exposures of the same double star with my telescope and robotic telescopes and compared the results. In the field, I found three additional WDS catalogue doubles, two of which I measured in addition to the original target. Also, I discovered a dim, approximately 1.3" separation new potential binary, which I was unable to measure but which warrants further study. After comparing the measurements between my 4-inch telescope and the 0.4 meter robotic telescopes, I concluded that my setup performed similarly despite having only one fourth the aperture.

Introduction

To perform research without access to major telescopes that are actively monitored by humans, researchers depend upon robotic telescopes to receive images. Such networks include Skynet and the Las Cumbres Observatory Network. The convenience of these robotic networks is due to their automation and ability to operate without a person, yet this also can lead to some issues. There is no "quality check", meaning images might be returned that are out of focus, misaligned, or have misshapen stars. Also, the exposure time cannot be dynamically checked. Because of this, excessive amounts of telescope time might be used by researchers submitting multiple exposures with 5s, 10s, 20s, and 30s exposure times.

One night, having recently acquired a telescope, mount, and camera designed for astrophotography, I was trying to take a picture of a Messier 103, an open star cluster in Cassiopeia. My mount did not "goto" properly, and when I took the image, it was only a random starfield. I was disappointed until I noticed a double star in the image. I measured its separation to be 6.49 arcseconds, and then looked up its coordinates in the Washington Double Star Catalog and on the Second Data Release of the European Space Agency's Gaia Collaboration. It turned out to be WDS 01210+5920 STI 1576, and my measurement agreed well with the Position Angle (PA) and separation (sep) listed in the WDS. Figure 1 shows this "fortuitous discovery", as I call it, that shows the possibility for research with backyard telescopes.

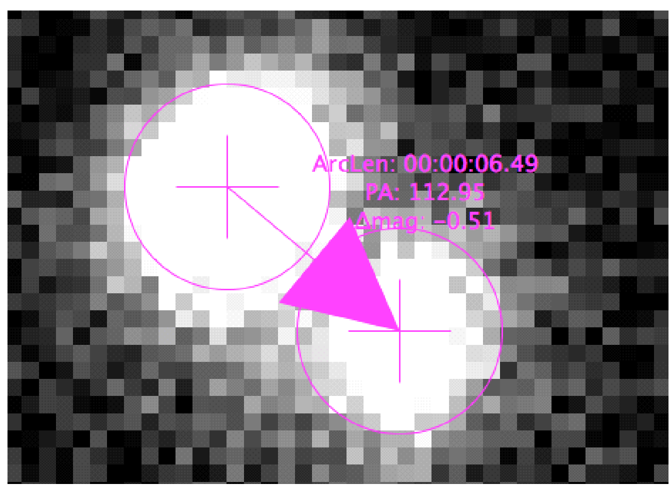

Figure 1. *Fortuitous discovery of WDS 01210+5920 STI 1576.*

Amateur telescopes can make significant contributions to research, as with the recent discovery of a 2.6-km Kuiper belt object (too dim for Hubble to image directly) by stellar occultation using an amateur telescope in Japan (Arimatsu, 2019). In this paper, I explore the prospect of performing research with my personal backyard setup. I selected a star by going to Stelledoppie and filtering the stars that are in Cassiopeia and have a separation of less than 6 arcseconds. I chose Cassiopeia because it was near zenith around midnight for my Texas location during late fall, and 6 arcseconds as the separation because I wanted to test the limits of my setup. I chose to image WDS 00057+4549 STT 547AB, taking images from my telescope, the Skynet Robotic Observatory Network (Skynet), and the Las Cumbres Observatory Network (LCO).

Double Stars

Double stars are important because some of them are binary, and measuring the separation and position angle allows researchers to calculate the orbits of those that are gravitationally bound. That allows a range of other values to be derived which can either provide new information or check other methods. Moreover, double stars are accessible and a good entry point into backyard research. However, oftentimes double stars are separated by only a few arcseconds, which makes measuring them very difficult. For telescopes, the phrase "bigger is better" usually applies, but there are many factors that influence the quality of an image that are not related to telescope size. These include mount tracking, camera noise, and seeing. With such tight tolerances, sometimes the "human element" is needed for quality-control and to apply changes on-the-spot.

Setup

My telescope is an Explore Scientific ED102 Apochromatic Refractor Essential Series, which has FCD1 series glass. The aperture is 102mm, and the focal ratio is $f/7$, giving the focal length to be 714mm. Refractors are well-known for having chromatic aberration, a type of optical aberration that results from different wavelengths of light refracting at different angles and therefore coming to focus at different focal lengths. However, the ED102 is a triplet lens, hence the "apochromatic" designation. The triplet lens system works to focus three wavelengths of light at the same focal point, unlike most normal refractors of today, which only focus two wavelengths (as most today are achromats, a doublet lens). The triplet lens reduces the chromatic aberration significantly to the point where it can barely be observed. Although my telescope has the slightest bit of chromatic aberration on the brightest stars such as Vega, it is very minimal and does not affect research.

My mount is a Skywatcher AZ-EQ5, one of the many variants of Skywatcher's EQ5 design. This mount is a German Equatorial Mount design, so once it is polar aligned, it can track the sky perfectly and long exposures can be taken. Otherwise, the stars will trail, and the images will be unusable. An alt-az mount, in contrast, has field rotation as it tracks the sky, so even if it tracks perfectly, a "de-rotater" is required to rotate the image exactly opposite to the amount the tracking incurs, which adds complexity and cost. Furthermore, a German equatorial mount only needs to rotate one axis to track the sky, and the rotation rate is always constant. No matter where in the sky the mount is pointed, the right ascension axis, as it is called, will track the sky perfectly rotating once every sidereal day. This is in contrast to an alt-az mount where both axes must rotate, and each must rotate at a different speed depending on where in the sky it is pointing. Overall, a German equatorial mount is much simpler, which means good images are easier to acquire.

My camera is a ZWO - ASI 1600mm cool, version 3. Contrary to most astronomical research cameras, it is not a CCD but a CMOS sensor. This type of sensor is what is found in smartphones and most consumer cameras. However, CMOS sensors in astronomical cameras are optimized to have an extremely low read noise, dark current, and almost no amp glow. Essentially, when the camera sees black, the sensor records a value extremely close to black even at long exposures, so that faint stars are able to be captured with a relatively high signal-to-noise ratio (SNR). The sensor is a 22mm diagonal, which means it has a large field of view. This is wonderful for finding targets. Also, unlike normal cameras, it has a Peltier-type cooler. This cooler is able to cool to 40 ^{o}C below ambient temperature, however I run it around 30 ^{o}C to save battery. The use of a cooler is absolutely essential for good images, because for every 7 - 8 ^{o}C of cooling, the noise level is reduced by half (Bracken, 2017). Therefore, the SNR is further increased. Combined with the sensor's already-low read noise, very dim stars can be observed with relatively short exposures. For example, the camera is able to record (although quite faintly) magnitude 14 stars with 30 second exposures in moderate light pollution.

The "optical train" is the accessories that come after the focuser. The optical train on my setup includes a 2x Barlow lens. This effectively doubles the focal length of my telescope, turning my $f/7$ into a $f/14$ telescope. If I had an $f/14$ refractor, I would certainly use it for the high magnification, but I currently do not, so a 2x Barlow lens is used for magnification purposes. The reason why a long focal length is needed is that double stars are very close together, and I need to be able to "split" the components. At $f/14$, my telescope and

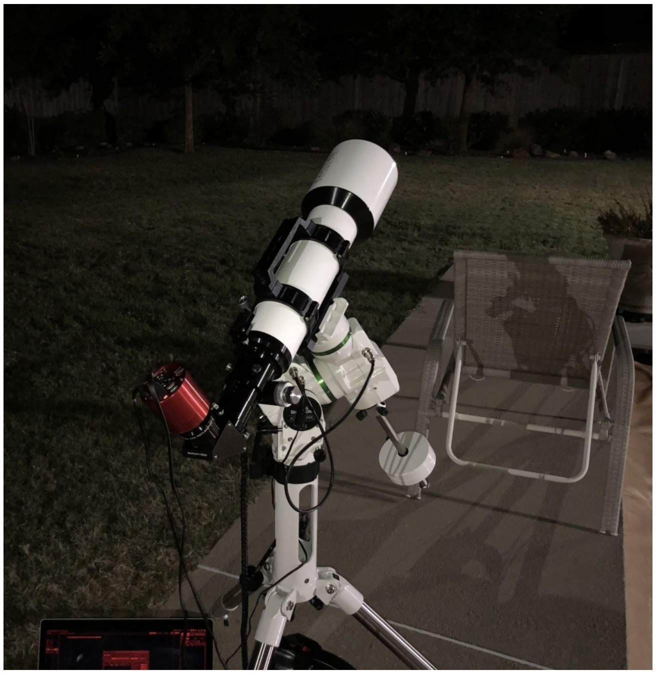

Figure 2. My setup for imaging.

camera combination have a true field of view of 0.71 x 0.54 degrees, with each pixel representing 0.55". The camera, Barlow lens, and telescope were chosen to optimize the pixel scale, specifically to prevent under sampling for my telescope's focal length (Buchheim 2007). Figure 2 shows my setup but without the Barlow lens in the optical train. Note that as of completing this project, several parts have been "polished" and improved. The diagonal has been removed and replaced with extenders, there is an Astronomik L-3 luminance filter located in front of the sensor, the polar alignment scope has been removed, a small counterweight to improve balance has been added directly onto the telescope, a guide scope and guide camera has been mounted to the top, and a regulated AC/DC power converter has replaced the battery.

Advantages of My Setup Relative to Robotic Telescopes

There are several advantages to using a backyard approach to gathering data. In conducting prior research using robotic telescopes, I had to wait for the images to come back. For LCO, this time was usually minimal, but for Skynet there sometimes were significant delays. Oftentimes I would request an image to be taken that night, but it would not come back for a week or two. When I use my own telescope, however, I have control over when my images will be taken.

Figure 3 shows the image I obtained of the target pair STT 547AB displayed in AstroImageJ, an astronomical image processing software (Collins, 2017). There is a slight asymmetry to the stars, but the bright region is significantly rounder than the stars' halos, meaning centroid measurements are not affected.

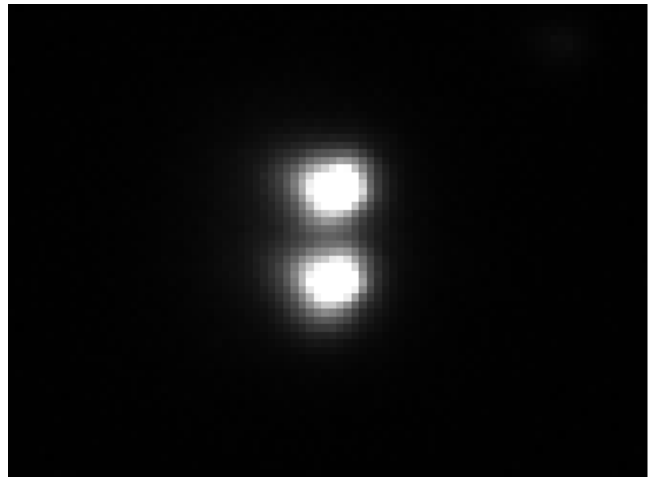

Figure 3: My best image of STT 547AB.

For comparison purposes, I took pictures of this starfield using Skynet on two telescopes, DSO-17 in North Carolina and AURT in Alberta, Canada. In both cases, the returned images were unusable. From AURT, the mount did not track properly, which resulted in the streaks shown in Figure 4.

For DSO-17, the mount did not track perfectly, and the stars were too bloated to perform accurate centroid measurements. This effect might occur if the target was low in the sky, but Skynet only takes images if the target is above thirty degrees. When DSO-17 imaged the double star (4 AM on October 30, 2018), it was 70 degrees above the horizon. It is possible that the atmosphere may have been unstable on the night the image was taken, but such conditions of bad seeing would not

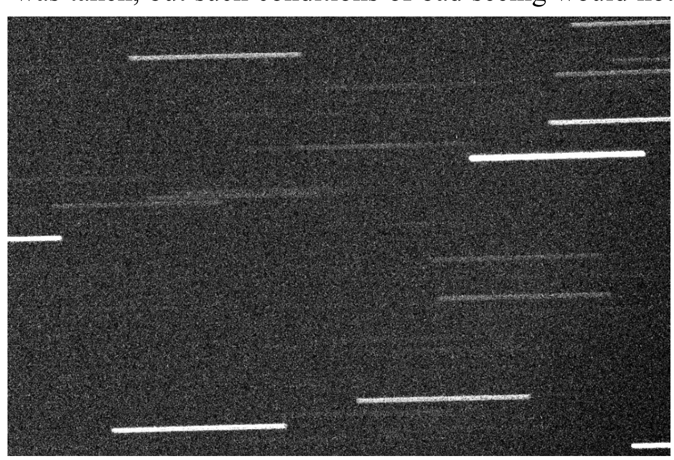

Figure 4. *AURT image showing incorrect tracking.*

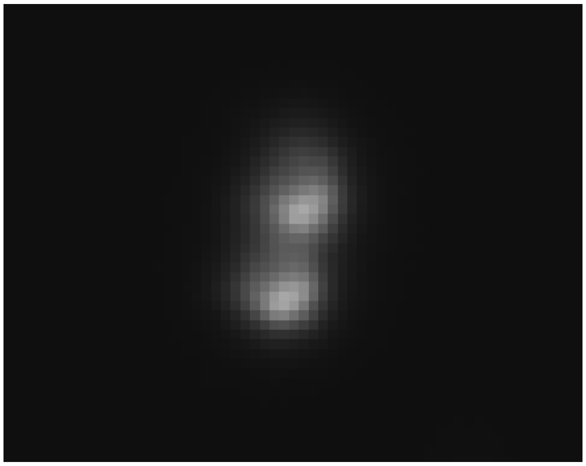

Figure 5: DSO-17 Bloated Stars with a slight drift along the NE/SW corners.

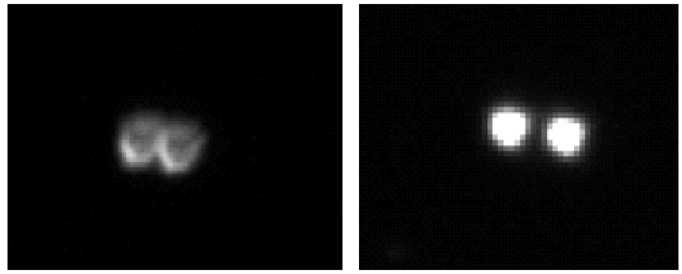

Figure 6: Bad LCO image, left; and good LCO image.

cause the stars to be asymmetric, just larger. The asymmetry of these stars indicates a problem with the mount that seeing could not have caused. Figure 5 shows a 30 -second exposure taken by DSO-17.

The Las Cumbres Observatory telescopes gave much better results, and by visual inspection the stars appeared rounder than the ones that are in my images. One of the images was not focused or collimated properly and had donut shaped stars (due to the central obstruction), but the rest of the images were very high quality as shown in Figure 6.

Because the LCO telescopes are 0.4m in aperture and their mounts are much more advanced than mine, the images are expected to be better. Our first images from LCO, however, were overexposed with exposures of 30 seconds and 60 seconds. To perform accurate centroid measurements, the stars must not be too overexposed. After some trial-and-error, we found the optimal exposure time to be three seconds. This process of trial and error takes time on the researcher's part and wastes telescope time that other people could use. The ability to make adjustments to elements like gain, focus, and specific framing of the field during the course of an observation is possible for human but not robotic researchers. Despite this, LCO gave back impressive results, both in the quality of the image and the speed with which they were taken.

One extremely important necessity for high quality images is the "seeing," which is the measure of the stability of the atmosphere. The seeing is completely out of the control of the observer; it is simply a function of the weather and air currents that day. Seeing is the prime reason why large telescopes cannot achieve their maximum resolution because the atmosphere "smears" out the stars. On nights of bad seeing, imaging double stars is almost hopeless because the stars will be very bloated. For example, with excellent seeing, I can split doubles under an arcsecond visually, but on nights of terrible seeing, splitting doubles under seven arcseconds is a challenge. On an average night, anything under two arcseconds reduces to mush in the eyepiece. For robotic telescope networks, images are taken when the skies are clear but not necessarily when seeing is good. However, when I do the imaging myself, I am outside looking at the stars. Therefore, I can evaluate the seeing and whether imaging a target is feasible, taking into account the difficulty of resolving the double star and the local hour-to-hour conditions.

Limitations of my Setup Relative to Robotic Telescopes

There are some limitations to my telescope, mostly related to its small aperture. Since it is only 102mm (4 inches) in aperture, the diffraction limit is around 1.23 arcseconds (Nave, 2000). However, for practical reasons, stars separated by anything less than three arcseconds are too close to image accurately with a single exposure. For this reason, speckle interferometry is in increasingly common use for close doubles (Wasson, 2018). This limitation is not that restrictive, though, as there are plenty of double stars that have separations above three arcseconds.

I was also limited by my mount. At the time of imaging for this project, I did not have a guiding solution, either by an autoguider or an off-axis guider. Every mount experiences periodic and sinusoidal movement known as "periodic error" because of imperfections in the worm and drive gears (Saunders 2012). This means that no matter how well a mount is polar aligned, there will be back-and-forth drift in the right ascension direction as the mount tracks the sky. As a result, my mount could not do unguided images for longer than around 60 seconds, and I sometimes struggled to have round stars. The addition of an autoguider has fixed this problem.

My camera does not have any major limitations that

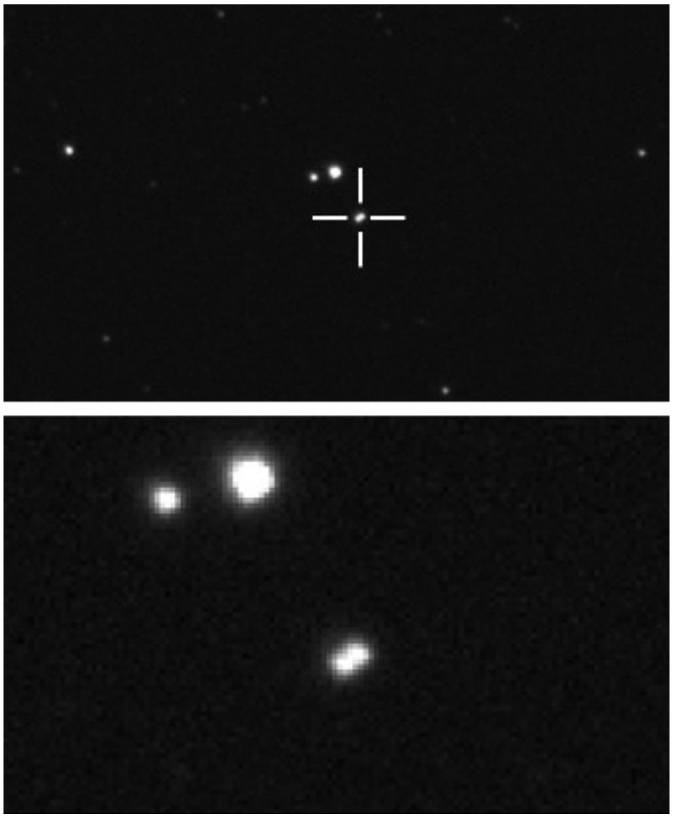

Figure 7. Fortuitously discovered potential binary at 00 06 32.31, +45 54 30.95, in a 60-second LCO exposure. Bottom image is zoomed in further.

are glaring problems. Certainly a more expensive sensor would give better results, as is the case for almost everything that is more expensive, but there is not a single main problem with the camera. Overall, my camera is the best piece of equipment in my setup.

Observations

The starfield of STT 547AB held some surprises. In addition to the target binary, I spotted several other known binaries and a potential binary by closely examining the image. Figure 7 shows one of these fortuitously-discovered doubles that has not been previously recorded in the WDS. This new double could potentially be gravitationally-bound because of its similar parallax and proper motion shown in Table 1 (Harshaw, 2018). In Figure 7, we zoom in on this double on a 60-second exposure from LCO. My telescope, while being able to capture these stars, only did so very faintly and the two stars cannot be resolved.

Image Analysis

The images were platesolved using Astrometry.net which produces a downloadable platesolved .fits file. The .fits files were then opened in AstroImageJ, which was used to find the position angle and separation of the stars. My images were not calibrated against a dark, bias, or flat frame, but the target star was bright enough not to need noise reduction. The LCO images are automatically calibrated using the network's calibration algorithm.

In Figure 8 and Table 1, all of the double stars - binary or not - that were found in the field are tabulated

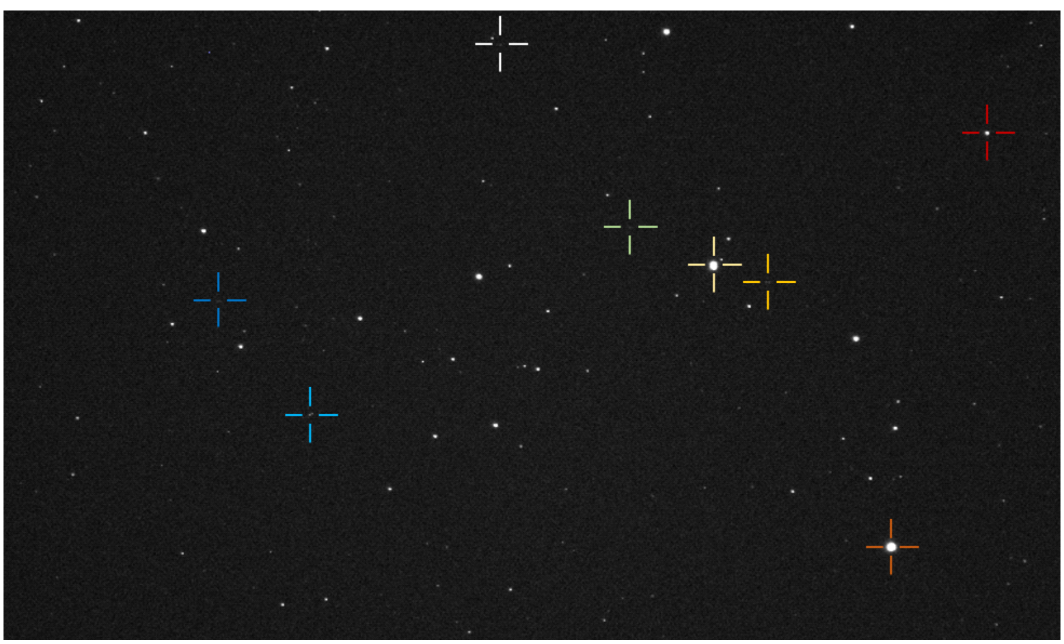

Figure 8. Starfield with double stars in Table 1 indicated.

Table 1. WDS and Gaia star data.

Coordinates	Name	Orbit in WDS?	Gaia Plxs	PM's (ra1, ra2; dec1, dec2)	Magnitudes	Measurable by my Telescope
00 04 55.317 +45 54 53.80	VYS 1	unsolved	4.1509, 4.3027	6.858, 6.547; -4.171, -4.013	10.5, 10.5	No
00:04:57.622+45:40:25.20	BU 997	unsolved	13.6562, 13.6018	18.385, 18.465; -65.374, -68.095	7.4, 9.5	No, high Δmag
00 05 31.350, +45 48 26.30	PAL 2	unsolved	0.9229, .9543	5.164, 5.362; -0.196, 0.144	13.9, 14.7	Yes
00 05 41.03 +45 48 43.3	**STT 547AB**	Yes	86.8735, 86.9402	888.615, 845.89; -162.47, -148.54	8.2, 8.3	Yes
00 06 00.27, +45 49 20.05	**POP 217YG**	Linear solution	0.7087, 0.7429	4.795, -3.695; -3.720, -4.805	14.8, 15.8	Optical
00 06 32.31, +45 54 30.95	**Potential binary!**	-	0.5394, 0.6123	-2.73, -2.707; 0.06, 0.064	14.9, 15.1	No, small sep
00:06:54.192 +45:40:52.95	-	-	0.6912, 1.1713	-0.653, -12.158; -0.602, 1.749	13.4, 14.2	Optical
00 07 15.96, +45 44 03.27-	-	-	0.8739, 1.4887	-3.004, 21.835; -2.610, 4.247	14.7, 14.9	Optical

along with their WDS Catalogue designations where applicable, corresponding data from the Gaia space telescope, and notes regarding whether it was possible to measure them in my images. The double stars were noted by visual inspection of the image, so there are some optical doubles that are not tabulated in the WDS and were not measured in the images. The white crosshair in Figure 8 is the same as in Figure 7; it gives a reference for the location of the new double in relation to the entire starfield.

Tables 2, 3, and 4 and the corresponding Figures 9, 10, and 11 show the various double stars and contain measurements of position angle and separation of each system. The measurements are made on both my images and the LCO images. The stars of WDS BU 997 have a delta mag too high to resolve in my images or the LCO images, so this system was not measured. Note that I only took 30 second images appropriate for a magnitude 8 star, as I did not anticipate measuring other, much dimmer stars, so the dimmer stars would be more accurate if the exposure had been adjusted for them. Although the original LCO images were overexposed for most of the stars in the field, they made possible the measurement of magnitude 14 stars. For each of the tables that follow, the last row is the average ± standard error of the mean.

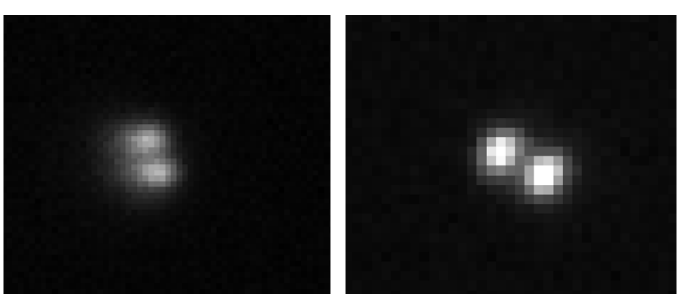

Figure 9: *VYS 1 through my telescope (left) and LCO (right).*

VYS 1

Although the nature of this double is uncertain, the parallaxes and proper motions are similar. The measurements of this system did not vary much, and my images gave essentially the same error as the LCO images. This star system is pushing what any telescope can resolve using a single exposure, and speckle interferometry is needed to give a reliable measurement. Still, the fact that my four-inch telescope can accurately record this double is impressive. Figure 9 shows my image and the LCO image. My image looks substantially less "sharp," as the stars are more smeared out, yet the measurements have low error. Table 2 shows the measurements of my images and the LCO images.

PAL 2

PAL 2 is a very dim star system, around magnitude

Table 2. Measurements made of VYS 1 from my images and LCO.

My Telescope		LCO (3 second exposures)	
Position Angle	Separation	Position Angle	Separation
26.21	2.78	25.83	2.78
27.98	2.74	28.66	2.88
25.73	2.89	28.80	2.84
25.02	2.91	26.58	3.00
		27.55	2.76
26.2 ± 0.63	**2.83 ± 0.041**	**27.5 ± 0.67**	**2.85 ± 0.042**

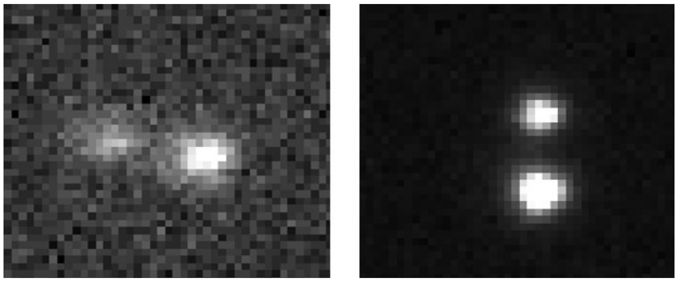

Figure 10. PAL 2 through my telescope (left) and LCO.

14, so my 30-second exposure is too short to record the stars with enough SNR to perform accurate measurements. The LCO images that I originally thought were horrendously overexposed turned out to be essential to measure this magnitude 14 double, so the LCO measurements have a very low error. My images are not good enough to be reliable. If I had taken a longer exposure, perhaps around two minutes, the stars would have been properly exposed. However, at this point, periodic error starts to creep in and the starfield will show drift, so a guiding solution is needed to measure this system accurately. Figure 10 shows the system through my telescope and LCO, and Table 3 lists the measurements from my images and LCO.

Table 3. Measurements made of PAL 2 from my images and LCO.

My Telescope		LCO (60 second exposures)	
Position Angle	Separation	Position Angle	Separation
90.99	5.77	91.61	6.06
92.43	6.11	91.66	6.07
90.32	5.54	91.12	6.02
91.33	5.75	91.64	6.06
		91.46	6.05
91.3 ± 0.44	**5.8 ± 0.118**	**91.5 ± 0.12**	**6.05 ± 0.010**

STT 547 AB

STT 547 AB was the original target for this project, and so the exposure was tuned for this double. My images were exceptionally accurate, with the separation having a standard mean error of 0.004. LCO, by comparison, was a very respectable 0.03 standard mean error for the separation, yet this is almost 10 times larger than mine. The position angle standard error of the mean also is much lower on my images, although the difference is not quite as dramatic as the separation. My images gave much more precise results despite the LCO image stars appearing rounder than mine. This shows that the quality of an image is based not only on its visual appearance, but also on factors that are much harder to readily observe. Figure 11 shows a comparison of this system in my images and LCO images, and Table 4 lists the measurements.

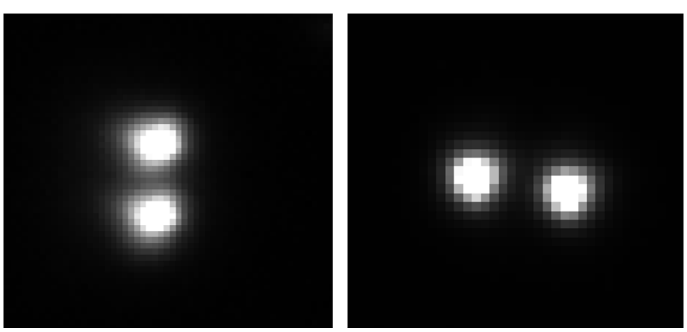

Figure 11. *STT 547 AB through my telescope (left) and LCO.*

Conclusion

Due to the greater control over real-time variables that impact observing, human-monitored telescope setups can perform quite well, even when limited in aperture compared to much larger robotic telescope networks. In comparing my four-inch telescope to 0.4-meter robotic telescopes on a three double stars in the same starfield, my setup performed similarly to LCO. The magnitude 14 star system, PAL 2, was the only double that I could not measure, but if I were able to take longer exposures, I am certain my setup would take images approaching the quality of the LCO images. In fact, as of completing this project, I have acquired more astrophotography gear, most importantly an autoguider. With this autoguider, I can take exposures in excess of several minutes, allowing me to push past the periodic error which was my limiting factor. Therefore, my future projects are likely to yield even better measurements, especially for the closer and dim-

Table 4. Measurements made of STT 547 from my images and LCO.

My Telescope		LCO (60 second exposures)	
Position Angle	Separation	Position Angle	Separation
189.59	5.99	189.55	6.07
189.38	6.01	189.14	5.95
189.62	5.99	188.94	6.02
189.77	6.00	190.04	6.07
		189.78	5.97
189.59 ± 0.080	**6.00 ± 0.004**	**189.5 ± 0.218**	**6.03 ± 0.03**

mer double star targets. Furthermore, actually looking at the sky and being outside while the images are being taken is a refreshing break from astronomy of today, in which observations are either done remotely or by trained telescope operators, not the astronomers themselves. Observations such as this demonstrate that small aperture astrometry is a viable alternative to large robotic telescopes because the limitations of the small aperture are offset by the human element.

Acknowledgements

Special thanks to Kalée Tock for helping me throughout the entire process, from being up with me during the cold late nights of imaging to the final editing process!

Special thanks to my parents, who (with much persuasion) bought me an astrophotography setup and support such an expensive hobby.

This research has made use of the Washington Double Star Catalog maintained at the U.S. Naval Observatory, Astrometry.net to plate solve image, and the AstroImageJ software written by Karen Collins and John Kielkopf at the University of Louisville, updated for double star astrometry by Karen Collins.

Special thanks to the Las Cumbres Observatory (LCO) network for time on the 0.4m telescopes.

This work has also made use of data from the European Space Agency (ESA) mission Gaia (https://www.cosmos.esa.int/gaia), processed by the Gaia Data Processing and Analysis Consortium (DPAC, https://www.cosmos.esa.int/web/gaia/dpac/consortium). Funding for the DPAC has been provided by national institutions, in particular the institutions participating in the Gaia Multilateral Agreement.

References

Arimatsu, K., K. Tsumura, F. Tsui, Y. Shinnaka, K. Ishikawa, T. Ootsubo, T. Kotani, T. Wada, K. Nahase, and J. Watanabe, 2019, "A kilometer-sized Kuiper belt object discovered by stellar occultation using amateur telescopes", *Nature Astronomy*, **3**, 301-306. https://www.nature.com/articles/s41550-018-0685-8.

Bracken, Charles, 2017, *The Deep Sky Imaging Primer, 2nd Edition*, Deep Sky Publishing. ISBN 978-0999470909.

Buchheim, Robert, 2007, *The Sky is Your Laboratory: Advanced Astronomy Projects for Amateurs*, Praxis Publishing, Chichester, UK. ISBN 978-0-387-73995-3.

Collins, Karen, John F. Kielkopf, Keivan G. Stassun, and Frederic V. Hessman, 2017, "AstroImageJ: Image Processing and Photometric Extraction for Ultra-Precise Astronomical Light Curves", *The Astronomical Journal*, 153:77.

Harshaw, Richard. "Gaia DR2 and the Washington Double Star Catalog: A Tale of Two Databases", *Journal of Double Star Observations*, **14**, 734 - 740.

Nave, Carl Rod. "The Rayleigh Limit." From the hyperphysics website: http://hyperphysics.phy-astr.gsu.edu/hbase/phyopt/Raylei.html . Described in "Doing It by the Numbers: JavaScript Calculations in Web-Based Physics Instructional Material: A presentation from the 121st AAPT National Meeting: Guelph, Ontario, Canada", 2000.

Saunders, Rick, 2012, "Gears and Periodic Errors," *Journal of the Royal Astronomical Society of Canada*, **106**, 162 - 164.

Wasson, Rick. "Speckle Interferometry with the OCA Kuhn 22" Telescope," *JDSO*, **14**, 223 - 241.

A Report on Double Stars Observed During the Year 2015 by Students and Faculty of the Humacao University Observatory

R.J. Muller, D. Cotto, J.C. Cersosimo, B.S.Torres, N.Vergara, J. Martinez, M. Reyes, B. Morales, E. Gonzalez, N. Marquez, O. Reyes, J. Garcia, O. Carromero, T. Ortiz, A. López, Yashira Del Valle, G. Espinosa and D. Ortiz

Humacao University Observatory
Department of Physics and Electronics
The University of Puerto Rico at Humacao
Call Box 860, Humacao, Puerto Rico 00792
Desiree.cotto@upr.edu

Abstract: We are hereby reporting on the measurements of separation and position angle of 70 binary stars. We used the NURO Telescope at the Anderson Mesa location of Lowell Observatory, 20 miles east of Flagstaff, Arizona, at an altitude of 7000 feet to obtain our data. We observed on September 26, 27, and 28 of 2015 and gathered the data using the 2K x 2K CCD camera, NASACAM, at the prime focus of the 31 inch telescope. The data was transferred and analyzed at the Humacao University Observatory of the University of Puerto Rico by undergraduate students undertaking astronomy research projects.

We report measurements of separation and position angle of 70 binary stars gathered from CCD images obtained with the NASACAM CCD at the prime focus of the National Undergraduate Research Observatory (NURO) telescope. The Humacao Campus of the University of Puerto Rico is a member of NURO, a consortium of primarily undergraduate institutions (www.nuro.nau.edu) with access to a 31-inch telescope, property of Lowell Observatory. It is located roughly 20 miles east of Flagstaff, Arizona at Anderson Mesa, at an altitude of 7200 feet. We use the NURO telescope twice a year, and at present we use it for both binary star measurements and asteroid research.

The data presented in this report was acquired on one trip to NURO on 2015, on September 26, 27 and 28. We were rained out on our May/June trip.

The NASA cam is a 2K x 2K CCD camera with 15 micron pixels. The camera does not need liquid nitrogen to cool down to -100, saving us a lot of time in the camera-telescope setup. The field of view of the old camera was 4 arc minutes by 4 arc minutes. The field of view of the new camera is 16 arc minutes by 16 arc minutes. However, an optical reducer with ratio 2:1 lies in the optical path, so the separation of binaries in the images looks almost the same as before, in a much wider field.

Procedure

As in past reports, the CCD images where analyzed by students with undergraduate astronomy research projects at our department at the University of Puerto Rico, Humacao Campus. The students used the pixelation of the CCD images to obtain the separation and position angle (Muller et al, 2003). Then various of the CCD images where analyzed a second time using the softwareAstronomical Image Processing for Windows (Berry et al, 2002). Since the software does not provide for introducing the telescope's plate scale in the computations one has to perform final number crunching with a hand calculator. The software in the program is also mirror reversed as far as position angle is concerned, so one must be very careful to figure the correct angle from the one given by the software. The design value for the plate scale with the new NASA CAM is .515 arc seconds/pixel. We used 22 binaries with very long periods to obtain an experimental value for the plate scale. With this small sample it came to be .524 ± .009, in close agreement with the design value provided by the manufacturer. We are using our value when calculating the separation of the binaries. There is also a systematic error in position angle that occurs because the CCD camera cannot be inserted into the telescope with an absolute level. This error can be corrected by using well known binary systems and binary systems that "don't move". Binary systems that "don't move" can be found in the neglected section of the Washington Double Star catalog, as binary stars that have been measured for the last 100 years and show no change in position angle. By imaging a mix of well known binaries and fixed binaries (we use around 20 of them total) and comparing the value of position angle given in the WDS with the value obtained from our images, the systematic error in the position angle can be corrected. We call such error the offset error and are incorporated in the position angle values given in the accompanying table.

Data

The following table includes the 70 entries for the binary stars for which we obtained useful results. The table is divided with the first column containing the name of the system. The second and third columns contain the R.A. and Dec of the system, acquired from the Washington Double Star Catalog (WDS).The fourth column contain our measurement of separation and the fifth our position angle measurements. The next two columns are the visual magnitudes of the primary and secondary, obtained from the WDS. The last column is the date of the observation in fractional date. We obtained only one image per night per system. That image was pixelized and three or more copies were made of each pixelized image. Then, three students analyzed the images separately and then an average of all measures was reported as the final result.

We have gathered data for many of these binaries during many years (Muller et al., 2007 and following years) until 2014; we are putting together yearly observations of various systems to obtain information on them. Any findings will be reported in this journal.

Acknowledgements

This research has made extensive use of the Washington Double Star Catalog maintained at the U. S. Naval Observatory.We want to thank Lowell Observatory for its continuous support of this project by allowing us the use of the 31-inch NURO telescope. We also thank Ed Anderson of NURO for his efforts on behalf of our students.

References:

Muller, Rafael, *et al.*, 2003, *The Double Star Observer*, **9**, 4-16.

Muller, Rafael, *et al*., 2007, *Journal of Double Stars Observations*, **3**, 11-16.

The Handbook of Astronomical Image Processing, R. Berry, J. Burnell, Willmann-Bell Inc., Virginia 2002.

Day 1: Sept 26 2015							
Star Name	**RA**	**DEC**	**Separation**	**θ**	**M1**	**M2**	**Date**
ARA 243	160106.51	-174216.7	13.21	118^0	11.7	12.1	2015.7369
AG 349	160104.36	+280642.4	12.36	227^0	9.59	10.86	2015.7369
HJ 580	160250.56	+370526.8	39.46	9^0	9.21	12.97	2015.7369
BEM 21	160258.26	+5111140.4	18.52	105^0	10.54	11.02	2015.7369
BAL1911	160320.00	+023126.8	16.36	238^0	12.19	12.7	2015.7369
STF1999 AB	160425.96	-112657.6	12.28	102.3^0	7.52	8.05	2015.7369
HJ 582	160716.96	+350741.6	22.5	234^0	11.11	13.61	2015.7369
ALI 370	160726.70	+354827.8	12.5	148^0	12.0	13.0	2015.7369
POU3214	160748.84	+230529.9	12.2	83.8^0	11.1	13.3	2015.7369
ES 627	161835.71	+511951.5	12.37	290^0	9.88	10.98	2015.7369
STF2098 AB	164543.4	+300017.2	15.5	147^0	8.77	9.61	2015.7369
BAL2429	165451.18	+031840.8	10.53	53^0	11.77	12.8	2015.7369
BAL1931	170605.4	+432857.4	17.95	189^0	12.4	13.23	2015.7369
COU 109	170627.8	+220756.7	10.34	140^0	10.01	13.1	2015.7369
AG 353	170701.3	+121321.6	9.53	250^0	9.83	11.7	2015.7369
STF2127	170704.4	+310535.1	15.17	280^0	8.7	12.3	2015.7369
SLE 9	170706.2	+202921.7	19.9	174^0	10.49	12.3	2015.7369
GRV 946	170714.1	+254434.5	20.65	43^0	10.54	11.71	2015.7369
BAL1934	171745.8	+020705.9	11.99	236^0	10.8	10.8	2015.7369
STI2366	180033.7	+584056.1	10.97	300^0	10.65	12.1	2015.7369
SLE 107	180149.8	+263123.4	13.3	207.4^0	12.45	12.6	2015.7369
HJ 1314	180705.3	+322254.6	17.25	155^0	10.33	11.09	2015.7369
SLE 110	180714.4	+271603.6	11.94	114^0	10.56	13.3	2015.7369
BAL2474	180803.4	+034312.1	16.27	284^0	10.0	11.0	2015.7369

Day 2: Sept 27 2015							
Star Name	RA	DEC	Separation	θ	M1	M2	Date
SLE 111	180853.96	+272456.6	14.02	317.3^0	10.8	12.5	2015.7397
POU3353	180855.05	+231900.4	14.97	346.1^0	12.26	12.4	2015.7397
STF2293	180953.83	+482405.7	12.42	85.4^0	8.08	10.34	2015.7397
ARA 267	180954.03	-170938.3	14.63	351^0	11.22	12.4	2015.7397
SEI 559	181027.80	+335555.6	11.89	174.8^0	11.0	11.0	2015.7397
BAL2481	181037.28	+032723.7	11.08	110^0	11.3	11.3	2015.7397
AG 217	181105.89	+532937.8	14.14	240^0	10.77	11.85	2015.7397
ALI 140	181125.14	+350645.5	14.62	251^0	10.97	11.79	2015.7397
BAL2483	181441.54	+034205.5	12.98	197^0	12.00	12.7	2015.7397
STF 2459	190722.01	+255823.9	13.68	232.7^0	9.12	10.07	2015.7397
SLE 931	191020.34	+024958.7	11.03	81.2^0	9.9	12.0	2015.7397
POU3745	191200.71	+234617.6	11.3	24.4^0	12.47	13.7	2015.7397
HJ 1375	191229.96	+281426.7	11.49	87^0	11.0	13.6	2015.7397
SLE 935	191426.85	+021204.9	8.46	222^0	10.5	13.1	2015.7397
ARA1175	191533.51	-195421.4	12.43	14^0	12.4	13.2	2015.7397
HJ 2868	191756.98	+580758.2	11.58	102^0	11.9	11.9	2015.7397
POU3940	193512.15	+250129.6	10.23	31^0	10.6	10.7	2015.7397
HJ 1421	193621.95	+353551.5	15.53	232^0	9.37	11.72	2015.7397
ALI 892	193720.68	+390419.2	11.27	65^0	10.74	12.6	2015.7397
HJ 1429	193757.45	+561405.9	8.89	239^0	10.6	11.0	2015.7397
SMA 101	195048.4	+444442.1	10.26	53^0	12.8	13.2	2015.7397
POU4178	200012.2	+242045.5	11.65	6^0	11.3	12.3	2015.7397

Day 3: September 28 2015							
Star Name	**RA**	**DEC**	**Separation**	**θ**	**M1**	**M2**	**Date**
BAL1230	212750.4	+010448.4	11.65	277.7^0	11.4	11.5	2015.7424
STI2586	214240.4	+561456.9	9.65	1.0^0	10.71	11.72	2015.7424
STI2720	222130.2	+583648.7	12.49	161.7^0	12.1	12.1	2015.7424
STI2722	222158.8	+561953.9	14.10	73.7^0	10.67	13.1	2015.7424
ES 837 AC	223145.7	+500424.4	12.05	241.3^0	9.6	12.9	2015.7424
HO 475 AC	223245.5	+262432.7	10.07	221.5^0	9.34	11.3	2015.7424
POU5723	223511.5	+234155.6	10.81	181.7^0	12.8	13.3	2015.7424
CHE 347	224037.3	+301949.0	8.03	53^0	13.1	13.6	2015.7424
STF2999 AD	231846.44	+051118.7	26.67	24^0	8.90	11.9	2015.7424
HJ 1876	232556.79	+365032.5	8.78	212.7^0	11.1	11.6	2015.7424
HJ 986	232707.3	+352028.2	9.85	294^0	11.23	12.2	2015.7424
CHE 501	233011.3	+421440.4	24.08	275^0	13.45	13.42	2015.7424
STF3019	233040.7	+051458.0	12.19	182^0	7.77	8.37	2015.7424
MLB 506	233828.6	+284456.2	8.06	239^0	11.1	11.6	2015.7424
STI3007	233642.8	+581948.7	8.88	123^0	13.2	13.2	2015.7424
ES 269 AB	234903.2	+411926.2	10.06	227.08^0	9.93	12.1	2015.7424
BAL1611	004318.5	255101.2	19.54	177^0	12.68	13.09	2015.7424
HJ 1288	161240.87	-164518.6	17.93	123^0	11.0	12.3	2015.7424
LDS4705	165624.44	+033029.1	13.73	56^0	15.2	17	2015.7424
STF2123	170657.50	+064803.0	17.5	217^0	9.82	9.98	2015.7424
STN 34	171642.44	-170911.5	15.96	290.3^0	9.57	10.58	2015.7424
HDS2441	171556.29	-132939.0	12.46	237^0	9.63	11.74	2015.7424
BAL1934	171745.8	+020705.9	12	239^0	10.8	10.8	2015.7424
BAL1952	180734.4	+022407.8	14.31	157^0	11.52	12.8	2015.7424

Astronomical Association of Queensland 2016 Results: Bluestar Observatory Measurement of Twenty Neglected Southern Multiple Stars

Peter N. Culshaw, Diane Hughes, John Hughes, Graeme Jenkinson, D. Janke

Astronomical Association of Queensland.
bluestars@iprimus.com.au

Abstract: This paper presents the final results of a 2016 program of photographic measurements of twenty southern multiple stars. All results were obtained using an Atik 460EX mono CCD camera used in conjunction with an equatorially mounted 400mm F4.5 Newtonian reflector.The mean 95% confidence intervals for the new measures were ± 0.758° in PA and ± 0.158" in separation.

Introduction

Commencing in 2008, the Double Star Section of the AAQ submits the 2016 results given in Table 1 as part of an ongoing program. The target stars were selected from the Washington Double Star Catalog (WDSC) and were observed in Queensland from a latitude of approximately 27° S.

Method

Once obtained with the equipment described above, the images were analysed using the astrometric double star program REDUC (Losse, 2008). Approximately ten stacked images of each target were taken per night for seven nights and the results averaged to obtain measures of separation and position angle with sufficient confidence.

Full details of the method are given in Napier-Munn and Jenkinson (2009). Some recent work on the errors inherent in the method is described in Napier-Munn and Jenkinson (2014). As proficiency has grown in the use of this equipment with the 400mm reflector, close doubles with considerable magnitude difference between the components have been successfully measured.

Results

For all of the systems shown below the WDSC information is first reproduced, showing the epoch 2000 position, magnitudes, separation, PA, and the last recorded measurement. The new measurements are then given in tabular form, including the mean and standard deviation and 95% confidence limits. Any uncertainties between the images and the last recorded measurements are discussed. Finally a conclusion is given as to whether any movement of the component stars has occurred in PA or separation, based on the P-value for the t-test comparing the new mean values with the cataloged value ($P < 0.05$ is considered as evidence of change).

For reference purposes a sample image of each target pair has been included with this report. Please note that all attached images are aligned with North to the bottom and East to the right.

Acknowledgements

This research has made use of the Washington Double Star Catalog maintained at the U.S. Naval Observatory.

The Edward Corbould Research Fund administered by the Astronomical Association of Queensland for granting of funds to upgrade imaging camera and observatory computer to suit.

Fellow AAQ member Des Janke for his work in processing the original FITS image files into JPEG photographs for this Circular.

Fellow AAQ members Culshaw, Hughes and Hughes provided invaluable assistance with image processing using Losse's REDUC software.

(Text continues on page 428)

Table 1

SYSTEM	Last listed measure			New measure			COMMENTS
	PA°	Sep"	Epoch	PA°	Sep"	Epoch*	
ARA1961	71	5.9	1921	231.19	18.15	2016.849	Very large movement
B 32	226	4.9	1954	225.77	5.18	2016.833	Slight increase in PA only
I 1142	41	3.7	1933	39.86	3.73	2016.843	Minor reduction in PA
HU 18	250	4.3	1919	251.39	4.29	2016.857	Slight change in PA only
RSS 73	98	10.7	1976	150.43	34.14	2017.019	Large movement over 41 years
RST2355	351	5.8	1949	351.41	6.06	2017.019	Minor change in both axes
I 554AB	183	3.2	1933	184.76	4.01	2016.513	Slight increases since 1933
I 554AC	159	5.6	1972	154.07	5.76	2016.513	Movement in PA only
RST 814	113	4.5	1967	114.16	4.97	2016.476	Small change since first measure
CPO 460	27	7.4	1902	29.80	6.53	2016.506	Movement evident
LDS 696	116	31.7	1999	115.84	31.60	2016.616	Slight decrease in PA
HDO 156AB	89	6.4	2010	88.69	6.60	2016.605	Possible slight changes
HDO 156AC	54	8.4	1999	53.66	8.29	2016.605	Possible slight changes
HO 277	68	3.6	1939	67.53	3.01	2016.627	Little probable change
I 1047AB	331	9.6	1912	330.97	6.20	2016.556	Definite decrease in separation
RSS 568	50	10.6	1974	53.77	9.72	2016.702	Clear changes evident
CPO 632	1	3.0	1901	0.66	3.58	2016.706	Little probable change
CPO 97	135	4.2	1932	135.47	4.1	2016.702	Little probable change
PRO 240	270	4.7	1910	238.26	35.72	2016.764	Considerable movement
DAW 28AB	74	3.8	1933	76.39	3.63	2016.764	Clear change in PA only

Astronomical Association of Queensland 2016 Results: Bluestar Observatory Measurement ...

ARA1961 Cetus	RA. 01 09.2	DEC. -22 39	Last Measure 1921
	MAG. 11.78 & 12.7	PA. 71°	SEP. 5.9"
Date	**No. images**	**PA°**	**Sep"**
24 Oct 2016	10	231.38	18.170
01 Nov 2016	10	231.76	18.241
04 Nov 2016	10	231.28	18.108
05 Nov 2016	10	231.13	18.202
06 Nov 2016	10	230.99	18.050
07 Nov 2016	10	230.86	18.125
18 Nov 2016	10	230.95	18.154
Mean		**231.193**	**18.150**
Std dev		0.311	0.063
95% CI +/-		0.287	0.058
P(t) movement		0.00	0.00

COMMENTS
Large movement. Only one other possible secondary candidate even further away in SE quadrant. North at bottom, east to the right.

B32 Fornax	RA. 02 15.5	DEC. -29 25	Last Measure 1954
	MAG. 9.6 & 13.3	PA. 226°	SEP. 4.9"
Date	**No. images**	**PA°**	**Sep"**
15 Oct 2016	10	225.82	5.144
29 Oct 2016	10	225.97	5.160
01 Nov 2016	10	225.67	4.957
04 Nov 2016	10	225.13	5.304
05 Nov 2016	10	224.98	5.392
07 Nov 2016	10	227.22	4.999
18 Nov 2016	10	225.61	5.286
Mean		**225.771**	**5.177**
Std dev		0.732	0.161
95% CI +/-		0.677	0.149
P(t) movement		0.440	0.004

COMMENTS
No change in PA since first measurement in 1926. Slight increase in separation consistent with the two previous recordings.

I 1142 Eridanus	RA. 02 23.5	DEC. -52 08	Last Measure 1933
	MAG. 9.65 & 12.6	PA. 41°	SEP. 3.7"
Date	**No. images**	**PA°**	**Sep"**
15 Oct 2016	10	40.99	3.609
29 Oct 2016	10	39.59	3.858
05 Nov 2016	10	38.98	3.949
06 Nov 2016	10	40.66	3.872
07 Nov 2016	10	38.97	3.758
20 Nov 2016	10	40.61	3.507
22 Nov 2016	10	39.20	3.568
Mean		**39.857**	**3.732**
Std dev		0.871	0.171
95% CI +/-		0.806	0.158
P(t) movement		0.013	0.643

COMMENTS
Minor reduction in PA consistent with the two previous measurements. No change in separation over the same period.

HU18 Cetus	RA. 02 28.6	DEC. -10 37	Last Measure 1919
	MAG. 8.77 & 12.8	PA. 250.0°	SEP. 4.3"
Date	**No. images**	**PA°**	**Sep"**
29 Oct 2016	10	251.34	4.257
04 Nov 2016	10	250.81	4.445
05 Nov 2016	10	…..	…..
06 Nov 2016	10	251.08	4.220
07 Nov 2016	10	251.98	4.165
18 Nov 2016	10	252.13	4.333
20 Nov 2016	10	251.01	4.302
Mean		**251.392**	**4.287**
Std dev		0.543	0.098
95% CI +/-		0.570	0.102
P(t) movement		0.002	0.757

COMMENTS
Slight change in PA since first measurement in 1900. Poor quality images obtained 05 Nov 2016 not used for reduction.

RSS73 Caelum	RA. 04 41.7	DEC. -32 51	Last Measure 1976
	MAG. 8.67 &	PA. 98°	SEP. 10.7"
Date	**No. images**	**PA°**	**Sep"**
25 Nov 2016	10	150.28	34.061
27 Dec 2016	10	150.51	34.220
28 Dec 2016	10	150.28	34.159
30 Dec 2016	10	150.43	34.182
09 Jan 2017	10	150.43	34.099
10 Jan 2017	10	150.51	34.151
23 Jan 2017	10	150.55	34.082
Mean		**150.427**	**34.136**
Std dev		0.110	0.057
95% CI +/-		0.101	0.053
P(t) movement		0.000	0.000

COMMENTS
Large movement over a period of 41 years.

RST2355 Pictor	RA. 04 41.7	DEC. -48.09	Last Measure 1949
	MAG. 8.67 & 14.9	PA. 351°	SEP. 5.8"
Date	**No. images**	**PA°**	**Sep"**
25 Nov 2016	10	352.14	5.965
27 Dec 2016	10	351.72	6.051
28 Dec 2016	10	351.71	6.058
30 Dec 2016	10	351.83	6.168
09 Jan 2017	10	351.49	6.115
10 Jan 2017	10	349.97	6.119
23 Jan 2017	10	351.00	5.932
Mean		**351.409**	**6.058**
Standard deviation		0.724	0.085
95% CI +/-		0.669	0.079
P(t) movement		0.000	0.000

COMMENTS
Minor movement in both axes consistent with changes since the first measure in 1936.

Astronomical Association of Queensland 2016 Results: Bluestar Observatory Measurement ...

I 554AC Norma	RA. 16 01.6	DEC. -54 09	Last Measure 1972
	MAG. 8.17 & 11.4	PA. 159°	SEP. 5.6"
Date	**No. images**	**PA°**	**Sep"**
14 June 2016	10	154.69	5.787
28 June 2016	10	154.12	5.835
09 July 2016	10	153.20	5.947
23 July 2016	10	151.64	5.426
27 July 2016	10	155.43	5.922
29 July 2016	10	153.81	5.688
30 July 2016	10	155.59	5.708
Mean		**154.069**	**5.759**
Standard deviation		1.371	0.177
95% CI +/-		1.268	0.163
P(t) movement		0.000	0.000

COMMENTS
Movement evident in PA only.

I 554AB Norma	RA. 16 01.6	DEC. -54 09	Last Measure 1933
	MAG. 8.17 & 11.4	PA. 183°	SEP.3.2"
Date	**No. images**	**PA°**	**Sep"**
14 June 2016	10	183.45	4.137
28 June 2016	10	187.39	4.073
09 July 2016	10	187.42	3.969
23 July 2016	10	183.02	3.101
27 July 2016	10	192.27	8.368
29 July 2016	10	182.51	4.787
30 July 2016	10	190.48	3.887
Mean		**184.758**	**4.013**
Standard deviation		2.439	0.602
95% CI +/-		3.029	0.748
P(t) movement		0.000	0.000

COMMENTS
Very slight increases possible since 1933. Reduction measures of 27 July and 30 July 2016 excluded from final calculation due to poor quality images.

RST814 Norma	RA. 16 10.5	DEC. -55 21	Last Measure 1967
	MAG. 7.65 & 13.4	PA. 113°	SEP. 4.5"
Date	**No. images**	**PA°**	**Sep"**
20 May 2016	10	113.82	5.111
07 June 2016	10	114.39	4.985
08 June 2016	10	113.89	4.936
28 June 2016	10	114.50	5.009
23 July 2016	10	113.63	4.765
27 July 2016	10	114.76	5.008
28 July 2016	10	116.77	4.379
Mean		**114.165**	**4.969**
Standard deviation		0.447	0.115
95% CI +/-		0.469	0.121
P(t) movement		0.000	0.000

COMMENTS
Consistent with very small changes since the first 1929 measure. Reduction measure of 28 July 2016 excluded from final calculation due to poor quality images.

CPO460 Norma	RA. 16 15.2	DEC. -48.38	Last Measure 1902
	MAG. 9.16 & 14.6	PA. 27°	SEP. 7.4"
Date	**No. images**	**PA°**	**Sep"**
08 June 2016	10	29.56	6.534
14 June 2016	10	29.56	6.393
28 June 2016	10	29.53	6.486
09 July 2016	10	30.12	6.607
27 July 2016	10	29.36	6.626
30 July 2016	10	30.63	6.531
31 July 2016	10	29.87	6.503
Mean		**29.804**	**6.526**
Standard deviation		0.443	0.078
95% CI +/-		0.410	0.072
P(t) movement		0.000	0.000

COMMENTS
Movement evident since the only previous measure in 1902.

LDS696 Pavo	RA. 20 01.4	DEC. -57.25	Last Measure 1999
	MAG. 11.5 & 14.2	PA. 116°	SEP. 31.7"
Date	**No. images**	**PA°**	**Sep"**
05 August 2016	10	115.89	31.65
06 August 2016	10	115.79	31.622
08 August 2016	10	115.85	31.67
12 August 2016	10	115.94	31.512
15 August 2016	10	115.77	31.604
20 August 2016	10	115.8	31.554
21 August 2016	10	115.85	31.606
Mean		**115.841**	**31.603**
Standard deviation		0.060	0.054
95% CI +/-		0.056	0.050
P(t) movement		0.000	0.000

COMMENTS
Slight decrease in PA over the previous measure in 1999 would seem to be consistent with change since the first 1920 measurement. Little apparent change in separation.

HDO156AB Capricorn	RA. 20 06.9	DEC. -08 55	Last Measure 2010
	MAG. 7.89 & 10.3	PA.89°	SEP. 6.4"
Date	**No. images**	**PA°**	**Sep"**
30 July 2016	10	89.03	6.612
01 August 2016	10	89.23	6.623
06 August 2016	10	88.63	6.543
08 August 2016	10	88.84	6.588
12 August 2016	10	88.11	6.635
15 August 2016	10	88.72	6.577
20 August 2016	10	88.25	6.629
Mean		**88.687**	**6.601**
Standard deviation		0.401	0.033
95% CI +/-		0.371	0.031
P(t) movement		0.000	0.000

COMMENTS
Possible slight change in both axes since last recent measurement.

Astronomical Association of Queensland 2016 Results: Bluestar Observatory Measurement ...

HDO156AC Capricorn	RA. 20 06.9	DEC. -08 55	Last Measure 1999
	MAG. 7.89 & 12.8	PA. 54°	SEP. 8.4"
Date	**No. images**	**PA°**	**Sep"**
30 July 2016	10	54.05	8.212
01 August 2016	10	54.05	8.315
06 August 2016	10	53.35	8.222
08 August 2016	10	53.26	8.302
12 August 2016	10	53.96	8.319
15 August 2016	10	53.49	8.312
20 August 2016	10	53.48	8.354
Mean		**53.663**	**8.291**
Standard deviation		0.344	0.053
95% CI +/-		0.318	0.049
P(t) movement		0.000	0.000

COMMENTS
Possible very minor change in both axes since last recent measurement.

HO277 Aquila	RA. 20 21.7	DEC. -07 45	Last Measure 1939
	MAG. 8.91 & 13.3	PA. 68°	SEP. 3.6"
Date	**No. images**	**PA°**	**Sep"**
30 July 2016	10	68.26	2.965
06 August 2016	10	66.27	3.094
12 August 2016	10	66.02	3.191
20 August 2016	10	70.38	3.029
27 August 2016	10	67.79	2.909
03 September 2016	10	68.39	2.985
05 September 2016	10	65.61	2.88
Mean		**67.531**	**3.008**
Standard deviation		1.684	0.108
95% CI +/-		1.558	0.100
P(t) movement		0.000	0.000

COMMENTS
Little probable movement.

I 1047AB Pavo	RA. 20 33.0	DEC. -71 19	Last Measure 1912
	MAG. 8.21 & 12.6	PA. 331°	SEP. 9.6"
Date	**No. images**	**PA°**	**Sep"**
09 July 2016	10	331.69	6.439
23 July 2016	10	330.39	6.230
27 July 2016	10	331.53	6.126
28 July 2016	10	329.90	6.088
30 July 2016	10	330.08	6.060
01 August 2016	10	331.51	6.317
05 August 2016	10	331.70	6.133
Mean		**330.971**	**6.199**
Standard deviation		0.809	0.138
95% CI +/-		0.748	0.127
P(t) movement		0.000	0.000

COMMENTS
Measurable decrease in sep. since the previous two recordings. Little probable movement in PA.

RSS568 Grus	RA. 22 12.0	DEC. -43.08	Last Measure 1974
	MAG. 8.5 & n/a	PA. 50°	SEP. 10.6"
Date	**No. images**	**PA°**	**Sep"**
27 August 2016	10	53.8	9.752
28 August 2016	10	53.71	9.824
03 September 2016	10	54.7	9.629
05 September 2016	10	53.06	9.71
13 September 2016	10	54.12	9.771
30 September 2016	10	53.51	9.78
01 October 2018	10	53.48	9.612
Mean		**53.769**	**9.725**
Standard deviation		0.524	0.079
95% CI +/-		0.485	0.073
P(t) movement		0.000	0.000

COMMENTS
Clear movement on both axes since the initial measure in 1974.

CPO632 Grus	RA. 22 33.6	DEC. -42 41	Last Measure 1901
	MAG. 10.9 & 12.6	PA. 1°	SEP. 3.0"
Date	**No. images**	**PA°**	**Sep"**
27 August 2016	10	1.06	3.525
28 August 2016	10	0.87	3.623
03 September 2016	10	0.23	3.588
05 September 2016	10	-0.13	3.693
30 September 2016	10	0.23	3.532
01 October 2016	10	0.98	3.636
04 October 2016	10	1.35	3.489
Mean		**0.656**	**3.584**
Standard deviation		0.544	0.072
95% CI +/-		0.503	0.067
P(t) movement		0.000	0.000

COMMENTS
Little probable movement since 1901.

CPO97 Grus	RA. 23 10.4	DEC. -46 53	Last Measure 1932
	MAG. 9.82 & 13.0	PA. 135°	SEP. 4.2"
Date	**No. images**	**PA°**	**Sep"**
27 August 2016	10	135.52	4.161
28 August 2016	10	135.86	4.065
03 September 2016	10	136.55	4.083
05 September 2016	10	136.91	4.059
13 September 2016	10	136.16	4.113
30 September 2016	10	133.29	4.084
01 October 2016	10	133.99	4.107
Mean		**135.469**	**4.096**
Standard deviation		1.342	0.035
95% CI +/-		1.242	0.032
P(t) movement		0.000	0.000

COMMENTS
Little probable movement since last measurement.

Astronomical Association of Queensland 2016 Results: Bluestar Observatory Measurement ...

PRO240 Sculptor	RA. 23 16.2	DEC. -31 31	Last Measure 1910
	MAG. 10.0 & 10.3	PA. 270°	SEP. 4.7"
Date	**No. images**	**PA°**	**Sep"**
01 October 2016	10	238.19	35.695
04 October 2016	10	238.24	35.743
05 October 2016	10	238.30	35.665
06 October 2016	10	238.28	35.769
07 October 2016	10	238.33	35.815
10 October 2016	10	238.19	35.672
12 October 2016	10	238.27	35.702
Mean		**238.257**	**35.723**
Standard deviation		0.053	0.055
95% CI +/-		0.049	0.051
P(t) movement		0.000	0.000
COMMENTS Considerable change in both axes over 106 years.			

DAW28AB Phoenix	RA. 23 43.1	DEC. -46 19	Last Measure 1933
	MAG. 6.65 & 11.1	PA. 74°	SEP. 3.8"
Date	**No. images**	**PA°**	**Sep"**
01 October 2016	10	74.66	3.493
04 October 2016	10	77.79	3.676
07 October 2016	10	76.3	3.706
10 October 2016	10	75.37	3.816
12 October 2016	10	77.81	3.461
Mean		**76.386**	**3.630**
Standard deviation		1.416	0.150
95% CI +/-		1.758	0.186
P(t) movement		0.000	0.000
COMMENTS Two nights poor quality data not used. Clear change evident in PA only.			

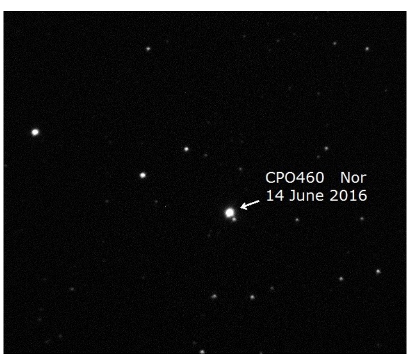

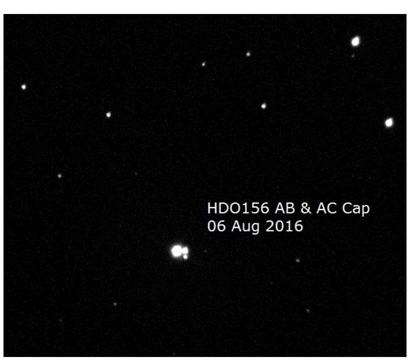

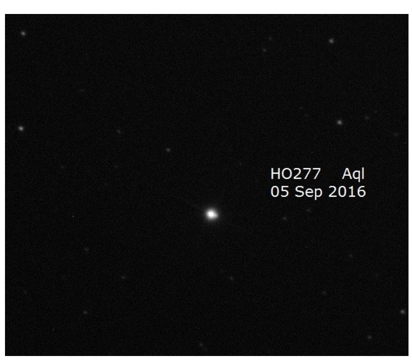

Astronomical Association of Queensland 2016 Results: Bluestar Observatory Measurement ...

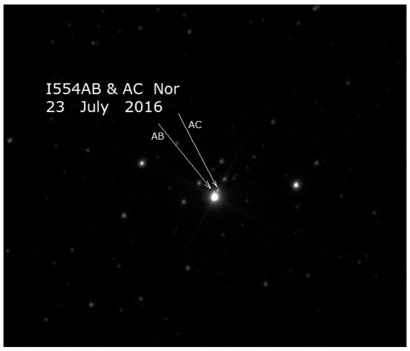

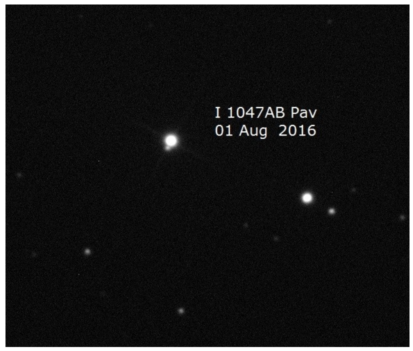

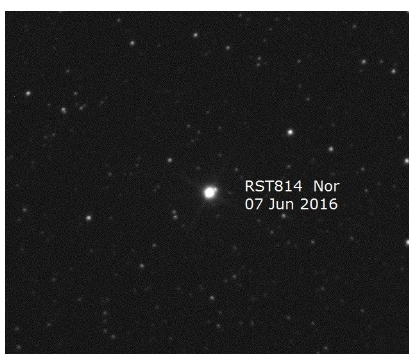

(Continued from page 421)

References

Losse, F. Reduc software, V4.5.1.

http://www.astrosurf.com/hfosaf/uk/tdownload.htm

Napier-Munn, T.J. and Jenkinson, G., 2009, "Measurement of some neglected southern multiple stars in Pavo", *Webb Society Double Star Section Circular*, **17**, 6-12.

Napier-Munn, T.J and Jenkinson G., 2014, "Analysis of Errors in the Measurement of Double Stars Using Imaging and the Reduc Software", *Journal of Double Star Observations*, **10**(3), 193-198.

Argyle, R.W., 2012, *Observing and Measuring Visual Double Stars*, 2nd edition, Springer.

Near Infrared Robotic Observation of Double Star System WDS 13513-3928

Stephen White[1, 2], James Gallegos[1], Grady Boyce[2], Pat Boyce[2], and Carson Barnett[1]

1. New Mexico Institute of Mining and Technology, Socorro, NM
2. Boyce Research Initiatives and Educational Foundation, San Diego, CA

Abstract: A near infrared robotic observation of the double star system WDS 13513-3928 was performed at the Siding Spring Observatory in New South Wales, Australia—part of the Las Cumbres Observatory Network. The mean position angle (θ) and separation (ρ) were measured to be 51.79° ± 0.01° and 28.32" ± 0.006", respectively, and were calculated from a series of twenty images. The mean values obtained, along with historical measurements from the United States Naval Observatory (USNO) and astrometric data collected by the European Space Agency's (ESA) Gaia satellite, substantiate the claim that the system is likely an optical double system.

Introduction

In observational astronomy, a double star system is a system of two or more stars which visually appear near each other in the sky (Genet 2015). As Genet explains in the Small Telescope Astronomical Research (STAR) Handbook (2015), these can be classified further as either optical doubles—stars which "appear close to each other in the sky because of their chance alignment along the line-of-sight from Earth"—or physical doubles—stars which are "traveling together as 'common proper motion pairs' or…gravitationally-bound binaries that rotate around a common center of gravity".

This research focused on making astrometric measurements of the double star system WDS 13513-3928 (hereafter HJ 4618), Figure 1. HJ 4618 was chosen for this project because it was listed in the Washington Double Star (WDS) Catalog as a non-physical binary, but showed some signs of possible orbital motion. HJ 4618 also had a body of historical data dating back to John Herschel's initial measurement in 1834, Table 1, and has been observed a total of 10 times—with the last time being in 2010.

The initial criteria laid out for choosing a star system for this project was specified as a right ascension (RA) between 12 and 18 hours, a delta magnitude of no greater than 6, and a separation of no less than 7". HJ 4618 fit our requirements with a RA of 13h 51m 17.77s, a delta magnitude of 2.78, and a separation of 27.4".

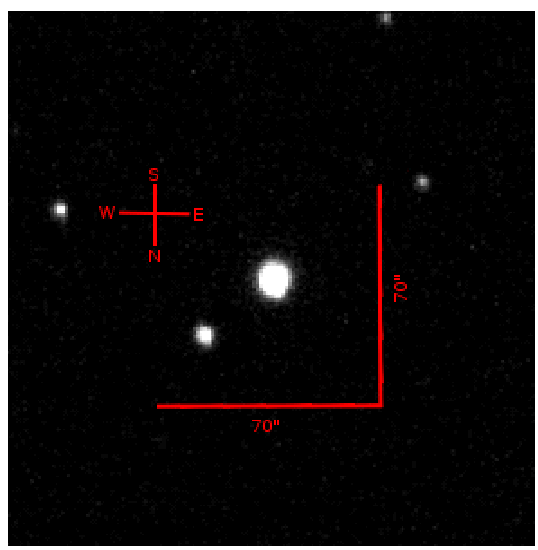

Figure 1. Near infrared CCD image of HJ 4618. ~38 second exposure using a PanSTARRS zs filter.

Table 1: Historical measurements for the double star system HJ 4618 acquired from the United States Naval Observatory.

Epoch	θ	ρ
1834.48	339.6°	12.0"
1907.49	18.5°	16.1"
1913.63	22.5°	17.7"
1920.17	22.5°	17.6"
1929.43	28.9°	18.3"
1959.46	38.5°	21.3"
1998.52	48.1°	25.9"
1999.29	48.4°	26.1"
2004.36	49.0°	26.7"
2010.50	50.1°	27.4"

Equipment and Observations

The observations were made remotely at the Siding Springs Observatory in New South Wales, Australia, on epoch 2018.261. The equipment utilized was a robotically controlled 0.4 meter Meade telescope, Figure 2, mounted with a SBIG STX6303 Charged Coupled Device (CCD). The telescopes were accessed via the Los Cumbres Observatory network online observing portal.

A total of 20 images were ordered using the Pan-STARRS zs (near infrared) filter. The exposure times, Table 2, ranged between 38.277 and 40.297 seconds.

Processing and Analysis

Prior to receiving the images, they were processed in Michael Fitzgerald's Our Solar Siblings (OSS) pipeline. This process consisted of the following:

1. Any compression of the fits file is removed.
2. Files are renamed to something more human-readable. It contains the object name, the filter, the exposure time, the UTC time and date, the air mass, the MJD and the camera (and hence observatory location) the image was taken from.
3. The known bad parts of the image for that camera are marked bad. A database of the bad pixels for each camera in the pipeline access is stored.
4. For a smaller format camera, 20 edge pixels are removed from the image, because many CCD images misbehave around the edges.
5. A lower threshold count value for the image is estimated and pixels below this value are marked bad. Due to the known count distribution for any particular given image, it can be very clearly ascertained what the smallest physically reasonable value in the image should be. Any values below this are marked bad.
6. Cosmic rays are removed as much as possible. The parameters are set quite conservatively such that targets of actual interest are not affected, but even still, about 99% of the cosmic rays do get removed at this step.
7. The bad pixels are interpolated. The bad pixels are interpolated currently using a Gaussian Kernel.
8. Preview TIFs and JPGs are made. This makes it easy for project personnel as well as users to flip through the images quickly to see if any images need to be resubmitted.
9. A new World Coordinate System (WCS) is calculated and implemented. Any existing WCS is removed from the image, as the shape of the image has changed.
10. Adjustments to the fits header are made. A number of different software packages have different quirks that require fits header items to be set a particular way. These changes are made at this point to facilitate easy usage.
11. Images are distributed to users' Google drive accounts. Based on the USERID in the fits header, the final processed images are distributed straight into the user's Google drive account.

Figure 2: Robotically controlled 0.4m Meade telescope at Siding Springs Observatory, NSW, Australia, with SBIG STX6303 CCD camera.

(for more on the OSS pipeline, see Fitzgerald 2018)

After the images were processed in the OSS pipeline, Mira Pro x64 was used to make the astrometric measurements. Mira utilizes an auto-centroiding feature that calculates the centroid based on a user provided sample pixel radius. The distance and angle tool is uti-

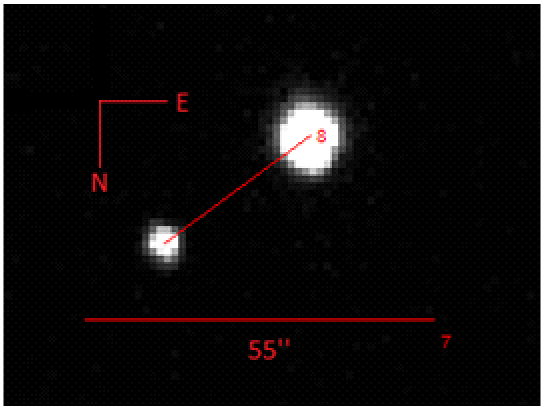

Figure 3. Position angle and separation measurements made with Mira Pro x64.

lized to draw a measurement line between the primary and secondary centroids of each image, Figure 3, and a table of all 20 measurements was exported into an Excel spreadsheet, Table 2.

Results

The mean, standard deviation (σ), and standard deviation of the mean (σ/√n) were calculated utilizing the measured θ and ρ values, Table 3. A mean measurement of 51.79° ± 0.01° and 28.32" ± 0.006" was calculated for θ and ρ, respectively.

Discussion

The new measurements, along with the historical data acquired from the USNO, were plotted on a Cartesian xy-plane showing the change in location of the secondary with respect to the primary star, Figure 4. This was done so that any trends or patterns could be observed in the data.

The parallax data collected by the European Space Agency's Gaia satellite (Gaia Collaboration et al., 2016) was also utilized in order to determine the rough distances to each star from Earth, and therefore allowed us to calculate the approximate distance between the primary and secondary stars.

It was found that the primary star had a parallax of 11.72 milli-arcseconds, and the secondary star had a parallax of 2.2559 milli-arcseconds (Gaia Collaboration et al., 2018). By utilizing the small angle approximation, the rough distance to each star from earth in parsecs (pc) can be calculated by

$$\text{Distance (pc)} \approx \frac{R}{\tan\theta} \approx \frac{R}{\theta} \qquad [1]$$

where R is the radius of the earth's orbit around the sun (1 astronomical unit) and θ is the parallax of the star in arcseconds. Using the Gaia parallax data for HJ 4618

Table 2: Table depicting the exposure times, position angle, and separation measurements of HJ 4618.

New Measurements of HJ 4618		
Exposure Time (sec)	**θ (degrees)**	**ρ (arcseconds)**
38.277	51.78	28.36
38.281	51.78	28.35
38.282	51.79	28.32
38.282	51.82	28.30
38.284	51.78	28.32
38.284	51.86	28.33
38.285	51.85	28.28
38.287	51.81	28.29
38.288	51.79	28.34
38.289	51.70	28.37
40.280	51.80	28.31
40.279	51.81	28.32
40.279	51.76	28.29
40.281	51.73	28.34
40.283	51.84	28.29
40.283	51.79	28.33
40.285	51.86	28.30
40.286	51.85	28.35
40.291	51.77	28.35
40.297	51.73	28.35

Table 3: The calculated mean, standard deviation (σ), and standard deviation of the mean (σ/√n) of HJ 4618 using the 20 measurements in Table 2

Statistical Analysis of Measurements		
	θ (degrees)	**ρ (arcseconds)**
Mean	51.79	28.32
σ	0.05	0.03
σ/√n	0.01	0.006

with Equation 1, the approximate distances to the primary and secondary stars were calculated to be 85.3 pc and 443.3 pc, or 278.3 ly and 1445.8 ly, respectively.

We were then able to take the distances calculated above, along with the right ascension and declination, and translate them from an earth-centered spherical coordinate system into a more familiar Cartesian coordinate plane, Figure 5, in R^3.

By translating into a Cartesian coordinate system,

Near Infrared Robotic Observation of Double Star System WDS 13513-3928

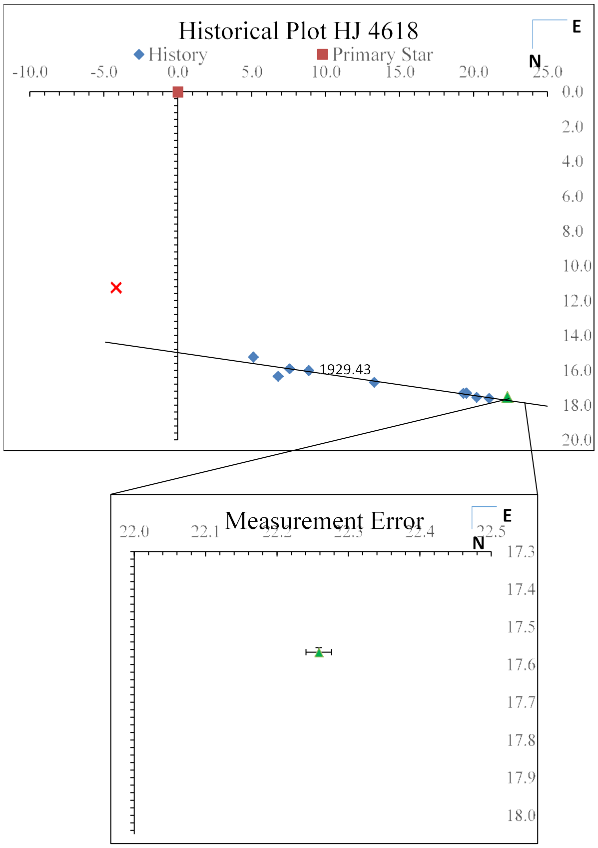

Figure 4: Historical plot showing all of the known measurements to date (upper). This plot shows the relative change in position of the secondary star in relation to the primary star. Please note the Herschel measurement (denoted with a red x) on 1834.48 was regarded as an outlier with respect to the trend line shown here.The exploded plot (lower) shows the error bars on the newest measurement, because the marker hides them in the original plot.

we were then able to utilize the distance formula in order to find the approximate separation between the primary and secondary stars in R^3, Equation 2.

$$\text{Separation (ly)} = \sqrt{(x_2 - x_1)^2 + (y_2 - y_1)^2 + (z_2 - z_1)^2} \quad [2]$$

The approximate separation between the primary and secondary stars was calculated to be 1167.5 light years.

Based on the available data, the authors have concluded that HJ 4618 is likely a visual binary system. This conclusion has been reached utilizing all of the available historical data along with the newest data point we recorded, and the astrometric data provided by the ESA Gaia satellite.

When the Herschel measurement in Figure 4 is regarded as an outlier, the plot shows a continuing linear motion trend between the primary and secondary stars.

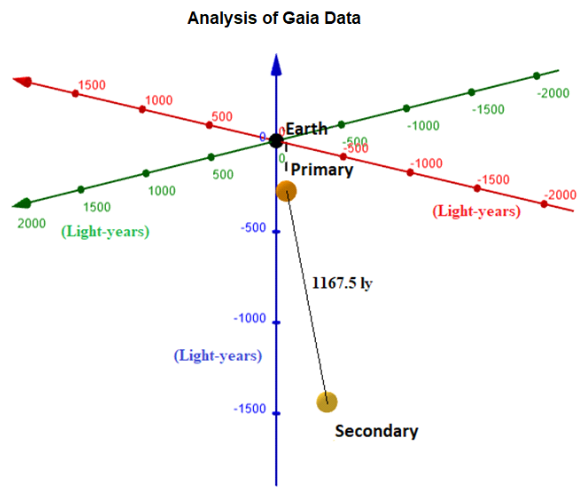

Figure 5: Plot showing the approximate distances between earth and the components of HJ 4618.

Given the successive measurements that lie on or near the linear trend line, the secondary star appears to be moving away from the primary star with no gravitational effects. The data point that we recorded fit this linear trend line very well with minimal deviation.

Given the estimated 1167.5 light year separation of the primary and secondary stars, Figure 5, the authors have determined it is highly unlikely that they are exerting any noticeable gravitational effects on each other. Future research would likely include an examination of the proper motion of these stars in order to determine their velocity toward or away from each other.

Conclusion

On epoch 2018.261, near-infrared images of possible binary star system HJ 4618 were taken at the Siding Springs Observatory in New South Wales, Australia. The calculated θ and ρ values were 51.79° ± 0.01° and 28.32" ± 0.006", respectively.

The authors have concluded, based on the available data, that HJ 4618 is likely a visual binary system, and are not gravitationally influencing each other

Acknowledgements

The authors would like to thank the Boyce Research Initiative and Education Foundation for their support in conducting this research, Alexander Beltzer-Sweeney for his help in finding a suitable system to conduct this research on, the Los Cumbres Observatory who provided the telescope time, and Michael Fitzgerald for the use of the Our Solar Siblings Pipeline.

The authors would also like to thank the Physics

Department at the New Mexico Institute of Mining and Technology for supporting this research.

This work has made use of data from the European Space Agency (ESA) mission Gaia (https://www.cosmos.esa.int/gaia), processed by the Gaia Data Processing and Analysis Consortium (DPAC,https://www.cosmos.esa.int/web/gaia/dpac/consortium). Funding for the DPAC has been provided by national institutions, in particular the institutions participating in the Gaia Multilateral Agreement.

References

Fitzgerald, M., 2018, “The Our Solar Siblings Pipeline: Tackling the data issues of the scaling problem for robotic telescope based astronomy education projects”, in *Robotic Telescopes, Student Research, and Education Proceedings*, Fitzgerald, M. T., James, C. R., Buxner, S., and White, S., ed., pp 347–358.

Gaia Collaboration et al., 2016, “The Gaia Mission”, *Astronomy & Astrophysics*, **595**, A1, 36 pp.

Gaia Collaboration et al., 2018, Gaia Data Release 2: Summary of the contents and survey properties”, *A & A*, **616**, A1, 22 pp.

Genet, R., Johnson, J., Buchheim, R., & Harshaw, R., 2015, *Small Telescope Astronomical Research Handbook,* Collins Foundation Press.

USNO (2018). The Washington Double Star Catalog. Retrieved March 1, 2018, from http://ad.usno.navy.mil/wds/

About the Authors: Stephen, James, and Carson are all undergraduate Physics and Astronomy students at the New Mexico Institute of Mining and Technology in Socorro, New Mexico.

New Binary Systems from Data of Gaia DR2

Filipp Dmitrievich Romanov

Moscow, Russian Federation
filipp.romanov.27.04.1997@gmail.com

Abstract: The author describes the discovery of 4 new pairs of stars with almost identical proper motions and parallaxes (from Gaia DR2 data).

During the search for missed outbursts of cataclysmic variable stars, I found new stars with visible proper motions in images from the Digitized Sky Survey (DSS). I found 4 pairs of stars with almost identical proper motions and parallaxes from the data of Gaia DR2 (Gaia Collaboration et al., 2018). It almost certainly indicates they are gravitationally bound. There is no information about these stars in past issues of the JDSO and in SIMBAD or in the VizieR catalogs of double stars or of stars with high proper motions.

Table 1 (next page) shows the information (names added for abbreviations in this paper, RBS means “Romanov – binary system”) about these stars (from Gaia DR2, sorted by right ascension): id – unique source identifier; RA - barycentric right ascension at Epoch = 2015.5; RA er - error of RA, millisecond of arc (mas); DE - barycentric declination at Epoch = 2015.5; DE er - error of DE, mas; Plx - absolute stellar parallax, mas; Plx er - standard error of parallax, mas; pmR - proper motion in right ascension direction, mas/yr; pmR e - standard error of pmR, mas; pmD - proper motion in declination direction, mas/yr; pmD e - standard error of pmD, mas/yr; G mag - G-band mean magnitude.

RBS 1A - RBS 1B is the closest pair among those mentioned in this paper. Stars RBS 3A and RBS 3B are present in the catalog of white dwarfs (Fusillo et al., 2019) therefore, most likely, they are a binary system of white dwarfs.

References

Gaia Collaboration et al., 2018, *Astronomy & Astrophysics*, **616**, A1.

Gentile Fusillo et al., 2019, *Monthly Notices of the Royal Astronomical Society*, **482**, 4570-4591.

New Binary Systems from Data of Gaia DR2

Table 1. Information about four pairs of stars from Gaia DR2.

Name	RBS 1A	RBS 1B	RBS 2A	RBS 2B	RBS 3B	RBS 3A	RBS 4A	RBS 4B
id	3058016822133524480	3058016822128695296	3048609087110484480	3048609091409752832	6065382021191694848	6065382021191695104	4126306649019342720	4126306649001765760
RA	109.42080407456	109.42105417528	109.74350321881	109.74407846527	204.82866809402	204.83342065405	254.36277171202	254.36346389038
RA er	0.0952	0.2386	0.0347	0.0655	0.1991	0.1885	0.0566	0.0913
DE	-06.77789155663	-06.77783089737	-08.34934877282	-08.34940354930	-54.82734656238	-54.82715314856	-21.68766640292	-21.68656443809
DE er	0.1082	0.2789	0.0379	0.0676	0.2231	0.2123	0.0367	0.0581
Plx	4.9279	5.0536	5.5013	5.4496	13.7966	13.8552	8.8331	8.6609
Plx er	0.1183	0.1714	0.0507	0.0866	0.2485	0.2347	0.0676	0.1065
pmR	-33.825	-33.383	-65.400	-64.764	-7.570	-8.419	-91.116	-91.163
pmR e	0.197	0.470	0.075	0.147	0.493	0.467	0.119	0.190
pmD	-42.465	-42.452	-37.807	-37.800	-92.137	-92.395	-89.127	-90.831
pmD e	0.206	0.498	0.072	0.143	0.544	0.518	0.069	0.107
G mag	16.4721	17.4292	15.3856	16.5317	18.7468	18.6777	15.5139	16.6666

Measurements of 628 Pairs: The 2018 Observing Run at Brilliant Sky Observatory

Richard Harshaw

Brilliant Sky Observatory, Cave Creek, AZ
rharshaw51@cox.net

Abstract: This paper presents measurements of Theta (θ) and Rho (ρ) for 628 double stars listed in the Washington Double Star Catalog (WDS). The measurements were made between November of 2017 and December of 2018.

1. Introduction

This paper presents measurements of 628 double star systems studied between November 2017 and December 2018 at Brilliant Sky Observatory located in Cave Creek, Arizona (a northern suburb of Phoenix, Arizona). The observatory and methodology used in these measurements are well-covered elsewhere in the pages of this journal (for example, references [1] - [3]) Harshaw 2018, Harshaw 2017A, and Harshaw 2017B).

2. Methodology

There are two major types of observation reported: S and CV.

S measurements are done with speckle interferometry. Speckle requires two major conditions: (1) the stars are no farther apart than 5 arc seconds, and (b) the stars are bright enough to both register on the camera in 40 milliseconds or less.

CV measurements were done on stars that did not meet the speckle criteria—that is, they were farther apart than 5 milliarcseconds, or needed more than 40 milliseconds to record both stars on the camera's CCD chip (or both). The CV code is a relatively new code, and it signifies that speckle reduction software was used to analyze the data of a pair that does not fit true speckle criteria. The experience of this author is that using speckle reduction software to analyze double star images is more precise than using traditional CCD image measuring software.

The results will be presented in two tables. Table 1 will report the measurements of 32 pairs with known orbits or rectilinear solutions. Such pairs have published ephemerides which allow the observer to check his or her accuracy and to make residual calculations.

Table 2 will present measurements of 596 pairs which have not yet been classified as having orbits or rectilinear solutions.

At the end of each table is a summary line under the "Change per Year" column. The first row is the sum of all the annual changes while the second row is the mean change. One would expect that for any large collection of double star measurements, changes in theta and rho would tend to lie about a normal distribution, meaning that the cumulative total of the changes for both theta and rho should approach zero. The smaller the mean values are for the annual change in theta and rho, the better the overall accuracy of the measurements being reported. Ideally, both means should be zero, but that will rarely, if ever, be achieved in practice.

3. Acknowledgements

This research has made use of the Washington Double Star Catalog maintained at the U.S. Naval Observatory.

4. References

[1] Harshaw, Richard W. "Measurements of 427 Double Stars With Speckle Interferometry: The Winter/Spring 2017 Observing Program at Brilliant Sky Observatory, Part 1", *JDSO*, **14** (2), 284-330, 2018.

[2] Harshaw, Ricard W., "The Autumn 2016 Observing Program of Brilliant Sky Observatory", *JDSO*, **13** (4), 511-528, 2017.

[3] Harshaw, Richard W., "The Speckle Toolbox: A Powerful Data Reduction Tool for CCD Astrometry", *JDSO*, **13** (1), 52-67, 2017.

Measurements of 628 Pairs: The 2018 Observing Run at Brilliant Sky Observatory

Table 1: Measures of 32 Pairs with Known Orbits or Rectilinear Solutions, with Residuals

Double Star Measures, 2017-2018													
					Last Reported			Measured		Changes from Last		Change per Year	
Date	WDS Number	Discoverer	Observations	Method	Year	θ	ρ	θ	ρ	θ	ρ	θ	ρ
2017.9041	00424+0410	STT 18 AB	5	S	2014	210.2	2.05	211.42 ± 0.0	2.065 ± 0.002	1.22	0.015	0.312	0.004
			Type:	ORB (4)	Solution:	HRT 2001	Ephem:	209.4	2.038		Residuals:	-2.020	-0.027
2018.0356	01030+4723	STT 21	5	S	2015	175.0	1.30	175.2 ± 0.1	1.300 ± 0.002	0.20	0.000	0.066	0.000
			Type:	ORB (5)	Solution:	HEI	Ephem:	175.7	1.143		Residuals:	-0.500	0.157
2018.0329	01055+2107	AG 14	5	S	2010	314.7	0.76	309.0 ± 0.3	0.822 ± 0.004	-5.70	0.062	-0.710	0.008
			Type:	ORB (4)	Solution:	FMR 2014	Ephem:	309.3	0.851		Residuals:	0.300	-0.029
2018.0329	01213+1132	BU 4 AB	5	S	2015	117.0	0.50	113.8 ± 2.3	0.639 ± 0.021	-3.20	0.139	-1.055	0.046
			Type:	ORB (4)	Solution:	SCA 2001	Ephem:	105.8	0.554		Residuals:	8.000	0.085
2017.9945	01424-0645	A 1	5	S	2014	253.9	0.85	254.1 ± 0.0	0.785 ± 0.000	0.20	-0.065	0.050	-0.016
			Type:	ORB	Solution:	TOK 2015	Ephem:	253.5	0.868		Residuals:	0.600	-0.083
2018.0110	01437+0934	BU 509	5	S	2015	44.0	0.80	41.8 ± 0.1	0.782 ± 0.002	-2.20	-0.018	-0.731	-0.006
			Type:	ORB (3)	Solution:	HRT 2010	Ephem:	45.1	0.767		Residuals:	-3.300	0.015
2018.0356	01467+3310	STF 158 AB	5	S	2013	269.0	2.20	271.3 ± 0.0	2.237 ± 0.001	2.30	0.037	0.457	0.007
			Type:	ORB (5)	Solution:	HRT 2011	Ephem:	272.7	2.032		Residuals:	-1.400	0.205
2018.0329	01532+1526	BU 260	5	S	2015	259.0	1.10	260.7 ± 0.1	1.110 ± 0.001	1.70	0.010	0.561	0.003
			Type:	ORB (5)	Solution:	CVE 2006	Ephem:	260.7	1.091		Residuals:	0.000	0.019
2018.0110	01559+0151	STF 186	5	S	2015	71.0	0.70	71.3 ± 0.1	0.726 ± 0.001	0.30	0.026	0.100	0.009
			Type:	ORB (2)	Solution:	USN 2007	Ephem:	70	0.755		Residuals:	1.300	-0.029
2018.0603	02140+4729	STF 228	5	S	2015	300.0	0.60	305.4 ± 0.3	0.636 ± 0.016	5.40	0.036	1.765	0.012
			Type:	ORB (2)	Solution:	SCA 2015	Ephem:	299.6	0.714		Residuals:	5.400	-0.078
2018.0329	02280+0158	KUI 8	5	S	2008	38.8	0.51	38.4 ± 1.4	0.536 ± 0.016	-0.40	0.026	-0.040	0.003
			Type:	ORB (4)	Solution:	ZIR 2013	Ephem:	39.4	0.49		Residuals:	-1.000	0.046

Table 1 continues on the next page.

Measurements of 628 Pairs: The 2018 Observing Run at Brilliant Sky Observatory

Table 1. (continued). Measures of 32 Pairs with Known Orbits or Rectilinear Solutions, with Residuals

Double Star Measures, 2017-2018													
					Last Reported			Measured		Changes from Last		Change per Year	
Date	**WDS Number**	**Discoverer**	**Observations**	**Method**	**Year**	**θ**	**ρ**	**θ**	**ρ**	**θ**	**ρ**	**θ**	**ρ**
2018.0466	02407+2637	STT 43	5	S	2015	338.0	0.60	342.5 ± 0.5	0.646 ± 0.017	4.50	0.046	1.477	0.015
			Type:	ORB (4)	Solution:	SCA 2001	Ephem:	337.9	0.618		Residuals:	4.600	0.028
2018.0110	02460-0457	BU 83	5	S	2015	13.2	0.98	11.8 ± 0.2	1.006 ± 0.002	-1.40	0.026	-0.465	0.009
			Type:	ORB (5)	Solution:	HRT 2011	Ephem:	11.7	0.99		Residuals:	0.100	0.016
2018.0658	02563+7253	STF 312 AB	5	S	2013	47.0	1.80	48.8 ± 0.1	1.800 ± 0.005	1.80	0.000	0.355	0.000
			Type:	ORB (5)	Solution:	CVE 2006	Ephem:	46.9	1.745		Residuals:	1.900	0.055
2018.0329	02572+0153	A 2413	5	S	2015	163.1	0.60	163.3 ± 0.7	0.564 ± 0.014	0.20	-0.036	0.066	-0.012
			Type:	ORB (3)	Solution:	HRT 2010	Ephem:	163.5	0.581		Residuals:	-0.200	-0.017
2018.0466	02589+2137	BU 525	5	S	2015	271.0	0.60	273.7 ± 0.9	0.585 ± 0.006	2.70	-0.015	0.886	-0.005
			Type:	ORB (4)	Solution:	RBR 2018	Ephem:	275.6	0.489		Residuals:	-1.900	0.096
2018.0959	03127+7133	STT 50 AB	10	S	2013	147.0	1.00	144.6 ± 0.0	1.015 ± 0.001	-2.40	0.015	-0.471	0.003
			Type:	ORB (4)	Solution:	SCA 2012	Ephem:	145.4	0.915		Residuals:	-0.800	0.100
2018.0877	03130+4417	STT 51	5	S	2014	340.0	0.70	346.2 ± 0.4	0.552 ± 0.002	6.20	-0.148	1.517	-0.036
			Type:	ORB (5)	Solution:	LIN 2012	Ephem:	345.7	0.582		Residuals:	0.500	-0.030
2018.0466	03140+0044	STF 367	5	S	2012	131.4	1.22	129.2 ± 0.0	1.293 ± 0.000	-2.20	0.073	-0.364	0.012
			Type:	ORB (4)	Solution:	RAO 2014	Ephem:	127.8	1.154		Residuals:	1.400	0.139
2018.0959	03196+6714	HU 1056	10	S	2012	80.7	1.09	79.5 ± 0.1	1.063 ± 0.001	-1.20	-0.027	-0.197	-0.004
			Type:	ORB (5)	Solution:	ZIR 2015	Ephem:	79.8	1.056		Residuals:	-0.300	0.007
2018.0466	03217+0845	STF 380	5	S	2015	6.0	0.90	4.0 ± 0.3	0.888 ± 0.012	-2.00	-0.012	-0.656	-0.004
			Type:	ORB (5)	Solution:	POP 1996	Ephem:	4.4	0.889		Residuals:	-0.400	-0.001
2018.0630	03344+2428	STF 412 AB	15	S	2015	352.0	0.80	352.6 ± 0.5	0.759 ± 0.002	0.60	-0.041	0.196	-0.013
			Type:	ORB (3)	Solution:	SCA 2002	Ephem:	350.8	0.76		Residuals:	1.200	-0.001
2018.0959	03350+6002	STF 400 AB	10	S	2015	267.0	1.60	268.8 ± 0.1	1.634 ± 0.002	1.80	0.034	0.581	0.011
			Type:	ORB (3)	Solution:	USN 2006	Ephem:	268.4	1.612		Residuals:	0.400	0.022
2018.0603	03520+0632	KUI 15 AB	15	S	2012	203.8	0.82	206.2 ± 0.3	0.824 ± 0.001	2.40	0.004	0.396	0.001
			Type:	ORB	Solution:	ZIR 2015	Ephem:	206.6	0.799		Residuals:	-0.600	0.025

Table 1 concludes on the next page.

Table 1. (conclusion). Measures of 32 Pairs with Known Orbits or Rectilinear Solutions, with Residuals

Double Star Measures, 2017-2018													
					Last Reported			Measured		Changes from Last		Change per Year	
Date	WDS Number	Discoverer	Observations	Method	Year	θ	ρ	θ	ρ	θ	ρ	θ	ρ
2018.0877	04041+3931	STF 483	5	S	2015	53.0	1.60	52.6 ± 0.0	1.606 ± 0.001	-0.40	0.006	-0.130	0.002
			Type:	ORB (4)	Solution:	USN 2006	Ephem:	53.7	1.533		Residuals:	-1.100	0.073
2018.0630	04227+1503	STT 82 AB	5	S	2015	328.0	1.20	327.1 ± 0.2	1.222 ± 0.003	-0.90	0.022	-0.294	0.007
			Type:	ORB (3)	Solution:	WSI 2004	Ephem:	328.9	1.19		Residuals:	-1.900	0.032
2018.0630	04233+1123	STF 535	5	S	2013	271.3	1.13	266.9 ± 0.1	1.090 ± 0.001	-4.40	-0.040	-0.869	-0.008
			Type:	ORB (5)	Solution:	HRT 2000	Ephem:	265	1.021		Residuals:	1.000	0.069
2018.0877	04385+2656	STF 572 AB	5	S	2014	188.6	4.35	188.7 ± 0.1	4.393 ± 0.010	0.10	0.043	0.024	0.011
			Type:	LIN	Solution:	HRT 2011	Ephem:	188.6	4.37		Residuals:	0.100	0.023
2018.0877	04422+3731	STF 577	5	S	2014	329.0	0.70	325.7 ± 0.3	0.763 ± 0.002	-3.30	0.063	-0.807	0.015
			Type:	ORB (4)	Solution:	RAO 2014	Ephem:	322.9	0.519		Residuals:	2.800	0.244
2018.2384	08554+7048	STF1280 AB	5	S	2012	353.1	2.67	357.5 ± 0.2	3.419 ± 0.007	4.40	0.749	0.705	0.120
			Type:	ORB (4)	Solution:	HEI 1997	Ephem:	355.8	2.962		Residuals:	1.700	0.457
2018.9233	22226+3328	ES 390	5	CV	2010	267.4	8.50	268.45 ± 0.04	8.404 ± 0.013	1.05	-0.096	0.118	-0.011
			Type:	LIN	Solution:	HRT 2011	Ephem:	268.6	8.241		Residuals:	0.150	-0.163
2018.9233	23133+2205	STF2990 AB	5	S	2010	55.8	2.51	55.95 ± 0.05	2.625 ± 0.002	0.15	0.115	0.017	0.013
			Type:	LIN	Solution:	HRT 2011	Ephem:	55.32	2.557		Residuals:	-0.630	-0.068
											Cumulative:	15.400	1.387
											Mean:	0.481	0.043

Measurements of 628 Pairs: The 2018 Observing Run at Brilliant Sky Observatory

Table 2: Measures of 596 Pairs Without Known Orbits or Rectilinear Solutions

					Last Reported			Measured		Changes from Last		Change per Year	
Date	WDS Number	Discoverer	Observations	Method	Year	θ	ρ	θ	ρ	θ	ρ	θ	ρ
2017.9041	00028+0208	BU 281 AB	5	S	2014	160.3	1.59	159.4 ± 0.1	1.585 ± 0.006	-0.90	-0.005	-0.231	-0.001
2017.9370	00029+2844	MLB 509	3	CV	2002	325.1	3.28	328.89 ± 0.2	3.268 ± 0.013	3.79	-0.012	0.238	-0.001
2017.9205	00065+0155	HJ 1000	3	CV	2005	205.9	7.41	205.2 ± 0.0	7.259 ± 0.007	-0.70	-0.151	-0.054	-0.012
2017.9370	00083+2029	BOW 3	3	CV	2011	47.5	3.28	47.99 ± 0.1	3.336 ± 0.015	0.49	0.056	0.071	0.008
2017.9370	00084+1843	COU 246	3	CV	2008	252.3	1.63	251.63 ± 0.2	1.637 ± 0.007	-0.67	0.007	-0.067	0.001
2017.9041	00137+0635	BU 998	5	S	2006	107.6	1.29	107.73 ± 0.1	1.275 ± 0.003	0.13	-0.015	0.011	-0.001
2017.9205	00162-0359	ROE 115	3	CV	2010	303.0	5.50	301.98 ± 0.0	5.512 ± 0.003	-1.02	0.012	-0.129	0.002
2017.9041	00174+0853	STF 22 AB-C	5	S	2012	235.0	4.00	234.52 ± 0.0	3.942 ± 0.001	-0.48	-0.058	-0.081	-0.010
2017.9370	00174+1002	A 1804	3	CV	2005	27.4	1.34	27.32 ± 0.2	1.233 ± 0.003	-0.08	-0.107	-0.006	-0.008
2017.9205	00199+0317	BAL1607	3	CV	2002	189.4	3.17	189.45 ± 0.5	3.127 ± 0.020	0.05	-0.043	0.003	-0.003
2017.9370	00344+1844	COU 250	3	CV	2005	36.5	1.20	40.44 ± 0.2	1.267 ± 0.001	3.94	0.067	0.305	0.005
2017.9370	00414+1439	KU 6	3	CV	2009	224.9	1.90	226.07 ± 0.2	1.850 ± 0.006	1.17	-0.050	0.131	-0.006
2017.9370	00419+1751	A 2303	3	CV	2001	218.3	1.17	221.23 ± 0.9	1.073 ± 0.050	2.93	-0.097	0.173	-0.006
2017.9205	00486-0146	HDO 35	3	CV	2010	34.1	7.26	34.06 ± 0.0	7.292 ± 0.007	-0.04	0.032	-0.005	0.004
2018.0329	01004+1803	BRT1927	5	S	2013	172.0	2.00	169.6 ± 0.2	1.894 ± 0.005	-2.40	-0.106	-0.477	-0.021
2018.0110	01007+0929	STF 82 AB	5	S	2008	304.0	1.80	304.2 ± 0.0	1.858 ± 0.002	0.20	0.058	0.020	0.006
2018.0356	01070+3014	A 929 AB	5	S	2015	135.0	0.70	127.7 ± 0.2	0.645 ± 0.012	-7.30	-0.055	-2.405	-0.018
2017.9945	01072-0144	STF 91	5	S	2012	314.0	4.30	314.41 ± 0.0	4.321 ± 0.003	0.41	0.021	0.068	0.004
2018.0356	01089+4512	AC 13 AB	5	S	2015	266.0	0.70	264.8 ± 0.3	0.616 ± 0.021	-1.20	-0.084	-0.395	-0.028
2018.0329	01097+2348	BU 303	5	S	2015	293.0	0.70	292.1 ± 0.4	0.551 ± 0.009	-0.90	-0.149	-0.297	-0.049
2018.0466	01099+4011	AG 15	5	S	2012	70.0	2.80	70.0 ± 0.0	2.818 ± 0.001	0.00	0.018	0.000	0.003
2018.0466	01121+4700	BU 236	5	S	2010	113.0	5.40	114.2 ± 0.1	5.362 ± 0.007	1.20	-0.038	0.149	-0.005
2018.0356	01151+3416	HU 803	5	S	2013	209.0	0.90	215.7 ± 0.2	0.932 ± 0.004	6.70	0.032	1.331	0.006
2017.9945	01163-0709	STF 106	5	S	2009	308.0	4.60	306.52 ± 0.0	4.620 ± 0.002	-1.48	0.020	-0.165	0.002

Table 2 continues on the next page.

Table 2 (continued). Measures of 596 Pairs Without Known Orbits or Rectilinear Solutions

					Last Reported			Measured		Changes from Last		Change per Year	
Date	**WDS Number**	**Discoverer**	**Observations**	**Method**	**Year**	**θ**	**ρ**	**θ**	**ρ**	**θ**	**ρ**	**θ**	**ρ**
2018.0466	01119+4748	BU 398	5	S	2008	44.0	1.74	43.6 ± 0.0	1.820 ± 0.000	-0.40	0.080	-0.040	0.008
2017.9945	01198-0031	STF 113 A-BC	5	S	2015	22.0	1.60	20.94 ± 0.1	1.616 ± 0.002	-1.06	0.016	-0.354	0.005
2018.0110	01205+0418	J 1807	3	CV	2008	249.9	3.10	248.6 ± 0.1	3.112 ± 0.008	-1.30	0.012	-0.130	0.001
2018.0329	01208+1813	A 2212	5	S	2015	214.0	1.30	213.5 ± 0.1	1.331 ± 0.003	-0.50	0.031	-0.165	0.010
2018.0329	01255+2832	HO 310	5	S	2013	357.0	1.60	355.9 ± 0.0	1.692 ± 0.008	-1.10	0.092	-0.219	0.018
2018.0110	01291+0347	A 2317	5	S	2009	58.4	1.09	58.9 ± 0.2	1.031 ± 0.008	0.50	-0.059	0.055	-0.007
2018.0329	01321+1218	AG 20	5	S	2015	247.0	2.50	249.1 ± 0.0	2.633 ± 0.010	2.10	0.133	0.692	0.044
2018.0356	01355+3118	STF 137	5	S	2011	85.0	3.30	85.4 ± 0.2	3.385 ± 0.003	0.40	0.085	0.057	0.012
2018.0356	01359+3304	HLD 6	5	S	2009	294.5	2.15	294.6 ± 0.0	2.140 ± 0.001	0.10	-0.010	0.011	-0.001
2018.0110	01360+0739	STF 138 AB	5	S	2015	58.0	1.80	59.7 ± 0.0	1.736 ± 0.001	1.70	-0.064	0.565	-0.021
2018.0329	01391+2656	BU 508 AB	5	S	2015	53.0	0.70	53.2 ± 1.0	0.668 ± 0.016	0.20	-0.032	0.066	-0.011
2018.0356	01401+3858	STF 141	5	S	2013	303.0	1.70	303.2 ± 0.0	1.670 ± 0.002	0.20	-0.030	0.040	-0.006
2018.0110	01443+0929	STF 155 AB	5	S	2012	325.0	5.00	324.7 ± 0.0	4.942 ± 0.001	-0.30	-0.058	-0.050	-0.010
2018.0356	01445+3957	STF 149	5	S	2015	81.0	1.40	81.2 ± 0.1	1.436 ± 0.002	0.20	0.036	0.066	0.012
2018.0110	01479-0057	BU 871	5	S	2008	349.1	1.93	346.6 ± 0.0	2.089 ± 0.002	-2.50	0.159	-0.250	0.016
2018.0329	01492+2815	A 2009	5	S	2009	321.9	0.86	321.4 ± 0.0	0.893 ± 0.005	-0.50	0.033	-0.055	0.004
2018.0329	01501+2217	STF 174	5	S	2015	163.0	2.80	163.9 ± 0.1	2.909 ± 0.003	0.90	0.109	0.297	0.036
2018.0329	01520+1049	STF 178	5	S	2013	205.0	3.00	205.1 ± 0.1	3.049 ± 0.005	0.10	0.049	0.020	0.010
2018.0356	01532+3719	STF 179	5	S	2007	160.0	3.50	160.4 ± 0.0	3.511 ± 0.003	0.40	0.011	0.036	0.001
2018.0329	01551+2847	STF 183 AB-C	5	S	2011	162.6	5.64	161.8 ± 0.1	5.635 ± 0.002	-0.80	-0.005	-0.114	-0.001
2018.0356	01557+3620	HU 1033	5	S	2015	215.0	1.30	216.2 ± 0.0	1.229 ± 0.001	1.20	-0.071	0.395	-0.023
2018.0356	01579+3310	A 1920	5	S	2011	233.3	1.71	236.2 ± 0.3	1.776 ± 0.015	2.90	0.066	0.412	0.009
2017.9945	01579-1158	HU 13	5	S	2001	111.4	1.00	114.06 ± 0.0	1.035 ± 0.003	2.66	0.035	0.157	0.002
2018.0329	01593+2450	STF 194	5	S	2013	280.0	1.20	278.9 ± 0.0	1.295 ± 0.001	-1.10	0.095	-0.219	0.019
2018.0603	02002+4427	STF 195	15	S	2008	194.3	3.02	194.6 ± 0.0	3.012 ± 0.001	0.30	-0.008	0.030	-0.001
2018.0877	02045+4750	WFC 7	5	CV	2010	122.0	5.20	120.4 ± 0.0	5.318 ± 0.018	-1.60	0.118	-0.198	0.015

Table 2 continues on the next page.

Measurements of 628 Pairs: The 2018 Observing Run at Brilliant Sky Observatory

Table 2 (continued). Measures of 596 Pairs Without Known Orbits or Rectilinear Solutions

					Last Reported			Measured		Changes from Last		Change per Year	
Date	WDS Number	Discoverer	Observations	Method	Year	θ	ρ	θ	ρ	θ	ρ	θ	ρ
2018.0110	02052-0058	BU 516	5	S	2015	316.0	0.60	317.4 ± 0.3	0.699 ± 0.004	1.40	0.099	0.465	0.033
2018.0110	02070-0413	HDS 283	5	S	2010	267.8	0.91	263.5 ± 0.3	0.871 ± 0.025	-4.30	-0.039	-0.537	-0.005
2018.0466	02140+3431	STF 229	5	S	2013	356.0	2.40	356.1 ± 0.0	2.490 ± 0.001	0.10	0.090	0.020	0.018
2018.0356	02174+2353	STF 240	5	S	2013	53.0	4.80	52.1 ± 0.0	4.786 ± 0.001	-0.90	-0.014	-0.179	-0.003
2018.0356	02176+2214	STF 244	5	S	2013	290.0	4.30	289.7 ± 0.0	4.415 ± 0.005	-0.30	0.115	-0.060	0.023
2018.0356	02211+2956	A 962	5	S	2013	67.0	0.90	66.7 ± 0.0	0.876 ± 0.001	-0.30	-0.024	-0.060	-0.005
2018.0466	02213+3726	STF 250	5	S	2009	136.0	3.20	136.4 ± 0.0	3.159 ± 0.002	0.40	-0.041	0.044	-0.005
2018.0603	02213+4436	STF 249	5	S	2006	195.2	2.43	197.2 ± 0.0	2.429 ± 0.002	2.00	-0.001	0.166	0.000
2018.0466	02217+3923	STF 251	5	S	2008	265.0	2.10	266.3 ± 0.1	2.217 ± 0.001	1.30	0.117	0.129	0.012
2018.0466	02218+3830	STT 40	5	S	2014	53.0	0.80	46.0 ± 0.1	0.655 ± 0.009	-7.00	-0.145	-1.730	-0.036
2018.0658	02231+5233	HU 536	10	S	2015	320.0	0.70	322.3 ± 0.7	0.627 ± 0.018	2.30	-0.073	0.750	-0.024
2018.0603	02261+4914	HU 537	15	S	2010	21.2	2.15	21.7 ± 0.0	2.152 ± 0.001	0.50	0.002	0.062	0.000
2018.0466	02270+3117	HO 216	5	S	2013	6.0	1.40	6.3 ± 0.0	1.431 ± 0.000	0.30	0.031	0.059	0.006
2018.0356	02282+2952	STF 269	5	S	2012	345.0	1.70	345.0 ± 0.1	1.677 ± 0.002	0.00	-0.023	0.000	-0.004
2018.0329	02284+1722	A 2330	5	S	2013	207.0	1.20	210.1 ± 0.3	1.211 ± 0.007	3.10	0.011	0.616	0.002
2018.0658	02292+5352	HJ 2136	10	S	2010	38.0	4.70	36.1 ± 0.1	4.655 ± 0.009	-1.90	-0.045	-0.236	-0.006
2018.0658	02292+5637	A 1275	5	S	2015	21.0	0.80	20.6 ± 0.8	0.856 ± 0.011	-0.40	0.056	-0.130	0.018
2018.0658	02294+5532	STF 268	10	S	2012	129.7	2.80	131.2 ± 0.1	2.865 ± 0.007	1.50	0.065	0.247	0.011
2018.0630	02313+4703	A 968	5	S	2009	26.2	1.69	27.1 ± 0.1	1.767 ± 0.004	0.90	0.077	0.099	0.008
2018.0658	02333+5619	A 1276 AB	5	S	2015	203.0	0.90	201.6 ± 0.2	0.939 ± 0.005	-1.40	0.039	-0.457	0.013
2018.0712	02343+4017	AG 42	5	CV	2010	144.0	6.20	143.9 ± 0.1	6.369 ± 0.008	-0.10	0.169	-0.012	0.021
2018.0329	02344+1148	HLD 63	5	S	2013	292.0	1.30	292.3 ± 0.1	1.489 ± 0.011	0.30	0.189	0.060	0.038
2018.0712	02348+4924	ES 458 AB	5	CV	2010	316.2	4.80	316.9 ± 0.4	5.072 ± 0.006	0.70	0.272	0.087	0.034
2018.0712	02366+4921	ES 459	5	CV	2002	142.7	3.42	143.2 ± 0.1	3.441 ± 0.006	0.50	0.021	0.031	0.001
2018.0110	02368-0334	BU 520	5	S	2004	188.3	0.87	189.7 ± 0.3	0.893 ± 0.022	1.40	0.023	0.100	0.002
2018.0712	02376+4839	ES 460 AB	5	CV	2002	318.4	2.88	319.4 ± 0.5	2.910 ± 0.008	1.00	0.030	0.062	0.002

Table 2 continues on the next page.

Measurements of 628 Pairs: The 2018 Observing Run at Brilliant Sky Observatory

Table 2 (continued). Measures of 596 Pairs Without Known Orbits or Rectilinear Solutions

					Last Reported			Measured		Changes from Last		Change per Year	
Date	WDS Number	Discoverer	Observations	Method	Year	θ	ρ	θ	ρ	θ	ρ	θ	ρ
2018.0603	02388+3325	STF 285	15	S	2012	163.0	1.70	161.5 ± 0.1	1.738 ± 0.004	-1.50	0.038	-0.248	0.006
2018.0110	02389-0135	HO 315	5	S	2008	356.9	1.63	354.7 ± 0.2	1.748 ± 0.010	-2.20	0.118	-0.220	0.012
2018.0329	02391+1430	BU 1315 AB	5	S	2006	131.3	1.72	129.6 ± 0.1	1.527 ± 0.005	-1.70	-0.193	-0.141	-0.016
2018.0466	02393+2552	A 2023	5	S	2015	226.0	0.60	228.3 ± 1.0	0.563 ± 0.025	2.30	-0.037	0.755	-0.012
2018.0712	02405+4535	ES 1308	5	CV	2010	276.1	6.93	276.0 ± 0.2	6.908 ± 0.026	-0.10	-0.022	-0.012	-0.003
2018.0658	02405+6129	STF 283 AB	5	S	2007	208.8	1.79	210.3 ± 0.1	1.849 ± 0.006	1.50	0.059	0.136	0.005
2018.0329	02409+0452	STT 45	5	S	2015	263.0	0.80	256.8 ± 0.5	0.829 ± 0.004	-6.20	0.029	-2.044	0.010
2018.0712	02412+4241	HJ 2154	5	CV	2010	140.2	9.99	140.4 ± 0.0	9.980 ± 0.006	0.20	-0.010	0.025	-0.001
2018.0466	02446+2928	STF 300	5	S	2012	314.3	3.09	316.1 ± 0.1	3.170 ± 0.005	1.80	0.080	0.298	0.013
2018.0658	02470+5007	ARG 9	10	S	2006	149.9	2.60	151.0 ± 0.1	2.564 ± 0.002	1.10	-0.036	0.091	-0.003
2018.0603	02478+3103	BU 262	5	S	2009	51.7	1.71	50.0 ± 0.0	1.722 ± 0.000	-1.70	0.012	-0.188	0.001
2018.0712	02506+4904	ES 1135	5	CV	2004	41.5	4.48	41.2 ± 0.1	4.532 ± 0.015	-0.30	0.052	-0.021	0.004
2018.0658	02511+6025	STF 306 AB	5	S	2008	92.6	2.15	92.9 ± 0.0	2.199 ± 0.001	0.30	0.049	0.030	0.005
2018.0658	02529+5300	STF 314 AB-C	10	S	2015	317.0	1.60	315.8 ± 0.1	1.608 ± 0.004	-1.20	0.008	-0.391	0.003
2018.0712	02548+4244	BRT 334	5	CV	2002	251.8	3.48	251.9 ± 0.7	3.637 ± 0.027	0.10	0.157	0.006	0.010
2018.0658	02581+6912	STF 317	5	S	2012	84.0	4.07	83.4 ± 0.0	4.137 ± 0.008	-0.60	0.067	-0.099	0.011
2018.0712	02593+4502	ES 1363	5	CV	2011	205.9	5.59	206.6 ± 0.0	5.834 ± 0.008	0.70	0.244	0.099	0.035
2018.0329	02594+0639	STF 334	5	S	2015	307.0	1.10	307.3 ± 0.0	1.112 ± 0.000	0.30	0.012	0.099	0.004
2018.0712	02595+4110	ES 1510	5	CV	2011	144.2	4.81	144.1 ± 0.2	4.897 ± 0.012	-0.10	0.087	-0.014	0.012
2018.0959	03034+6051	KR 17	10	S	2011	219.2	3.09	219.3 ± 0.1	3.113 ± 0.002	0.10	0.023	0.014	0.003
2018.0904	03061+5303	ARG 10	10	S	2015	265.0	3.90	264.2 ± 0.0	4.053 ± 0.003	-0.80	0.153	-0.259	0.050
2018.0877	03072+4306	A 1702 AB	5	S	2011	230.6	4.28	230.5 ± 0.0	4.359 ± 0.003	-0.10	0.079	-0.014	0.011
2018.0877	03150+3543	HO 502	5	S	2014	14.0	0.80	15.3 ± 0.9	0.843 ± 0.014	1.30	0.043	0.318	0.011
2018.0904	03158+5057	HU 544	10	S	2008	102.2	1.60	102.5 ± 0.1	1.674 ± 0.002	0.30	0.074	0.030	0.007
2018.0630	03163+1920	A 2244	5	S	2015	332.0	0.90	331.0 ± 0.1	0.790 ± 0.001	-1.00	-0.110	-0.326	-0.036
2018.0877	03182+4915	HU 545	5	S	2009	81.3	3.52	81.7 ± 0.0	3.617 ± 0.001	0.40	0.097	0.044	0.011

Table 2 continues on the next page.

Table 2 (continued). Measures of 596 Pairs Without Known Orbits or Rectilinear Solutions

					Last Reported			Measured		Changes from Last		Change per Year	
Date	WDS Number	Discoverer	Observations	Method	Year	θ	ρ	θ	ρ	θ	ρ	θ	ρ
2018.0630	03206+1911	STF 377 AB	5	S	2015	110.0	1.10	110.3 ± 0.2	1.119 ± 0.005	0.30	0.019	0.098	0.006
2018.0959	03218+6830	STF 368 AB	10	S	2015	172.0	1.70	158.7 ± 0.0	2.042 ± 0.001	-13.30	0.342	-4.296	0.110
2018.0630	03233+2058	STF 381	5	S	2015	108.0	1.00	108.7 ± 0.1	1.090 ± 0.002	0.70	0.090	0.229	0.029
2018.0877	03250+4013	HU 1058	5	S	2015	111.0	0.80	114.1 ± 0.0	0.863 ± 0.001	3.10	0.063	1.004	0.020
2018.0904	03260+4536	HO 322	10	S	2008	124.7	1.86	125.6 ± 0.1	1.887 ± 0.004	0.90	0.027	0.089	0.003
2018.0630	03261+2015	A 2344 AB	5	S	2015	195.0	1.20	193.0 ± 0.3	1.166 ± 0.027	-2.00	-0.034	-0.653	-0.011
2018.0959	03280+5511	STF 386	10	S	2011	59.0	2.67	59.3 ± 0.0	2.711 ± 0.003	0.30	0.041	0.042	0.006
2018.0959	03285+5954	STF 384 AB	10	S	2012	272.0	2.00	272.5 ± 0.1	1.974 ± 0.005	0.50	-0.026	0.082	-0.004
2018.0630	03286+2904	STF 395	5	S	2015	89.0	1.80	89.8 ± 0.0	1.790 ± 0.001	0.80	-0.010	0.261	-0.003
2018.0959	03287+5026	STF 388	10	S	2007	213.5	2.76	214.3 ± 0.0	2.753 ± 0.002	0.80	-0.007	0.072	-0.001
2018.0904	03293+4503	STF 391	10	S	2007	96.0	4.00	95.9 ± 0.0	3.944 ± 0.005	-0.10	-0.056	-0.009	-0.005
2018.0959	03302+5922	STF 389 AB	10	S	2012	71.1	2.67	71.5 ± 0.0	2.625 ± 0.003	0.40	-0.045	0.066	-0.007
2018.0904	03306+4947	HLD 8	10	S	2009	176.6	2.31	176.7 ± 0.1	2.356 ± 0.001	0.10	0.046	0.011	0.005
2018.0466	03307-0416	STF 408	5	S	2008	322.9	1.18	319.0 ± 0.4	1.096 ± 0.000	-3.90	-0.084	-0.388	-0.008
2018.0466	03318+0749	A 1931	5	S	2014	56.0	0.80	47.3 ± 1.3	0.801 ± 0.025	-8.70	0.001	-2.150	0.000
2018.0630	03332+2817	HO 14	5	S	2009	25.9	2.15	25.8 ± 0.3	2.164 ± 0.019	-0.10	0.014	-0.011	0.002
2018.0603	03355+0625	A 1933	15	S	2015	136.0	1.10	136.8 ± 0.0	1.255 ± 0.003	0.80	0.155	0.261	0.051
2018.0603	03372+0121	A 2419	5	S	2015	99.0	0.80	98.4 ± 0.0	0.802 ± 0.001	-0.60	0.002	-0.196	0.001
2018.0904	03377+4807	HLD 9 AB	10	S	2016	54.0	1.30	54.9 ± 0.0	1.329 ± 0.001	0.90	0.029	0.431	0.014
2018.0466	03379-0739	BU 308	5	S	2006	323.9	1.82	324.3 ± 0.7	1.864 ± 0.012	0.40	0.044	0.033	0.004
2018.0959	03427+6950	STF 419 AB	10	S	2010	72.2	2.99	73.1 ± 0.1	2.907 ± 0.002	0.90	-0.083	0.111	-0.010
2018.0877	03435+2244	STF 438 AB	5	S	2012	242.5	1.74	241.9 ± 0.1	1.698 ± 0.004	-0.60	-0.042	-0.099	-0.007
2018.0904	03454+4952	HU 103 AB	10	S	2014	202.0	1.10	201.6 ± 0.0	1.179 ± 0.001	-0.40	0.079	-0.098	0.019
2018.0877	03466+2728	COU 694	5	S	2012	134.0	2.51	135.7 ± 0.1	2.539 ± 0.003	1.70	0.029	0.279	0.005
2018.0630	03490+1459	HO 324	5	S	2013	330.0	1.20	328.2 ± 0.4	1.155 ± 0.019	-1.80	-0.045	-0.356	-0.009
2018.0877	03491+3216	STT 516	5	S	2010	43.4	2.22	44.3 ± 0.1	2.205 ± 0.006	0.90	-0.015	0.111	-0.002

Table 2 continues on the next page.

Table 2 (continued). Measures of 596 Pairs Without Known Orbits or Rectilinear Solutions

					Last Reported			Measured		Changes from Last		Change per Year	
Date	WDS Number	Discoverer	Observations	Method	Year	θ	ρ	θ	ρ	θ	ρ	θ	ρ
2018.0877	03503+2241	STF 457 AB	5	S	2013	91.0	0.90	90.9 ± 0.2	0.722 ± 0.015	-0.10	-0.178	-0.020	-0.035
2018.0959	03507+6007	STF 445	10	S	2010	258.5	3.05	259.2 ± 0.0	3.107 ± 0.001	0.70	0.057	0.086	0.007
2018.0904	03521+4048	STT 66	10	S	2015	145.0	1.00	145.7 ± 0.2	1.012 ± 0.001	0.70	0.012	0.227	0.004
2018.0959	03556+5216	BU 743	10	S	2014	261.0	1.10	261.0 ± 0.1	1.085 ± 0.001	0.00	-0.015	0.000	-0.004
2018.0877	03565+3311	BU 263	5	S	2007	105.1	0.69	110.0 ± 0.2	0.706 ± 0.001	4.90	0.020	0.442	0.002
2018.0904	04020+4151	STF 477	10	S	2012	211.3	3.07	212.0 ± 0.0	3.088 ± 0.004	0.70	0.018	0.115	0.003
2018.0877	04038+2549	COU 562	5	S	2008	337.5	1.85	339.8 ± 0.7	1.881 ± 0.004	2.30	0.031	0.228	0.003
2018.0904	04045+5544	STF 480	10	S	2012	326.5	3.29	327.0 ± 0.1	3.375 ± 0.003	0.50	0.085	0.082	0.014
2018.0877	04089+2306	STF 494	5	S	2015	187.0	5.20	188.1 ± 0.0	5.289 ± 0.002	1.10	0.089	0.356	0.029
2018.0904	04092+4010	STF3114	10	S	2013	158.0	3.10	157.1 ± 0.0	3.114 ± 0.001	-0.90	0.014	-0.177	0.003
2018.0904	04115+4152	BU 546	10	S	2015	229.0	0.90	230.0 ± 0.1	0.980 ± 0.004	1.00	0.080	0.324	0.026
2018.0904	04116+4016	STF 500	10	S	2011	79.4	3.84	78.7 ± 0.1	3.954 ± 0.001	-0.70	0.114	-0.099	0.016
2018.0904	04158+4524	STF 512	10	S	2010	220.0	5.20	217.8 ± 0.0	5.294 ± 0.005	-2.20	0.094	-0.272	0.012
2018.0877	04182+2248	STF 520	5	S	2015	81.0	0.70	80.9 ± 0.2	0.705 ± 0.001	-0.10	0.005	-0.032	0.002
2018.0959	04315+6232	HU 1079	10	S	2006	160.3	0.64	160.2 ± 0.5	0.664 ± 0.003	-0.10	0.024	-0.008	0.002
2018.0630	04335+1801	STF 559	15	S	2014	277.2	3.11	277.0 ± 0.1	3.103 ± 0.004	-0.20	-0.007	-0.049	-0.002
2018.0630	04367+1930	STF 567	5	S	2015	344.0	2.10	344.9 ± 0.1	2.046 ± 0.008	0.90	-0.054	0.294	-0.018
2018.0904	04381+4207	STF 565 AB	10	S	2016	166.0	1.30	166.7 ± 0.1	1.375 ± 0.003	0.70	0.075	0.335	0.036
2018.0904	04401+4220	WEI 4	10	S	2009	111.0	2.59	110.2 ± 0.2	2.634 ± 0.005	-0.80	0.044	-0.088	0.005
2018.0959	04551+6104	HU 1088	10	S	2003	157.7	2.62	158.4 ± 0.1	2.757 ± 0.001	0.70	0.137	0.046	0.009
2018.0904	04567+3917	HU 1091	10	S	2015	36.0	0.80	37.6 ± 0.3	0.908 ± 0.001	1.60	0.108	0.518	0.035
2018.0630	04583+1357	STF 620	15	S	2012	238.0	4.00	238.1 ± 0.1	4.413 ± 0.009	0.10	0.413	0.016	0.068
2018.2685	07001-1200	HU 111	5	S	2013	16.8	2.94	17.9 ± 0.0	2.990 ± 0.002	1.10	0.050	0.209	0.009
2018.2685	07018-1053	BU 573	5	S	1997	300.5	0.79	311.0 ± 0.7	0.820 ± 0.004	10.50	0.030	0.494	0.001
2018.2685	07046-1131	STF1016	5	S	2003	149.2	5.35	150.0 ± 0.1	5.372 ± 0.004	0.80	0.022	0.052	0.001
2018.2685	08001-0937	J 2862	3	CV	2000	58.9	2.54	61.1 ± 0.2	2.413 ± 0.006	2.20	-0.127	0.120	-0.007

Table 2 continues on the next page.

Table 2 (continued). Measures of 596 Pairs Without Known Orbits or Rectilinear Solutions

					Last Reported			Measured		Changes from Last		Change per Year	
Date	WDS Number	Discoverer	Observations	Method	Year	θ	ρ	θ	ρ	θ	ρ	θ	ρ
2018.2959	08049-0819	A 1582	5	S	2010	227.4	1.46	229.1 ± 0.2	1.474 ± 0.011	1.70	0.014	0.205	0.002
2018.2959	08059-0146	AG 148	5	CV	2010	178.0	6.60	176.1 ± 0.0	6.839 ± 0.006	-1.90	0.239	-0.229	0.029
2018.2959	08136-0159	HJ 1778	5	S	2002	138.2	4.84	138.8 ± 0.1	4.862 ± 0.008	0.60	0.022	0.037	0.001
2018.2685	08174-1125	BRT2708	3	CV	2005	116.4	4.70	116.3 ± 0.3	4.606 ± 0.008	-0.10	-0.094	-0.008	-0.007
2018.2685	08226-1041	HJ 784 AC	3	CV	2000	10.4	18.03	12.6 ± 0.0	17.862 ± 0.008	2.20	-0.168	0.120	-0.009
2018.2685	08226-1041	HU 116 AB	3	CV	1991	170.1	1.94	167.9 ± 0.5	1.765 ± 0.049	-2.20	-0.175	-0.081	-0.006
2018.2959	08244-0431	A 3059 AB	5	S	2005	137.2	3.57	136.7 ± 0.3	3.536 ± 0.007	-0.50	-0.034	-0.038	-0.003
2018.3151	08255-0207	A 1336	5	CV	2010	211.0	5.40	206.5 ± 0.0	5.670 ± 0.000	-4.50	0.270	-0.541	0.032
2018.3151	08287-0018	BAL1137	5	CV	2005	191.5	5.47	189.4 ± 0.0	5.720 ± 0.000	-2.10	0.250	-0.158	0.019
2018.2685	08298-1015	HJ 789	3	CV	2004	47.9	10.20	47.7 ± 0.1	10.232 ± 0.004	-0.20	0.032	-0.014	0.002
2018.3151	08423-0824	STF1264	5	CV	2004	269.0	6.41	268.7 ± 0.0	6.400 ± 0.010	-0.30	-0.010	-0.021	-0.001
2018.2384	08514+5732	STF1275 AB	5	S	2012	197.9	1.87	198.6 ± 0.1	1.883 5 0.002	0.70	0.013	0.112	0.002
2018.2384	08519+6308	KR 32	5	S	2005	13.6	4.80	15.1 ± 0.0	4.945 ± 0.006	1.50	0.145	0.113	0.011
2018.2384	08554+6414	STI 684	5	S	2003	214.2	8.00	214.5 ± 0.0	8.058 ± 0.011	0.30	0.058	0.020	0.004
2018.2384	08590+6326	BU 408	5	S	2001	343.2	2.95	344.9 ± 0.1	2.777 ± 0.005	1.70	-0.173	0.099	-0.010
2018.2959	09013+4843	ES 1083	5	CV	2010	335.0	6.20	336.4 ± 0.0	6.338 ± 0.003	1.40	0.138	0.169	0.017
2018.2685	09015-0816	BRT 546	3	CV	2000	138.3	2.81	139.9 ± 0.1	2.683 ± 0.003	1.60	-0.127	0.088	-0.007
2018.3205	09043+0511	ALD 85	5	CV	2009	37.7	2.58	36.2 ± 0.0	2.660 ± 0.001	-1.50	0.080	-0.161	0.009
2018.3205	09057+3227	AG 161	5	CV	2009	224.0	4.40	224.6 ± 0.04	4.340 ± 0.002	0.60	-0.060	0.064	-0.006
2018.2685	09072-0357	A 342	3	CV	2010	151.4	5.50	151.9 ± 0.0	5.603 ± 0.006	0.50	0.103	0.060	0.012
2018.3205	09077+6459	STF1303	5	CV	2012	282.0	2.70	282.2 ± 0.0	2.800 ± 0.007	0.20	0.100	0.032	0.016
2018.2685	09078-0013	SCJ 12	3	CV	2012	261.0	6.60	261.8 ± 0.0	6.610 ± 0.003	0.80	0.010	0.128	0.002
2018.2959	09081+4510	HJ 1164 AB	5	CV	2010	174.0	6.20	173.1 ± 0.0	6.084 ± 0.003	-0.90	-0.116	-0.108	-0.014
2018.3205	09082+2353	POU3029	5	CV	2009	316.0	7.90	315.4 ± 0.0	8.120 ± 0.002	-0.60	0.220	-0.064	0.024
2018.3205	09129+2420	BRT 155 AB	5	CV	2011	269.8	4.37	269.8 ± 0.0	4.550 ± 0.003	0.00	0.180	0.000	0.025
2018.3151	09136+4659	STF1318	5	S	2013	228.0	2.60	227.7 ± 0.2	2.440 ± 0.010	-0.30	-0.160	-0.056	-0.030

Table 2 continues on the next page.

Measurements of 628 Pairs: The 2018 Observing Run at Brilliant Sky Observatory

Table 2 (continued). Measures of 596 Pairs Without Known Orbits or Rectilinear Solutions

					Last Reported			Measured		Changes from Last		Change per Year	
Date	WDS Number	Discoverer	Observations	Method	Year	θ	ρ	θ	ρ	θ	ρ	θ	ρ
2018.2685	09147-0212	BAL 517	3	CV	2007	51.0	5.03	50.4 ± 0.1	4.848 ± 0.010	-0.60	-0.182	-0.053	-0.016
2018.2685	09167-0941	HDO 122	3	CV	2011	92.4	8.84	92.9 ± 0.1	8.913 ± 0.038	0.50	0.073	0.069	0.010
2018.3151	09225+4933	STF1340 AB	5	CV	2012	321.0	6.30	319.0 ± 0.0	6.280 ± 0.010	-2.00	-0.020	-0.317	-0.003
2018.3205	09229-0753	BRT 428	5	CV	2010	190.0	4.20	191.1 ± 0.0	4.340 ± 0.002	1.10	0.140	0.132	0.017
2018.3205	09238+3825	AG 164	5	CV	2004	18.0	4.50	18.7 ± 0.0	4.610 ± 0.003	0.70	0.110	0.049	0.008
2018.3205	09424-0750	BRT 547	5	CV	2009	222.1	3.94	223.9 ± 0.1	3.930 ± 0.003	1.80	-0.010	0.193	-0.001
2018.3205	09505+0337	J 83	5	CV	2001	237.6	2.20	238.1 ± 0.1	2.140 ± 0.004	0.50	-0.060	0.029	-0.003
2018.4027	09514+7436	STF1378	5	CV	2011	357.5	5.19	357.2 ± 0.0	5.249 ± 0.002	-0.30	0.059	-0.041	0.008
2018.3205	09562+0328	J 426	5	CV	2012	208.0	3.41	207.3 ± 0.1	3.450 ± 0.002	-0.70	0.040	-0.111	0.006
2018.3205	09564+1040	STF1396 AB	5	CV	2009	129.5	3.95	129.7 ± 0.1	3.890 ± 0.004	0.20	-0.060	0.021	-0.006
2018.2959	10220+4354	STF1427	5	CV	2012	214.0	9.00	214.1 ± 0.0	9.355 ± 0.004	0.10	0.355	0.016	0.056
2018.4027	10429+4641	STF1463	5	CV	2007	258.0	7.90	258.0 ± 0.0	7.943 ± 0.001	0.00	0.043	0.000	0.004
2018.4027	10473+5815	MLB 167	5	CV	2011	322.0	5.60	322.0 ± 0.0	5.527 ± 0.006	0.00	-0.073	0.000	-0.010
2018.4027	10545+4730	STF1483	5	S	2010	243.0	2.30	242.3 ± 0.0	2.345 ± 0.003	-0.70	0.045	-0.083	0.005
2018.3918	11029-1001	RST3726	5	CV	2003	283.0	1.99	283.5 ± 0.5	2.023 ± 0.035	0.50	0.033	0.032	0.002
2018.3918	11029-1001	RST3726	5	CV	2003	283.0	1.99	283.5 ± 0.5	2.023 ± 0.035	0.50	0.033	0.032	0.002
2018.3918	11086-0442	J 1372	5	CV	2011	21.8	8.25	22.0 ± 0.1	8.242 ± 0.002	0.20	-0.008	0.027	-0.001
2018.3918	11086-0442	J 1572	5	CV	2011	21.8	8.25	22.0 ± 0.1	8.242 ± 0.002	0.20	-0.008	0.027	-0.001
2018.3918	11114-0921	STF3068	5	CV	2012	312.6	19.36	312.4 ± 0.0	19.426 ± 0.013	-0.20	0.060	-0.031	0.009
2018.3918	11114-0921	STF3068	5	CV	2012	312.6	19.36	312.4 ± 0.0	19.426 ± 0.013	-0.20	0.066	-0.031	0.010
2018.3918	11246-0156	BAL 536	5	CV	2011	146.8	11.84	145.6 ± 0.0	11.463 ± 0.004	-1.20	-0.380	-0.162	-0.051
2018.3918	11246-0156	BAL 536	5	CV	2011	146.8	11.84	145.6 ± 0.0	11.463 ± 0.004	-1.20	-0.377	-0.162	-0.051
2018.3918	12108+3953	STF1606	5	S	2015	151.0	0.60	143.7 ± 0.8	0.631 ± 0.005	-7.30	0.031	-2.152	0.009
2018.3918	12108+3953	STF1606	5	S	2015	151.0	0.60	143.7 ± 0.8	0.631 ± 0.005	-7.30	0.031	-2.152	0.009
2018.3918	12207+2255	STF1634	5	S	2014	147.0	5.10	147.1 ± 0.0	5.367 ± 0.005	0.10	0.267	0.023	0.061

Table 2 continues on the next page.

Measurements of 628 Pairs: The 2018 Observing Run at Brilliant Sky Observatory

Table 2 (continued). Measures of 596 Pairs Without Known Orbits or Rectilinear Solutions

					Last Reported			Measured		Changes from Last		Change per Year	
Date	WDS Number	Discoverer	Observations	Method	Year	θ	ρ	θ	ρ	θ	ρ	θ	ρ
2018.3918	12207+2255	STF1634	5	S	2014	147.0	5.10	147.1 ± 0.0	5.367 ± 0.005	0.10	0.267	0.023	0.061
2018.4027	14218+4229	A 1618	5	CV	2009	161.5	3.95	161.7 ± 0.0	3.810 ± 0.002	0.20	-0.140	0.021	-0.015
2018.4027	14222+4832	BU 615	5	CV	2000	235.7	2.91	235.1 ± 0.1	2.969 ± 0.002	-0.60	0.059	-0.033	0.003
2018.4027	14319+5758	A 1106	5	CV	2013	28.0	2.27	29.0 ± 0.3	2.224 ± 0.008	1.00	-0.046	0.185	-0.009
2018.4027	14416+5124	STF1871	5	S	2012	312.0	1.80	312.7 ± 0.2	1.858 ± 0.008	0.70	0.058	0.109	0.009
2018.4027	14539+5734	HJ 1261	5	CV	2009	17.0	8.89	16.7 ± 0.0	8.796 ± 0.010	-0.30	-0.094	-0.032	-0.010
2018.4027	14565+5923	STF1898	5	CV	2006	217.9	2.78	217.8 ± 0.1	2.798 ± 0.012	-0.10	0.018	-0.008	0.001
2018.4822	15019+1506	HU 1155	5	CV	2010	15.0	3.90	15.0 ± 0.0	3.964 ± 0.004	0.00	0.064	0.000	0.008
2018.4822	15056+1138	STF1907	5	S	2015	349.0	0.90	347.5 ± 0.2	0.853 ± 0.003	-1.50	-0.047	-0.431	-0.013
2018.4986	15076+5056	ES 774	5	CV	2006	230.5	3.29	230.4 ± 0.0	3.377 ± 0.002	-0.10	0.087	-0.008	0.007
2018.4822	15077+1158	STF1911	5	CV	2015	291.0	2.00	291.5 ± 0.1	1.966 ± 0.004	0.50	-0.034	0.144	-0.010
2018.4986	15187+5334	ES 740	5	CV	2011	39.0	3.42	38.3 ± 0.0	3.451 ± 0.001	-0.70	0.031	-0.093	0.004
2018.4822	15190-0713	HJ 4758	5	CV	2009	78.8	8.93	78.6 ± 0.0	6.015 ± 0.003	-0.20	-2.915	-0.021	-0.307
2018.4822	15227-1654	HU 307	5	CV	1999	2.7	2.94	3.20 ± 0.1	2.981 ± 0.003	0.50	0.041	0.026	0.002
2018.4822	15252+0932	HEI 784	5	CV	2009	275.5	3.95	274.7 ± 0.0	3.923 ± 0.002	-0.80	-0.027	-0.084	-0.003
2018.4986	15261+2128	STF1942	5	CV	2008	91.4	9.62	91.6 ± 0.0	9.737 ± 0.002	0.20	0.117	0.019	0.011
2018.4986	15269+4610	KU 50	5	CV	2002	335.3	2.91	335.9 ± 0.0	2.948 ± 0.002	0.60	0.038	0.036	0.002
2018.4986	15288+2038	HU 150	5	CV	2010	25.6	4.36	26.0 ± 0.0	4.542 ± 0.001	0.40	0.182	0.047	0.021
2018.4986	15347+3446	STF1959	5	CV	2009	244.7	2.11	243.5 ± 0.0	2.155 ± 0.001	-1.20	0.045	-0.126	0.005
2018.4822	15352+1456	LEO 33	5	CV	2015	258.0	1.60	260.7 ± 0.1	1.543 ± 0.005	2.70	-0.057	0.775	-0.016
2018.4822	15370-0041	HJ 1276	5	CV	2009	258.6	5.43	258.1 ± 0.0	5.410 ± 0.004	-0.50	-0.020	-0.053	-0.002
2018.4822	15379+3006	STF1963 AB	5	S	2010	298.0	5.10	298.3 ± 0.0	5.321 ± 0.006	0.30	0.221	0.035	0.026
2018.4986	15448+3534	PRT 5	5	CV	2009	44.0	4.44	44.7 ± 0.0	4.533 ± 0.003	0.70	0.093	0.074	0.010
2018.4822	15501-0311	STF3126 AB	5	CV	2013	278.6	2.29	278.5 ± 0.1	2.309 ± 0.001	-0.10	0.019	-0.018	0.003
2018.4986	15513+2509	STF1981	5	CV	2010	3.5	12.01	3.90 ± 0.0	12.056 ± 0.001	0.40	0.046	0.047	0.005
2018.4822	15521+0528	A 1128	5	CV	2005	349.7	1.57	349.5 ± 0.0	1.552 ± 0.003	-0.20	-0.018	-0.015	-0.001

Table 2 continues on the next page.

Measurements of 628 Pairs: The 2018 Observing Run at Brilliant Sky Observatory

Table 2 (continued). Measures of 596 Pairs Without Known Orbits or Rectilinear Solutions

					Last Reported			Measured		Changes from Last		Change per Year	
Date	WDS Number	Discoverer	Observations	Method	Year	θ	ρ	θ	ρ	θ	ρ	θ	ρ
2018.4986	15568+1229	STF1988	5	CV	2011	249.0	1.90	249.3 ± 0.1	1.808 ± 0.003	0.30	−0.092	0.040	−0.012
2018.4986	15578+1737	BRT2422	5	CV	2010	179.0	4.53	179.0 ± 0.0	4.554 ± 0.002	0.00	0.024	0.000	0.003
2018.7288	17021+0713	STF2113	5	S	2010	116.6	4.88	115.56 ± 0.04	5.230 ± 0.009	−1.04	0.350	−0.119	0.040
2018.7288	17057+0620	HEI 859	5	CV	2010	56.3	3.11	55.07 ± 0.05	3.190 ± 0.005	−1.23	0.080	−0.141	0.009
2018.7288	18004+2112	A 1375	5	CV	2014	92.0	1.80	91.63 ± 0.05	1.817 5 0.003	−0.37	0.017	−0.078	0.004
2018.7288	18009+2633	STF2263	5	CV	2004	160.4	7.41	158.40 ± 0.03	7.707 ± 0.007	−2.00	0.297	−0.136	0.020
2018.7260	18014+0406	BAL2910	5	CV	2002	111.3	3.72	112.36 ± 0.01	4.003 ± 0.001	1.06	0.283	0.063	0.017
2018.7260	18030-0237	A 35	5	S	2005	300.9	1.37	297.23 ± 0.18	1.398 ± 0.006	−3.67	0.028	−0.267	0.002
2018.7260	18033+0745	HEI 867	5	CV	2001	339.2	3.39	337.94 ± 0.03	3.495 ± 0.001	−1.26	0.105	−0.071	0.006
2018.7288	18033+2751	ES 470	5	CV	2011	208.6	8.15	208.48 ± 0.04	8.270 ± 0.013	−0.12	0.120	−0.016	0.016
2018.7233	18056+1242	J 1220	5	CV	2015	129.0	1.50	128.34 ± 0.04	1.548 ± 0.002	−0.66	0.048	−0.177	0.013
2018.7233	18067+1359	AG 358 AB	5	CV	2009	330.2	3.45	330.16 ± 0.24	3.660 ± 0.012	−0.04	0.210	−0.004	0.022
2018.7288	18069+2933	SLE 135	5	CV	2002	126.2	9.30	125.69 ± 0.03	9.676 ± 0.008	−0.51	0.376	−0.030	0.022
2018.8301	18094+3144	A 237 AB	5	CV	2002	102.2	2.32	103.41 ± 0.22	2.214 ± 0.027	1.21	−0.106	0.072	−0.006
2018.7233	18096+1801	BRT2441	5	CV	2003	27.7	4.66	26.37 ± 0.05	4.764 ± 0.015	−1.33	0.104	−0.085	0.007
2018.7260	18146-1113	HLD 142	5	S	1991	253.4	1.17	252.99 ± 0.16	1.270 ± 0.002	−0.41	0.100	−0.015	0.004
2018.7288	18204+2048	WFC 206	5	CV	2011	43.9	9.15	44.63 ± 0.01	9.422 ± 0.003	0.73	0.272	0.094	0.035
2018.8301	18209+3220	ES 347	5	CV	2000	64.9	1.78	64.11 ± 0.20	1.754 ± 0.015	−0.79	−0.026	−0.042	−0.001
2018.7288	18216+2030	HO 430	5	CV	2002	193.6	2.40	194.01 ± 0.02	2.498 ± 0.002	0.41	0.098	0.025	0.006
2018.7342	18234+2327	STF2314	5	S	2013	330.0	2.58	331.03 ± 0.07	2.670 ± 0.008	1.03	0.090	0.180	0.016
2018.7342	18273+2012	TDS 922	5	S	2002	205.4	2.32	206.04 ± 0.08	2.375 ± 0.009	0.64	0.055	0.038	0.003
2018.7342	18276+2423	AG 223	5	S	2002	50.3	2.59	50.91 ± 0.07	2.637 ± 0.005	0.61	0.047	0.036	0.003
2018.7342	18280+2708	ES 475	5	CV	2006	219.8	10.91	222.98 ± 0.02	10.654 ± 0.003	3.18	−0.256	0.250	−0.020
2018.7342	18330+2420	POU3427	5	CV	2011	79.7	6.61	80.65 ± 0.04	6.783 ± 0.003	0.95	0.173	0.123	0.022
2018.7342	18335+2102	COU 204	5	CV	2004	129.4	10.08	130.47 ± 0.04	11.872 ± 0.013	1.07	1.792	0.073	0.122
2018.8301	18375+3112	A 250	5	CV	2003	114.3	2.52	113.81 ± 0.47	2.447 ± 0.053	−0.49	−0.073	−0.031	−0.005

Table 2 continues on the next page.

Table 2 (continued). Measures of 596 Pairs Without Known Orbits or Rectilinear Solutions

					Last Reported			Measured		Changes from Last		Change per Year	
Date	WDS Number	Discoverer	Observations	Method	Year	θ	ρ	θ	ρ	θ	ρ	θ	ρ
2018.7342	18386+2706	HJ 1333	5	S	2012	225.6	2.84	226.36 ± 0.15	2.910 ± 0.004	0.76	0.070	0.113	0.010
2018.7342	18413+2506	SLE 502	5	CV	2010	93.2	5.82	94.48 ± 0.05	6.218 ± 0.007	1.28	0.398	0.147	0.046
2018.7342	18422+2739	STF2371	5	CV	2010	55.0	9.30	55.53 ± 0.02	9.971 ± 0.005	0.53	0.671	0.061	0.077
2018.7342	18425+2537	ROE 7	5	CV	2010	197.4	9.45	198.05 ± 0.04	9.835 ± 0.04	0.65	0.385	0.074	0.044
2018.7342	18455+2815	STF2381	5	S	2008	122.1	8.50	122.45 ± 0.01	8.919 ± 0.005	0.35	0.419	0.033	0.039
2018.7260	18459-1030	STF2373	5	S	2007	336.9	4.44	335.96 ± 0.03	4.259 ± 0.006	-0.94	-0.181	-0.080	-0.015
2017.8383	18472+3125	STF2397	5	S	2011	265.8	3.87	269.28 ± 0.0	3.887 ± 0.001	3.48	0.017	0.509	0.002
2017.8383	18487+3401	HU 936	5	S	2011	97.8	1.83	101.21 ± 0.0	1.844 ± 0.001	3.41	0.014	0.499	0.002
2018.7342	18500+2043	HU 328	5	CV	2003	188.8	4.62	187.38 ± 2.32	4.772 ± 0.004	-1.42	0.152	-0.090	0.010
2017.8383	18576+3209	A 260	5	S	2010	245.8	0.88	246.63 ± 0.6	0.912 ± 0.004	0.83	0.032	0.106	0.004
2017.8383	18584+3625	STF2429	5	S	2006	285.2	5.43	288.63 ± 0.0	5.490 ± 0.003	3.43	0.060	0.290	0.005
2018.7425	19015+2724	AG 370	5	S	2014	341.0	4.00	340.53 ± 0.08	4.114 ± 0.002	-0.47	0.114	-0.099	0.024
2018.7425	19019+2718	ES 479	5	CV	2008	141.5	8.23	141.57 ± 0.01	8.345 ± 0.010	0.07	0.115	0.007	0.011
2018.7370	19023+0652	A 359	5	CV	2002	272.5	2.17	273.73 ± 0.10	2.287 ± 0.003	1.23	0.117	0.073	0.007
2018.7425	19025+2640	BRT 36 AB	5	CV	2011	45.7	4.75	46.77 ± 0.06	4.923 ± 0.008	1.07	0.173	0.138	0.022
2018.7425	19031+2202	BRT2451	5	CV	2003	65.1	4.78	65.14 ± 0.04	4.896 ± 0.002	0.04	0.116	0.003	0.007
2018.7397	19041+1106	AG 371	5	CV	2010	159.5	5.49	159.24 ± 0.03	5.637 ± 0.003	-0.26	0.147	-0.030	0.017
2018.7233	19042+3245	BRD 4	5	S	2009	310.1	2.54	309.71 ± 0.08	2.600 ± 0.002	-0.39	0.060	-0.040	0.006
2018.7753	19050+2904	AG 372 AB	5	CV	2006	184.4	6.14	181.80 ± 0.02	6.029 ± 0.002	-2.60	-0.111	-0.204	-0.009
2018.7342	19077-0421	J 1639	5	CV	2010	337.3	6.58	334.76 ± 2.29	6.744 ± 0.007	-2.54	0.164	-0.291	0.019
2018.7370	19078+0928	J 812	5	CV	2007	120.3	2.42	120.22 ± 0.08	2.436 ± 0.004	-0.08	0.016	-0.007	0.001
2018.8301	19078+3040	STF2465	5	CV	2010	248.6	1.25	249.05 ± 0.33	1.195 ± 0.009	0.45	-0.055	0.051	-0.006
2018.7397	19080+1945	STF2460	5	CV	2005	197.9	9.38	197.80 ± 0.04	9.488 ± 0.012	-0.10	0.108	-0.007	0.008
2018.7397	19082+1448	ROE 125 AB	5	CV	2010	265.2	7.79	265.62 ± 0.03	7.949 ± 0.002	0.42	0.159	0.048	0.018
2018.7370	19102+0841	STF2468	5	CV	2010	257.0	7.70	257.40 ± 0.07	7.765 ± 0.008	0.40	0.065	0.046	0.007
2018.7397	19104+1744	STF2475	5	CV	2007	321.1	6.55	320.86 ± 0.04	6.790 ± 0.009	-0.24	0.240	-0.020	0.020

Table 2 continues on the next page.

Measurements of 628 Pairs: The 2018 Observing Run at Brilliant Sky Observatory

Table 2 (continued). Measures of 596 Pairs Without Known Orbits or Rectilinear Solutions

					Last Reported			Measured		Changes from Last		Change per Year	
Date	WDS Number	Discoverer	Observations	Method	Year	θ	ρ	θ	ρ	θ	ρ	θ	ρ
2018.8301	19106+3701	A 152 AB	5	CV	2008	2.9	2.54	2.900 ± 0.01	2.594 ± 0.002	0.00	0.054	0.000	0.005
2018.7425	19113+2705	AG 373	5	S	2013	327.0	2.80	327.61 ± 0.05	2.991 ± 0.007	0.61	0.191	0.106	0.033
2018.7753	19118+2443	MRG 3	5	CV	2010	144.4	5.25	144.34 ± 0.02	5.428 ± 0.004	-0.06	0.178	-0.007	0.020
2018.7753	19124+2435	HO 445	5	CV	2010	244.0	5.20	242.90 ± 0.02	5.283 ± 0.003	-1.10	0.083	-0.125	0.009
2018.8301	19129+3100	HO 101	5	CV	1999	112.7	2.17	113.37 ± 0.03	2.162 ± 0.001	0.67	-0.008	0.034	0.000
2018.7370	19144+0053	J 1035	5	S	2000	76.3	4.21	73.94 ± 0.32	4.112 ± 0.022	-2.36	-0.098	-0.126	-0.005
2018.7397	19153+1522	J 483	5	CV	2002	216.8	2.67	217.55 ± 0.20	2.731 ± 0.006	0.75	0.061	0.045	0.004
2018.7397	19162+1534	KU 57 AB	5	CV	2010	229.8	9.79	229.82 ± 0.05	10.230 ± 0.006	0.02	0.440	0.002	0.050
2018.7342	19164-0925	A 99 AB	5	CV	2002	63.1	2.31	64.93 ± 0.13	2.397 ± 0.011	1.83	0.087	0.109	0.005
2018.7342	19170-0713	BRT 492	5	CV	2010	188.4	5.43	188.96 ± 0.08	5.421 ± 0.018	0.56	-0.009	0.064	-0.001
2018.7397	19172+1853	HU 336	5	CV	2008	190.7	1.50	191.43 ± 0.16	1.581 ± 0.008	0.73	0.081	0.068	0.008
2018.7370	19184+0654	BRT2181	5	CV	2011	178.3	3.65	177.31 ± 0.13	3.826 ± 0.011	-0.99	0.176	-0.128	0.023
2018.7753	19186+2038	WFC 219	5	CV	2010	70.0	8.60	70.71 ± 0.02	8.763 ± 0.001	0.71	0.163	0.081	0.019
2018.7370	19188+0451	BAL2938	5	CV	2011	91.6	9.89	91.03 ± 0.02	9.892 ± 0.016	-0.57	0.002	-0.074	0.000
2018.7397	19192+1540	A 1646	5	S	2003	205.5	4.31	205.40 ± 0.05	4.496 ± 0.006	-0.10	0.186	-0.006	0.012
2018.7370	19203+0056	BAL1202	5	CV	2004	20.1	8.39	19.69 ± 0.08	8.478 ± 0.013	-0.41	0.088	-0.028	0.006
2018.7370	19213+0404	BAL2509	5	CV	2000	212.7	9.57	212.60 ± 0.04	9.723 ± 0.017	-0.10	0.153	-0.005	0.008
2018.7342	19215-0807	J 2265	5	CV	1999	279.6	3.27	278.44 ± 0.11	3.494 ± 0.015	-1.16	0.224	-0.059	0.011
2018.7370	19217+0014	BAL1203	5	CV	2002	127.4	8.76	125.86 ± 0.04	9.365 ± 0.011	-1.54	0.605	-0.092	0.036
2018.7342	19218-0122	J 116	5	CV	2013	142.0	5.70	143.22 ± 0.07	5.992 ± 0.002	1.22	0.292	0.213	0.051
2018.7370	19233+0931	STF2510 A-BC	5	CV	2010	181.2	8.71	180.95 ± 0.04	8.978 ± 0.006	-0.25	0.268	-0.029	0.031
2018.7233	19236-0424	A 103	5	S	2000	4.3	3.36	3.11 ± 0.06	3.489 ± 0.020	-1.19	0.129	-0.064	0.007
2018.7753	19237+2746	AG 378	5	CV	2004	45.0	8.39	45.19 ± 0.05	8.776 ± 0.007	0.19	0.386	0.013	0.026
2018.7233	19251+2150	STF3111	5	CV	2009	117.2	2.50	155.21 ± 0.04	2.560 ± 0.001	38.01	0.060	3.909	0.006
2018.7397	19265+1839	BOW 7	5	CV	2008	250.6	9.38	250.63 ± 0.02	9.590 ± 0.007	0.03	0.210	0.003	0.020
2018.8301	19267+3221	STF2528 AB	5	CV	2004	243.5	14.32	243.66 ± 0.05	14.677 ± 0.024	0.16	0.357	0.011	0.024

Table 2 continues on the next page.

Table 2 (continued). Measures of 596 Pairs Without Known Orbits or Rectilinear Solutions

					Last Reported			Measured		Changes from Last		Change per Year	
Date	WDS Number	Discoverer	Observations	Method	Year	θ	ρ	θ	ρ	θ	ρ	θ	ρ
2018.7397	19268+1252	STF2520 AB	5	S	2009	233.8	1.84	234.24 ± 0.10	1.856 ± 0.004	0.44	0.016	0.045	0.002
2018.7260	19281+3521	HU 1194 AB	5	S	2009	37.3	0.95	36.02 ± 0.20	0.983 ± 0.002	-1.28	0.033	-0.132	0.003
2018.7753	19282+2013	STF3132 AB	5	CV	2008	39.9	7.85	39.33 ± 0.06	7.975 ± 0.007	-0.57	0.125	-0.053	0.012
2018.7425	19282+2942	AG 380	5	S	2009	228.4	2.46	225.51 ± 2.32	2.571 ± 0.006	-2.89	0.111	-0.297	0.011
2018.7342	19282-0932	STF2519	5	CV	2003	124.5	11.85	123.74 ± 0.01	12.038 ± 0.010	-0.76	0.188	-0.048	0.012
2018.7425	19284+2019	STF2530	5	S	2006	158.5	5.57	154.93 ± 0.16	5.641 ± 0.004	-3.57	0.071	-0.280	0.006
2018.7370	19288+0939	J 2970	5	CV	2001	37.4	6.28	37.09 ± 0.08	6.510 ± 0.011	-0.31	0.230	-0.017	0.013
2018.7370	19290+0343	HJ 872 AB	5	CV	2007	115.8	6.34	111.45 ± 0.02	9.809 ± 0.006	-4.35	3.469	-0.371	0.296
2018.7233	19296+1800	AG 231	5	CV	2009	240.3	4.35	239.32 ± 0.04	4.490 ± 0.001	-0.98	0.140	-0.101	0.014
2018.7425	19298+2522	DOO 75	5	CV	2002	238.3	2.92	239.58 ± 0.08	3.033 ± 0.006	1.28	0.113	0.076	0.007
2018.7397	19299+1241	BRT1318	5	CV	2010	84.7	5.93	83.61 ± 0.04	6.035 ± 0.009	-1.09	0.105	-0.125	0.012
2018.7397	19329+0831	A 1185	5	S	2009	193.2	3.38	193.27 ± 0.04	3.537 ± 0.005	0.07	0.157	0.007	0.016
2018.7233	19333+2025	STF2540 AB	5	S	2005	146.1	5.05	145.47 ± 0.02	5.404 ± 0.008	-0.63	0.354	-0.046	0.026
2018.7425	19340+2729	ES 488	5	S	2005	52.4	2.70	52.54 ± 0.12	2.784 ± 0.010	0.14	0.084	0.010	0.006
2018.7233	19356+2944	AG 387	5	S	2010	119.6	3.53	118.81 ± 0.02	3.695 ± 0.002	-0.79	0.165	-0.091	0.019
2018.7260	19356+3617	AG 234	5	S	2002	321.2	2.59	319.85 ± 0.03	2.679 ± 0.002	-1.35	0.089	-0.081	0.005
2018.7425	19358+2334	A 2787	5	CV	2010	111.0	4.20	110.73 ± 0.09	3.937 ± 0.006	-0.27	-0.263	-0.031	-0.030
2018.7425	19366+2700	BRT3345	5	CV	2002	12.3	3.33	11.79 ± 0.07	3.408 ± 0.005	-0.51	0.076	-0.030	0.005
2018.7397	19370+1430	A 1655	5	S	2013	69.0	1.90	67.97 ± 0.16	2.027 ± 0.004	-1.03	0.127	-0.179	0.022
2018.7397	19371+1723	HU 342	5	S	2011	254.3	4.44	255.14 ± 0.06	4.710 ± 0.007	0.84	0.270	0.109	0.035
2018.7397	19373+1534	TDT1590	5	CV	2010	349.0	6.20	349.62 ± 0.06	6.344 ± 0.008	0.62	0.144	0.071	0.016
2018.7425	19374+2249	STF2551	5	CV	2008	41.9	6.50	41.43 ± 0.04	6.889 ± 0.012	-0.47	0.389	-0.044	0.036
2018.7397	19377+1422	BRT1321	5	CV	2003	157.1	4.43	156.78 ± 0.03	4.616 ± 0.006	-0.32	0.186	-0.020	0.012
2018.7233	19379+1922	STF2552	5	S	2011	196.3	5.10	194.10 ± 0.01	5.393 ± 0.005	-2.20	0.293	-0.285	0.038
2018.7397	19384+1153	BRT1323	5	CV	2001	157.1	3.95	157.29 ± 0.08	4.095 ± 0.006	0.19	0.145	0.011	0.008
2018.7397	19392+1152	BRT1324	5	CV	2004	78.5	4.82	75.88 ± 0.09	5.064 ± 0.007	-2.62	0.244	-0.178	0.017

Table 2 continues on the next page.

Measurements of 628 Pairs: The 2018 Observing Run at Brilliant Sky Observatory

Table 2 (continued). Measures of 596 Pairs Without Known Orbits or Rectilinear Solutions

					Last Reported			Measured		Changes from Last		Change per Year	
Date	WDS Number	Discoverer	Observations	Method	Year	θ	ρ	θ	ρ	θ	ρ	θ	ρ
2018.7342	19394-0118	J 120	5	CV	2002	93.6	1.71	94.01 ± 0.17	1.950 ± 0.003	0.41	0.240	0.025	0.014
2018.7397	19402+1211	A 1190	5	CV	2010	198.0	5.00	199.94 ± 1.33	4.897 ± 0.101	1.94	-0.103	0.222	-0.012
2018.7342	19413-0128	BAL 605	5	CV	2010	280.3	6.98	279.89 ± 0.07	7.158 ± 0.012	-0.41	0.178	-0.047	0.020
2018.7233	19415+1838	HO 112	5	CV	2001	260.1	2.69	258.65 ± 0.02	2.785 ± 0.002	-1.45	0.095	-0.082	0.005
2018.8301	19417+3103	A 371	5	CV	2008	18.6	1.90	19.16 ± 0.13	1.857 ± 0.016	0.56	-0.043	0.052	-0.004
2018.7397	19429+0502	HWE 50	5	S	2001	16.3	2.61	15.69 ± 0.08	2.662 ± 0.003	-0.61	0.052	-0.034	0.003
2018.7260	19435+3450	AG 236 AB	5	S	2008	148.6	4.44	147.01 ± 0.02	4.292 ± 0.003	-1.59	-0.148	-0.148	-0.014
2018.7342	19436-0904	HO 579 AB	5	CV	2002	305.9	2.52	306.09 ± 0.05	2.817 ± 0.003	0.19	0.297	0.011	0.018
2018.7397	19445+1418	BRT1953	5	CV	2010	197.0	6.40	194.55 ± 0.09	6.470 ± 0.004	-2.45	0.070	-0.280	0.008
2018.7425	19451+2359	J 492 AB	5	CV	2008	296.4	4.83	296.39 ± 0.09	5.009 ± 0.010	-0.01	0.179	-0.001	0.017
2018.7260	19453+3048	AG 237	5	S	2011	140.7	2.43	139.52 ± 0.04	2.491 ± 0.003	-1.18	0.061	-0.153	0.008
2018.8301	19453+3656	POP 121	5	CV	1995	324.8	1.51	323.46 ± 0.04	1.675 ± 0.001	-1.34	0.165	-0.056	0.007
2018.7425	19456+2512	AG 390	5	CV	2007	96.2	7.11	96.69 ± 0.09	7.263 ± 0.004	0.49	0.153	0.042	0.013
2018.7397	19469+0610	BU 828	5	S	2002	10.4	2.96	14.56 ± 0.00	3.036 ± 0.004	4.16	0.076	0.249	0.005
2018.7260	19471+3321	HU 758	5	S	2012	144.2	0.88	144.06 ± 0.20	0.920 ± 0.002	-0.14	0.040	-0.021	0.006
2018.8301	19476+3557	ES 2182	5	CV	1996	48.1	1.88	43.52 ± 0.01	1.942 ± 0.003	-4.58	0.062	-0.201	0.003
2018.7288	19483+3710	STT 386	5	S	2013	69.9	0.95	71.22 ± 0.04	0.964 ± 0.004	1.32	0.014	0.230	0.002
2018.7397	19485+1958	J 1865	5	CV	2011	21.8	5.82	21.87 ± 0.05	6.252 ± 0.007	0.07	0.432	0.009	0.056
2018.7288	19489+3202	A 375	5	S	2011	158.8	1.18	158.66 ± 0.06	1.213 ± 0.002	-0.14	0.033	-0.018	0.004
2018.7753	19493+2726	MLB 603	5	CV	2005	28.0	7.75	27.70 ± 0.02	8.309 ± 0.004	-0.30	0.559	-0.022	0.041
2018.7397	19496+0235	BAL2005	5	CV	2010	285.0	6.50	285.51 ± 0.02	6.537 ± 0.006	0.51	0.037	0.058	0.004
2018.7397	19513+1430	HJ 1442	5	CV	2007	275.8	7.55	275.62 ± 0.04	7.751 ± 0.005	-0.18	0.201	-0.015	0.017
2018.7397	19517+0738	A 376	5	CV	2012	129.3	2.21	128.99 ± 0.09	2.271 ± 0.003	-0.31	0.061	-0.046	0.009
2018.7425	19518+2356	POU4122	5	CV	2008	74.6	6.89	73.73 ± 0.12	7.115 ± 0.011	-0.87	0.225	-0.081	0.021
2018.7288	19530+3704	AG 242	5	S	2013	179.0	2.00	180.37 ± 0.03	2.061 ± 0.004	1.37	0.061	0.239	0.011
2018.7425	19534+2923	J 25	5	S	1994	8.4	1.67	11.88 ± 0.05	1.666 ± 0.006	3.48	-0.004	0.141	0.000

Table 2 continues on the next page.

Measurements of 628 Pairs: The 2018 Observing Run at Brilliant Sky Observatory

Table 2 (continued). Measures of 596 Pairs Without Known Orbits or Rectilinear Solutions

					Last Reported			Measured		Changes from Last		Change per Year	
Date	WDS Number	Discoverer	Observations	Method	Year	θ	ρ	θ	ρ	θ	ρ	θ	ρ
2018.7425	19537+2805	ES 494	5	CV	2009	198.0	3.78	198.12 ± 0.04	3.847 ± 0.008	0.12	0.067	0.012	0.007
2018.7397	19542+1744	J 830	5	CV	2009	194.3	3.40	194.15 ± 0.03	3.502 ± 0.004	-0.15	0.102	-0.015	0.010
2018.7425	19554+2449	J 1156 AB	5	CV	2006	226.7	3.25	225.89 ± 0.04	3.336 ± 0.005	-0.81	0.086	-0.064	0.007
2018.7342	19567-0737	RST4646	5	CV	2010	195.8	4.35	195.49 ± 0.04	4.590 ± 0.005	-0.31	0.240	-0.035	0.027
2018.7397	19568+0155	STF2601 AB-C	5	CV	2010	161.9	6.92	161.76 ± 0.02	7.119 ± 0.006	-0.14	0.199	-0.016	0.023
2018.7397	19568+1935	J 3036 AB	5	CV	2004	257.9	6.81	256.41 ± 0.03	7.200 ± 0.002	-1.49	0.390	-0.101	0.026
2018.7397	19570+0514	BAL2956	5	CV	2011	245.8	9.47	245.71 ± 0.04	9.975 ± 0.011	-0.09	0.505	-0.012	0.065
2018.7342	19576-0608	BRT 496	5	CV	2010	339.1	3.57	339.65 ± 0.05	3.711 ± 0.004	0.55	0.141	0.063	0.016
2018.7342	19583-0037	J 1386	5	CV	2010	319.2	3.73	318.96 ± 0.07	3.860 ± 0.005	-0.24	0.130	-0.027	0.015
2018.7288	19586+3806	STF2609	5	S	2013	22.3	1.95	23.12 ± 0.05	1.977 ± 0.003	0.82	0.027	0.143	0.005
2018.8219	20003+4621	A 719	5	CV	2003	108.5	2.93	108.62 ± 0.05	3.029 ± 0.004	0.12	0.099	0.008	0.006
2017.8356	20004+5627	ES 1756	5	CV	1991	185.8	2.19	188.76 ± 0.9	2.141 ± 0.042	2.96	-0.049	0.110	-0.002
2018.7342	20006-0911	BRT 554	5	CV	2002	26.0	2.56	25.28 ± 0.06	2.550 ± 0.002	-0.72	-0.010	-0.043	-0.001
2018.7753	20010+2956	L 32	5	CV	2003	127.6	3.26	128.79 ± 0.08	3.347 ± 0.006	1.19	0.087	0.075	0.006
2017.8356	20031+5921	ES 1757	3	CV	1997	212.0	1.89	209.31 ± 0.0	1.960 ± 0.002	-2.69	0.070	-0.129	0.003
2018.8466	20034+1528	STF2618	5	CV	2005	114.9	5.43	114.73 ± 0.04	5.627 ± 0.003	-0.17	0.197	-0.012	0.014
2018.8466	20041+1700	STF2622 AB	5	CV	2010	194.2	5.83	193.22 ± 0.02	6.033 ± 0.005	-0.98	0.203	-0.111	0.023
2017.8383	20046+3641	A 1413	5	CV	1999	138.0	2.36	138.85 ± 0.0	2.393 ± 0.001	0.85	0.033	0.045	0.002
2018.8493	20047+4938	KU 58 AB	5	CV	2011	190.3	2.72	186.38 ± 0.06	2.868 ± 0.004	-3.92	0.148	-0.499	0.019
2018.8301	20066+0207	HJ 902	5	CV	2004	18.4	6.91	17.14 ± 0.03	7.119 ± 0.010	-1.26	0.209	-0.085	0.014
2018.8466	20070+1220	BRT1336	5	CV	2011	292.5	5.12	292.09 ± 0.03	5.499 ± 0.001	-0.41	0.379	-0.052	0.048
2017.8383	20083+3714	ES 2185	5	CV	2002	242.0	2.20	244.05 ± 0.0	2.195 ± 0.002	2.05	-0.005	0.129	0.000
2018.8466	20099+1149	BRT1339	5	CV	2001	177.9	4.27	177.71 ± 0.16	4.382 ± 0.001	-0.19	0.112	-0.011	0.006
2018.8137	20102+3644	ES 87	5	CV	2004	298.0	8.89	298.43 ± 0.03	8.793 ± 0.004	0.43	-0.097	0.029	-0.007
2018.8493	20104+4949	STF2648	5	CV	2008	117.1	6.75	117.24 ± 0.04	6.862 ± 0.001	0.14	0.112	0.013	0.010
2018.8493	20105+4923	ES 1099	5	CV	2006	183.8	6.58	185.98 ± 0.02	4.932 ± 0.005	2.18	-1.648	0.170	-0.128

Table 2 continues on the next page.

Table 2 (continued). Measures of 596 Pairs Without Known Orbits or Rectilinear Solutions

					Last Reported			Measured		Changes from Last		Change per Year	
Date	WDS Number	Discoverer	Observations	Method	Year	θ	ρ	θ	ρ	θ	ρ	θ	ρ
2017.8356	20111-1252	HO 119	5	S	2002	198.1	3.14	197.52 ± 0.0	3.120 ± 0.001	-0.58	-0.020	-0.037	-0.001
2018.7753	20120+2554	DOO 14	5	S	2000	271.0	1.93	273.14 ± 0.27	1.909 ± 0.005	2.14	-0.021	0.114	-0.001
2018.8466	20128+1210	A 722	5	CV	2009	162.8	2.65	162.43 ± 0.04	2.736 ± 0.001	-0.37	0.086	-0.038	0.009
2018.7945	20129+2913	HJ 1492 A-BC	5	CV	2005	53.9	18.27	54.13 ± 0.01	18.740 ± 0.020	0.23	0.470	0.017	0.034
2018.8137	20129+3429	AG 250	5	CV	2006	50.8	8.71	53.10 ± 0.01	8.889 ± 0.003	2.30	0.179	0.179	0.014
2018.8493	20137+4050	DOO 13	5	CV	2009	258.4	2.91	258.28 ± 0.02	3.021 ± 0.002	-0.12	0.111	-0.012	0.011
2018.8219	20142+4744	ES 799 AB	5	CV	2011	17.0	2.07	14.38 ± 0.04	2.199 ± 0.001	-2.62	0.129	-0.335	0.016
2018.7753	20145+2808	BRT 47 AB	5	CV	2007	232.2	4.67	232.29 ± 0.07	4.773 ± 0.003	0.09	0.103	0.008	0.009
2018.8219	20158+4233	ES 1567	5	CV	1991	183.6	2.19	181.86 ± 0.03	2.391 ± 0.001	-1.74	0.201	-0.063	0.007
2017.8356	20160+2703	A 389	5	S	2013	211.0	1.70	212.74 ± 0.3	1.690 ± 0.007	1.74	-0.010	0.360	-0.002
2017.8356	20164+5542	KR 49	5	CV	1997	114.7	1.68	113.56 ± 0.0	1.700 ± 0.000	-1.14	0.020	-0.055	0.001
2018.8301	20166+0405	J 1641	5	CV	2002	215.7	7.19	215.27 ± 0.07	7.378 ± 0.003	-0.43	0.188	-0.026	0.011
2018.8301	20186+1100	STF2662	5	CV	2007	37.2	1.80	42.44 ± 0.04	1.961 ± 0.004	5.24	0.161	0.443	0.014
2018.8301	20186+1318	A 1671	5	CV	2005	231.6	2.17	229.02 ± 0.02	2.197 ± 0.005	-2.58	0.027	-0.187	0.002
2017.8383	20192+3859	HO 126 AB	5	CV	2002	159.7	2.18	162.79 ± 0.0	2.184 ± 0.005	3.09	0.004	0.195	0.000
2018.8137	20193+3635	AG 253 AB	5	CV	2008	118.9	9.49	117.64 ± 0.02	9.784 ± 0.002	-1.26	0.294	-0.117	0.027
2018.8466	20209+1948	HJ 2954 AB	5	CV	2009	303.3	2.97	302.62 ± 0.02	3.075 ± 0.002	-0.68	0.105	-0.069	0.011
2018.7753	20237+2710	TDS1067	5	S	2000	203.8	1.78	202.68 ± 0.35	1.797 ± 0.012	-1.12	0.017	-0.060	0.001
2017.8383	20255+3553	A 47	5	CV	2000	176.2	1.56	175.95 ± 0.8	1.565 ± 0.002	-0.25	0.005	-0.014	0.000
2018.8466	20260+1212	J 1704	5	CV	2009	202.0	6.03	202.05 ± 0.01	6.223 ± 0.005	0.05	0.193	0.005	0.020
2018.8137	20263+3728	AG 255	5	CV	2008	286.0	4.94	286.68 ± 0.01	5.208 ± 0.001	0.68	0.268	0.063	0.025
2018.7753	20278+2411	TDT2295	5	CV	2003	29.4	2.79	28.69 ± 0.04	2.796 ± 0.007	-0.71	0.006	-0.045	0.000
2018.8301	20279+0958	AG 256 AB	5	CV	2011	351.3	4.97	351.41 ± 0.09	5.214 ± 0.007	0.11	0.244	0.014	0.031
2018.8137	20282+3024	HJ 1517	5	CV	2002	104.8	12.74	104.78 ± 0.02	13.100 ± 0.002	-0.02	0.360	-0.001	0.021
2018.8466	20284+1713	HJ 2969	5	CV	2004	169.4	5.79	169.57 ± 0.03	5.986 ± 0.002	0.17	0.196	0.011	0.013
2018.8137	20288+3810	ES 206	5	CV	2008	124.4	3.95	124.15 ± 0.02	4.162 ± 0.002	-0.25	0.212	-0.023	0.020

Table 2 continues on the next page.

Measurements of 628 Pairs: The 2018 Observing Run at Brilliant Sky Observatory

Table 2 (continued). Measures of 596 Pairs Without Known Orbits or Rectilinear Solutions

					Last Reported			Measured		Changes from Last		Change per Year	
Date	WDS Number	Discoverer	Observations	Method	Year	θ	ρ	θ	ρ	θ	ρ	θ	ρ
2018.7945	20291+2956	AG 406	5	CV	2011	332.6	8.30	332.79 ± 0.03	8.478 ± 0.005	0.19	0.178	0.024	0.023
2018.8219	20300+4940	HU 589	5	CV	2005	201.6	1.54	203.56 ± 0.06	1.615 ± 0.001	1.96	0.075	0.142	0.005
2018.8466	20306+1404	AG 408	5	CV	2003	284.8	4.87	285.05 ± 0.02	5.060 ± 0.001	0.25	0.190	0.016	0.012
2018.8493	20308+1347	STF2688	5	CV	2011	175.0	7.66	174.88 ± 0.01	8.040 ± 0.004	-0.12	0.380	-0.015	0.048
2018.7342	20312-0328	J 1395	5	CV	2011	298.0	5.62	297.82 ± 0.07	5.701 ± 0.014	-0.18	0.081	-0.023	0.010
2018.8137	20319+3920	HJ 1531	5	CV	2010	317.7	6.37	317.89 ± 0.02	6.448 ± 0.002	0.19	0.078	0.022	0.009
2018.8493	20329+1803	HJ 2977	5	CV	2004	317.4	19.75	316.64 ± 0.02	20.11 ± 0.002	-0.76	0.360	-0.051	0.024
2018.7753	20338+2125	TDS1083	5	CV	2013	354.0	2.50	353.47 ± 0.04	2.616 ± 0.004	-0.53	0.116	-0.092	0.020
2018.8137	20338+3336	HJ 1538	5	CV	2009	120.5	5.43	121.94 ± 0.01	5.542 ± 0.003	1.44	0.112	0.147	0.011
2018.7945	20382+2224	HJ 1550	5	CV	2001	223.3	7.61	223.26 ± 0.04	7.912 ± 0.011	-0.04	0.302	-0.002	0.017
2017.8356	20383+5023	HU 588 AB	5	CV	2008	245.2	2.08	244.64 ± 0.1	2.010 ± 0.001	-0.56	-0.070	-0.057	-0.007
2018.7945	20410+2001	HJ 2987	5	CV	2007	115.7	10.78	115.73 ± 0.05	11.146 ± 0.011	0.03	0.366	0.003	0.031
2018.7945	20411+2133	HJ 922	5	CV	2004	312.3	7.41	313.05 ± 0.02	7.752 ± 0.004	0.75	0.342	0.051	0.023
2018.7342	20417-0424	BU 267	5	CV	2001	239.2	1.84	237.46 ± 0.07	1.935 ± 0.003	-1.74	0.095	-0.098	0.005
2018.8301	20431+0253	AG 262	5	CV	2011	94.0	5.30	93.69 ± 0.02	5.678 ± 0.005	-0.31	0.378	-0.040	0.048
2018.8137	20431+3411	ES 2310	5	CV	2002	33.2	4.61	33.08 ± 0.02	4.751 ± 0.003	-0.12	0.141	-0.007	0.008
2018.8301	20444+1205	A 875	5	CV	2005	210.2	2.29	207.81 ± 0.01	2.529 ± 0.001	-2.39	0.239	-0.173	0.017
2018.7945	20445+2856	MLB 710	5	CV	2011	180.0	7.36	180.37 ± 0.08	7.583 ± 0.006	0.37	0.223	0.047	0.029
2018.7342	20447-0721	A 2999	5	CV	2001	222.0	2.04	221.44 ± 0.10	2.052 ± 0.008	-0.56	0.012	-0.032	0.001
2018.7945	20448+2051	A 172	5	CV	2009	219.5	2.81	219.41 ± 0.05	2.889 ± 0.008	-0.09	0.079	-0.009	0.008
2018.8219	20449+4332	ES 1448	5	CV	2000	141.9	1.95	142.38 ± 0.03	2.013 ± 0.001	0.48	0.063	0.026	0.003
2018.7370	20456-0853	HDO 160	5	CV	2010	201.0	5.74	201.17 ± 0.13	5.844 ± 0.005	0.17	0.104	0.019	0.012
2018.8137	20457+3647	AG 265	5	CV	2008	207.5	6.91	206.98 ± 0.03	6.843 ± 0.006	-0.52	-0.067	-0.048	-0.006
2018.7945	20461+2638	BRT 217	5	CV	2006	79.9	4.14	80.06 ± 0.07	4.297 ± 0.006	0.16	0.157	0.013	0.012
2018.8219	20480+4126	ES 1681	5	CV	2001	153.7	2.10	145.82 ± 0.02	2.134 ± 0.001	-7.88	0.034	-0.442	0.002
2018.8301	20484+0426	AG 267	5	CV	2010	260.8	5.90	260.46 ± 0.05	6.066 ± 0.002	-0.34	0.166	-0.039	0.019

Table 2 continues on the next page.

Table 2 (continued). Measures of 596 Pairs Without Known Orbits or Rectilinear Solutions

					Last Reported			Measured		Changes from Last		Change per Year	
Date	WDS Number	Discoverer	Observations	Method	Year	θ	ρ	θ	ρ	θ	ρ	θ	ρ
2018.7945	20490+2932	BRT 51 AB	5	CV	2010	355.0	6.59	354.87 ± 0.03	6.916 ± 0.005	-0.13	0.326	-0.015	0.037
2018.7945	20490+2932	BRT 51 AC	5	CV	2010	38.0	4.90	37.22 ± 0.05	5.053 ± 0.005	-0.78	0.153	-0.089	0.017
2018.7945	20493+2026	HJ 926	5	CV	2009	190.1	5.73	189.67 ± 0.06	6.001 ± 0.005	-0.43	0.271	-0.044	0.028
2018.7945	20497+2535	J 3112	5	CV	2009	75.2	5.57	75.10 ± 0.06	5.788 ± 0.005	-0.10	0.218	-0.010	0.022
2018.8137	20505+3635	SEI1271 AB	5	CV	2002	27.2	14.52	27.03 ± 0.01	14.917 ± 0.003	-0.17	0.397	-0.010	0.024
2018.8137	20505+3635	SEI1271 AC	5	CV	2002	184.7	19.81	184.77 ± 0.01	20.395 ± 0.002	0.07	0.585	0.004	0.035
2017.8356	20506+3024	STT 415	5	S	2009	231.6	3.66	234.2 ± 0.0	3.740 ± 0.000	2.60	0.080	0.294	0.009
2018.8301	20516+07341	A 612	5	CV	2000	9.2	2.01	6.95 ± 0.15	2.026 ± 0.014	-2.25	0.016	-0.119	0.001
2018.7945	20523+2839	BRT 52	5	CV	2009	86.6	8.39	86.62 ± 0.04	8.830 ± 0.008	0.02	0.440	0.002	0.045
2018.8137	20540+3124	ES 371	5	CV	2002	34.4	3.39	33.61 ± 0.03	3.477 ± 0.003	-0.79	0.087	-0.047	0.005
2018.8301	20554+0653	BRT2188	5	CV	2010	45.6	4.06	45.92 ± 0.05	4.290 ± 0.006	0.32	0.230	0.036	0.026
2017.8356	20559+5906	A 754	5	S	2008	2.4	0.93	6.29 ± 0.1	0.980 ± 0.002	3.89	0.050	0.396	0.005
2017.8356	20559+5906	AG 258	5	S	2009	9.4	4.14	10.75 ± 0.0	4.160 ± 0.001	1.30	0.020	0.147	0.002
2018.8466	20567+1300	STF2736	5	CV	2009	217.1	5.43	219.13 ± 0.02	5.251 ± 0.005	2.03	-0.179	0.206	-0.018
2018.8219	20576+4058	A 400	5	CV	2011	68.1	1.42	69.41 ± 0.03	1.931 ± 0.001	1.31	0.511	0.167	0.065
2017.8356	20577+5849	A 756 AB	5	S	2011	209.6	0.57	209.73 ± 0.2	0.580 ± 0.016	-0.60	0.010	-0.088	0.001
2017.8356	20588+0921	BU 764	5	S	1991	357.9	0.71	1.46 ± 0.5	0.730 ± 0.015	3.56	0.020	0.133	0.001
2018.8137	20596+3703	HJ 1601	5	CV	2008	143.2	6.42	140.76 ± 0.03	6.524 ± 0.005	-2.44	0.104	-0.226	0.010
2017.8383	21001+3627	J 1219	5	CV	2007	171.4	3.62	172.12 ± 0.0	3.684 ± 0.003	0.72	0.064	0.066	0.006
2017.8383	21020+3745	COU2223	5	CV	2009	178.6	1.93	180.33 ± 0.3	1.893 ± 0.013	1.73	-0.037	0.196	-0.004
2017.8383	21020+3914	LV 9	5	CV	2009	193.0	2.33	194.93 ± 0.1	2.283 ± 0.006	1.93	-0.047	0.218	-0.005
2018.8219	21022+4235	ES 1577	5	CV	2004	40.4	5.59	40.79 ± 0.01	5.783 ± 0.003	0.39	0.193	0.026	0.013
2018.8219	21024+4236	ES 1578	5	CV	1997	233.1	2.68	233.12 ± 0.06	2.822 ± 0.001	0.02	0.142	0.001	0.007
2017.8383	21029+3554	J 1078 AB	5	CV	2000	109.7	2.59	112.0 ± 0.0	2.659 ± 0.005	2.30	0.069	0.129	0.004
2018.8466	21031+1434	A 1689	5	CV	2000	340.4	2.25	340.86 ± 0.05	2.430 ± 0.002	0.46	0.180	0.024	0.010
2018.8219	21044+4057	ROE 44	5	CV	2008	43.2	7.07	42.84 ± 0.02	7.193 ± 0.001	-0.36	0.123	-0.033	0.011

Table 2 continues on the next page.

Measurements of 628 Pairs: The 2018 Observing Run at Brilliant Sky Observatory

Table 2 (continued). Measures of 596 Pairs Without Known Orbits or Rectilinear Solutions

					Last Reported			Measured		Changes from Last		Change per Year	
Date	WDS Number	Discoverer	Observations	Method	Year	θ	ρ	θ	ρ	θ	ρ	θ	ρ
2018.8301	21052-1004	AOT 104	5	CV	2008	172.8	7.33	173.63 ± 0.07	7.573 ± 0.005	0.83	0.243	0.077	0.022
2018.8219	21055+4758	ES 816	5	CV	2003	35.5	2.52	35.63 ± 0.05	2.640 ± 0.002	0.13	0.120	0.008	0.008
2018.8301	21066-0534	BRT 557	5	CV	2010	280.1	4.02	280.54 ± 0.11	4.301 ± 0.013	0.44	0.281	0.050	0.032
2017.8383	21067+3715	SEI1406	5	CV	2002	172.8	3.18	174.61 ± 0.0	3.235 ± 0.003	1.81	0.055	0.114	0.003
2018.8959	21074+2429	STF2761	5	CV	2009	112.1	5.49	111.44 ± 0.01	5.729 ± 0.003	-0.66	0.239	-0.067	0.024
2018.8493	21076+3546	ES 2254	5	CV	2010	275.3	8.16	275.22 ± 0.03	8.579 ± 0.005	-0.08	0.419	-0.009	0.047
2018.8137	21082+3449	ES 2255 AB	5	CV	2004	249.3	4.80	249.17 ± 0.01	4.951 ± 0.001	-0.13	0.151	-0.009	0.010
2018.8219	21082+4055	AG 414	5	CV	2004	105.0	5.43	107.53 ± 0.02	5.267 ± 0.001	2.53	-0.163	0.171	-0.011
2018.8301	21086-0427	BRT 514	5	CV	2003	135.0	4.49	136.06 ± 0.12	4.769 ± 0.006	1.06	0.279	0.067	0.018
2018.8137	21088+3102	ES 375	5	CV	2003	41.3	4.42	41.80 ± 0.02	4.536 ± 0.003	0.50	0.116	0.032	0.007
2018.8219	21100+4326	ES 1453	5	CV	2007	68.4	5.43	68.00 ± 0.02	5.463 ± 0.002	-0.40	0.033	-0.034	0.003
2018.8466	21116+1251	ROE 102	5	CV	2010	127.4	6.45	128.18 ± 0.05	6.686 ± 0.004	0.78	0.236	0.088	0.027
2018.8219	21119+4838	HJ 1624	5	CV	2004	189.4	5.94	189.69 ± 0.02	6.204 ± 0.002	0.29	0.264	0.020	0.018
2018.8301	21127-0045	J 1403	5	CV	2011	343.9	3.77	343.85 ± 0.14	4.013 ± 0.007	-0.05	0.243	-0.006	0.031
2018.8466	21130+1802	J 577	5	CV	2000	20.2	2.39	19.10 ± 0.11	2.434 ± 0.004	-1.10	0.044	-0.058	0.002
2018.8959	21158+4719	ES 514	5	CV	2003	195.0	4.25	194.94 ± 0.03	4.392 ± 0.003	-0.06	0.142	-0.004	0.009
2018.8466	21167+1459	HU 961	5	CV	1999	13.7	2.13	13.86 ± 0.08	2.156 ± 0.005	0.16	0.026	0.008	0.001
2018.8493	21189+3909	AG 270	5	CV	2007	111.8	5.93	112.20 ± 0.01	5.791 ± 0.003	0.40	-0.139	0.034	-0.012
2017.8383	21210+3304	J 1229	5	CV	2001	302.7	2.23	304.56 ± 0.0	2.215 ± 0.003	1.86	-0.015	0.110	-0.001
2018.8959	21230+2858	STF2791	5	CV	2010	330.2	7.25	330.58 ± 0.02	7.412 ± 0.004	0.38	0.162	0.043	0.018
2018.8466	21236+1030	BRT1356	5	CV	2004	63.2	5.48	62.70 ± 0.13	5.685 ± 0.018	-0.50	0.205	-0.034	0.014
2018.8959	21240+2236	KU 60	5	CV	2011	227.6	7.08	227.86 ± 0.01	7.319 ± 0.002	0.26	0.239	0.033	0.030
2018.8493	21278+3835	KU 61 AB	5	CV	2002	271.4	3.80	271.24 ± 0.04	3.919 ± 0.003	-0.16	0.119	-0.009	0.007
2018.9041	21282+4713	ES 1171 AB	5	CV	2003	196.5	3.66	196.58 ± 0.03	3.772 ± 0.001	0.08	0.112	0.005	0.007
2018.9041	21287+4952	STF2800	5	CV	2010	249.0	9.00	254.36 ± 0.01	9.337 ± 0.007	5.36	0.337	0.602	0.038
2018.9041	21293+4512	ES 100 AB	5	CV	2011	157.0	4.33	156.64 ± 0.04	4.387 ± 0.002	-0.36	0.057	-0.046	0.007

Table 2 continues on the next page.

Table 2 (continued). Measures of 596 Pairs Without Known Orbits or Rectilinear Solutions

					Last Reported			Measured		Changes from Last		Change per Year	
Date	WDS Number	Discoverer	Observations	Method	Year	θ	ρ	θ	ρ	θ	ρ	θ	ρ
2018.8466	21300-0637	BRT 517	5	CV	2001	206.7	4.27	204.57 ± 0.08	4.407 ± 0.007	-2.13	0.137	-0.119	0.008
2018.8466	21309+1141	J 178	5	CV	2001	187.4	2.72	185.20 ± 0.16	2.938 ± 0.012	-2.20	0.218	-0.123	0.012
2018.9041	21309+4228	TDT3004	5	CV	2002	173.3	5.97	163.76 ± 0.02	5.933 ± 0.003	-9.54	-0.037	-0.564	-0.002
2018.9041	21317+4508	AG 272	5	CV	2011	183.4	4.10	183.70 ± 0.05	4.240 ± 0.002	0.30	0.140	0.038	0.018
2018.8493	21322+3850	ES 259	5	CV	2009	318.3	3.77	318.98 ± 0.03	3.937 ± 0.004	0.68	0.167	0.069	0.017
2018.9041	21324+4002	HO 162	5	CV	2009	330.0	3.42	329.97 ± 0.02	3.537 ± 0.001	-0.03	0.117	-0.003	0.012
2018.8493	21327+3948	HO 604	5	CV	2011	316.1	4.94	316.06 ± 0.03	5.291 ± 0.003	-0.04	0.351	-0.005	0.045
2018.8959	21374+2454	POU5440	5	CV	2003	305.0	4.16	304.67 ± 0.05	4.219 ± 0.005	-0.33	0.059	-0.021	0.004
2018.8301	21385+0513	BAL2981	5	CV	2010	265.7	4.12	265.33 ± 0.01	4.284 ± 0.001	-0.37	0.164	-0.042	0.019
2018.8466	21388-0121	BAL 624	5	CV	2003	331.1	3.43	330.85 ± 0.05	3.599 ± 0.004	-0.25	0.169	-0.016	0.011
2018.8959	21389+3623	STF2814	5	CV	2004	159.9	7.93	159.85 ± 0.01	8.143 ± 0.004	-0.05	0.213	-0.003	0.014
2018.8466	21399+1427	AG 419	5	CV	2009	222.5	3.64	222.58 ± 0.06	3.803 ± 0.005	0.08	0.163	0.008	0.017
2018.8301	21403+0344	STT 446	5	CV	2004	173.9	6.58	173.33 ± 0.02	6.769 ± 0.003	-0.57	0.189	-0.038	0.013
2018.8301	21423+0715	HU 279	5	CV	2009	355.5	2.42	356.08 ± 0.08	2.482 ± 0.002	0.58	0.062	0.059	0.006
2018.8466	21456+0251	BAL2056	5	CV	2010	269.3	7.88	269.11 ± 0.03	8.128 ± 0.008	-0.19	0.248	-0.021	0.028
2018.8959	21474+2834	A 300 AB	5	CV	2001	251.5	2.40	251.81 ± 0.13	2.312 ± 0.006	0.31	-0.088	0.017	-0.005
2017.8383	21474+3453	HO 466	5	CV	2005	143.1	2.26	144.57 ± 0.0	2.291 ± 0.003	1.47	0.031	0.115	0.002
2017.8383	21522+3252	ES 2321	5	CV	2005	277.3	2.04	279.03 ± 0.1	2.007 ± 0.008	1.73	-0.033	0.135	-0.003
2018.8959	21551+2523	AG 421	5	CV	2010	198.9	6.36	199.05 ± 0.01	6.799 ± 0.006	0.15	0.439	0.017	0.049
2018.8493	21557+3301	AG 278	5	CV	2010	158.4	3.40	158.69 ± 0.02	3.542 ± 0.003	0.29	0.142	0.033	0.016
2018.8959	21561+2420	STT 454 AB	5	CV	2009	277.9	7.05	278.06 ± 0.01	7.429 ± 0.003	0.16	0.379	0.016	0.038
2018.8493	21571+3858	SEI1545	5	CV	2004	324.5	5.60	324.49 ± 0.04	5.800 ± 0.002	-0.01	0.200	-0.001	0.013
2018.8301	21591+0116	HJ 3078	5	CV	2003	182.7	4.39	180.78 ± 0.06	4.564 ± 0.011	-1.92	0.174	-0.121	0.011
2018.8466	21595+0617	HJ 3079	5	CV	2010	74.3	9.78	74.24 ± 0.01	10.02 ± 0.002	-0.06	0.240	-0.007	0.027
2018.9233	22002+4545	A 777	5	CV	2005	81.7	2.30	81.57 ± 0.03	2.322 ± 0.001	-0.13	0.022	-0.009	0.002
2018.8493	22006+5411	STF2852	5	CV	2005	172.7	7.90	172.25 ± 0.02	7.862 ± 0.006	-0.45	-0.038	-0.032	-0.003

Table 2 continues on the next page.

Table 2 (continued). Measures of 596 Pairs Without Known Orbits or Rectilinear Solutions

					Last Reported			Measured		Changes from Last		Change per Year	
Date	WDS Number	Discoverer	Observations	Method	Year	θ	ρ	θ	ρ	θ	ρ	θ	ρ
2017.9205	22013+2751	ES 527	3	CV	2011	213.7	3.46	214.03 ± 0.0	3.494 ± 0.008	0.33	0.034	0.048	0.005
2018.8493	22029+4717	A 781	5	CV	2001	199.6	2.85	199.64 ± 0.12	2.919 ± 0.005	0.04	0.069	0.002	0.004
2017.9370	22040+3841	COU1341	3	CV	2005	272.2	1.57	272.64 ± 0.2	1.612 ± 0.002	0.44	0.042	0.034	0.003
2017.9205	22044+2500	POU5269	3	CV	2004	235.9	5.38	235.23 ± 0.1	5.562 ± 0.012	-0.67	0.182	-0.048	0.013
2017.9205	22058+2951	J 1225	3	CV	2002	114.3	3.19	115.2 ± 0.0	3.195 ± 0.002	0.90	0.005	0.057	0.000
2017.9205	22060+2036	STF2859	3	CV	2013	344.0	3.70	343.92 ± 0.1	3.765 ± 0.010	-0.08	0.065	-0.016	0.013
2017.9205	22061+2034	BRT2840	3	CV	2013	318.0	2.30	315.88 ± 0.2	2.350 ± 0.002	-2.12	0.050	-0.431	0.010
2017.9205	22092+2346	TDS1160	3	CV	2003	115.5	1.38	116.78 ± 0.5	1.468 ± 0.003	1.28	0.088	0.086	0.006
2017.9041	22104+1925	BRT2527	3	CV	2010	12.0	5.80	10.71 ± 0.0	5.613 ± 0.003	-1.29	-0.187	-0.163	-0.024
2017.9342	22108+2151	J 2365	3	CV	2004	260.6	5.45	261.14 ± 0.0	5.508 ± 0.001	0.54	0.058	0.039	0.004
2017.9041	22110+1543	J 1794	3	CV	2011	229.9	5.28	229.3 ± 0.0	5.209 ± 0.004	-0.60	-0.071	-0.087	-0.010
2018.8959	22117+3149	A 1228	5	CV	2002	350.0	3.77	349.92 ± 0.02	3.830 ± 0.007	-0.08	0.060	-0.005	0.004
2017.9205	22120+2546	MLB 723	3	CV	2006	337.9	2.33	338.8 ± 0.1	2.337 ± 0.011	0.90	0.007	0.076	0.001
2018.8959	22126+3358	KU 63	5	CV	2003	241.1	4.16	240.97 ± 0.13	4.245 ± 0.005	-0.13	0.085	-0.008	0.005
2017.9342	22132+2148	HJ 958	3	CV	2010	231.0	5.70	232.51 ± 0.2	5.839 ± 0.015	1.51	0.139	0.190	0.018
2018.8301	22133+3207	ES 388	5	CV	2010	263.7	7.33	263.43 ± 0.11	7.855 ± 0.005	-0.27	0.525	-0.031	0.059
2018.8301	22159+3125	BU 477	5	CV	2010	41.5	6.14	41.45 ± 0.07	6.559 ± 0.013	-0.05	0.419	-0.006	0.047
2018.9041	22159+3125	BU 477	5	CV	2010	41.5	6.14	41.32 ± 0.07	6.572 ± 0.004	-0.18	0.432	-0.020	0.049
2018.8301	22161+3037	ES 389	5	CV	2010	258.6	7.57	257.93 ± 0.02	7.640 ± 0.004	-0.67	0.070	-0.076	0.008
2018.9233	22176+4503	ES 1343	5	CV	2000	76.0	1.72	73.97 ± 0.05	1.744 ± 0.003	-2.03	0.024	-0.107	0.001
2017.9205	22221+2155	J 2578	3	CV	2000	351.4	2.09	351.18 ± 0.1	2.095 ± 0.002	-0.22	0.005	-0.012	0.000
2017.9342	22242+2712	HJ 1760	3	CV	2007	335.9	6.93	336.17 ± 0.0	6.977 ± 0.023	0.27	0.047	0.025	0.004
2017.9041	22254+1842	HJ 963	3	CV	2010	59.6	7.00	59.62 ± 0.0	7.170 ± 0.006	0.02	0.170	0.003	0.022
2017.9041	22265+1925	HU 596	3	CV	2005	19.4	3.09	16.56 ± 0.0	1.111 ± 0.001	-2.84	-1.979	-0.220	-0.153
2017.9342	22292+2621	J 3168 AB	3	CV	2006	149.4	7.91	149.46 ± 0.2	8.036 ± 0.43	0.06	0.126	0.005	0.011
2017.9370	22293+3008	MLB 581 AB	3	CV	2006	236.2	2.24	235.74 ± 0.1	2.278 ± 0.016	-0.46	0.038	-0.039	0.003

Table 2 continues on the next page.

Measurements of 628 Pairs: The 2018 Observing Run at Brilliant Sky Observatory

Table 2 (continued). Measures of 596 Pairs Without Known Orbits or Rectilinear Solutions

					Last Reported			Measured		Changes from Last		Change per Year	
Date	WDS Number	Discoverer	Observations	Method	Year	θ	ρ	θ	ρ	θ	ρ	θ	ρ
2017.9370	22297+3259	TDT3548	3	CV	2002	136.6	1.50	135.6 ± 0.2	1.498 ± 0.012	-1.00	-0.002	-0.063	0.000
2018.9233	22314+4753	A 2397	5	CV	2010	267.4	8.50	271.46 ± 0.04	2.054 ± 0.004	4.06	-6.446	0.455	-0.722
2017.9342	22318+2953	MLB 582	3	CV	2010	341.6	5.49	342.01 ± 0.2	5.406 ± 0.024	0.41	-0.084	0.052	-0.011
2017.9342	22339+2635	HO 476	3	CV	2010	206.9	6.75	207.4 ± 0.0	6.921 ± 0.009	0.50	0.171	0.063	0.022
2017.9370	22364+3007	MLB 624	3	CV	2009	298.6	1.93	298.45 ± 0.6	1.927 ± 0.038	-0.15	-0.003	-0.017	0.000
2017.9041	22379+1131	J 165	3	CV	2001	137.3	1.96	137.29 ± 0.0	2.077 ± 0.002	-0.01	0.117	-0.001	0.007
2018.9041	22395+3653	HJ 968	5	CV	2011	109.2	4.32	110.44 ± 0.02	4.415 ± 0.004	1.24	0.095	0.157	0.012
2017.9041	22432+1913	TDT3676	3	CV	2002	348.4	2.03	348.89 ± 0.0	1.982 ± 0.003	0.49	-0.048	0.031	-0.003
2018.9233	22439+3337	ES 265	5	CV	2011	5.2	8.65	5.250 ± 0.02	8.853 ± 0.003	0.05	0.203	0.006	0.026
2017.9370	22445+3303	ES 2271	3	CV	1997	206.9	1.75	205.78 ± 0.2	1.730 ± 0.007	-1.12	-0.020	-0.053	-0.001
2017.9370	22455+3359	HU 782	3	CV	2009	321.3	1.98	322.73 ± 0.0	1.966 ± 0.015	1.43	-0.014	0.160	-0.002
2018.9233	22459+3358	HJ 969	5	CV	2009	26.3	5.86	26.19 ± 0.03	6.131 ± 0.005	-0.11	0.271	-0.011	0.027
2017.9370	22492+3310	ES 2272	3	CV	2002	23.2	2.10	21.5 ± 0.7	2.020 ± 0.009	-1.70	-0.080	-0.107	-0.005
2017.9205	22519+2219	COU 239	3	CV	2005	296.2	2.13	296.55 ± 0.0	2.105 ± 0.003	0.35	-0.025	0.027	-0.002
2017.9205	22524+2819	TDT3763	3	CV	2009	13.4	1.56	12.59 ± 0.0	1.652 ± 0.000	-0.81	0.092	-0.091	0.010
2017.9342	22546+2020	BU 847	3	CV	2010	35.6	6.92	36.17 ± 0.0	6.872 ± 0.002	0.57	-0.048	0.072	-0.006
2018.9233	22550+3304	KU 66	5	CV	2009	2.5	3.46	2.610 ± 0.03	3.658 ± 0.004	0.11	0.198	0.011	0.020
2017.9342	22580+2240	BRT2510	2	CV	2005	268.8	3.02	269.98 ± 0.0	3.056 ± 0.000	1.18	0.036	0.091	0.003
2017.9205	23002+2409	TDT3834	3	CV	2009	16.3	2.45	15.91 ± 0.2	2.496 ± 0.034	-0.39	0.046	-0.044	0.005
2017.9342	23042+2438	J 211	3	CV	2009	147.9	2.60	149.48 ± 0.5	2.426 ± 0.057	1.58	-0.174	0.177	-0.019
2017.9041	23049+0122	J 622	3	CV	2010	320.1	4.06	320.18 ± 0.0	4.155 ± 0.006	0.08	0.095	0.010	0.012
2017.9205	23055+0407	HO 485	3	CV	2010	46.9	5.38	47.2 ± 0.1	5.665 ± 0.013	0.30	0.285	0.038	0.036
2018.9233	23134+4603	A 199	5	CV	2009	278.0	2.25	279.62 ± 0.16	2.206 ± 0.022	1.62	-0.044	0.163	-0.004
2017.9370	23171+2045	BRT2512	3	CV	2010	350.4	3.64	351.4 ± 0.0	3.709 ± 0.011	1.00	0.069	0.126	0.009
2017.9342	23180+1032	FOX 47	3	CV	2010	279.8	4.83	280.24 ± 0.5	4.736 ± 0.062	0.44	-0.094	0.055	-0.012
2017.9370	23204+2915	FOX 101	3	CV	2009	45.7	2.38	47.22 ± 0.2	2.262 ± 0.021	1.52	-0.118	0.170	-0.013

Table 2 continues on the next page.

Measurements of 628 Pairs: The 2018 Observing Run at Brilliant Sky Observatory

Table 2 (continued). Measures of 596 Pairs Without Known Orbits or Rectilinear Solutions

					Last Reported			Measured		Changes from Last		Change per Year	
Date	WDS Number	Discoverer	Observations	Method	Year	θ	ρ	θ	ρ	θ	ρ	θ	ρ
2017.9370	23232+2439	TDT4012	3	CV	2009	36.6	2.30	40.04 ± 0.5	2.153 ± 0.039	3.44	-0.147	0.385	-0.016
2017.9342	23279+1108	STF3014	3	CV	2011	277.0	8.10	278.52 ± 0.0	8.148 ± 0.031	1.52	0.048	0.219	0.007
2017.9370	23280+1024	ROE 137	3	CV	2010	61.2	8.40	61.76 ± 0.1	8.464 ± 0.018	0.56	0.064	0.071	0.008
2017.9205	23287+1157	A 1239	3	CV	2008	53.2	2.02	52.99 ± 0.0	2.074 ± 0.001	-0.21	0.054	-0.021	0.005
2017.9370	23293+2949	ES 400	3	CV	2008	211.0	6.15	211.05 ± 0.0	6.046 ± 0.006	0.05	-0.104	0.005	-0.010
2017.9205	23302+1359	HU 999	3	CV	2005	141.9	1.59	141.25 ± 0.1	1.608 ± 0.010	-0.65	0.018	-0.050	0.001
2017.9205	23314+0317	BAL2068	3	CV	2010	74.7	7.14	74.45 ± 0.0	7.178 ± 0.001	-0.25	0.038	-0.032	0.005
2017.9370	23345+2703	COU 440	2	CV	2009	235.6	1.78	236.31 ± 0.1	1.779 ± 0.011	0.71	-0.001	0.079	0.000
2017.9342	23352+1133	HJ 3203	3	CV	2010	211.2	6.59	211.71 ± 0.1	6.621 ± 0.005	0.51	0.031	0.064	0.004
2017.9205	23355+0850	BRT3372	3	CV	2010	120.0	5.20	119.66 ± 0.0	5.535 ± 0.006	-0.34	0.335	-0.043	0.042
2017.9370	23356+2816	BRT 230	3	CV	2011	5.8	3.20	6.53 ± 0.2	3.190 ± 0.002	0.73	-0.010	0.105	-0.001
2018.9233	23357+3830	AG 296	5	CV	2008	55.2	5.93	54.00 ± 0.02	5.727 ± 0.002	-1.20	-0.203	-0.110	-0.019
2018.8301	23372+3439	HO 201	5	CV	2010	346.7	3.53	346.71 ± 0.06	3.637 ± 0.005	0.01	0.107	0.001	0.012
2018.9233	23372+3439	HO 201	5	CV	2010	346.7	3.53	346.77 ± 0.05	3.640 ± 0.003	0.07	0.110	0.008	0.012
2018.8301	23392+3535	HO 203	5	CV	2009	131.5	3.80	130.51 ± 0.02	3.879 ± 0.003	-0.99	0.079	-0.101	0.008
2018.9233	23392+3535	HO 302	5	CV	2009	131.5	3.80	130.47 ± 0.05	3.886 ± 0.002	-1.03	0.086	-0.104	0.009
2017.9342	23397+1403	HEI 298	3	CV	2009	315.3	3.15	315.39 ± 0.6	3.056 ± 0.024	0.09	-0.094	0.010	-0.011
2018.8301	23415+3247	ES 2327	5	CV	2009	55.6	3.29	54.99 ± 0.08	3.435 ± 0.003	-0.61	0.145	-0.062	0.015
2018.9233	23415+3247	ES 2327	5	CV	2009	55.6	3.29	55.08 ± 0.07	3.408 ± 0.005	-0.52	0.118	-0.052	0.012
2018.8301	23417+3147	HJ 992	5	CV	2010	255.4	6.77	255.67 ± 0.03	6.930 ± 0.006	0.27	0.160	0.031	0.018
2017.9342	23455+1223	AG 248	3	CV	2010	85.0	4.90	86.69 ± 0.2	4.592 ± 0.010	1.69	-0.308	0.213	-0.039
2017.9370	23467+2521	TDT4186	3	CV	2009	230.3	1.84	231.17 ± 0.0	1.825 ± 0.008	0.87	-0.015	0.097	-0.002
2018.9233	23472+3044	A 1244	5	CV	2009	270.7	2.62	272.02 ± 0.01	2.658 ± 0.002	1.32	0.038	0.133	0.004
2017.9205	23474+0928	A 1245	3	CV	1999	30.0	2.04	30.3 ± 0.1	2.063 ± 0.003	0.30	0.023	0.016	0.001
2018.9233	23512+4847	A 795	5	CV	2001	317.8	1.26	317.97 ± 0.17	1.239 ± 0.003	0.17	-0.021	0.009	-0.001
2017.9370	23522+2835	HO 204	3	CV	2010	356.6	5.66	356.75 ± 0.0	5.930 ± 0.009	0.15	0.270	0.019	0.034

Table 2 concludes on the next page.

Measurements of 628 Pairs: The 2018 Observing Run at Brilliant Sky Observatory

Table 2 (conclusion). Measures of 596 Pairs Without Known Orbits or Rectilinear Solutions

					Last Reported			Measured		Changes from Last		Change per Year	
Date	WDS Number	Discoverer	Observations	Method	Year	θ	ρ	θ	ρ	θ	ρ	θ	ρ
2018.9233	23544+3700	ES 2005	5	CV	2004	148.9	5.79	147.95 ± 0.06	6.071 ± 0.009	-0.95	0.281	-0.064	0.019
2017.9370	23560+2815	A 425	3	CV	2009	160.9	1.85	161.23 ± 0.0	1.878 ± 0.001	0.33	0.028	0.037	0.003
									Cumulative	29.55	42.03	-3.39	4.33
									Mean	0.05	0.07	-0.01	0.01

The "True" Movement of Double Stars in Space

Wilfried R.A. Knapp

Vienna, Austria

wilfried.knapp@gmail.com

Abstract: Common movement of any kind (proper motion, transverse velocity, radial velocity, total or spatial velocity) of double star components is neither a sufficient nor a necessary criterion to consider a double star as likely physical. This proposition is substantiated by analysis of the movement of double star components in space and confirmed by counter-checking with double stars listed in the 6th Catalog of Orbits of Visual Binary Stars. An earlier suggested assessment scheme for potential gravitational relationship (PGR) based on the likely distance between the components of a double star is discussed more in detail.

1. Introduction

Several recent papers like for example:

- Harshaw 2018 with the statement that in general, doubles with an orbit should have common proper motion
- Greaves 2019 with the assumption that common radial velocity allows for the conclusion that a double star is physically related
- Bryant 2019 with the assumption that common spatial velocity allows for the conclusion that a double star is physically related
- Jiménez-Esteban et al. 2019 with the idea that co-moving systems should be considered as physically bound
- Winter et al. 2019 with the statement "A wide companion would have a similar proper motion to its primary and would thus appear to move in the same direction at the same speed across the sky"

made me aware, that the common notion that common movement of any kind is required for a double star to be considered as likely physical needs a closer look. I have reported myself a considerable number of double stars as likely physical by means of common proper motion (Knapp 2018 – 495 and 2126 CPM pairs) for which a critical review already took place (Knapp 2019) with the result that only ~20% of these pairs are potentially bound by gravitation. See also Appendix B for a counter-check of object samples from the reports mentioned above.

2. Data on Movement of Double Stars

RA/Dec coordinates, angular separation, position angle, magnitude, spectral class, proper motion, parallax, radial velocity and in best case orbital elements are the data usually used to describe the properties of double stars. The "true" movement through space of the components of a double star can at least for a given point of time derived from such data and used for the purpose to draw conclusions if a double star might be considered physical or not. During the work on the "A Catalog of High Proper Motion Stars in the Southern Sky" report (Knapp and Nanson 2019) I became aware that especially common proper motion (meaning very similar to identical proper motion vector length and direction) is not necessarily required for a double star to be considered physical but also that common proper motion pairs are very often most likely not (or not anymore) bound by gravitation.

The term "motion" suggests that proper motion data indicate a specific movement of stars – but as a matter of fact these data reflect "only" the position change of a star in the used RA/Dec coordinate system between two observation epochs given as *pmRA* and *pmDE* in mas/yr for RA and Dec calculated as

The "True" Movement of Double Stars in Space

$$pmRA = \left(RA2 - RA1\right)\frac{\cos\left(DE1\right)}{\Delta t}$$

and

$$pmDE = \frac{DE2 - De1}{\Delta t}$$

with *RA1* and *DE1* for the coordinates of observation 1 and *RA2* and *DE2* for the coordinates of observation 2 and Δt for the time delta between the observations. The cosine of *DE1* is needed due to the spherical property of the coordinate system with the caveat that this formula is sufficiently precise only for small position deltas which is usually the case even for stars with very high proper motion.

Proper motion data thus depend on the time frame given and are for this reason not constant values but usually slightly changing when considering different time frames and as already mentioned proper motion data give no direct information on star movement itself but reflect only the effects of the true motion of the star related to the RA/Dec coordinate system.

Identical proper motion vector length and direction values might even stand for very different star movement depending on the distance of the star – for example a *pmVL* (proper motion vector length calculated from *pmRA* and *pmDE* as $mVL = (pmRA^2 + pmDE^2)^{1/2}$) of 50mas/yr indicates a star movement perpendicular to our line of sight (transverse or tangential velocity *Vt*) of ~145km/s if the distance to the star is 100 light years but only ~14.5km/s with a distance of 10 light years. The distance of a star in parsecs can easily be calculated with the simple if less reliable parallax inversion $d = 1000/Plx$ or be determined by looking up the VizieR I/347 catalog ("Distances to 1.33 billion stars in Gaia DR2" from Bailer-Jones et al. 2018) and the distance in light years can then be calculated by multiplication of parsec with 3.261631. The transverse velocity can in a shortcut be calculated directly from *pmVL* and *Plx* as

$$Vt = 4.74\frac{pmVL}{Plx}$$

But also transverse velocity *Vt* is not the "true" movement of a star because it does not reflect the depth of the space, but only the apparent tangential star movement.

The movement of the star along the line of sight away from or towards our solar system is the radial velocity *Vr*, usually given in km/s and can be quite high even if proper motion and, consequently, the transverse velocity is near zero.

Finally the combination of transverse and radial velocity using Pythagoras' theorem gives the overall star velocity V in space again in km/s:

$$V = \sqrt{Vt^2 + Vr^2}$$

Here the proper motion data joins in again as the proper motion vector direction indicates in combination with the direction of the radial velocity the plane of the star's movement (up/down and left/right) and the angle between total and radial velocity indicates if the movement is more radial if zero to 45° or more transverse if 45 to 90°, both in relation to the RA/Dec coordinate system.

GAIA DR2 provides for many objects not only precise coordinates but also proper motion, parallax and radial velocity data so everything is in place to calculate the movement of a star through space if only for a specific point of time.

It is usually assumed that if significantly high movement data values overlap each other for both stars within the given error range this allows for assessing a double star for being likely a physical pair – the WDS catalog uses for such cases the code "V" standing for "Proper motion or other technique indicates that this pair is physical". Indeed the selection of double stars by criteria of this kind certainly increases the chance for a positive hit significantly if only because high motion values are mostly connected with stars rather close to

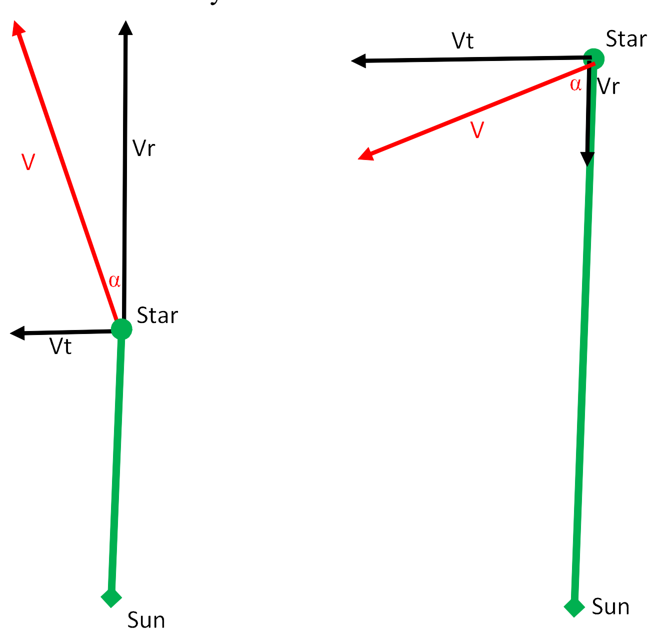

Figure 1: Velocity of stars. Vt = transverse velocity, Vr = radial velocity, V = total velocity of the star, α = angle of total velocity

our solar system. Yet the likelihood that common proper motion pairs qualify for PGR seems to be in average less than 25% as is shown for example in two reports on such objects (Knapp 2019 on KPP and SKF objects). And the overall quality of such a selection process is certainly less than satisfying because the hit rate gets the larger the larger the error range gets and on the other side it leads to the exclusion of double stars being very well likely physicals – so common proper motion, common transverse velocity, common radial velocity, common total velocity, common parallax are obviously not sufficient criteria to declare a pair of stars as likely physical. Stars close enough for potential gravitational relationship (PGR) will in many if not most cases not have "common" movements due to gravitational forces as even the most simple idea of an orbit defines the movements of the secondary as significant different from the movements of the primary depending on the position of the secondary in the orbit. The speed of the secondary in very eccentric orbits can change from nearly zero in apastron (maximum distance to barycenter) to 100km/s or more in periastron (smallest distance to barycenter) and can thus be a significant part of the total velocity of the secondary. The total velocity of the secondary is for this reason often very different from the total velocity of the primary.

This means in consequence a total switch of perspective: Not common but over time changing movement of the components of a visual double star over time is useful for assessing if a pair is likely physical or optical. This concept is already some time in use if so far mostly for detecting the wobble of the primaries of visually unresolved pairs. For example searching for radial velocity variations is especially useful for detecting binaries with very short periods (Ashley at al. 2019) or looking for proper motion anomalies helps to detect so far unrecognized companions (Graczyk at al. 2019). A recent paper on the topic of proper motion anomalies (Kervella et al. 2019) gives a detailed discussion of this approach aiming at the detection of long period orbit multiples by comparing long term proper motion values based on comparison of Hipparcos to GAIA DR2 coordinates with the short term proper motion values of Hipparcos and GAIA DR2. And Bessel published already 175 years ago his report about variations of the proper motion values of Sirius (Bessel 1844) assumed to be caused by an unseen companion – visually resolved for the first time about 20 years later.

3. True Movement of Double Star Components with Gravitational Relationship

While in many cases gravitational relationship might simply mean traveling through space close enough to influence the direction and velocity of nearby star movements for some time to a measurable extent the most interesting form of such a relationship is a common center of gravitation (barycenter) with both stars traveling on ellipses around this center.

As the movement of the barycenter of a star system is usually not zero what we see is a wobble of the primary along the path of the barycenter and a larger wobble of the secondary along the path of the primary depending on the masses and other properties of the components of the star system like velocity and direction and speed of spin. This effect on the primary is true even for very unequal masses of the components – even the Sun wobbles due to the effects of the masses of the planets.

The basic model of a double star orbit corresponds to the movement of planets around a star: A low mass secondary moves on an elliptical path around a high mass primary with the barycenter inside the primary as shown in Figures 2 to 4. This basic model is obviously more fiction than fact but certainly a useful concept for describing true physical pairs.

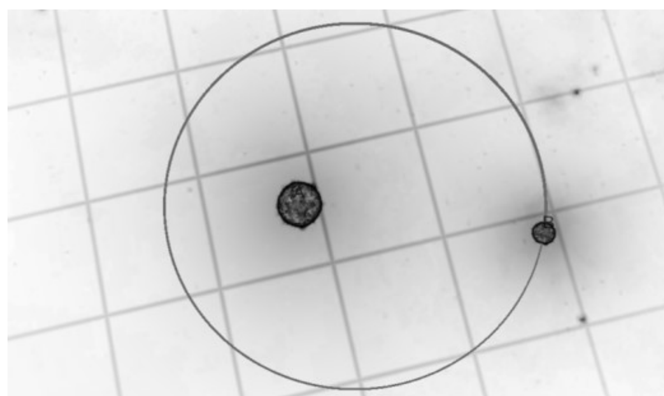

Figure 2: Basic model of an orbit

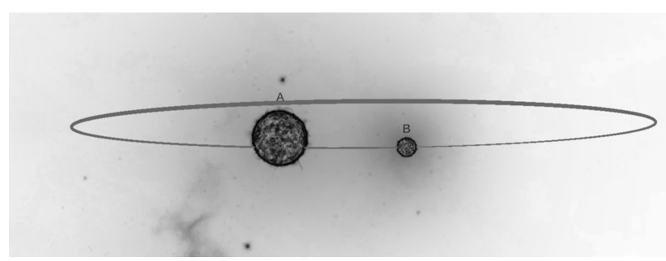

Figure 3: Same apparent orbit seen with different plane

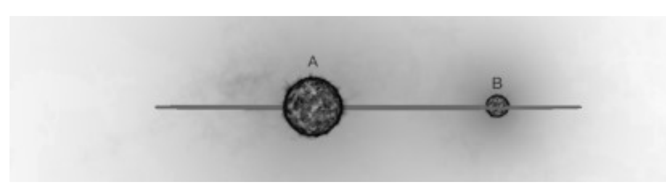

Figure 4: Same apparent orbit seen from the side – B seems to move just back and forth

The "True" Movement of Double Stars in Space

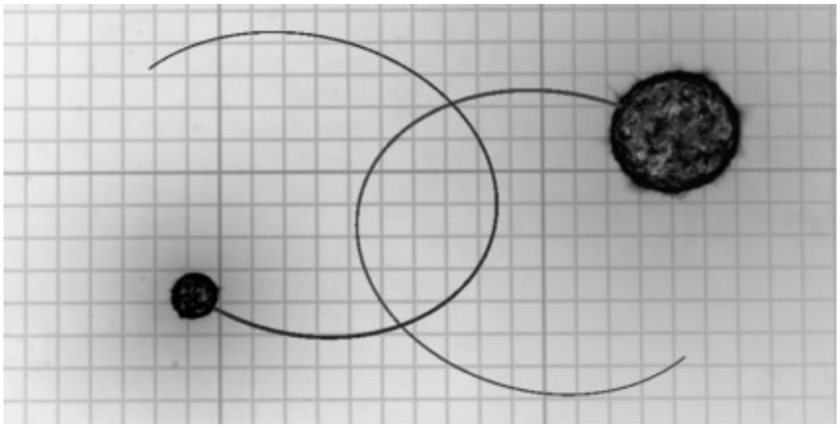

Figure 5. Two stars move on separate orbits around the barycenter

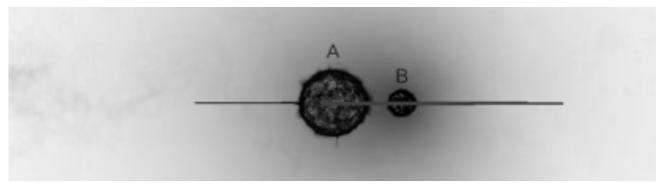

Figure 6. Same two orbits seen from the side – again B seems to simply move back and forth

The more realistic model of a double star orbit: Two components move on their own ellipses around the barycenter of the system (Figures 5 and 6).

Adding some velocity to the double star as system gives a more dynamic picture: The primary wobbles along the movement of the barycenter, the secondary moves in a spiral around the path of the primary (Figures 7 and 8).

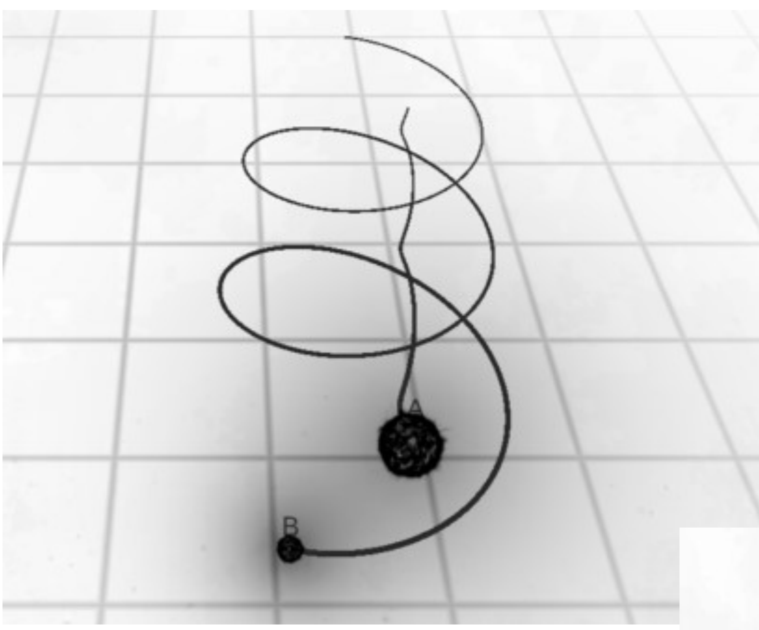

Figure 7. Primary wobbles along the movement of the barycenter, the secondary moves in a spiral around the path of the primary

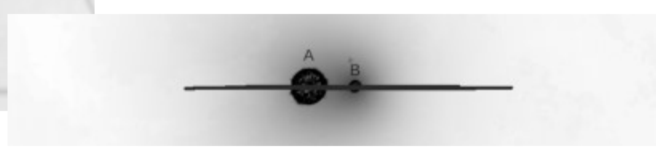

Figure 8. Same scenario seen from the side – again B seems to move back and forth

The "True" Movement of Double Stars in Space

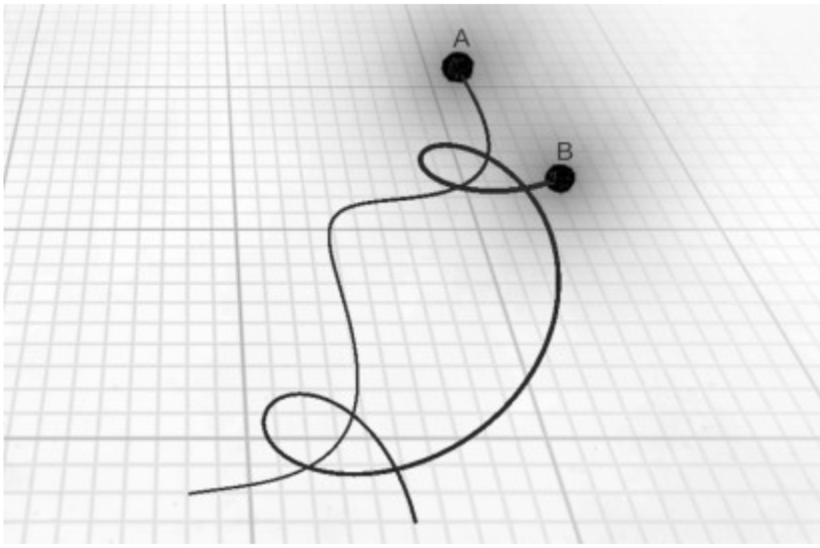

Figure 9: Wobble of the primary more pronounced by larger mass of the secondary

Similar scenario as above but wobble of the primary gets more pronounced due to a larger mass of the secondary, illustrated in Figure 9.

Another possible scenario is a high velocity binary system with equal mass components moving more or less parallel with similar speed despite very eccentric orbits just overtaking each other from time to time combined with switching lanes as illustrated in Figure 10. This scenario allows for common proper motion as well as common transverse, radial and total velocity despite gravity influences between the components. Such a scenario is certainly possible but rather not the rule.

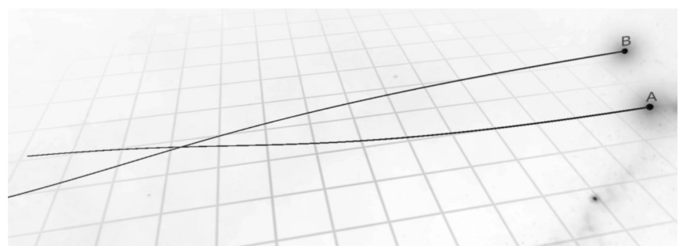

Figure 10: Fast moving double star system

Next we have the scenario of high total velocity stars crossing the path of other stars nearby leading to changes for the path of all involved stars without inducing an orbit, Figure 11.

Similarly there is the scenario of stars born in the same cloud of dust and gas traveling with similar speed in similar direction but without noticeable gravitational relationship between at least most of the stars – this is then the field of Open Clusters.

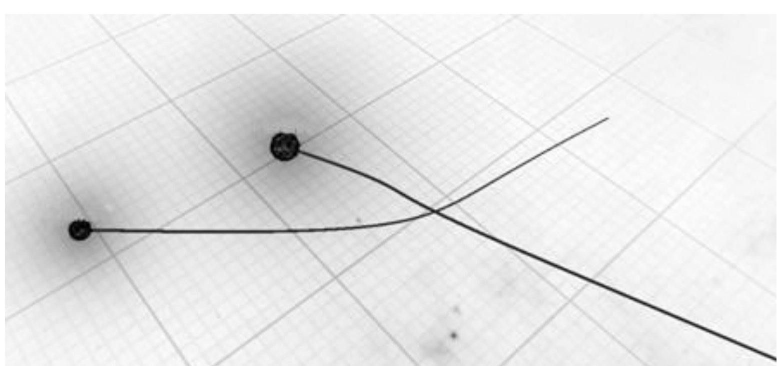

Figure 11: Crossing paths

The different scenarios described above support very strongly the proposition that common movement data of any kind starting with common proper motion up to common total velocity seem to be no good criteria for assessing a double star for PGR. At least in cases with rather fast orbits speed and direction of the motion of especially the secondaries depend very much on the current position in the orbit and there is only a random chance that at any given point in an orbit both components share common movement values.

A closer look at the data of a double star with a known orbit provides additional evidence for this proposition. The example of the 6th orbit catalog object KR 60 AB shows clearly the effect of the orbit on the apparent proper motion of the secondary – in Figure 12, the black line represents the proper motion for the primary (assuming that the barycenter is within or close to the primary) and the red line for the secondary for the time frame 1950 to 1968 (just for demonstration, not to scale) – it is obvious, that the components of a double star with an orbit do not have common movement of any kind besides being members of a system with additional movements added to the path of the barycenter. Only the rare case of an observation epoch delta equal to the orbit period would provide common proper motion for a pair with a fast orbit and in case of a slow orbit any small observation epoch delta might also provide common proper motion if the data changes are smaller than the error range of the measurements – but both cases are rather exceptions than the rule.

4. Cross-matching WDS 6th orbit catalog with GAIA DR2

According to Lindegren et al. 2018 (see conclusions paragraph) GAIA DR2 does not discriminate between the movement of a binary system and the by gravitationally-induced extra movement of the components within the system. Both the parallax and the proper motion values are calculated under the assumption that each object is a single star. The deviation from the single star model may be large enough to give for the components of a star system incorrect proper motion and parallax values depending on the properties of a binary like mass, velocity, distance between the components and the different aspects of the observations like number of observation epochs and scanning angles with respect to the plane of a potential orbit. According to Graczyk et al. 2019 this might be a minor issue for close binaries not resolved but examples like KR 60AB give very good evidence for such issues with visually resolved binaries: While the parallaxes for both components are similar enough to suggest PGR with 100% likelihood the given proper motion values result in completely different proper motion vectors caused by the extra orbit motion as demonstrated by the CDS Aladin tool (see Image 1). A side effect of this issue are definitely wrong J2000 positions calculated by CDS VizieR using the GAIA DR2 J2015.5 positions and applying the given proper motion data. This situation seems to be a regular pattern especially for binaries with a rather short period orbit.

That the given parallax error range is in such cases

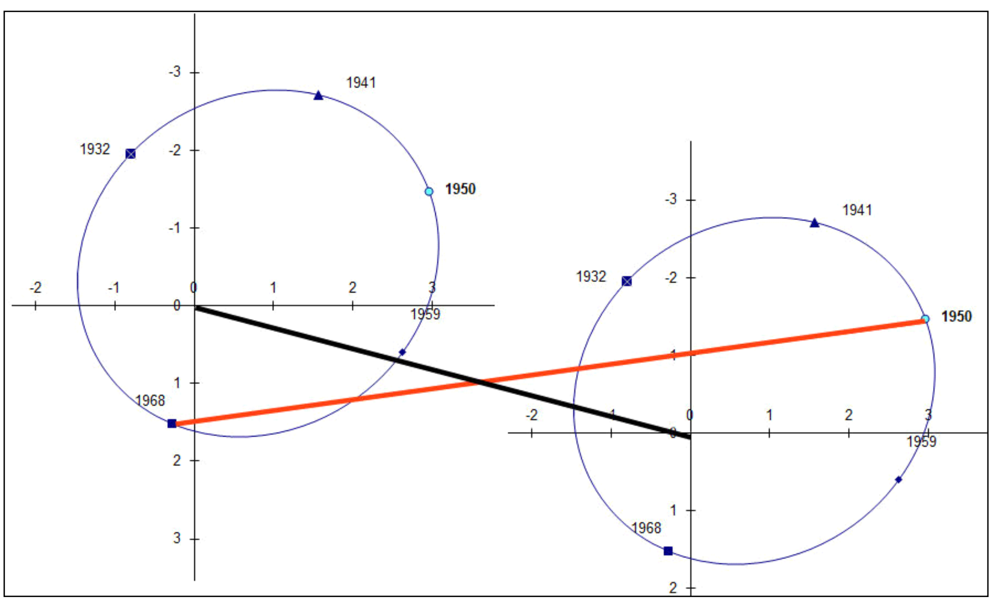

Figure 12: Example Orbit KR 60 AB

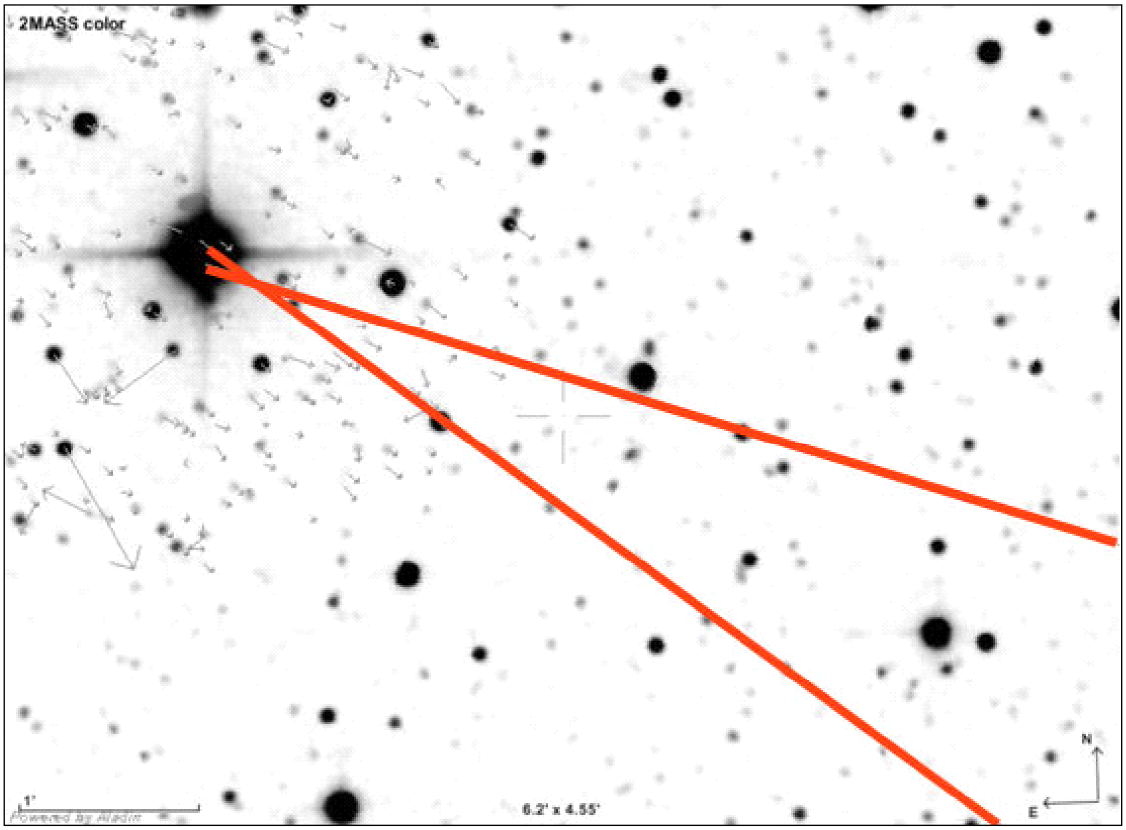

Image 1: GAIA DR2 proper motion vectors for KR 60AB according to CDS Aladin

often rather large when compared with the GAIA DR2 average might be a hint that there is also a minor issue with the given parallax values.

With the caveat that this DR2 data issue might result in proper motion and parallax errors far beyond any given error range a cross-match of the WDS 6th orbit with the GAIA DR2 catalog should provide additional evidence for the proposition that common movement of any kind is neither a sufficient nor a required condition to consider a double star as physical and that the criterion "distance between the components" is far more efficient. This statement refers not only to proper motion but also to transverse velocity and spatial velocity – especially proper motion alone seems to me no longer of significance because it represents only a small part of the relevant data necessary to calculate the spatial movement of a star. But common spatial movement (same speed and direction) might be of interest even in the case of small to no PGR likelihood, indicating that these stars are potentially born in the same molecular cloud if the spatial distance is smaller than 100 light years.

The WDS 6th orbit catalog lists per end of Nov 2018 a total of 2,941 suggested orbits for 2,868 objects as for a few objects two or more different orbits were calculated. These apparent orbits are the projection of the true orbits on the plane of the sky (Alzner 2012) with the movement of the barycenter considered to be identical with the movement of the primary and are listed with a grade rating 1 to 9 suggesting very high to very low reliability. The WDS catalog lists 2,179 objects with note code "O" indicating a given orbit – the difference to the number of 6th orbit catalog are explained by the large number of orbits with grade 9 considered not reliable enough to give an "O".

A first attempt to cross-match WDS objects with an orbit with GAIA DR2 was already done in Knapp and Nanson 2019 (HPMS3 catalog, Appendix B) but this time the intention is to go more into the details and to check as many WDS objects as possible with code "O" for common movement and for PGR based on parallax and angular separation of the components.

About 2/3 of the WDS code "O" objects have a separation of less than 0.4 arcseconds meaning below the GAIA DR2 resolution limit (Arenoux et al. 2018) – this limitation reduces the number of objects suited for

The "True" Movement of Double Stars in Space

cross-matching to 883.

The cross-match with DR2 for the primaries of these 883 objects was then done with CDS X-match with a search radius of 10 arcseconds around the J2000 positions to avoid possible position issues due to high proper motion and other movements. The total number of matches was 1,400 including all resolved secondaries up to 10 arcsecond separation. The usual next step would have been the cross-match for the secondaries based on the calculated positions with the given separation and position angle but to avoid again issues with orbit induced changes of separation and position angle I decided to work through this list manually limiting this way the overall cross-matching process to the pairs with less than 10 arcseconds separation. The manual matching process allows also for checking for missing primaries not found within the 10" search radius.

Results of the manual matching process:

- 103 or close to 12% of the selected WDS 6th orbit catalog objects were not found at all simply due to missing DR2 objects for the primary
- For 393 or close to 45% of the selected WDS 6th orbit catalog objects no secondary was found in DR2 mostly with separations below 1" (a known weakness of DR2 – see Knapp 2019, Cross-Match of WDS TDS/TDT objects with GAIA DR2)
- 5 of the selected WDS 6th orbit catalog objects could not be matched with DR2 due to combined components like for example for STF1196AB,C
- The remaining 344 pairs or 39% were considered correct matches.

Next step was then checking for proper motion and parallax data with the result that 77 pairs had to be eliminated due to missing proper motion and parallax data necessary for assessment regarding common proper motion and potential gravitational relationship with a meagre remaining number of 267 pairs suited for assessment.

These numbers suggest that the double star resolution performance of GAIA DR2 is overall quite poor.

Next step was then to check these 267 objects for common movement of any kind:

- Proper motion: Only 18 means less than 7% of these pairs were found with proper motion data similar enough to allow for positive CPM assessment according to the Knapp & Nanson scheme (see Appendix A) – this strongly suggests that common proper motion is not a suitable criterion for detecting physical pairs
- Radial velocity: Out of the 267 pairs only 34 (only about 13%) have DR2 radial velocity data for both components with 12 of them with overlapping error range as minimum criterion for common radial velocity – besides the fact that radial velocity data is still scarce this also indicates that common radial velocity seems of limited value for detecting physical pairs
- Total or spatial velocity: Existing radial velocity data allows for calculating total velocity. Only 6 cases out of the 34 pairs with radial velocity data available resulted in total velocity values similar enough to be considered common– so also common total velocity does not seem to provide any significant information valuable in this context.

Next step was then to check these 267 pairs for PGR based on distance between the components using the Knapp 2018 assessment scheme (see Appendix A). Several examples were additionally counter-checked with a Monte Carlo simulation (sample size 30,000) using normal distributions for the GAIA DR2 RA, Dec and Plx values with the given error range as standard deviation to get closer insights:

- 173 (about 65% out of 267) pairs got a positive assessment result for PGR by the criterion of distance between the components likely less than 200,000 AU. This shows that this criterion seems valuable for detecting probably physical pairs with good likelihood for an orbit. Examples are:
  - ◊ STF3007AB: Figure 13. With the given data for position and parallax and error range more than 99% of the simulation sample provide a distance below 200,000 AU with a mean value of ~60,000 AU and an asymmetrical distribution (see graph below) due to the simple fact that zero is a natural limit for a distance. The position angle 2015.5 does even with some allowance not match very well with the

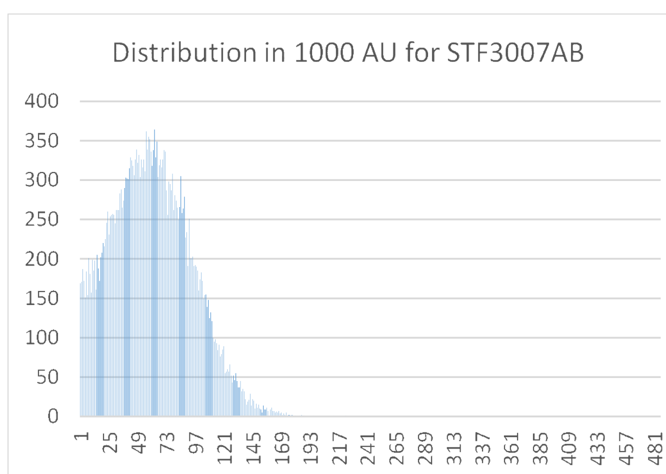

Figure 13: Distance distribution in 1000 AU for STF3007AB

The "True" Movement of Double Stars in Space

orbit data for 2016. The given orbit period is with 2161 years very long and the so far 276 observations cover only less than one tenth of the assumed orbit if in a rather conclusive part. Smallest distance by simulation is ~225 AU suggesting an orbit period of at least 2,400 years (using this distance as minimum semi-major axis of a potential orbit applying Keplers 3rd law with about Sun mass for both components). The currently given orbit might be a bit questionable but the likelihood for gravitational relationship seems quite high. A rather long period orbit might also be the reason that the proper motion values are similar enough for a positive CPM rating.

- ◊ WIR 1AB: Figure 14. This is a pair with a likelihood of 100% for a distance of less than 8,000 AU with a mean value of ~2,800 AU. The 2015.5 values for separation and position angle are a good match with the orbit values for 2016 and the 68 observations so far cover a good and significant part of the orbit with a period of 359 years. The smallest distance by simulation supports the given period so this seems to be a very solid physical pair even if the suggested orbit period would require a much smaller distance than the mentioned mean value. The proper motion values are very different resulting in a negative CPM rating.
- ◊ KAM 3AB: Figure 15. Simulation gives 100% likelihood for a distance less than 10,000 AU with a mean value of ~2,200 AU. Position angle and separation 2015.5 are a good match for the calculated orbit values. The given orbit shows a high eccentricity with the so far recorded observations in a not very conclusive part of the orbit so the orbit period might be much longer than currently assumed with 452 years. According to the simulation the smallest possible distance is ~ 79 AU suggesting a smallest possible orbit period of 500 years. Anyway this looks like a very high likelihood for gravitational relationship. The proper motion vector length is too different to allow for a positive CPM rating

- 15 of the assessed pairs were considered positive for both common proper motion and common parallax criteria which means that only 3 pairs showed common proper motion but with components too distant to suggest gravitational relationship. To check the possibility that common proper motion provides very well evidence for a like-

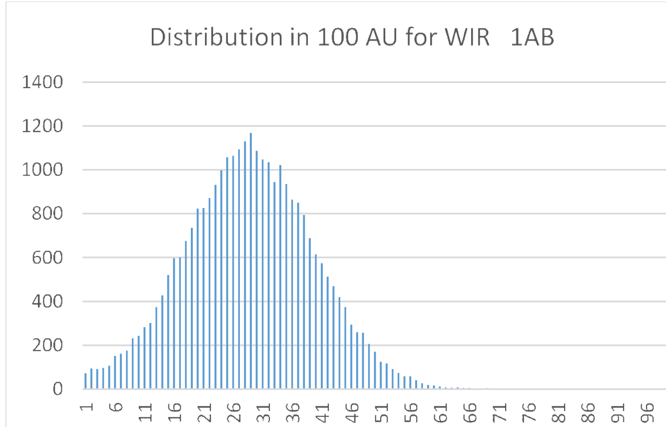

Figure 14: Distance distribution in 100 AU for WIR 1AB

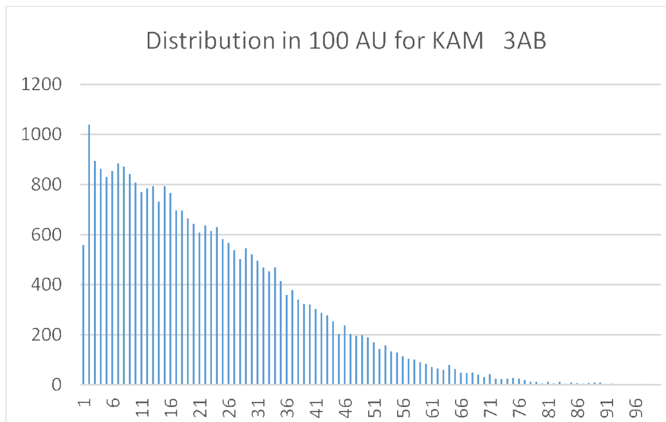

Figure 15: Distance distribution in 100 AU for KAM 3AB

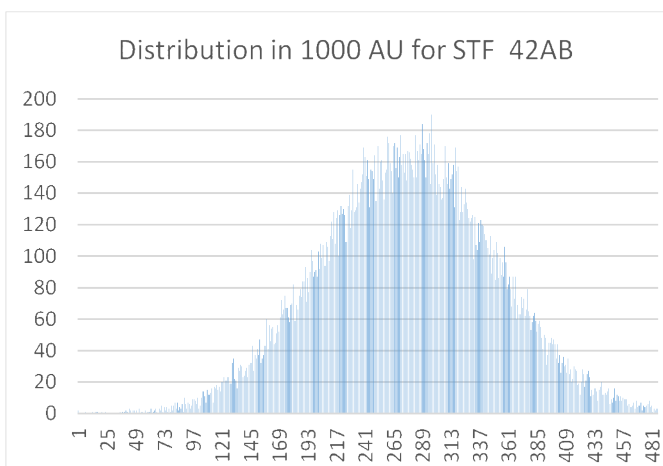

Figure 16: Distance distribution in 1000 AU for STF 42AB

The "True" Movement of Double Stars in Space

ly physical pair this needs also a closer look:

◊ STF 42AB: Figure 16. With the given data for position and parallax and error range about 15% of the simulation sample provide a distance below 200,000 AU with a mean value of ~275,000 AU and a distribution shown in the graph below. Position angle and separation 2015.5 match with some allowance very well with the orbit data for 2016 so this might be a valid orbit based on 142 observations but the given period is with 1900 years rather long and the observations cover only a small part of the assumed orbit. According to several runs of the simulation the spread for the smallest possible distance is very high and with a very tiny likelihood the smallest possible distance is ~300 AU suggesting a smallest possible orbit period of ~3,500 years. This suggests a small "might be" likelihood for gravitational relationship but with a significant longer orbit period than currently assumed

◊ I 226AB: With the given data for position and parallax and error range only a few outliers out of the simulation sample provide a distance between the components of less than 200,000 AU making the likelihood of any gravitational relationship close to zero. Position angle and separation 2015.5 do not very well match with the orbit data for 2016 and the number of observations is only 18 so this might be not such a valid orbit especially as the period is with 3,556 years very long and the observations so far cover only a tiny fraction of the assumed orbit. According to several runs of the simulation the spread for the smallest possible distance is very high and with a very tiny likelihood the smallest possible distance is ~2,500 AU suggesting a smallest possible orbit period of ~90,000 years. I 226AB seems with the given evidence to be most likely not physical

◊ STF2454AB: With the given data for position and parallax and error range about 24% of the simulation sample provide a distance below 200,000 AU with a mean value of ~380,000 AU and a rather flat distribution. Position angle and separation 2015.5 match with some allowance very well with the orbit data for 2016 so this might be a valid orbit based on 177 observations. The observations cover so far only about one third of the assumed orbit with a period of 560 years. The simulation suggests a smallest possible distance of ~100 AU meaning a smallest possible orbit period of ~700 years. Together this suggests a "might be" likelihood for gravitational relationship.

Back to the 94 (35% out of 267) pairs with a negative assessment for PGR – these need a closer look to find an explanation for the negative assessment:

- For 31 of these pairs "negative" assessment means simply a likelihood less than 50% as for the following examples:

  ◊ STF 2: With the given data for position and parallax and error range about 4% of a 30,000 simulation sample provide a distance below 200,000 AU with a mean value of ~3,250,000 AU. The huge spread caused by a rather large parallax measurement error for the primary makes this result questionable and suggests an "undecidable" likelihood for gravitational relationship due to poor parallax data quality. Position angle and separation 2015.5 match even with some allowance not this well with the orbit data for 2016. The given period is with 3,267 years very long and the so far 210 observations cover only about one tenth of the assumed orbit and this in a not very conclusive part. This one has to wait for better parallax data to come to a more conclusive assessment

  ◊ BU 391AB: A similar situation with parallax data like for STF 2 but less severe – 16% likelihood for a distance below 200,000 AU with a mean value of ~750,000 AU and again a very large spread. This suggests again an "undecidable" likelihood for gravitational relationship due to poor parallax data. Position angle and separation 2015.5 match very well with the orbit data for 2016. The given period is with 616 years not very long and the so far 79 observations cover only about one sixth of the assumed orbit but in a very conclusive part. The smallest possible distance by simulation would correspond with the given period. This one has also to wait for better parallax data to come to a more conclusive assessment but looks much better than STF 2

  ◊ STF 73AB: Figure 17. With the given data for position and parallax and error range about 14% of a 30,000 simulation sample provide a distance below 200,000 AU with a mean value of ~270,000 AU and a standard deviation of ~60,000. The parallax values for the components are similar but do not even overlap within the error range – so at first look rather not physical. But then position angle and separation 2015.5 match very well with the orbit data for 2016 and the orbit with a period of 168 years is nearly fully covered with so far 727 observations – this might then be one of the suspected cases with questionable GAIA DR2 parallax data due to the extra motion of an orbit. The GAIA DR2 data quality parameters indicate some issues with the data for the secondary with a high percentage of bad measurements and a suspected duplicity issue – may be a third component is involved.

◊ STT 21: Figure 18. With the given data for position and parallax and error range about 40% of a 30,000 simulation sample provide a distance below 200,000 AU with a mean value of ~290,000 AU with a large spread and a distribution shown in the graph below. Position angle and separation 2015.5 match very well with the orbit PA data for 2016 but not very well with separation. The given period is with 450 years not very long and the so far 128 observations cover a large but not significant part of the assumed orbit. According to simulation the smallest possible distance would be ~140 AU giving a smallest possible orbit period of ~1,170 years. This suggests a "might be" likelihood for gravitational relationship but with a much longer than assumed orbit period.

- For the remaining 63 pairs the negative assessment result means indeed a likelihood for PGR close to zero as for the following examples:

◊ HJ 2036: Figure 19. With the given data for position and parallax and error range only a few outliers of a 30,000 simulation sample provide a distance between the components of less than 200,000 AU making the likelihood of any gravitational relationship close to zero. Position angle and separation 2015.5 match very well with the orbit data for 2016 but the given period is with 1443 years very long and the 115 observations so far cover only a small fraction of the assumed orbit. The parallax error range seems acceptable for both components and the calculated distance between the components is in average about 10 light years – any gravitational relationship seems very questionable here.

◊ BU 1216: The parallax data suggests here a

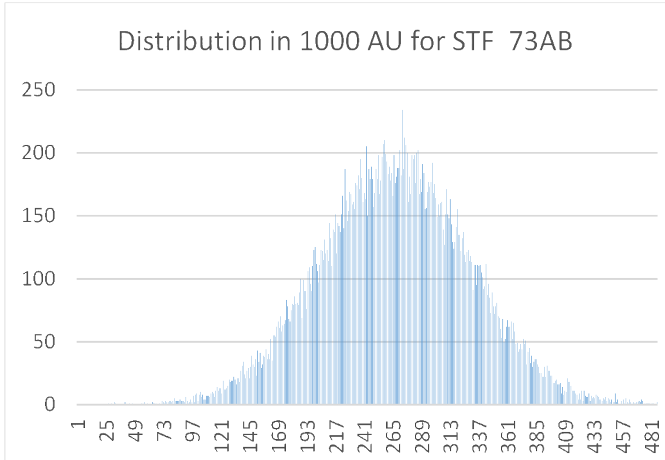

Figure 17: Distance distribution in 1000 AU for STF 73AB

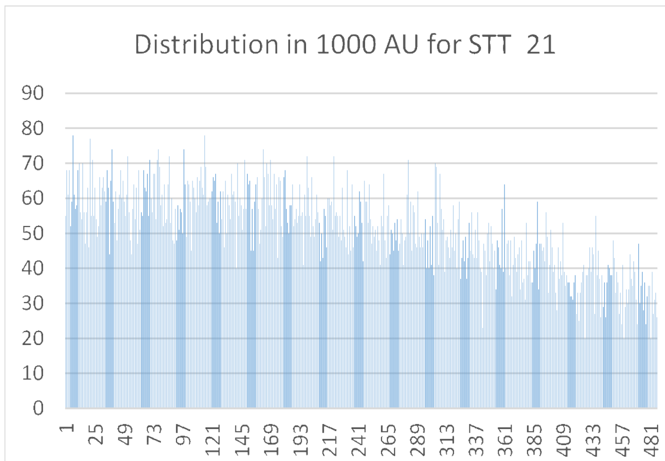

Figure 18: Distance distribution in 1000 AU for STT 21

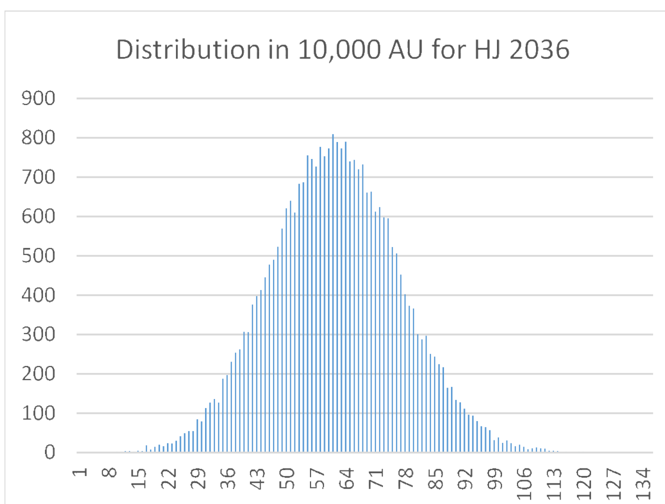

Figure 19: Distance distribution in 10,000 AU for HJ 2036

The "True" Movement of Double Stars in Space

zero likelihood for a distance between the components smaller than 200,000 AU with an average distance of 7,200,000 AU and a huge spread. The observation history with 82 observations covers a good but not very significant part of the calculated orbit. With some allowances the 2015.5 separation and PA values correspond acceptable with the orbit values for 2015 yet the given evidence speaks clearly against any gravitational relationship

◊ STF2118AB: With the given positions and parallax values only a few outliers out of a 30,000 simulation sample are within a distance of less than 200,000 AU between the components meaning a near zero likelihood for gravitational relationship. 281 observations starting with 1830 cover about half the calculated orbit with a period of 422 years. The 2015.5 measurements do not match very well with the orbit 2016 separation values putting a question mark on the reliability of the calculated orbit – overall it seems very questionable that STF2118AB should be a pair with gravitational relationship especially as the GAIA DR2 parallax values do not even overlap within the error range

◊ STT 507AB: The parallax values are completely different if with a rather larger error range excluding any possibility of gravitational relationship. The 2015.5 values for separation and position angle are at best a moderate match with the orbit values for 2016. The number of 135 observations cover about 1/3 of the orbit with a period of 566 years but the spread of the measurements compared to the calculated orbit seems a bit large – rather not a physical.

The full cross-match data set is available for downlodad from the JDSO website as fixed format text file "WDS_O_GE_0.4_X_DR2_R10.txt".

Note for HU 66BC: Confusing WDS data for HU 66: Bad match with 6th orbit catalog and STT 351 AC.

Finally I had a look at a small random sample of WDS code "O" objects with separations larger than 10 arcseconds and for this reason not included in the cross-match process described above:

◊ GRB 34AB: Figure 20 With the given data for position and parallax and error range 100% of the simulation sample suggest a distance less than 1,000 AU with a mean value ~300 AU and a standard deviation of ~136 AU. The 2015.5 values for separation and position angle are with some allowances a good match for the calculated orbit values for 2016 but the observations so far cover only a small part of the orbit period of 1,253 years so the reliability of the calculated values is a bit questionable. The likelihood for PRG seems extremely high but the orbit period might, according to the distances from to the simulation sample, be somewhat longer although also the given period is covered by the simulation results

◊ LDS1017: Figure 21 With the given data for position and parallax and error range 100% of the simulation sample suggest a distance less than 8,000 AU with a mean value ~2,640 AU and a standard deviation of ~1,330 AU. The 2015.5 values for separation and position angle (reversed) are with some allowances a

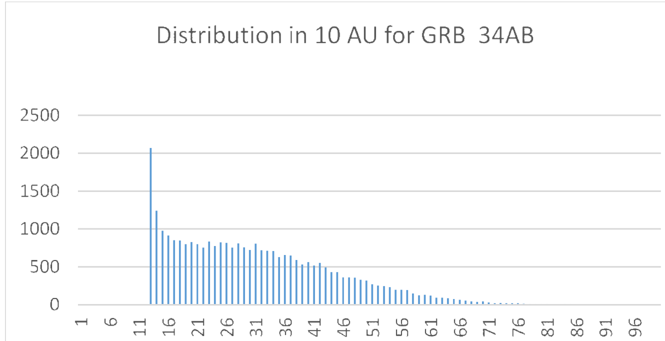

Figure 20: Distance distribution in 10 AU for GRB 34AB

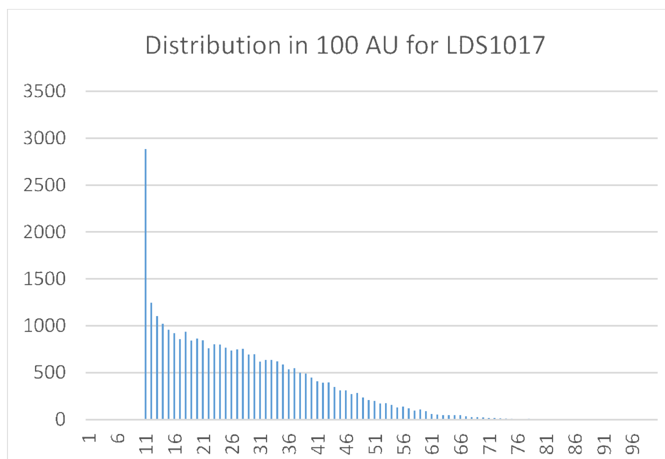

Figure 21: Distance distribution in 100 AU for LDS1017

The "True" Movement of Double Stars in Space

good match for the calculated orbit values for 2016 but the observations so far cover only a tiny part of the suggested orbit period of 360 years so the reliability of the calculated values is a bit questionable. The likelihood for PRG seems very high but the orbit period might, according to the distances from to the simulation sample, be significantly longer, the data from the simulation suggest even >20,000 years

◊ STF1217: Figure 22. With the given data for position and parallax and error range 100% of the simulation sample suggest a distance less than 100,000 AU with a mean value ~25,700 AU and a standard deviation of ~15,800 AU. The 2015.5 values for separation and position angle are with some allowances a good match for the calculated orbit values for 2016 but the observations so far cover only a tiny part of the orbit period of 1,600 years so the reliability of the calculated values is a bit questionable. Some likelihood for PRG seems given but the orbit period might according to the distances from to the simulation sample be significantly longer, the data from the simulation suggests even >25,000 years

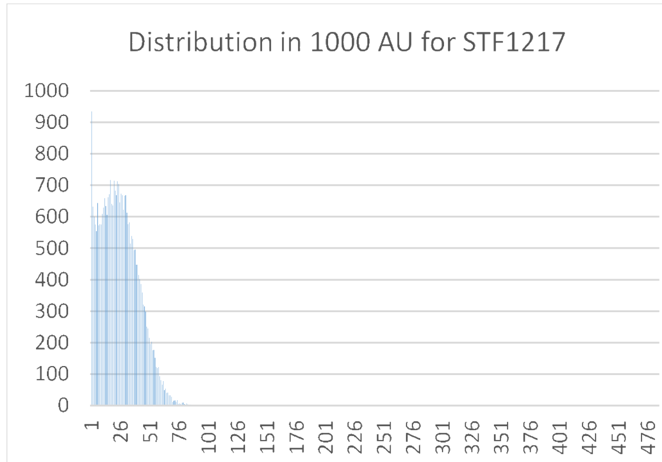

Figure 22. Distance distribution in 1000 AU for STF1217

5. Cross-Matching WDS L-Coded Objects with Gaia DR2

The WDS catalog lists per end of 2018 ~1,500 such systems with code "L" meaning significant but apparently not Keplerian motion since their discovery – a few of these systems might according to the description of the "L" code be long-period physicals but most of them are most likely optical pairs. This means that the assessment scheme for PGR should provide here only a very small number of positive results as proof of concept for a reliable hit rate not only for positive but as well also for negative assessment results.

For this purpose all L-coded WDS objects were twice cross-matched with GAIA DR2 with a 5 arcsecond search radius around the J2000 positions for the primary and the secondary. After elimination of all obviously wrong and suspect matches 1,196 objects with a delta in separation of less than 20% and a delta in position of less than 15° and reasonable delta in magnitudes were kept and only 32 (less than 3%) of these were assessed as likely physicals and 97% as most likely opticals.

A closer look at a few L-coded objects assessed as likely physical:

- STF 49: Figure 23. With the given data for position and parallax and error range 100% of a

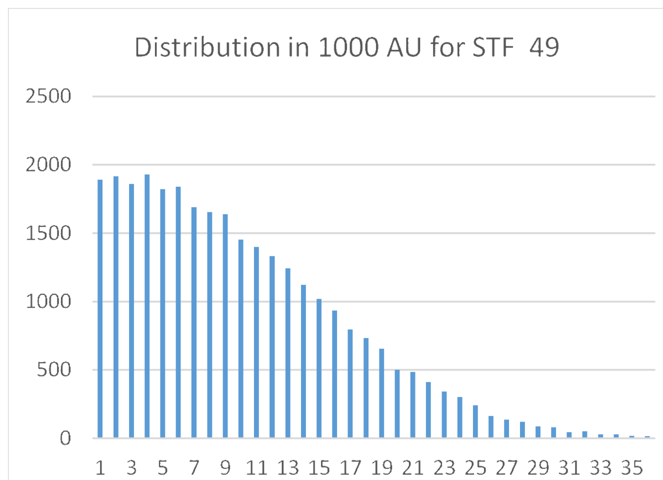

Figure 23. Distance distribution in 1000 AU for STF 49

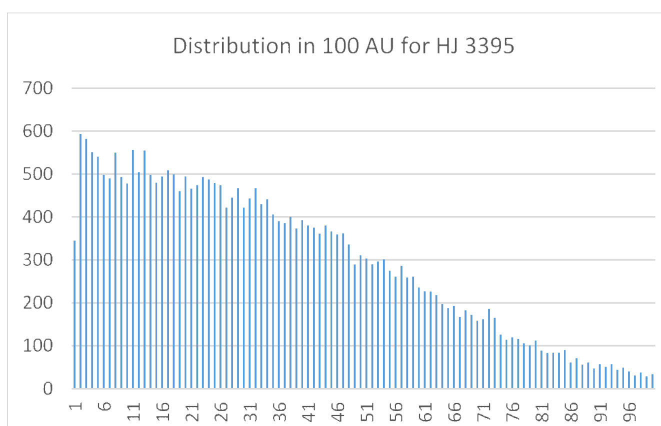

Figure 24: Distance distribution in 100 AU for HJ 3395

The "True" Movement of Double Stars in Space

30,000 simulation sample provide a distance below 200,000 AU with a mean value of ~9,450 AU and a rather large standard deviation. This suggests a realistic chance for gravitational relationship even if the mean distance value would mean a long-period orbit according to the smallest simulation results at least ~2,600 years.

- HJ 3395: Figure 24. With the given data for position and parallax and error range 100% of the simulation sample provide a distance below 200,000 AU with a mean value of ~3,400 AU and a very asymmetric distribution with 17% likelihood for a distance even below 1,000 AU. Most likely a physical pair if with a long-period orbit according to the smallest simulation results larger than ~460 years
- STF 315: Figure 25. With the given data for position and parallax and error range, 75% of the simulation sample provide a distance below 200,000 AU with a mean value of ~138,000 AU with a rather asymmetric distribution. If this distance is close enough for a realistic chance for an orbit is questionable, but there will be most likely some kind of gravitational relationship between the components.

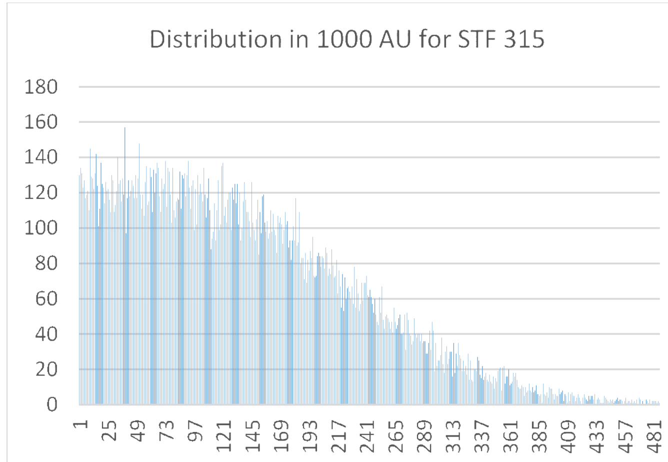

Figure 25: Distance distribution in 1000 AU for STF 315

The full cross-match data set is available for download from the JDSO website as fixed format text file "Code_L_XX_DR2_2x5s.txt".

6. Discussion of the Concept of the Assessment Scheme for Potential Gravitational Relationship (PGR)

PGR means a measureable influence of the tidal force of a single star/system on the movement of another single star/system. Gravitation works regardless of the underlying theory without a distance limit so basically all stellar objects are assumed to be in their movements influenced by gravitation. As relativistic effects seem here of little concern the equations of Newton and Kepler will provide good enough approximations. MOND suggests according to Banik 2019 additional orbit speed for wide pairs with distances between the components larger than 7,000 AU, but such small differences get lost in the overall error range of the data currently available.

To look for a radius of the gravitational field of a star might not be the best idea because in different directions nearby stars are in different large distances so the outer rim of the gravitational field of a star is most certainly not a perfect sphere and the hypothetical Oort cloud might be a fiction as there is so far no evidence that the number of objects expected to float here in space is large enough to be called a "cloud". But the assumption that a radius of ~100,000 AU corresponds with the outer rim of the gravitational field of the Sun seems plausible at least in the direction of Alpha Centauri generally considered the nearest star system next to the solar system with a distance of ~4.35 light years (Kervella et al 2016). The gravitational pull of the Sun is at 100,000 AU quite soft – about 20 days would be needed for a free floating low mass object there to move one single meter closer to the Sun if no other forces are involved and 5.6 million years would be needed to get such an object consumed by the Sun again if no other forces are involved allowing for example for a swing-by or even an orbit. Alpha Centauri (with >2 Sun masses for A plus B plus C) would already largely compensate this minimal movement and at 115,000 AU distance the free floating would go on indefinitely. On the other side even the huge distance of 100,000 AU between two stars allows for an orbit if with a very long period of ~22.5 million years and a very slow speed of only ~ 0.13km/s – an orbit of truly cosmic scale but certainly possible. Also to consider is the fact that the average star mass might be a bit smaller than the Sun mass (Winters et al. 2019) but this seems of minor consequence as gravitation works only linear with mass.

The vexing question here is how to detect such ultra-long period binaries with any degree of certainty. The availability of Gaia single position measurements over several years, in addition to the currently published summarized ones, might allow for conclusions here. I asked the Gaia team if such data will be available in the future and the answer was positive. While the measurement errors will certainly be greater than “real” changes in positions, such a data row should allow the detection of a trend in the position changes.

The average distance between single stars or star systems in our Galaxy might be somewhere around the distance between our Sun and the closest single stars/star systems nearby as there is no reason to assume that this distance is unusual. And even if this distance might be smaller than the galactic average, there remains the fact that the effective distribution of stars in space is far from equal—areas of higher density like the Solar neighborhood are separated by areas with thin star populations and the likelihood for gravitational relationship is most certainly higher in dense populated star areas. The number of stars within 100 parsec from our solar system is according to GAIA DR2 700,055 giving an average distance between the stars of ~7.3 light years (by taking a sphere volume with a radius of 100 parsec divided by equal distributed 700,000 stars). But there are some caveats regarding this number:

- The GAIA DR2 resolution of double stars is limited with 0.4 arcseconds and the resolution record for double stars with a separation up to 1 arcsecond is with an average of 36% (Knapp 2019 on TDS/TDT objects) rather low. The number of resolved systems might to some degree compensate the number of not resolved opticals but certainly by far not completely
- A small number of Gaia DR2 parallaxes is “horrendously wrong” (Lindegren et al. 2018, slide 47) – for example ~60 very faint objects are listed with a parallax larger than 760mas suggesting a distance to our Sun of less than ~4 light years and this result is highly questionable. The relation to the number of ~1,720 Gaia DR2 objects within a distance of 10 parsec would then suggest a contamination rate of ~3.5% wrong parallaxes far beyond the given error range not counting the negative parallaxes. Gaia DR2 might have some specific issues with the nearby stars because there seems to be a significant large positive bias in the parallax values for these stars compared with the overall given small negative bias of about -0.05mas (Schönrich et al. 2019). But the total number of objects is large enough to render these facts as of little significance for the average distance between stars
- Several hundred objects with very high proper motion >600mas/yr are missing, but again the total number of objects is large enough to render this fact as of little significance
- The main issue remaining is the question of overall resolution rate of Gaia DR2 for all existing stars within this distance besides the question of stars fainter than ~20Gmag.

Overall there seems currently no serious star count estimation possible based on Gaia DR2 numbers. The number of missed stars is hard to estimate due to the different star density in the different areas – the higher the star density the higher the number of missed stars. Additionally the reliability of Gaia degrades heavily with fainter stars. But even if the “real” number of stars is assumed to be twice the Gaia DR2 count we get ~ 6 light years as average distance between single stars or star systems and this seems still a bit too high.

That single stars and star systems are equally distributed in space is, as already mentioned, an oversimplification because there are certainly areas of different star density with the consequence of average distances between star systems being likely smaller than equally distributed. Then there is the special case of open clusters: For example Lodieu et al. 2019 suggest for the Hyades cluster members to be bound up to a distances of 9 parsec from the barycenter of the cluster – this might be a bit over-optimistic but the gravitation effects within open clusters are different from single stars and several of the (in Lodieu et al. 2019 table C.1) listed objects have despite very large angular separations a >50% likelihood for gravitational relationship.

As a resort data from the RECONS “Solar Neighborhood” project (Henry et al. 2018) should allow for a precise counter-check. The 100 star systems closest to our solar system (using the RECONS list from http://www.recons.org/TOP100.posted.htm) suggest with assumed equally distribution an average distance of ~4.8 light years while the based on parallax and angular separation precisely calculated average distance between star systems is with 4.3 light years about 10% smaller (see Appendix C for the full table). GAIA DR2 suggests a few new members to this list even after eliminating the objects with obvious wrong parallaxes and the large number of very faint and for this reason suspect objects – on the other side several objects of the RECONS list are missing in GAIA DR2 due to the issue with very high proper motion objects. Some interesting side results from the RECONS counter-check: Distances between star systems vary from ~1 to ~10 light years with 16 cases below 3 light years suggesting potential gravitational relationship, especially Procyon and Luyten's Star seem close enough to be considered a system. All numbers given here do not take the spread caused by parallax data errors into account but this effect is with the very large parallax values given here of little concern.

It is certainly a bit arbitrary to declare a specific number as threshold for assumed gravitational relationship but ~3 light years or 200,000 AU seem with the given intelligence to be a reasonable choice. At such a distance there might still be some minimal gravitational relationship between two average mass stars in case of areas of thin star population but in most cases there will be most likely zero individual gravity besides the tidal force of the Galaxy even if this is a static point of view because all stars move through space with velocities large enough to change the relationship betweeb stars over time significantly. Bailer-Jones et al. 2018 for example expects 700 stars to come closer than 5 pc to the Sun over the next 15 million years with 26 of them having a >50% chance to come closer than 1 pc meaning serious gravitational disturbance of our solar system. We might not even have to wait millions of years for such a scenario to happen – several of the stars within the 10pc radius have a significant negative velocity means are moving towards our solar system and this might reduce the time span of a possible close encounter to less than a few 100,000 years.

The calculation of the distance between two stars is basically easy with the given distance of the stars from the sun using the simple parallax inversion or the Bailer-Jones GAIA DR2 Distances catalog (VizieR I/347) and the angular separation applying the law of cosines. Yet special attention is needed regarding data quality (issues with duplicity, numbers of visibility periods used and other issues discussed extensively in the GAIA DR2 documentation) and the parallaxes should have a reasonable size and a small measurement error range. The reason for this requirement is simply the exponentially increasing distance between two stars with decreasing parallax, but also the exponentially growing spread for the distance caused by an increasing relative error range. For example an error range of 0.04mas means for a pair with 5 arcsecond separation and parallaxes of ~40mas a spread of a few thousand AU in the distance between the components and for a pair with parallaxes of ~4mas already a spread of several hundred thousand AU. See Figure 26.

With positions and parallaxes available for a pair of stars the ad hoc expectation is that the calculated distance for the components of such a pair should correspond with the mean value of a normal distribution for this distance – at least this expectation was the base for the "realistic distance" value in the proposed PGR assessment scheme. But the mentioned non-linear effect of parallax errors has the consequence that this is the case only for large parallax values with a small error range but not for small parallax values with an in relation large error range. The requirement to stick with parallax data with a very small error relative error is

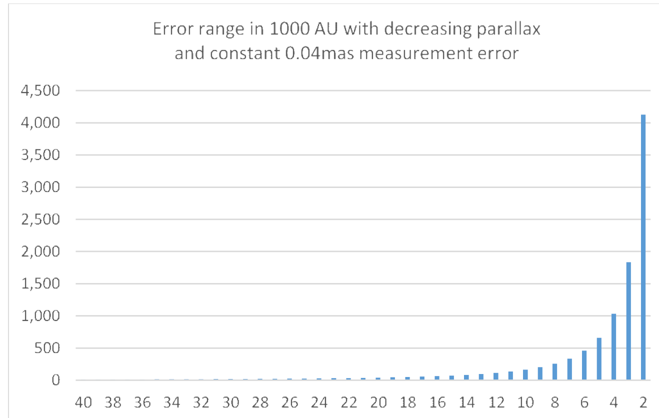

Figure 26: Error range in 1000 AU with decreasing parallax

often severely disregarded as for example by Igoshev and Perets 2019 according to the mentioned selection criterion "We keep only stars with measured parallax and proper motion with relative errors which are less than a third of their value". This is a reasonable approach to eliminate all objects with negative parallaxes including the very small ones potentially negative when applying the error range as standard deviation for a confidence interval of 99.73%. I used this approach myself in my first attempts for the PGR assessment scheme to get a grip on this issue and even Schönrich at al. 2019 work with a Plx/e_Plx ratio of 4 as data quality cut despite postulated highest precision requirements. Meanwhile it seems clear that a small parallax value with such an error size is close to meaningless at least for estimating the distance between double star components as explained above. As to expect also the difference between the lower and upper bound on the confidence interval of the estimated distances according to Bailer-Jones et al. 2018 gets in such cases quite huge – in some cases even larger than 1,000 parsec as for example for HD 313070 with Plx of 0.4269 and e_Plx of 0.0672 despite a seemingly solid Plx/e_Plx ratio of 6.35.

Using Monte Carlo simulation for the parameters involved makes quickly clear that the exponential effects of parallax errors for small parallax values results in average distance values much larger than expected combined with a very flat distribution with a huge standard deviation. For this reason the proposed PGR assessment scheme requires parallaxes > 5mas with an error range smaller than 0.5% (or Plx/e_Plx ratio >200) to work properly. These requirements reduce drastically the number of usable GAIA objects to ~430,000 so for a first impression this assessment scheme might be used also with data not meeting fully these requirements but the result needs then a very critical second look.

7. Summary

Selecting double stars with common but significant movement of any kind is basically a good approach for finding with some likelihood physical pairs but is combined with the high risk of selecting pairs with obviously no chance of gravitational relationship because the distance between the components is simply too large. So the concept of looking for common movements of any kind provides always a mixed bag of results missing at the same time good candidates for likely physical pairs with components close enough for PGR but movement data values different enough to be considered not "common". If star movement data is for whatever reasons considered as relevant for assessing a pair as potentially physical it is strongly to recommend to have additionally a closer look at the spatial distance between the components of a pair (based on parallax and angular separation) whether PGR seems likely or rather not. With accurate data on the mass of the components it would then be possible to compute the gravitational forces with some precision, but without this data, the assumption that all stars have on average a sun-like mass and that ~1 parsec distance between single stars or systems in our near Galaxy area can be considered as the edge of the gravitational field should work as an useful compromise. With a distance of less than 200,000 AU (~3 light years or ~1 parsec) between two stars gravitational relationship seems at least possible and using my assessment scheme for PGR gives an idea about the likelihood of being potentially physical or not.

The simple calculation of the distance between components using the given parallaxes leads to a wrong expectation about the average value of such a distance caused by the non-linear spread depending on parallax size and error range. Using the given GAIA DR2 coordinates and the parallax as mean values and the given error ranges as standard deviations of an assumed normal distribution (or alternatively use Bailer-Jones 2018/ VizieR I/347 distances) it is possible to calculate (at least approximately by numerical simulation) the probability for measurement results giving a specific distance between the components. This result can then be interpreted as likelihood that the pair in question has indeed a spatial distance between the components less than this specific distance. The proposal that a distance of 200,000 AU is a reasonable threshold for PGR is supported by the fact that this approach works reasonable good for positive as well as for negative results by the high hit rate when applied on the WDS code "O" objects as well as by the low hit rate when applied on the WDS code "L" objects.

The results of a Monte Carlo simulation can also be used to determine the smallest possible spatial distance between double star components as estimation of the minimum value for the semi-major axis of a potential orbit with zero inclination as for example done in Farihi et al. 2010 using photometric distance estimations. With the parallax data available in GAIA DR2 this can now be done with comparatively little effort and much higher precision – but it should be added that the likelihood for such minimum distances is usually very small so it makes sense to have also a look at the largest possible distance. And for a reasonable large PGR likelihood over 50% it is certainly better to stick with the average or median distance of such a simulation.

A weak point of the proposed PGR assessment scheme is the still often insufficient quality of the available data despite the huge step forward with GAIA DR2. Cross-matching components of multiple systems with GAIA DR2 objects seems often like kind of poking into the soft parts of this catalog:

- No resolution below 0.4 arcseconds angular separation
- Resolution performance between 0.4 and 1.0" separation far below 50%
- Insufficient coverage of the solar system neighborhood star population mostly due to insufficient coverage of very high proper motion stars
- Parallax data often of little value for calculating the distance between double star components beginning with "horrendously wrong" over negative to parallax values with an insufficient error range ratio
- All objects are treated as single stars even when obviously components of a star system without distinction between the proper motion of the barycenter of star systems and the extra motion of the components due to gravitational relationship with negative effects on proper motion and parallax data quality.

Additionally GAIA DR2 parallax data show a systematic bias of -0.03 to -0.05mas (depending on source and method applied - see Schönrich et al. 2019) although this is in the given context at least for rather large parallax values usually of little concern.

But according to the GAIA data release scenario (https://www.cosmos.esa.int/web/gaia/release) there is qualified hope that future GAIA data releases should do better in all mentioned aspects.

8. Acknowledgements:

The following tools and resources have been used for this research:

- 2MASS, DSS2 and PS1 images
- Aladin Sky Atlas v10.0
- GAIA DR2 catalog
- SIMBAD
- VizieR, TAP VizieR, X-Match
- Washington Double Star Catalog
- 6th Catalog of Orbits of Visual Binary Stars
- 6th Orbits_Calculator by Brian Workman
- My Pocket Galaxy (PocketLabs, Adam Lewis, Sean O'Neill) for creating the figures demonstrating the movement of stars bound by gravitation

Special thanks to John Greaves for his "Sprachkritik" regarding the use of the term "probability" and for his readiness to discuss in detail the question of orbit influences on proper motion values.

Special thanks to Brian Mason for giving me access to the most recent version of the Catalog of Rectilinear Elements.

9. References

Alzner A., Argyle R.W., 2012, "The Orbital Elements of a Visual Binary Star", *Observing and Measuring Visual Double Stars*, R.W. Argyle, ed., Chapter 7, Patrick Moore's Practical Astronomy Series. Springer, New York, NY.

F. Arenou, X. Luri, C. Babusiaux, et al., 2018, "Gaia Data Release 2: Catalogue validation", *Astronomy & Astrophysics*, **616**, A17.

P. Ashley, R & Farihi, J & R. Marsh, T & J. Wilson, D & T. Gaensicke, B., 2019, "Evidence for bimodal orbital separations of white dwarf-red dwarf binary stars", 10.1093/mnras/stz298

C.A.L. Bailer-Jones, J. Rybizki, M. Fouesneau, G. Mantelet and R. Andrae, 2018, "Estimating distances from parallaxes. IV. Distances to 1.33 billion stars in Gaia data release 2", *Astronomical Journal*, **156**, Number 2, pp 58.

C.A.L. Bailer-Jones, J. Rybizki, R. Andrae, M. Fouesneau, 2018, "New stellar encounters discovered in the second Gaia data release", *A & A*, **616**, A37.

Banik, Indranil, 2018, "A new line on the wide binary test of gravity", *Monthly Notices of the Royal Astronomical Society*, **480** (2), 2660–2688

Bessel, F. W., 1844, "On the variations of the proper motions of Procyon and Sirius", *Monthly Notices of the Royal Astronomical Society*, **6**, 136-141

Bryant, Tom, 2019, "New Doubles Found Using Data from the Gaia DR2 Catalog", *Journal of Double Star Observations*, **15** (1), 89.

J. Farihi, D. W. Hoard and S. Wachter, 2010, "White Dwarf–Red Dwarf Systems resolved with the Hubble Space Telescope. II. Full Snapshot Survey Results", *The Astrophysical Journal Supplement Series*, **190**, 275–296.

Dariusz Graczyk, Grzegorz Pietrzynski, et al., 2019, "Testing Systematics of GAIA DR2 Parallaxes with Empirical Surface Brightness Color Relations applied to Eclipsing Binaries", arXiv:1902.00589v1.

Greaves, John, 2019, "Using the Six Astrometric Parameters from Gaia DR2 II : Common Radial Velocity Pairs", *JDSO*, **15** (1), 77.

Harshaw, Richard, 2018, "Gaia DR2 and the Washington Double Star Catalog: A Tale of Two Databases", *JDSO*, **14**)4),734.

Todd J. Henry, Wei-Chun Jao, Jennifer G. Winters, et al., 2018, "The Solar Neighborhood XLIV: RECONS Discoveries within 10parsecs", *The Astronomical Journal*, **155**, 265 (23pp).

Andrei P. Igoshev, Hagai B. Perets, 2019, "Wide binary companions to massive stars and their use in constraining natal kicks", draft arXiv:1901.05972v1.

Jiménez-Esteban, F. M., Solano, E. and Rodrigo, C., 2019, "A catalogue of bright wide binary and multiple stars from GAIA-DR2 and the Virtual Observatory", arXiv:1901.03730, draft version submitted Jan 11th. Accepted to be published in the Astronomical Journal

P. Kervella, F. Mignard, A. Mérand and F. Thévenin, 2016, "Close stellar conjunctions of α Centauri A and B until 2050", arXiv:1610.06079v1 [astro-ph.SR].

Pierre Kervella, Frédéric Arenou, François Mignard, Frédéric Thévenin, 2019, "Stellar and substellar companions of nearby stars from Gaia DR2 - Binarity from proper motion anomaly". arXiv:1811.08902v2

Knapp, Wilfried R. A., 2018, "495 Common Proper Motion Pairs so far not WDS Listed", *JDSO*, **14** (3), 546.

Knapp, Wilfried R. A., 2018, "2126 Common Proper Motion Pairs so far not WDS Listed", *JDSO*, **14** (3), 587.

Knapp, Wilfried R. A., 2018, "A New Concept for Counter-Checking of Assumed Binaries", *JDSO*, **14** (3), 487.

Knapp, Wilfried R. A., Nanson, John, 2019, "A Catalog of High Proper Motion Stars in the Southern Sky (HPMS3 catalog)", JDSO, **15** (1), 21.

Knapp, Wilfried R. A., Nanson, John, 2019, "A Catalog of High Proper Motion Stars in the Northern Sky (HPMSNS catalog)", *JDSO*, **15** (1), 42.

Knapp, Wilfried R. A., 2019, "Cross-Match of WDS TDS/TDT objects with DAIA DR2", *JDSO*, **15**)1). 178.

Knapp, Wilfried R. A., 2019, "Recovery of KPP objects in GAIA DR2", submitted to DSSC 27 Dec 18, 2018

Knapp, Wilfried R. A.. 2019, "Recovery of SKF objects in GAIA DR2", submitted to DSSC 27 Oct 21, 2018.

L. Lindegren, J. Hernández, A. Bombrun, et al., 2018, "Gaia Data Release 2 – The astrometric solution", *A & A*, **616**, A2.

L. Lindegren, J. Hernandez, A. Bombrun, et al., 2018, "Gaia DR2 astrometry", Astronomical Conference Vienna, August 2, 2018.

N. Lodieu, R. L. Smart, A. Pérez-Garrido and R. Silvotti, 2019, "A 3D view of the Hyades stellar and sub-stellar population", submitted to *Astronomy & Astrophysics*, arXiv:1901.07534v1.

X. Luri, A.G.A Brown, L. Sarro, et al., 2018, "Gaia Data Release 2. Using Gaia parallaxes", *A & A*, **616**, A9.

Ralph Schönrich, Paul McMillan and Laurent Eyer, 2019, "Distances and parallax bias in Gaia DR2", arXiv:1902.02355v1.

Jennifer G. Winters, Todd J. Henry, Wei-Chun Jao, et al., 2019, "The Solar Neighborhood XLV. The Stellar Multiplicity Rate of M Dwarfs within 25 PC", draft version arXiv:1901.06364 [astro-ph.SR]

Appendix A

Description of the CPM rating procedure (according Knapp and Nanson 2017 and Knapp 2018)

- Four rating factors are used: Proper motion vector direction, proper motion vector length, size of position error in relation to proper motion vector length and relation separation to proper motion speed
- Proper motion vector direction ratings: "A" for within the error range of identical direction, "B" for similar direction within the double error range, "C" for direction within the triple error range and "D" for outside
- Proper motion vector length ratings: "A" for identical length within the error range, "B" for similar length within the double error range, "C" for length within the triple error range and "D" for outside
- Error size ratings: "A" for error size of less than 5% of the proper motion vector length, "B" for less than 10%, "C" for less than 15% and "D" for a larger error size
- Relation separation to proper motion speed: "A" for less than 100 years, "B" for less than 1000 years, "C" or less than 10000 years and "D" for above

To compensate for the extremely small proper motion GAIA DR2 errors resulting in a worse than "A" rating despite only very small deviations an absolute lower limit is applied regardless of calculated error size:

- Proper motion vector direction: Max. 1° difference for an "A"
- Proper motion vector length: Max. 1% difference for an "A"

The letter based scoring is then transformed into an estimated likelihood for being CPM

Description of the Plx rating procedure (according to Knapp 2018)

- Two rating factors are used: Distance between the components in AU and relationship Plx error to Plx value. The distance between the components is calculated from the inverted Gaia DR2 parallax data (if positive) and the angular separation using the law of cosine

$$\sqrt{a^2 - 2ab\cos\gamma + b^2}$$

- with a and b = distance vectors for the stars A and B in lightyears calculated as (1000/Plx)*3.261631 and γ = angular separation in degrees calculated for small position deltas as

$$\gamma = \sqrt{\left[abs\left(RA1 - RA2\right)\cos\left(DE1\right)\right]^2 + \left(DE2 - DE1\right)^2}$$

and for large position deltas as

$$\gamma = \arccos\left[\sin\left(DE1\right)\sin\left(DE2\right) + \cos\left(DE1\right)\cos\left(DE2\right)\cos\left(abs\left(RA1 - RA2\right)\right)\right]$$

Realistic case distance is based on the given Plx values and the best and worst case scenario uses the given e_Plx data on the Plx values to estimate a smallest and largest possible distance within this error range applied once (threefold might be better)

- "A" for worst case distance, "B" for realistic case distance and "C" for best case distance less than 200,000 AU (means touching Oort clouds for two stars with Sun-like mass) and "D" for above
- "A" for Plx error less than 0.5% of Plx, "B" for less than 1%, "C" for less than 1.5% and "D" for above

The letter based scoring is then transformed into an estimated likelihood for being potentially gravitationally bound.

- A Plx Score of
- less than 10 means a likelihood of or near zero
- less than 50 means a likelihood lower than 50%
- larger than 50 means a likelihood larger than 50%
- equal 100 means a likelihood of 100%
- for a distance between the components smaller than 200,000 AU.

These likelihoods are based on the assumption that RA and DEC coordinates as well as parallaxes are normal distributed measurements with the given error range as standard deviation.

Appendix B

Counter-check of object samples from some of the 2019 reports mentioned in the introduction:

- Greaves 2019 – 15 objects listed in table 1: 12 out of the 15 objects qualify for a likely gravitational relationship, a respectable ratio due to a selection process concentrating on objects with rather large parallax values with a small error range. Three objects were less convincing:
  - ◊ GRV1252: Not very close parallax values and a rather larger parallax error for the primary result in a zero likelihood for a gravitational relationship despite the nearly ident radial velocity. Using the error range values for positions and parallaxes in a simulation gives an average value for the distance between the components over 30 light years – so this is most certainly no physical
  - ◊ GRV1256: 35% likelihood for a distance between the components of less than 200,000 AU with a mean value of ~300,000 AU and a rather large standard deviation give a quite flat distribution – despite very similar radial velocity in best case a "might be" physical
  - ◊ GRV1261: 12% likelihood for a distance between the components of less than 200,000 AU with a mean value of ~600,000 AU and a rather large standard deviation give a quite flat distribution – despite very similar radial velocity with overlapping error range a "rather not" physical
- Bryant 2019 – sample of 140 objects from the table in the Appendix starting with page 92: 46 or 33% out of the 140 objects qualify at first look for a likely gravitational relationship but only 31 or 22% make the cut for the PGR assessment scheme with a parallax value > 5 - so the assessment result for the objects not meeting this cut threshold is not valid. The rest of 94 objects are assessed as "might be" to "rather not" physicals despite the within the error range overlapping spatial velocity. The reason for this result is to be found in the object selection process with as it seems a preference towards very small parallax values leading despite the rather small error range to a huge spread regarding the likely distances between the components. Small parallaxes mean also less reliable data quality (Luri et al. 2018) and exponentially increasing distances for a given angular separation even with ident parallax values. A few examples for the objects with invalid "positive" assessment combined with small parallax values:
  - ◊ 4620459781916118528: The parallax values ~4,25 combined with the given angular separation suggest a distance between the components of ~161,000 AU but the simulation with the given error range for positions and parallaxes suggests an average distance of 262,500 AU with a likelihood of 45% for a distance below 200,000 AU so this is a "might be" case
  - ◊ 5056129616471590784: Very small but nearly ident parallax values suggest a distance between the components of ~157,000 AU but the simulation using the error range suggests an average distance between the components of ~350,000 AU making gravitational relationship rather unlikely and the likelihood of ~4% for a distance below 200,000 AU makes this look a "rather not" case
  - ◊ 5895171990539248000: This is another example with a positive rating at first look but due to the small parallax values of less than 3 combined with a rather large error range the average distance by simulation is larger than 1,000,000 AU or 15 light years making gravitational relationship very questionable. The likelihood for a distance below 200,000 AU is 12% so this seems also a "rather not" physical

Jiménez-Esteban et al. 2019 – 3,055 doubles from the total data set of 3,741 multiples available for download: 152 or 5% out of the 3,055 objects qualify at first look for a likely gravitational relationship but a second look shows that only 58 such pairs have a parallax value larger than 5 corresponding with a valid assessment and 94 come with much smaller parallax values down to below 1 by chance with more or less identical parallax values allowing for the conclusion of a distance between the components of less than 200,000 AU. But with parallax values this small this means then within the given parallax errors an extremely flat distribution of distances with an average distance far beyond this threshold. Reporting such pairs as likely physicals needs then very good additional reasons beyond common parallaxes. A few examples:

- GroupID 66: Rather ident parallax values of 1.76 mas suggest together with the angular separation of 25.3 arcseconds a distance between the components of ~94,000 AU but the likelihood for a distance < 200,000 AU is with the given error range only about 3%
- GroupID 85: Similar situation, only slightly better – the given data suggest a distance between the components of ~64,000 AU but the likelihood for a distance < 200,000 AU is with the given error range only about 5%

- GroupID 807: Rather ident parallax values of 1.23 mas suggest together with the angular separation of 34.25 arcseconds a distance between the components of ~99,500 AU but the likelihood for a distance < 200,000 AU is with the given error range only about 2%
- GroupID 5 to give a positive example: Very similar parallax values of ~17,6 suggest despite the huge angular separation of 837 arcseconds a distance between the components of ~71,000 AU and the likelihood for a distance < 200,000 AU is with the given error range 99%

Appendix C

Table with distances between the 100 star systems closest to the solar system based on the RECONS list per 01 Jan 2012:

Nr	RA	Dec	Plx	Name	Lyrs	To Nr	Name
1	217.42916666666700	-62.67944444444440	768.85	Proxima Centauri	6.569	2	
2	269.45208333333300	4.69333333333333	545.51	Barnard's Star	5.512	7	
3	164.12166666666700	7.01472222222222	419.10	Wolf 359	3.896	11	
4	165.83416666666700	35.97000000000000	393.25	Lalande 21185	4.055	3	
5	101.28708333333300	-16.71611111111110	380.02	Sirius	5.251	14	
6	24.75541666666670	-17.95027777777780	373.70	BL Ceti	3.204	19	
7	282.45583333333300	-23.83611111111110	337.22	Ross 154	5.512	2	
8	355.47791666666700	44.17500000000000	316.37	Ross 248	1.837	16	GX Andromedae
9	53.23250000000000	-9.45833333333333	311.22	epsilon Eridani	5.084	6	
10	346.46666666666700	-35.85305555555560	305.08	Lacaille 9352	4.123	12	
11	176.93500000000000	0.80444444444445	298.14	Ross 128	3.896	3	
12	339.63916666666700	-15.30194444444440	289.50	EZ Aquarii A	4.031	40	
13	316.72458333333300	38.74944444444440	286.08	61 Cygni A	4.769	37	
14	114.82541666666700	5.22500000000000	285.17	Procyon	1.018	22	Luyten's Star
15	280.69458333333300	59.63027777777780	283.83		4.179	35	
16	4.59541666666667	44.02305555555560	279.87	GX Andromedae	1.837	8	Ross 248
17	330.84041666666700	-56.78611111111110	276.07	epsilon Indi A	4.299	26	
18	127.45625000000000	26.77694444444440	275.80	DX Cancri	4.988	14	
19	26.01708333333330	-15.93750000000000	273.97	tau Ceti	1.615	21	YZ Ceti
20	53.99875000000000	-44.51250000000000	272.01	Henry et al. 1997. Henry et al. 2006	3.721	25	
21	18.12750000000000	-16.99888888888890	269.08	YZ Ceti	1.615	19	tau Ceti
22	111.85208333333300	5.22583333333333	266.23	Luyten's Star	1.018	14	Procyon
23	281.27208333333300	-63.96333333333330	259.50	Henry et al. 2006	5.255	38	
24	43.25375000000000	16.88138888888890	259.41	Henry et al. 2006	3.680	34	

Table continues on the next page.

Appendix C

Table with distances between the 100 star systems closest to the solar system based on the RECONS list per 01 Jan 2012 (continued).

Nr	RA	Dec	Plx	Name	Lyrs	To Nr	Name
25	77.91916666666670	-45.01833333333330	255.67	Kapteyn's Star	3.721	20	
26	319.31375000000000	-38.86750000000000	253.44	AX Microscopii	4.214	46	
27	162.06125000000000	-39.93500000000000	248.53	Jao et al. 2005. Costa et al. 2005	5.809	42	
28	336.99791666666700	57.69583333333330	248.06	Kruger 60 A	4.575	8	
29	97.34750000000000	-2.81388888888889	244.44	Ross 614 A	3.843	22	
30	247.57541666666700	-12.66250000000000	234.38	Wolf 1061	7.420	76	
31	12.29125000000000	5.38861111111111	232.70	van Maanen's Star	4.324	41	
32	1.35166666666667	-37.35750000000000	230.32		4.324	10	
33	188.32166666666700	9.02083333333333	227.90	Wolf 424 A	4.546	11	
34	30.05500000000000	13.05222222222220	224.80	TZ Arietis	3.680	24	
35	264.10791666666700	68.33916666666670	220.47		4.179	15	
36	162.05250000000000	-11.33722222222220	220.30		5.731	11	
37	298.47583333333300	44.41527777777780	220.20	G 208-044 A	4.769	13	
38	262.16625000000000	-46.89527777777780	220.11		1.835	51	EV Lacertae
39	176.42875000000000	-64.84138888888890	216.12	WD 1142-645	2.140	42	
40	343.31958333333300	-14.26361111111110	214.47	Ross 780	4.031	12	
41	1.68250000000000	-7.53944444444444	213.00		4.450	31	
42	161.08833333333300	-61.21000000000000	209.70	Henry et al. 2006	2.140	39	WD 1142-645
43	166.36916666666700	43.52666666666670	205.67		3.045	44	
44	152.84208333333300	49.45416666666670	205.53		3.045	43	
45	154.90166666666700	19.86944444444440	204.60		5.591	54	
46	323.39166666666700	-49.00888888888890	202.03		4.214	26	
47	54.89666666666670	-35.42805555555560	201.40		4.022	48	
48	43.76541666666670	-47.01444444444440	201.37	Costa et al. 2005	3.966	80	
49	63.81791666666670	-7.65277777777778	200.65	omicron 2 Eridani	2.523	65	
50	341.70708333333300	44.33388888888890	198.21	EV Lacertae	4.817	28	
51	264.26541666666700	-44.31916666666670	198.09		1.835	38	
52	271.36375000000000	2.50000000000000	195.96	70 Ophiuchi A	6.090	70	
53	297.69583333333300	8.86833333333333	195.40	Altair	3.722	70	
54	134.56208333333300	19.76194444444440	191.20	EI Cancri	3.798	90	
55	90.01458333333330	2.70666666666667	190.77	Henry et al. 2006	3.302	63	
56	75.48916666666670	-6.94638888888889	187.92	Henry et al. 2006	2.776	63	
57	144.89791666666700	-24.80777777777780	187.30	Burgasser et al. 2008	6.435	36	
58	176.92250000000000	78.69111111111110	187.26		7.123	35	
59	206.43250000000000	14.89138888888890	184.72	Wolf 498	6.143	33	
60	67.79916666666670	58.97722222222220	180.52	Stein 2051	9.238	75	

Table continues on the next page.

Appendix C

Table with distances between the 100 star systems closest to the solar system based on the RECONS list per 01 Jan 2012 (continued).

Nr	RA	Dec	Plx	Name	Lyrs	To Nr	Name
61	103.70416666666700	33.26805555555560	178.11		2.617	84	
62	278.90791666666700	32.99833333333330	176.50	Reid et al. 2003	6.574	37	
63	82.86416666666670	-3.67722222222222	175.99	Wolf 1453	2.776	56	
64	313.13750000000000	-16.97472222222220	175.03		7.106	79	
65	63.83125000000000	-9.58527777777778	174.34	Vrba et al. 2004	2.523	49	
66	293.09000000000000	69.66111111111110	173.79	sigma Draconis	3.138	81	
67	92.64416666666670	-21.86472222222220	173.77		6.580	93	
68	85.53875000000000	12.48944444444440	171.50	Ross 47	3.883	55	
69	266.64250000000000	-57.31916666666670	171.10		4.800	51	
70	289.23041666666700	5.16888888888889	170.96	Wolf 1055	3.722	53	
71	224.36666666666700	-21.41555555555560	170.62		3.292	100	
72	290.20000000000000	-45.55750000000000	169.17	Jao et al. 2005	3.342	86	
73	233.05375000000000	-41.27555555555560	168.52		5.685	100	
74	3.86708333333333	-16.13388888888890	168.35		4.855	41	
75	12.27625000000000	57.81527777777780	168.23	eta Cassiopei A	4.945	99	
76	258.83750000000000	-26.60277777777780	168.12	36 Ophiuchi A	6.383	51	
77	357.30208333333300	2.40111111111111	168.02		5.239	41	
78	116.16750000000000	3.55250000000000	167.19	Ross 882	4.177	107	
79	302.79958333333300	-36.10111111111110	166.26		3.208	86	
80	49.98166666666670	-43.06972222222220	165.47	82 Eridani	3.966	48	
81	267.02791666666700	70.87472222222220	164.70		3.138	66	
82	138.59500000000000	52.68666666666670	163.73		5.008	44	
83	302.18166666666700	-66.18194444444450	163.71	delta Pavonis	6.377	69	
84	107.50750000000000	38.52944444444440	163.41	QY Aurigae A	2.617	61	
85	144.39541666666700	29.52805555555560	163.30	Vrba et al. 2004	4.118	90	
86	303.47250000000000	-45.16388888888890	161.35		3.208	79	
87	218.57000000000000	-12.51944444444440	160.78	HN Librae	3.782	71	
88	352.96750000000000	19.93722222222220	159.88	EQ Pegasi	3.850	106	
89	229.86166666666700	-7.72222222222222	157.80	Wolf 562	4.334	87	
90	135.09833333333300	21.83472222222220	156.87	Henry et al. 2006	3.798	54	
91	189.70458333333300	-38.38166666666670	156.78	Henry et al. 2006	9.831	27	
92	258.03291666666700	45.66583333333330	156.32		3.219	94	
93	88.79041666666670	-4.17138888888889	156.05	WD 0552-041	3.124	63	
94	247.82666666666700	40.86500000000000	156.00		3.219	92	
95	253.87000000000000	-8.33638888888889	154.96	Wolf 630 A	6.825	76	
96	246.35250000000000	54.30416666666670	153.14		4.216	92	

Table concludes on the next page.

The "True" Movement of Double Stars in Space

Appendix C

Table with distances between the 100 star systems closest to the solar system based on the RECONS list per 01 Jan 2012 (conclusion).

Nr	RA	Dec	Plx	Name	Lyrs	To Nr	Name
97	145.69333333333300	-68.88500000000000	153.05	Jao et al. 2005	6.573	42	
98	184.75125000000000	11.12527777777780	152.90	GL Virginis	7.130	33	
99	348.32083333333300	57.16833333333330	152.84		4.945	75	
100	224.16041666666700	-28.16416666666670	152.49		3.292	71	
				Average distance Lyrs	**4.298**		
				Minimum distance Lyrs	**1.018**		
				Maximum distance Lyrs	**9.831**		
				Objects with dis-tance to the next star smaller than 3 Lyrs	**16**		
Additional nearby objects:	Additional nearby objects:	Additional nearby objects:	Additional nearby objects:	Additional nearby objects:	Additional nearby objects:	Additional nearby objects:	Additional nearby objects:
101	165.01791666666700	22.83305555555560	149.32	Ross 104	6.200	105	
102	322.40333333333300	17.64333333333330	149.01	Ross 775 A	7.983	106	
103	134.73458333333300	8.47388888888889	147.66	Henry et al. 2006	4.496	107	
104	222.84750000000000	19.10055555555560	147.57	ksi Bootis A	7.136	59	
105	162.71708333333300	6.80805555555556	147.15	EE Leonis	6.200	101	
106	344.14500000000000	16.55333333333330	146.37	Ross 671	3.850	88	
107	122.98958333333300	8.77444444444444	146.30	Ross 619	4.177	78	
108	45.46416666666670	-16.59333333333330	143.81	Henry et al. 2006	7.935	65	

Measures of Ten Sco Doubles and the Determination of Two Orbits

Matthew James[1], Meg Emery[2], Graeme L. White[3], Roderick Letchford[4], Stephen Bosi[5]

1. University of New England, Armidale, NSW, Australia; m.b.james27@gmail.com
2. Kildare Catholic College, Wagga Wagga, NSW, Australia; megcolemery@gmail.com
3. Centre for Astronomy, University of Southern Queensland, Toowoomba, QLD, Australia; graemewhiteau@gmail.com
4. Vianney College Seminary, Wagga Wagga, NSW, Australia; rodvianney@yahoo.com.au
5. University of New England, Armidale, NSW, Australia; sbosi@une.edu.au

Abstract: We present measures for 10 pairs in the constellation of Scorpius using a C14 telescope, Lucky Imaging, and the Reduc software. The separations of Alpha Centauri AB, as determined from the orbital elements of Pourbaix and Boffin (2016), were used as an image scale and position angle calibrator.

Our internal uncertainties are ~0.06 arcsec in r and ~0.06 degree in PA. There is excellent agreement with historic data extrapolated to epoch of observation (~2018.53), and micro-arcsecond positions from the GAIA database where the differences are ~0.05 arcsec in r and ~0.15 degrees in PA.

In addition, we present rectilinear elements for the 10 Sco pairs and orbital elements for two of them. Ephemera are given for these pairs based on both the rectilinear elements and the orbital elements.

1. Introduction

We present here the first of two papers that explore the limits of uncertainty that can be obtained using different techniques to determine standard separation, ρ, and position angles, PA. In this first paper we undertake lucky imaging measures of 10 pairs in the constellation of Scorpio (Sco) using drifting images, with the image scale and the camera's position angle calibrated against an accurate ephemeris of Alpha Centauri. A second paper (James *et al.,* in preparation for journal submission) will undertake a more detailed analysis of the accuracy of different applications of lucky imaging.

We present measures for these pairs and look for uncertainty through comparison with extrapolations of historic data and micro-arcsecond positions from the Gaia DR2 database. One method to determine if a double star system is a visual double or a binary system is to observe the relative motions between the primary and secondary component over a period of time. The trend can be used to differentiate between orbital or rectilinear motion. Section 5 looks at the motion of the pairs over time utilising the historic record, and Section 6 determines the rectilinear motion of the pairs following the method of Letchford, White and Ernest (2018a). For binary systems with very short orbital arcs the method developed by Letchford, White and Ernest (2018b) is used in Section 7 to determine grade 5 orbits for two of the pairs in this study.

2. Selection of Pairs.

The objects in this study were chosen from the Carro Double Star Catalogue (Carro, 2013) that have a separation, ρ, larger than 4 arcseconds; a limit imposed by local seeing conditions.

The constellation Scorpius was specifically chosen since the constellation was near zenith at the time of observation. High elevations reduce the effects of airmass and give better video captures.

Table 1 lists the stars that make up the 10 pairs. Here the WDS designation is given along with the WDS Discovery Code (*Disc*). Both are adapted from the Washington Double Star Catalog (WDS, Mason, *et al.,* 2001). The names/identifiers of the stars are from the SIMBAD database (Wegner, *et al.,* 2000), the ASCC database (Kharchenko, 2001) and from the DR2 release (Brown, *et al.*, 2018) of the GAIA astrometric mission (Prusti, *et al.*, 2016).

3. Observations

Equipment and Software.

The telescope used to make the observations is the

Measures of Ten Sco Doubles and the Determination of Two Orbits

Table 1. Modern Identifications of the Stars that make up the 10 Sco Pairs

	WDS	Disc	SIMBAD	ASCC	GAIA
1	16029-2501	BU 38A,B	TYC 6784-1420-1	1683158	6235913255305953536
			TYC 6784-1425-1	1683157	6235913255305954432
2	16095-3239	BSO 11A,B	HD 144927	1778073	6035755719057732224
			TYC 7334-2610-1	1778075	6035755719057730816
3	16143-1025	STF2019AB,C	HD 145996	1401854	4344884406644977280
			BD-10 4276C	1401855	4344884406644973952
4	16195-3054	BSO 12A,B	HD 146836	1778791	6037514800199297152
			HD 146835	1778788	6037514800213601024
5	16201-2003	SHJ 225A,B	V* V933 Sco	1587367	6244725050721030528
			HD 147009	1587364	6244725905417556992
6	16247-2942	H N 39A,B	HD147723	1684185	6038073970589665280
			HD 147722	1684184	6038073970589665536
7	16482-3653	DUN 209A,B	HD 151315	1875678	5971596329361239808
			HD 151316	1875680	5971596260664472704
8	16510-3731	HJ 4889A,B	HD 151771A	1875852	5971527094516942720
			HD 151771B	1875854	5971527094516943488
9	17290-4358	DUN 217A,B	HD 158042	1978893	5958561447264080768
			CD-43 11741B	1978895	5958561447264078208
10	17512-3033	PZ 5A,B	HD 162220	1788279	4056340704108946176
			CD-30 14802B	1788278	4056340704108937600

Bill Webster 14-inch Celestron Schmidt-Cassegrain Telescope located at the Kirby Observatory of the University of New England, Armidale, NSW, Australia. See Figure 1. The telescope is equipped with a flip-mirror box which allows the user to switch between the camera and eyepiece. The camera, a ZWO ASI120MM-S USB 3.0 Monochrome CMOS, was used for its image resolution, temporal resolution, and the USB 3.0 download bandwidth. A red (approximating R) filter was used to reduce the effects of atmospheric distortion on the video captures.

Figure 1. The Kirby Observatory of the University of New England, Armidale, NSW, Australia. The dome covers the Bill Webster 14-inch Celestron Schmidt-Cassegrain Telescope used in this study.

The video capture software used was SharpCaps version 3.1, and the analysis software used was Reduc version 5.36, provided by Florent Losse. Reduc allows for the rapid disposal of data (capture frames) resulting in a text file output of the X and Y coordinates of the primary and secondary star on the chip, which were used in Microsoft Excel 2016 to calculate the PA and ρ along with their formal uncertainties.

Lucky Imaging

The lucky imaging technique is utilized which is akin to high speed photography; high frame-rate and low exposure times. When used on astronomical objects, like double stars, the short exposure time (<100 ms) has the effect of freezing the perturbed atmosphere, reducing image distortion and increasing the chance of obtaining higher quality images (Fried, 1977).

Video Drift Method.

Observations were made using the video drift method outlined by Nugent (2011). In brief, the pair is placed to the east side just outside of the video frame, the telescope's drive motor is deactivated and the video capture is then started, which results in the image of the pair drifting across the field of view of the camera (and out of the west side of the camera frame).

Calibration – Image Scale and Position Angle.

Calibration of the image scale and position angle was undertaken using the prominent southern hemisphere pair Alpha Centauri (α Cen). α Cen has been extensively studied (see White, Letchford and Ernest, 2018) over ~260 years and ~3.5 orbits. Precise orbital elements by Pourbaix and Boffin (2016) are available in the WDS Sixth Orbit Catalog, and these give precise predicted ρ and PA for the pair at the epoch of observation. Concurrent observations of α Cen underpin the calibration of the Sco measures presented here, and uncertainties in the calibration observations of α Cen contribute to the uncertainties in the measures presented below.

Analysis.

For each Sco pair, 5 AVI format video captures were taken using the video drift method. Each video capture was then reduced using all frames with ρ or PA outside of 2 standard deviations from the mean being removed. Further reduction was undertaken using Excel. Further details of the data analysis are given by James (2019).

Image Scale for the Calibration of Separation.

To determine the ρ for the 10 Sco pairs, a pixel per arcsecond ratio was calculated for the C14/ZWO ASI120MM-S telescope/camera based on the observations of α Cen; the image scale, $R_{px/as}$, was determined to be 5.664 pixels per arcsecond. Again further details of the data analysis are given in James (2019).

Position Angle.

The position angle was computed from the drift angle of the individual stars across the chip of the camera, the individual positions on each frame having been determined using Reduc. Again further details are given by James (2019).

$$SEM = \bar{M}\sqrt{\left(\frac{\sigma_M}{\bar{M}\sqrt{N_M}}\right)^2 + \left(\frac{\sigma_{cal}}{M_{cal}\sqrt{N_{cal}}}\right)^2}$$

Equation 1. The equation used to calculate the standard error in the mean for PA and ρ

4. Measures

The measures for the 10 Sco objects observed are given in Table 2. The formal uncertainties in these measures are the uncertainty of the observations of the Sco pairs combined with the uncertainty in the calibration observations of α Cen (for the ρ). These uncertainties are the Standard Error in the Mean (SEM) of 5 independent observations.

Equation 1 was used to calculate the Standard Error in the Mean (SEM) uncertainty of the measures. This equation combines both the uncertainty in the observations and in the calibrator into a single SEM uncertainty. Here N is the number of observations of a particular pair; always $N = 5$ for this paper. is the average measure (either PA or ρ) of the N number of observations. *cal* refers to the calibrator, i.e. α Cen. σ is the standard deviation (SD) of the measures of N observations.

5. Historic Observations.

Historic positional measures have been obtained from the supplementary catalogues of the WDS. For the 10 pairs studied here, there are a total of 420 observations starting as early as 1783.23 (for the pair WDS 16201-2003).

Table 2. Measures at Epoch for 10 Sco Pairs.

	WDS	Disc	Epoch	Sep (arcsec)	SEM (arcsec)	PA (deg)	SEM(deg)
1	16029-2501	BU 38	2018.542	4.472	0.023	343.091	0.280
2	16095-3239	BSO 11 AB	2018.526	7.636	0.033	83.610	0.024
3	16143-1025	STF2019 AB,C	2018.542	22.320	0.100	153.021	0.094
4	16195-3054	BSO 12 AB	2018.523	23.579	0.098	317.976	0.024
5	16201-2003	SHJ 225	2018.542	46.686	0.194	332.601	0.021
6	16247-2942	H N 39	2018.526	3.999	0.017	359.241	0.047
7	16482-3653	DUN 209AB	2018.545	23.914	0.100	137.972	0.034
8	16510-3731	HJ 4889	2018.526	6.761	0.028	4.224	0.058
9	17290-4358	DUN 217	2018.526	13.457	0.056	167.837	0.022
10	17512-3033	PZ 5 AB	2018.526	10.101	0.043	189.323	0.049

Measures of Ten Sco Doubles and the Determination of Two Orbits

Table 3. Linear fits Coefficient to the Historic Data for 10 Sco Pairs.

	WDS	Disc	Rho			PA		
			A	B	R^2	C	D	R^2
1	16029-2501	BU 38	0.00126	1.965	0.061	-0.0605	465.907	0.896
2	16095-3239	BSO 11 AB	-0.00448	16.606	0.118	-0.0148	113.872	0.300
3	16143-1025	STF2019 AB,C	0.00908	4.589	0.316	0.0032	147.704	0.014
4	16195-3054	BSO 12 AB	-0.00432	31.821	0.057	-0.0147	347.660	0.213
5	16201-2003	SHJ 225	-0.00124	49.204	0.033	-0.0027	338.412	0.067
6	16247-2942	H N 39	-0.01886	42.323	0.859	0.0503	256.409	0.617
7	16482-3653	DUN 209AB	0.00177	20.041	0.033	-0.0563	251.380	0.937
8	16510-3731	HJ 4889	-0.00144	9.612	0.056	-0.0090	22.915	0.201
9	17290-4358	DUN 217	-0.00449	22.343	0.375	-0.0065	181.831	0.043
10	17512-3033	PZ 5 AB	0.00023	9.671	0.002	-0.0017	192.841	0.027

Appendix 1 presents the ρ and PA for the 10 Sco pairs. Datapoints as orange squares were deemed to be outliers and rejected based on a subjective assessment of the trend. The green triangle datapoints are the measures from this work (taken from Table 2).

Precession of Position Angles.

All plots in Appendix 1 are for PA (and ρ) at the epoch and equinox of observation. The correction of the PA to bring them to a standard Equinox (say J2000) have not been applied. This precessional rotation of the frame is defined in Aitken (1935, p. 73) and Argyle (2004). As all pairs in the study are in close proximity (~16h 30m, -20^o) the PA precession of each pair is approximately 0.55 degree per century in the sense that the PA is decreasing with time. A much smaller component of PA precession based on the proper motion of the primary star (Argyle, 2004) was ignored in this work, except for those in Appendices 2 & 3, Tables 6, 7, & 9.

Uncertainties in Historic Measures.

White, Letchford and Ernest (2018) have shown that the precision of historic observations of double stars has improved with epoch; from ~0.6 arcseconds to ~0.14 arcseconds in ρ, and ~0.74 degree to ~0.5 degree in PA, over our period of interest (~1800 to the present). This trend towards better quality data is also visible here as it is seen that the spread of data points around the trend line converges with increasing time.

Fitted Trend Lines.

Each plot in Appendix 1 has been fitted by an unweighted linear trend line and the fitted parameters are given in Table 3 along with the derived correlation coefficient, R^2.

For the fit to the separation, ρ, with Epoch plot, the fit is defined as

$$\text{Separation, } \rho = A \times Epoch + B$$

and the fitted trend line for the Position Angle, PA, is

$$\text{Position Angle, } PA = C \times Epoch + D$$

The fitted parameters *A*, *B*, *C* and *D* are presented in Table 3 along with the fitted correlation coefficient, R^2.

6. Accuracy of the 10 Sco Measures.

The measures for the 10 Sco pairs in Table 2 were now compared with two external measures (*i*) the historic measures extrapolated to the epoch of observation, and (*ii*) the position given in the Gaia DR2 catalogue which was precessed to the epoch of observation.

Using a fitted linear trendline extrapolated from the historic measures from Table 3, ρ and PA are calculated for the epoch of observations and shown in Table 4 in column History.

The ρ and PA for the pairs obtained at epoch from the Gaia DR2 data base are given in Table 4 under heading GAIA.

The differences between the measures reported here (shown here as This Paper, TP) and those extrapolated from the historic data (shown as Hist) and the Gaia database are given in Table 5. Here units for differences in ρ are arcsecond, and degrees in PA respectively. There is excellent agreement between the measures of historic and Gaia values. The mean offset between the data sets (shown as Average =), and its formal uncertainty (shown as SEM =) are all self-consistent and consistent with the formal uncertainties quoted for the measures in Table 2. The average SEM in the offset of ρ is 0.04 arcseconds, and the average SEM in the offset

Measures of Ten Sco Doubles and the Determination of Two Orbits

Table 4. Comparison of Measures with (i) Extrapolated Historic Data and (ii) GAIA positions and Proper Motions.

	WDS	Disc	Rho			PA		
			This Work (arcsec)	History (arcsec)	GAIA (arcsec)	This Work (deg)	History (deg)	GAIA (deg)
1	16029-2501	BU 38	4.472	4.504	4.487	343.091	343.759	343.445
2	16095-3239	BSO 11 AB	7.636	7.571	7.649	83.610	83.947	83.644
3	16143-1025	STF2019 AB,C	22.320	22.924	21.625	153.021	154.089	155.359
4	16195-3054	BSO 12 AB	23.579	23.109	23.498	317.976	318.046	318.180
5	16201-2003	SHJ 225	46.686	46.703	46.637	332.601	332.982	332.707
6	16247-2942	H N 39	3.999	4.257	4.006	359.241	357.977	359.322
7	16482-3653	DUN 209 AB	23.914	23.616	23.888	137.972	137.740	138.120
8	16510-3731	HJ 4889	6.761	6.711	6.767	4.224	4.805	4.503
9	17290-4358	DUN 217	13.457	13.278	13.433	167.837	168.680	168.040
10	17512-3033	PZ 5 AB	10.101	10.136	10.110	189.323	189.498	189.580

Table 5. Differences of Measures with (i) Extrapolated Historic Data and (ii) GAIA positions and Proper Motions.

WDS	Disc	Diff Rho	Diff PA	Diff Rho	Diff PA	Diff Rho	Diff PA
		GAIA - TP	GAIA - TP	Hist - TP	Hist - TP	Hist - GAIA	Hist - GAIA
16029-2501	BU 38	0.015	0.353	0.032	0.668	0.017	0.314
16095-3239	BSO 11 AB	0.012	0.034	-0.065	0.337	-0.077	0.303
16143-1025	STF2019 AB,C						
16195-3054	BSO 12 AB	-0.081	0.204	-0.470	0.071	-0.389	-0.134
16201-2003	SHJ 225	-0.050	0.106	0.017	0.380	0.066	0.274
16247-2942	H N 39	0.007	0.080	0.258	-1.264	0.252	-1.344
16482-3653	DUN 209 AB	-0.027	0.148	-0.299	-0.232	-0.272	-0.379
16510-3731	HJ 4889	0.006	0.279	-0.050	0.582	-0.056	0.303
17290-4358	DUN 217	-0.024	0.202	-0.179	0.843	-0.155	0.640
17512-3033	PZ 5 AB	0.009	0.257	0.035	0.175	0.026	-0.082
	Average =	-0.015	0.185	-0.080	0.173	-0.065	-0.012
	SEM =	0.011	0.034	0.071	0.210	0.063	0.195

of PA is 0.12 degrees.

This comparison does not extend to WDS 16143-1025. The brightest (primary) component observed in this work is WDS 16143-1025 AB, a very close pair separated by only 0.2 arcseconds. The positions, and proper motions, reported for components AC by both the HIPPARCOS and GAIA mission are inconsistent and no comparison has been made with the measures reported in Table 2.

7. Rectilinear Motion.

The motion of the components of a double star may be characterised as a rectilinear motion of the secondary relative to the primary star. Rectilinear motion is usually visualized as a straight line on a Cartesian plot where the primary star is the origin (0,0) position.

Such descriptions are an important tool in distinguishing between optical doubles and physical binaries since it is the variations from linearity that allows a sensitive identification of a Keplerian system.

As stated above, White, Letchford and Ernest (2018) have shown the precision of historic observations of double stars to be ~0.14 arcsec in ρ, and ~0.5 degree in PA, at best, for recent measures, and where

(Text continues on page 495)

Measures of Ten Sco Doubles and the Determination of Two Orbits

Table 6. Rectilinear Elements for 10 Sco pairs.

	WDS	x0 (DE0)	xa	y0(RA0)	ya	t0	theta0	rho0	xb	yb	move	x-inter	y-inter
		+/-	+/-	+/-	+/-	+/-	+/-	+/-	+/-	+/-	+/-		
1	16029-2501	3.58	-32	-2.35	-0.0050	2200	326.7	4.28	10.9	8.8	5.9	5.12	-7.81
		0.02	0.0001	0.07	0.0003	200	0.8	0.04	0.2	0.6	0.2		
2	16095-3239	4.23	0.001079	3.6	-0.00127	5000	40.0	5.6	-1.34	10.2	1.67	7.28	8.59
		0.07	2.23E-05	0.5	0.00014	900	4.0	0.3	0.04	0.3	0.11		
3	16143-1025	-14	-0.005	15.4	-0.004	700	133.0	21	-11	19	6.2	-30.80	28.60
		2	0.002	2.5	0.002	1400	7.0	2	4	4	1.3		
4	16195-3054	9	0.0026	4	-0.0062	-1000	23.0	10	12	-3	6.7	10.99	26.16
		4	0.0012	4	0.0012	700	20.0	4	2	3	1.1		
5	16201-2003	3	-0.00115	-25.7	-0.00013	35000	276.0	25.8	43.80	-21	1.156	230.98	-25.98
		1	3.07E-05	1.5	4.33E-05	2000	2.0	1.5	0.06	0.09	0.004		
6	16247-2942	0.598	-0.02345	1.30	0.0090	2170	69.1	1.40	51.35	-18	25.11	3.91	1.49
		0.002	1.44E-05	0.02	0.0015	11	0.3	0.02	0.03	0.3	0.05		
7	16482-3653	-20.2	0.0038	4.0	0.0191	1390	168.8	20.6	-25.4	-22.5	19.4	-20.99	106.08
		0.3	0.0005	0.3	0.0005	90	0.8	0.3	0.9	0.9	0.4		
8	16510-3731	6.2	-3.40E-05	-2	-0.0001	17000	350.0	6.4	6.81	0.8	0.1	6.60	-26.89
		0.5	3.37E-05	4	0.0003	7000	40.0	1.1	0.07	0.6	0.3		
9	17290-4358	-6.9	-0.00032	-5	0.0004	-17000	220.0	9	-12.51	1.9	0.5	-11.03	-14.30
		1.8	8.98E-05	6	0.000303	17000	30.0	4	0.18	0.6	0.5		
10	17512-3033	-9.0	-0.00027	2.2	-0.001	-1500	170.0	9.3	-9.43	0.5	1.1	-9.55	39.47
		0.3	8.30E-05	1.2	0.004	1200	7.0	0.4	0.17	0.7	0.3		

Table 7. Ephemeris for the10 Sco Pairs based on the Rectilinear Motion.

	WDS	1991.25 PA°	1991.25 Sep"	2015.5 PA°	2015.5 Sep"	2020.0 PA°	2020.0 Sep"	2025.0 PA°	2025.0 Sep"	2030.0 PA°	2030.0 Sep"	2035.0 PA°	2035.0 Sep"	2040.0 PA°	2040.0 Sep"
		+/-	+/-	+/-	+/-	+/-	+/-	+/-	+/-	+/-	+/-	+/-	+/-	+/-	+/-
1	16029-2501	345.59	4.53	343.85	4.48	343.52	4.47	343.15	4.46	342.79	4.46	342.42	4.45	342.05	4.44
		0.09	0.00	0.00	0.00	0.02	0.00	0.04	0.00	0.05	0.00	0.07	0.00	0.09	0.00
2	16095-3239	83.99	7.68	83.77	7.65	83.73	7.65	83.69	7.64	83.64	7.64	83.60	7.63	83.55	7.62
		0.00	0.00	0.00	0.00	0.00	0.00	0.00	0.00	0.00	0.00	0.00	0.00	0.01	0.00
3	16143-1025	152.81	22.29	153.18	22.35	153.24	22.36	153.32	22.37	153.39	22.38	153.47	22.39	153.54	22.40
		0.12	0.05	0.00	0.00	0.03	0.01	0.05	0.02	0.08	0.03	0.10	0.04	0.13	0.05
4	16195-3054	318.52	23.32	318.35	23.46	318.32	23.49	318.28	23.52	318.25	23.55	318.21	23.58	318.18	23.61
		0.07	0.03	0.00	0.00	0.02	0.01	0.03	0.01	0.04	0.02	0.06	0.02	0.07	0.03
5	16201-2003	332.83	46.66	332.81	46.64	332.81	46.63	332.80	46.63	332.80	46.62	332.79	46.62	332.79	46.62
		0.00	0.00	0.00	0.00	0.00	0.00	0.00	0.00	0.00	0.00	0.00	0.00	0.00	0.00
6	16247-2942	356.55	4.65	359.13	4.07	359.69	3.97	0.35	3.85	1.05	3.73	1.79	3.62	2.58	3.50
		0.04	0.00	0.00	0.00	0.01	0.00	0.02	0.00	0.03	0.00	0.05	0.00	0.06	0.00
7	16482-3653	139.32	23.65	138.33	23.89	138.15	23.93	137.95	23.98	137.75	24.03	137.56	24.08	137.36	24.13
		0.03	0.01	0.00	0.00	0.01	0.00	0.01	0.00	0.02	0.01	0.02	0.01	0.03	0.01
8	16510-3731	4.66	6.76	4.63	6.76	4.63	6.76	4.62	6.76	4.62	6.76	4.61	6.76	4.60	6.76
		0.06	0.00	0.00	0.00	0.01	0.00	0.02	0.00	0.04	0.00	0.05	0.00	0.06	0.00
9	17290-4358	168.22	13.43	168.18	13.44	168.18	13.44	168.17	13.44	168.16	13.45	168.16	13.45	168.15	13.45
		0.03	0.00	0.00	0.00	0.01	0.00	0.01	0.00	0.02	0.00	0.03	0.00	0.03	0.00
10	17512-3033	189.58	10.10	189.72	10.11	189.75	10.12	189.78	10.12	189.81	10.12	189.84	10.12	189.87	10.12
		0.05	0.00	0.00	0.00	0.01	0.00	0.02	0.00	0.03	0.00	0.04	0.00	0.05	0.00

Measures of Ten Sco Doubles and the Determination of Two Orbits

Table 8. Orbital Elements for 2 Sco pairs.

	WDS	P yrs	a "	I °	Ω °	T yr	e	ω °
		+/-	+/-	+/-	+/-	+/-	+/-	+/-
2	16095-3239	150000	40	100.0	120	-11000	0.52	350
		20000	4	2.3	7	15000	0.02	115
4	16195-3054	33000	34	118.0	110	-1900	0.76	351
		5000	4	1.2	10	100	0.09	20

Table 9. Ephemeris for the 2 Sco Pairs based on the Orbital Motion.

	WDS	1991.25 PA°	1991.25 Sep"	2015.5 PA°	2015.5 Sep"	2020.0 PA°	2020.0 Sep"	2025.0 PA°	2025.0 Sep"	2030.0 PA°	2030.0 Sep"	2035.0 PA°	2035.0 Sep"	2040.0 PA°	2040.0 Sep"
2	16095-3239	84.00	7.68	83.78	7.65	83.74	7.65	83.69	7.64	83.65	7.64	83.60	7.63	83.55	7.62
4	16195-3054	318.53	23.31	318.36	23.46	318.32	23.49	318.29	23.52	318.25	23.55	318.22	23.58	318.18	23.61

(Continued from page 493)

the uncertainties for early measures are larger (~0.6 arcsec and ~74 degree). These uncertainties are dwarfed by the precisions of the HIPPARCOS and Gaia spacecraft (milli-arcsecond and micro-arcsecond respectively) and their inclusion in the rectilinear analysis presented here would not contribute to the accuracy of that analysis. The rectilinear analysis there is based only on the HIPPARCOS and Gaia positions and the historic measures are shown in Appendix 2 only for completeness, as are the measures from Table 2.

The rectilinear plots for the 10 Sco pairs are presented in Appendix 2.

Table 6 gives the Rectilinear Elements for the 10 pairs, where the column headings, x0, xa, y0, ya, t0, θ0 and ρ0 are defined in Letchford, White and Ernest, 2018a.

Armed with the Rectilinear Elements, it is possible to give an ephemeris for the ρ and PA. This is given in Table 7. Epochs are in the column headings.

8. Determination of the Orbit for Two Sco Pairs.

Following the technique presented in Letchford, White and Ernest, 2018b, it is possible to determine Grade 5 Orbital Elements for pairs that display very short arcs. For this analysis all historic data is considered as is the measure from Table 2.

The orbital elements for two Sco pairs are given in Table 8 and shown graphically in Appendix 3. Column headings in Table 8 are described in Letchford, White and Ernest, 2018b.

Again, armed with these Orbital Elements, it is possible to give an ephemeris for the ρ and PA. These are given in Table 9. Epochs are in the column headings. Units for ρ are arcseconds and units for PA are degrees.

These predictions are in exact agreement with the rectilinear predictions of Table 7.

9. Conclusion.

We presented measures for 10 pairs in the constellation of Scorpius using a C14 telescope, lucky imaging, drift scans and the Reduc software. The separations of α Cen AB, as determined from the orbital elements of Pourbaix and Boffin (2016) were used as the image scale and position angle calibrator, where PA calibration was undertaken using drift scans.

Our internal uncertainties are ~0.06 arcseconds in ρ and ~0.06 degree in PA. There is excellent agreement with historic data extrapolated to epoch of observation (~2018.53), and micro-arcsecond positions from the GAIA database where the differences were ~0.05 arcsecond in ρ and ~0.15 degrees in PA.

There is excellent agreement between the extrapolated historic observations and these from Gaia.

In addition, we presented rectilinear elements for 10 Sco pairs and Orbital Elements for two of them. Ephemera are given for these pairs based on both the rectilinear elements are the orbital elements.

10. Acknowledgements.

We acknowledge the use of the following resources:

- SIMBAD Astronomical Database, operated at CDS, Strasbourg, France, https://simbad.u-strasbg.fr/simbad
- The Aladin sky atlas developed at CDS, Strasbourg Observatory, France, https://aladin.u-strasbg.fr
- The Washington Double Star Catalog maintained by the USNO. (WDS), https://ad.usno.navy.mil/wds

- All-sky Compiled Catalogue of 2.5 million stars, 3rd version (ASCC), http://vizier.u-strasbg.fr/viz-bin/VizieR-3?-source=I/280B/ascc
- The Gaia Catalogue (Gaia DR2, Gaia Collaboration, 2018), from VizieR (GAIA DR2), http://vizier.u-strasbg.fr/viz-bin/VizieR-3?-source=I/345/gaia2
- SharpCap astrophotography software developed by Robin Glover, https://www.sharpcap.co.uk

In addition, we thank Jenny Stevens for her support for author Meg Emery, and Florent Losse for the Reduc software.

11. References.

Aitken, R.G., 1935. The Binary Stars". McGraw-Hill Book Company, Inc.

Argyle, B., 2004. "Observing and Measuring Visual Double Stars", Springer press.

Brown, A.G.A., et al., (Gaia Collaboration)., 2018. Gaia Data Release 2 - Summary of the contents and survey properties. Astronomy and Astrophysics, 616, A1.

Carro, J. M., 2013, "Useful Lists of Double Stars". *Journal of Double Star Observations*, **9**(3), 203-206.

Fried, D. L., 1977, "Probability of getting a lucky short-explosure image through turbulence", *Journal of the Optical Society of America*, **68**(12),1651-1658.

James, M., 2019, BSc Honours Thesis, University of New England, Australia.

Kharchenko, N.V., 2001, "All-Sky Compiled Catalogue", *Kinematika Fiz. Nebesn. Tel*., **17**(5) 409.

Letchford, Roderick R, Graeme L White, and Allan D Ernest., 2018a, "The Southern Double Stars of Carl Rümker II: Their Relative Rectilinear Motion." *JDSO*, **14**(2): 208–222. http://www.jdso.org/volume14/number2/Letchford_208_222.pdf.

Letchford, Roderick R, Graeme L White, and Allan D Ernest., 2018b, "The Southern Double Stars of Carl Rümker III: Quantified Probability of Boundedness and Preliminary Grade 5 Orbits for Some Very Long Period Doubles." *JDSO*, **14**(4): 761–70. http://www.jdso.org/volume14/number4/Letchford_761_770.pdf.

Mason, B.D., Wycoff, G.L., Hartkopf, W.I., Douglass, G.G. and Worley, C.E., 2001, "The 2001 US Naval Observatory double star CD-ROM. I. The Washington double star catalog." *Astron. J.*, **122**, 3466-3471.

Nugent, R. L., & Iverson, E. W., 2011, "A New Video Method to Measure Double Stars", *JDSO*, **7**(3),185-194.

Pourbaix, D. and Boffin, H.M.J., 2016, *Astronomy & Astrophysics*, **586**, 90P.

Prusti, T., et al., (Gaia Collaboration)., 2016, "The Gaia mission", *A & A*, **595**, A1.

Wenger et al., 2000, "The SIMBAD astronomical database", *Astronomy and Astrophysics Supplement*, **143**, 9.

White, Letchford and Ernest., 2018, "Uncertainties in Separation and Position Angle of Historic Measures – Alpha Centauri AB Case Study",. *JDSO*, **14**(3): 432.

Measures of Ten Sco Doubles and the Determination of Two Orbits

Appendix 1

Trends Shown by the Incorporation of Historic Data.

Historic positional measures have been obtained from supplementary catalogues of the WDS. For the 10 pairs a total of 420 observations are available dating from 1783.23.

This Appendix presents the ρ and PA for the 10 Sco pairs. All plots of PA (and ρ) are at the epoch and equinox of observation. Data points in orange have been rejected from the trend. The green points are the measures from this work (from Table 2).

A trend towards better quality data is visible as the spread of data points around the trend line is converging with epoch.

Each plot has been fitted by an unweighted linear trend line and the fitted parameters are given in Table 3 along with the derived correlation coefficient, R^2.

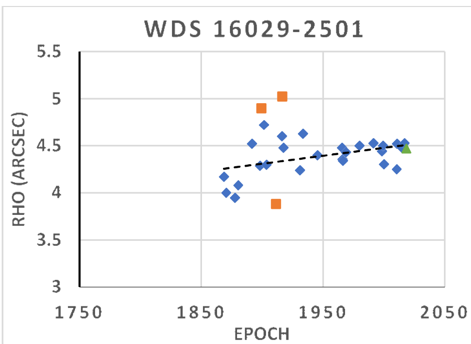

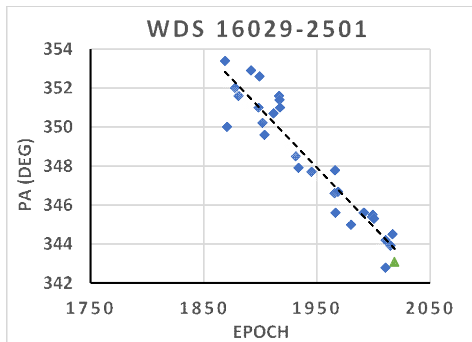

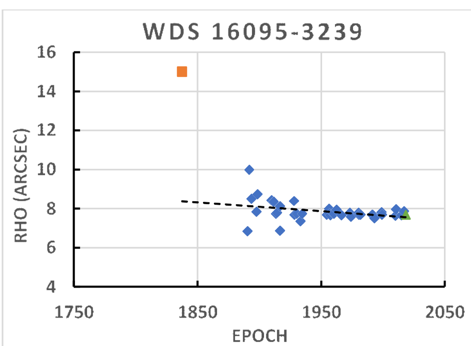

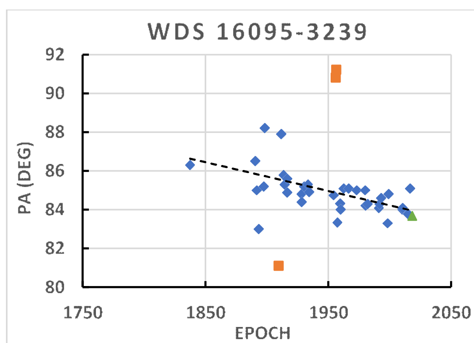

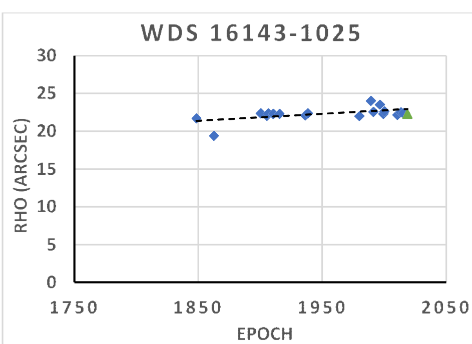

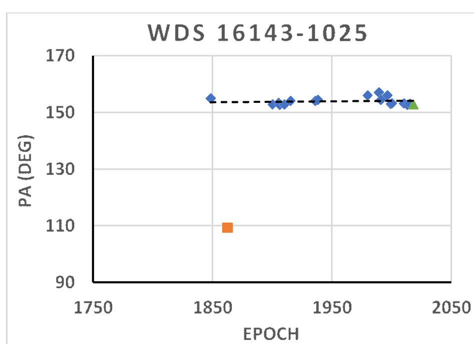

Measures of Ten Sco Doubles and the Determination of Two Orbits

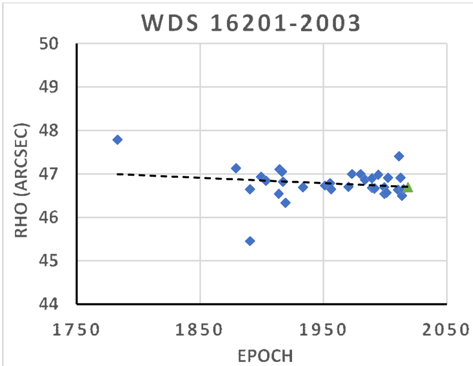

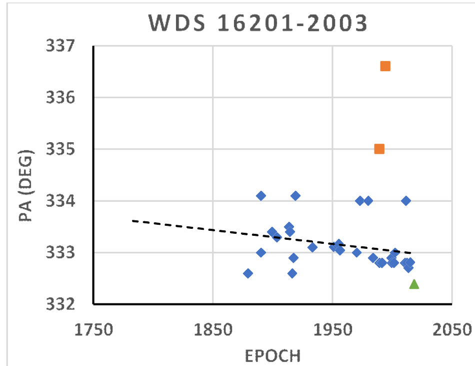

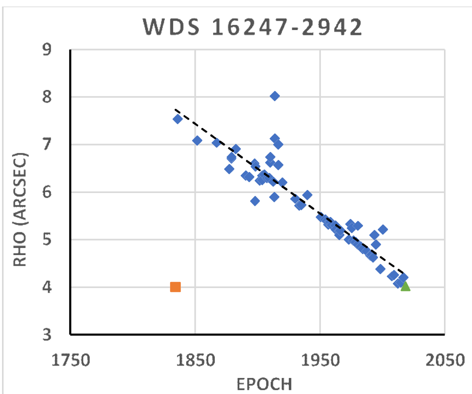

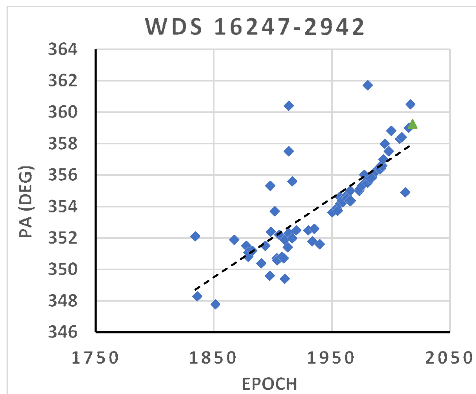

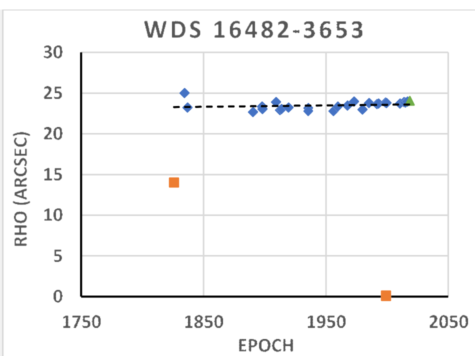

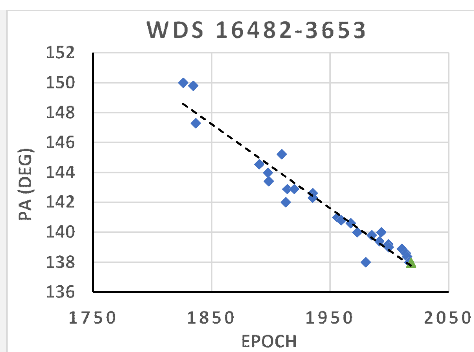

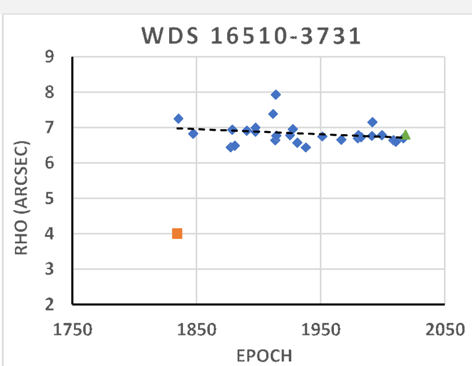

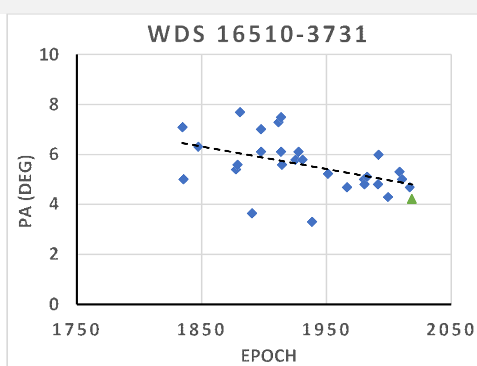

Measures of Ten Sco Doubles and the Determination of Two Orbits

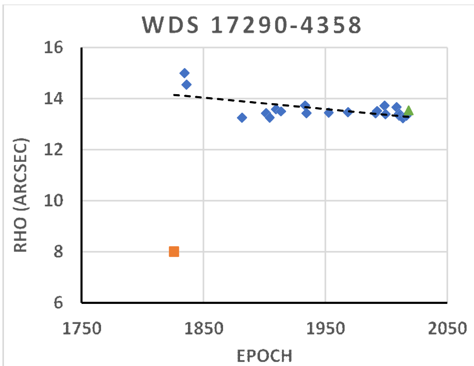

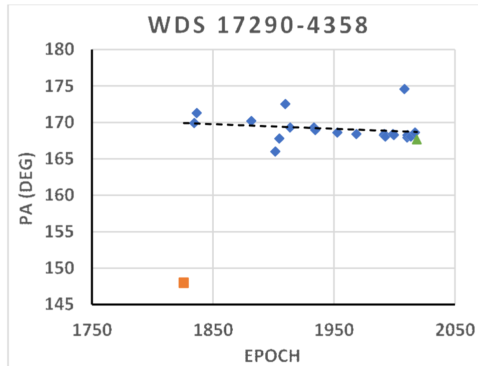

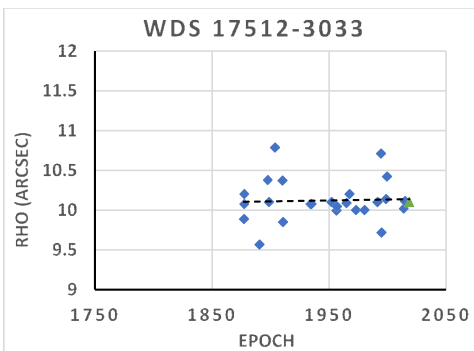

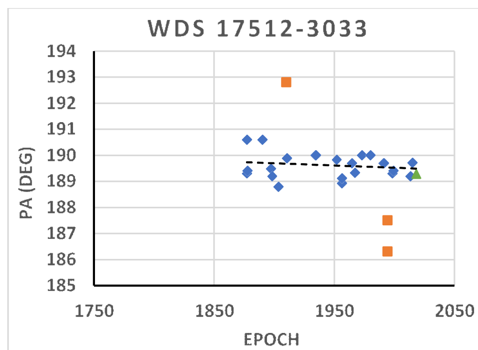

Appendix 2

Rectilinear Motion of the Ten Sco Pairs

Plots of the rectilinear motion of the 10 Sco doubles are given here. Left hand figures are unzoomed – right hand are zoomed. Historical data from the WDS have been incorporated and their position angles have been precessed from Equinox of date to Equinox J2000.0 using proper motions. The WDS data for 1991.25 (HIP – from the HIPPARCOS mission) are already at Equinox J2000.0. Precessed WDS observations are represented in the plots by a '+'.

The HIP and GAIA positions are represented by a red circle and green square respectively. The dotted ellipses are the uncertainty ellipses for the t0 (un-zoomed figure for each pair). If they cannot be seen in the plots, it is because of the plot scale. Uncertainty ellipses for the HIP and GAIA were also plotted but in each case they too may be too small to see at the scales that are needed to represent all relevant data.

Red line is HIP proper motion and Green is GAIA. The black line is the rectilinear motion based on the HIP and GAIA position. Rectilinear Elements are given in Table 6 and projected r and PA in Table 7.

For additional understanding into the this process, read in Letchford, White and Ernest, 2018b.

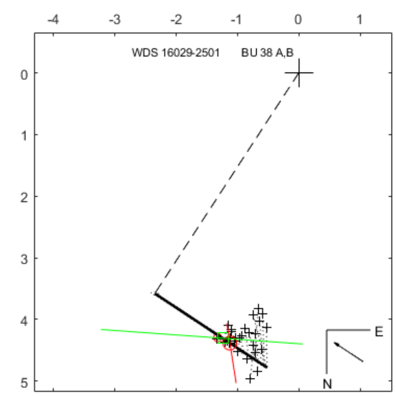

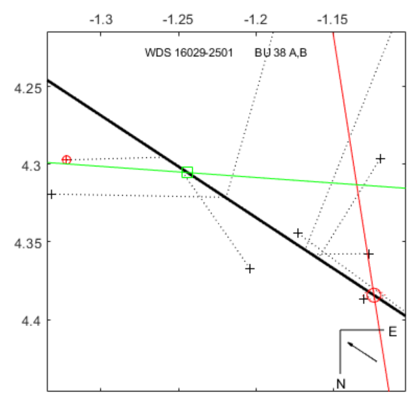

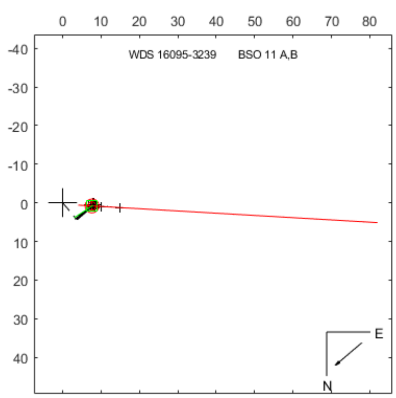

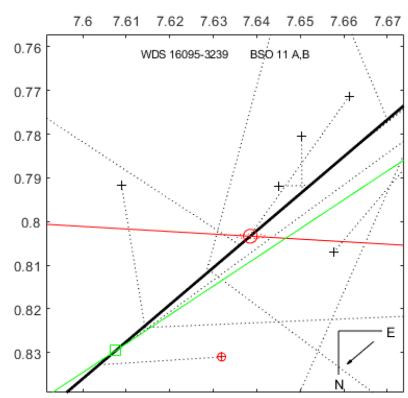

Measures of Ten Sco Doubles and the Determination of Two Orbits

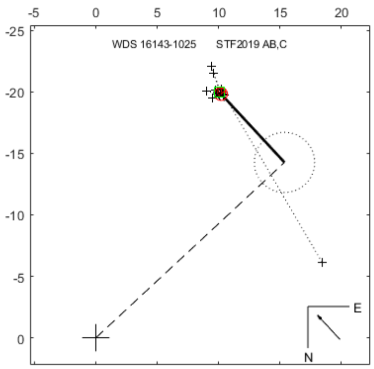

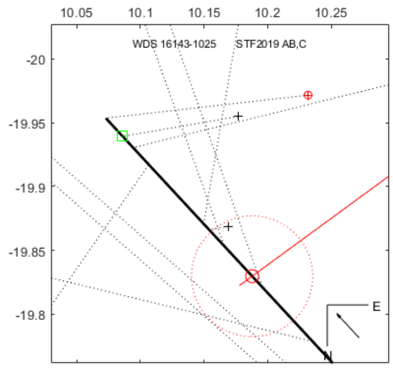

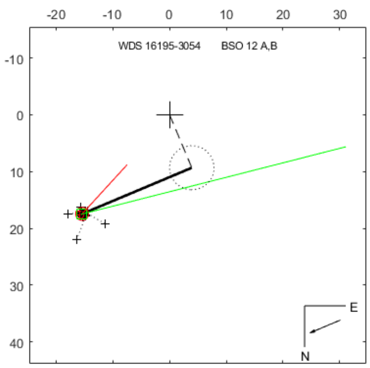

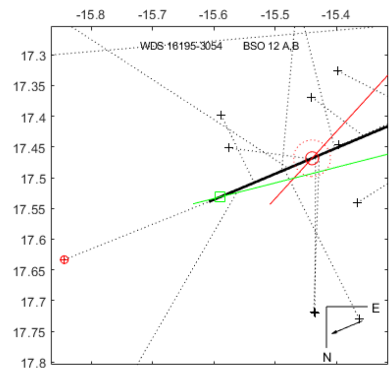

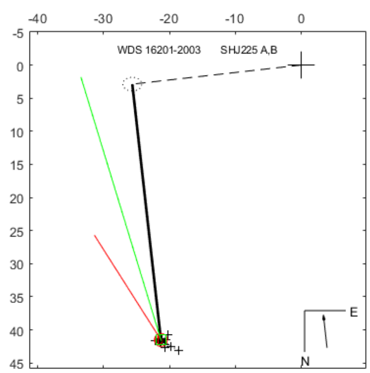

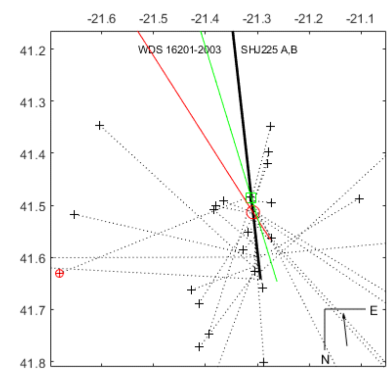

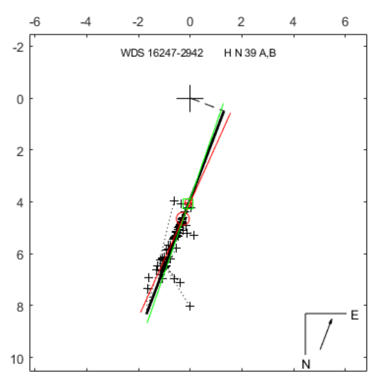

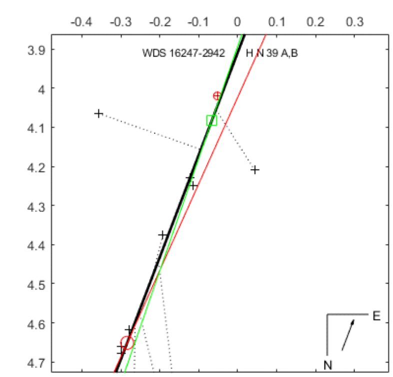

Measures of Ten Sco Doubles and the Determination of Two Orbits

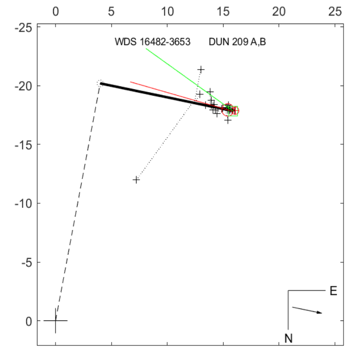

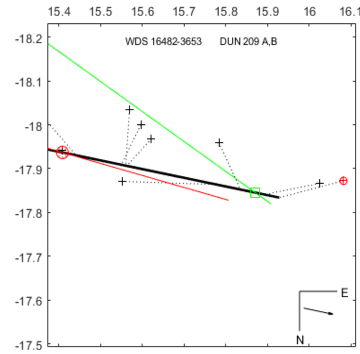

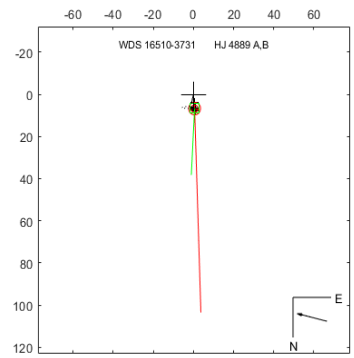

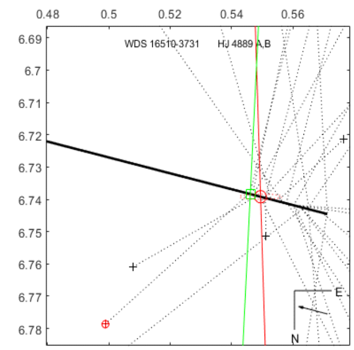

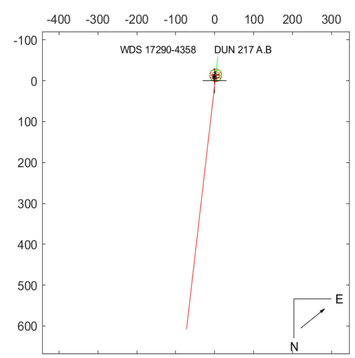

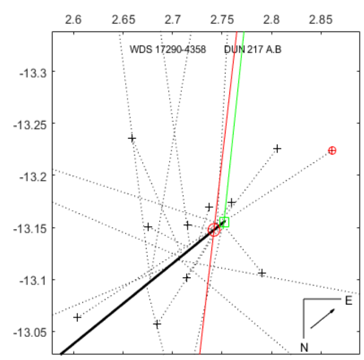

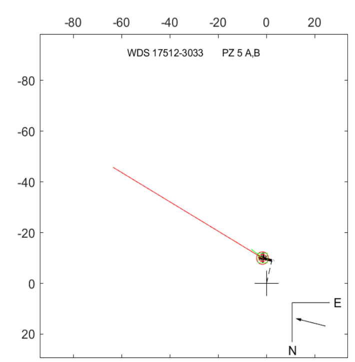

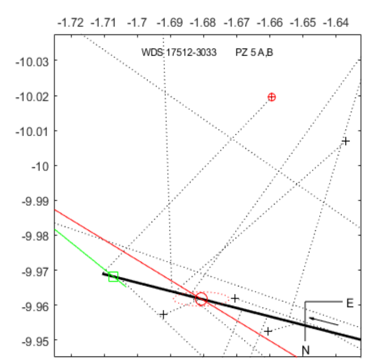

Appendix 3

Orbits Found for the Two Sco Pairs.

The family of orbits for 2 Sco pairs. The best orbit (smallest residuals from historic data) is bolded and the elements are in Table 8. Predicted r and PA based on the Orbital Elements are given in Table 9.

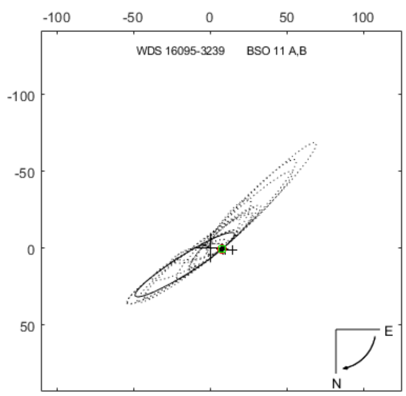

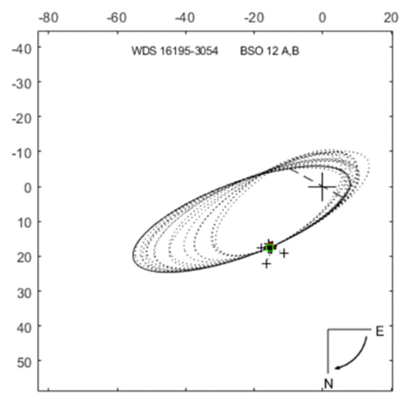

Addendum to "Using the Six Astrometric Parameters from Gaia DR2 II : Common Radial Velocity Pairs"

John Greaves

Northants, U.K.
jggaia@tutanota.com

In Greaves 2019 (*JDSO*, **15**, 77-86), an object entitled GRV 1251 was given as a pair of stars of common high proper motion. Subsequent closer inspection of the pair showed that the primary star had an even closer comites at a separation of 1.07" in a Position Angle of 214.8 degrees with very similar GAIA parallax (8.247 milliarcseconds) and proper motions (-142.44 millarcseconds per year in Right Ascension and 87.32 millarcseconds per year in Declination), but no radial velocity hence why it was missed. This object is therefore trinary. This object is GAIA magnitude 14.6. The figure below from the VISTA VHS confirms the reality of the closer pair as an extended object with the original noted companion approximately in line with the close pair.

All references and acknowledgements as per Greaves, J., *JDSO* **15**, 77-86, 2019.

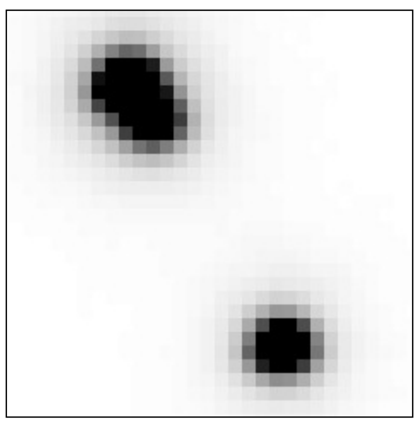

Journal of Double Star Observations

July 1, 2019
Volume 15, Number 3

The Journal of Double Star Observations (ISSN 2572-4436) is an electronic journal published quarterly. Copies can be freely downloaded from http://www.jdso.org.

Questions, comments, or submissions may be directed to rclark@southalabama.edu or to rmollise@bellsouth.net

The *Journal of Double Star Observations* (*JDSO*) publishes articles on any and all aspects of astronomy involving double and binary stars. The *JDSO* is especially interested in observations made by amateur astronomers. Submitted articles announcing measurements, discoveries, or conclusions about double or binary stars may undergo a peer review. This means that a paper submitted by an amateur astronomer will be reviewed by other amateur astronomers doing similar work.

Submitted manuscripts must be original, unpublished material and written in English. They should contain an abstract and a short description or biography (2 or 3 sentences) of the author(s). For more information about format of submitted articles, please see our web site at http://www.jdso.org

Submissions should be made electronically via e-mail to rclark@southalabama.edu or to rmolise@bellsouth.net. Articles should be attached to the email in Microsoft Word, Word Perfect, Open Office, or text format. All images should be in jpg or fits format.